THE LIGHTNING GROUND FLASH : AN ENGINEERING STUDY

by

ANDREW JOHN ERIKSSON

Thesis (Phd. - Electrical Engineering) Univ. of Natal.

Submitted in partial fulfilment of the requirements for the degree of Doctor of Philosophy in the Faculty of Engineering, University of Natal.

Pretoria
South Africa

December 1979

THE LIGHTNING GROUND FLASH - AN ENGINEERING STUDY

A B S T R A C T

The thesis is concerned with a study of the electrical engineering parameters of the lightning ground flash - i.e. the statistical distributions of peak current amplitudes, discharge current waveform characteristics, and flash striking distances - in the event of flashes to practical engineering structures. In view of its predominating frequency of occurrence in practical situations, the discharge of primary concern is the downward progressing and negatively charged ground flash.

A central feature of this work is the establishment of a lightning research station (incorporating a 60 m instrumented mast) in the Transvaal highveld region of South Africa. The design of this station and the related measurement techniques are fully described. Preliminary results accumulated over a 6-year period of observation are presented, and include recordings obtained during direct strikes to the mast, as well as data from associated measurements of additional thunderstorm and lightning parameters. The latter studies include the use of closed circuit television video recordings, together with electrostatic field mills and lightning flash counters. Analysis of the resultant data serves to provide a comprehensive characterisation of the thunderstorm and lightning climatology in the region - on the basis of electrical activity. With only few exceptions, it is concluded that the characteristics of lightning observed in the Transvaal region are generally consistent with the trends of data from other regions of the world.

A unique aspect of the project is a study of lightning striking distances. An attempt to estimate these distances using bi-directional photography of flashes to the research mast is described, and several preliminary results are also presented - in conjunction with the associated measurements of discharge current amplitude. These results are compared with previously used relationships between striking distance and peak current.

Thereafter .....

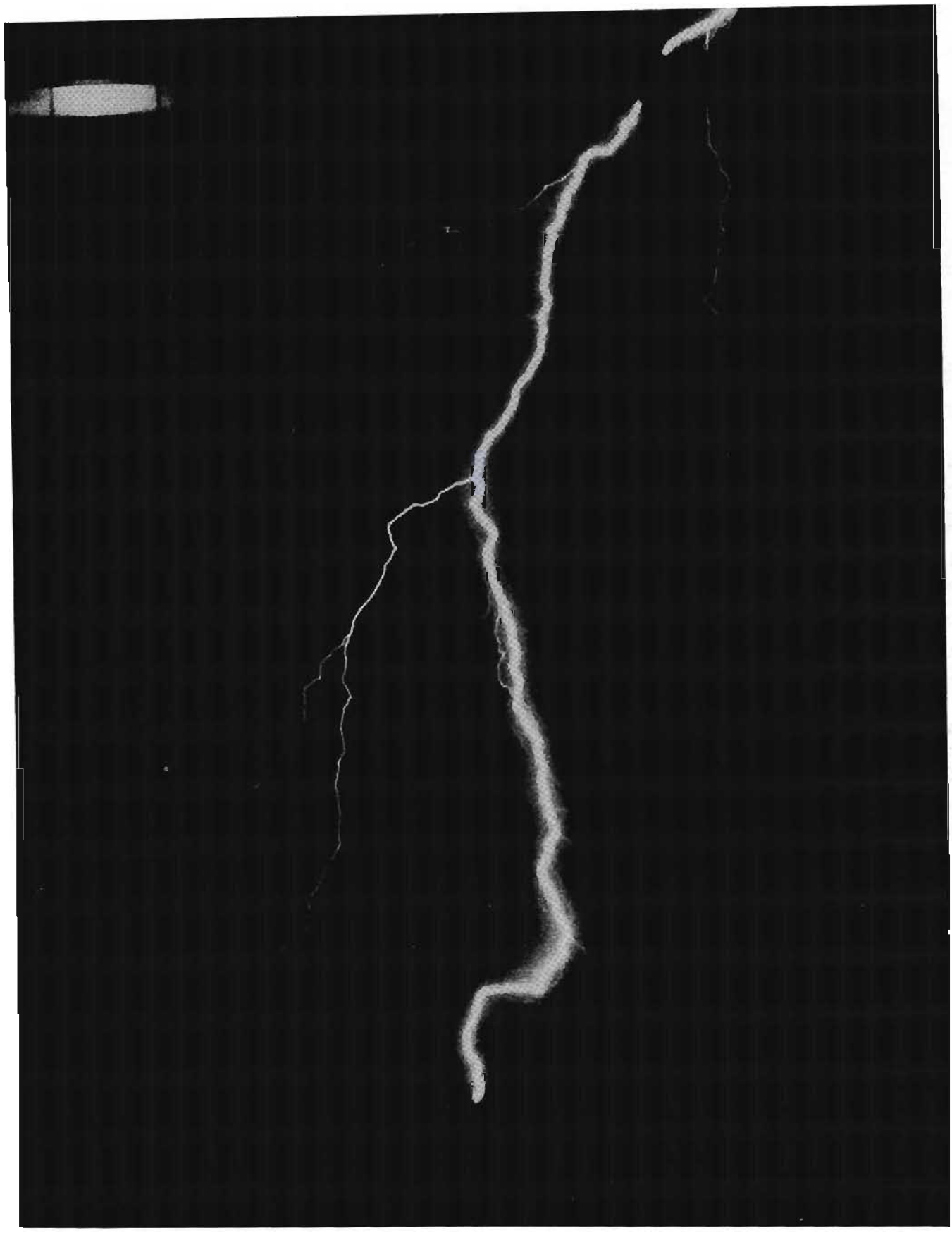

A SEVERE LIGHTNING FLASH TO THE RESEARCH MAST

THE LIGHTNING GROUND FLASH - AN ENGINEERING STUDY

CONTENTS

3.3.1 ..... /ii

5.4.3 ..... /iii

TABLES ..... /iv

TABLES

CONTENTS

FIGURES ..... /v

FIGURES

CONTENTS

4.11 ..... /vi

PREFACE

Lightning has long been an object of fascination and awe to man - perhaps because it is one of the most graphic manifestations of natural forces in a state of turmoil. The occurrence and consequences of lightning flashes have featured as integral aspects of many earlier mythologies and such atavistic attitudes have persisted until comparatively modern times. It has only been in the past 250 years that the physical nature of lightning has become clarified, and that steps have been taken to devise protective approaches against lightning - notably in the pioneering work of Franklin. More particularly, it has only been in the past 50 - 60 years that a comprehensive scientific understanding of the phenomenon has emerged.

Concomitant with scientific development has been technological advancement and increasing industrialisation. Thus it is only in the modern era that man's exposure and susceptibility to lightning has been widened beyond the individual or domestic level, to the collective - in that his technological systems (and society's increasing dependency thereon) are now also susceptible to disruption by lightning. A considerable amount of research effort has therefore been directed, over the past 30 - 40 years, towards clarification of the effects of lightning upon engineering systems, and toward the development of improved protective means whereby damage and disruption may be minimised.

The principal objective of this thesis is to report upon a research programme which attempts to arrive at an improved understanding of the ground flash - more particularly in the South African highveld region, but also in terms of the broader electrical engineering implications of the discharge process.

(Note: Except in isolated instances, as stated in the text, all the material presented in this thesis is the author's own original work.)

CHAPTER 1

INTRODUCTORY REVIEW

1.1 Background

The primary concern of this thesis is with the characteristics of the lightning ground flash, since it is this aspect of the discharge phenomenon which is mainly responsible for the damage, or disruption caused by lightning.

In presenting the material in this thesis, it is assumed that the reader is familiar with the main features of the lightning discharge. For completeness, however, a brief review of the phenomenology of the process is given in Appendix 1A and this also serves to define the terminology that has been adopted in this work. This Appendix also points out that in the majority of practical situations the most commonly encountered form of ground flash involves the transport of negative charge from the cloud to the ground (i.e. the negative downward ground flash). The study of this particular variant of ground flash therefore forms the main theme of this work.

The research programme which provides the basis of the material in this thesis was initiated in 1972 by the author, as a research project of the National Electrical Engineering Research Institute (NEERI) of the South African Council for Scientific and Industrial Research (CSIR). The background motivation to this project lay in the need to arrive at a better understanding of the ground flash and its characteristics, in order to arrive at more effective and optimised approaches to prevailing lightning protection problems in South Africa.

Again, by way of clarification to the non-specialist reader, Appendix 1B contains a brief review of contemporary thinking on lightning protective concepts and the electrical engineering implications of the problem. This demonstrates that implementation of an effective lightning protective approach - whether this relates to the protection of a house, or of an electrical engineering installation such as a transmission line - requires adequate knowledge of several primary aspects of the negative downward flash process; as follows:

(i) an understanding of the striking mechanism

(ii) a knowledge of the probability distribution of stroke current peak amplitudes.

(iii) a knowledge of the time dependent characteristics of the stroke discharge current waveform.

In ..... /2

In considering these requirements, it was recognised that a considerable body of information was already available from various experimental studies of the lightning phenomenon, which had been carried out over the past 50 years in different regions of the world. These ranged from physical studies of the discharge mechanism (such as the work of Schonland[1], Malan[2], Pierce[3], Brook[4], and their colleagues) to experimental investigations of the engineering characteristics and implications of the ground flash (e.g. McCann[5], Hagenguth[6], Wagner[7], Whitehead[8], Anderson[9], Popolansky[10], et al).

Much of this earlier material has now been collated and reviewed in several standard reference works (e.g. Uman[11], Golde[12][13], and it is generally agreed that probably the most comprehensive source of data on the parameters of the ground flash derives from the comprehensive investigations carried out by Berger[14], over a 30 year period of study, on top of Monte San Salvatore in Switzerland.

In a review of aspects of Berger's data in 1971, Anderson[15] drew attention to the fact that certain data accumulated earlier in Southern Africa raised the possibility that the lightning discharge in this region could be more intense in relation to the more temperate regions of the world, such as Switzerland. In particular, Anderson's review indicated the possibility that South African flashes could involve higher amplitude currents, as well as a greater incidence of multiple stroke and negative polarity flashes, and flashes of longer duration, than had generally been observed by Berger in Switzerland. This raised the question therefore, as to whether Berger's data (comprehensive as they were), were necessarily applicable to the study and resolution of lightning protection problems in Southern Africa.

A further question concerning Berger's data related to the fact that these were based upon direct stroke measurements carried out on masts located at the top of Monte San Salvatore. This mountain has an altitude of 914 m above sea level, and rises steeply, some 640 m, above the Lake of Lugano. The topography of this measurement situation is thus comparatively far removed from many practical problem situations, such as domestic houses or transmission lines in "normal" countryside, and therefore raised the additional question of whether the resultant measured data were representative of what might be encountered in common practical situations.

Arising ...../3

Arising out of this background study therefore, the principal objectives of the South African research programme - and thus of the work presented in this thesis - were as follows:

(a) Establishment of a research station for the measurement of the parameters of the ground flash during direct strikes to a structure - in a location more representative of practical engineering situations - with the emphasis primarily upon the negative downward flash.

(b) Accumulation of direct stroke data and a comparison of the results with data from other regions of the world, in order to establish to what extent local discharge characteristics may deviate in this climatic region.

(c) Rigorous characterisation of the local lightning and thunderstorm climatology and again, a comparison with data from other regions of the world.

(d) A study of the lightning striking process, in order to arrive at a better understanding of those aspects which could facilitate and optimise protective techniques.

1.2 Plan of research

Two main lines of approach were followed in the course of the research programme reviewed in this thesis. The first involved an experimental study of a variety of ground flash characteristics, using both direct and indirect techniques of observation, while the second included also an analytical examination of striking distance concepts and led to the development of a simple analytical model whereby structure effects upon the process could be clarified.

In considering the material in this thesis it may be helpful to review briefly the several distinct phases that delineated progress as the programme developed:

(a) The project was initiated in early 1972 and the first phase comprised essentially the design, development and commissioning of the requisite facilities making up the research station. This included the planning and erection of a research mast and the establishment of a suitable instrumentation facility, together with the necessary site services. The first direct flashes to the research station were registered successfully in November 1972.

(b) Thereafter ..... /4

(b) Thereafter, the second phase represented a period of evaluation and consolidation of measurement techniques, during which the principal objective was the attainment of a high reliability of all instrumentation systems, in order that as much data as possible could be accumulated. Station operation and data acquisition proceeded routinely until some 27 flash events had been registered by October 1977.

(c) At that stage it was considered that sufficient data had been obtained to justify preliminary analysis and the author published a research paper in June 1978[16], which presented the tentative trends emerging from these early measurements. In order to examine the implications of these data adequately, the author had in the same paper carried out an analysis of flash incidence and characteristics on a variety of structures in different regions of the world. This analysis drew attention to the important influence of structure height upon the incidence of flashes of different types (e.g. upward and downward flashes), and led also to the expression of an approximate empirical relation, which accounted for the observed incidence of downward flashes to various structures, in terms of an equivalent structure attractive radius, viz.:

$$N_d = N_g \pi R^2 \times 10^{-6} \text{ flashes/year}$$

where N_d = annual incidence of downward flashes to a structure

N_g = prevailing annual ground flash density ($km^{-2}yr^{-1}$)

and R_a = structure equivalent attractive radius, given by:

$$R_a = 16{,}3\ H_s^{0{,}61} \quad \ldots\ldots\ (m)$$

where H_s = structure height in m

Arising out of this analysis, the author also reached the tentative conclusion that the cumulative distribution of stroke current amplitudes registered during downward flashes to structures, could be largely independent of structure height and essentially similar to the distribution of current amplitudes associated with flashes to comparatively flat ground.

This ...../5

This postulate had important implications for engineering practice, but was contradictory to the trends derived from several comparatively well-established electro-geometric concepts, (e.g. Sargent[17]) and thus demonstrated the need for a better understanding of the striking process and particularly of the role of structures in this process.

(d) Accordingly, the most recent phase of the research programme (i.e. in its stage of development, as represented by the preparation of this thesis), involved a study of experimentally measured "striking distances" and the development of an analytical model which served to represent the final stages of a downward flash to a structure.

Application of this model in numerical simulation studies - as discussed later in this thesis - allowed examination of the effects of structures of varying heights upon flash incidence, (including also structure protective effects), as well as upon the anticipated distributio of stroke current amplitudes in structures.

Subject to the assumptions of the model studies, the results tend to support field observations and the author's earlier conclusions from the tall structures analysis.

It should be emphasised that preparation of this thesis does not represent termination of the research programme. This particular project remains an integral part of the ongoing lightning research programme of the NEERI.

1.3 Synopsis of the succeeding chapters

The material presented in the body of this thesis lends itself to being grouped into several comparatively distinct topics, or sections, although each remains an element of the overall research programme. Chapters 2 to 5 (inclusive) therefore, have each been prepared as integral units, comprising all the material germane to the particular topic of discussion (i.e. including results and conclusions), and, taken together with their associated Appendices, may thus be considered almost independently of each other. An attempt is made in the concluding section, however, (Chapter 6), to correlate the material presented in the preceding chapters, and, where necessary, to enlarge upon this further.

By way of clarification of the organisation of the body of the thesis, it may be helpful briefly to review the content of each of the succeeding chapters.

Chapter 2 ..... /6

Chapter 2 - provisions of the research station

The activities reviewed in this section represent the first phase of the research program and comprise the basic engineering steps involved in the establishment of the research station and the related site services.

No claim for originality is made in respect of the engineering principles employed, but the situation itself was comparatively unique, since, as far as the author is aware, it represented the first contemporary instance that a complete measurement station - including the mast structure - was established purely for lightning recordings. The few known research stations of similar nature have all taken advantage of existing structures, (typically, broadcast antennae of various types).

This chapter serves therefore to set on record the various design steps involved in establishing the station, as well as the reasoning behind the various specialised arrangements that were adopted.

The material presented includes firstly, an examination of those factors that led up to the choice of research station site on the CSIR campus in Pretoria. The following three sections (together with Appendices 2A and 2B) outline the design of various site facilities, including the structural support of the mast itself, as well as the specialised earth electrode and power supply provisions. The remaining sections review the measurement technique and instrumentation arrangements that were adopted for direct measurement of lightning currents, as well as lightning photography. A primary objective in planning the site facilities was to reconcile the need to ensure maximum reliability of all measurement systems at a time when the site services themselves were experiencing maximum disruption, that is, at the time of a strike. Considerable attention was paid therefore to effective grounding and shielding principles.

As a last resort, to allow for the eventuality that all systems might fail, a magnetic link system was introduced to provide a back-up measurement of maximum current amplitudes. In view of their importance to the project therefore, Appendix 2C reviews briefly the procedures adopted for the calibration of these magnetic links.

Chapter 3 ..... /7

Finally, in operation of the station, it was necessary to take account of the unpredictable nature and times of occurrence of thunderstorm activity. This necessitated an approach which combined continuous operation (24 hours) of certain strategic items of equipment, with selective radio control of the remaining instrumentation - thereby ensuring effective operation of all systems at the requisite times, (i.e. when lightning was in the immediate vicinity of the station).

Chapter 3 - Direct measurement of lightning flashes to the research mast and results

This chapter reviews the performance of the research station over the first seven years of operation (1972 - 1978). A total of 28 flash events was recorded on the research mast during this period and the circumstances surrounding each event are outlined in Appendix 3A, which also presents the relevant oscillograms and flash photographs.

A primary feature of the planning of the research station had been an emphasis upon the negative downward flash and it is encouraging therefore to note that the majority of the recorded flashes (15 in all), were identified as being of this type. In examining the incidence of flashes to the mast, it is also observed that the negative downward type mostly occurred during afternoon storms, while the remaining more unusual flash types (such as those involving upward leaders), tended to be associated with the less common, early morning "cold" frontal storms.

As experience developed in the operation of the research station, various modifications to the instrumentation systems were gradually introduced - leading to an improving measurement success rate as the programme progressed. Of the available records, meaningful data were extracted from measurements on 13 flashes. (The majority of the remaining flash events could not be analysed, either due to missed recordings through loss of site power supply in the early stages of the programme before a standby supply was arranged, or, because at least 4 of these events involved weak upward leader discharges in which the maximum currents were below the recording system threshhold).

Various waveform parameters were evaluated from the available discharge current oscillograms and these results are analysed in the body of the chapter. While the recorded data samples are too small to allow meaningful statistical analysis, it is generally concluded that the character of the preliminary results, as well as their trends, are consistent with results obtained from other direct discharge current measurements - such as those of Berger[18]

A preliminary cumulative frequency distribution of negative downward peak current amplitudes is also presented and yields a median value of 44 kA, but being based upon a small sample, is subject to wide confidence limits. Although suggesting marginally higher current amplitudes than have been recorded elsewhere - subject to the confidence limits - this result is again consistent with contemporary thinking on the probable distribution of negative downward flash current amplitudes.

Chapter 4 - Striking distance considerations

Following a short introductory review of the concept of striking distance, this chapter outlines a unique experimental technique which attempts to determine the striking distances of flashes to the research mast. This involves a system of bi-directional photography of direct strokes, coupled with a technique of geometrical analysis, which leads to estimations of the striking distance of the downward leader, as well as of the interception between the resultant upward and downward progressing leaders.

Tentative results are presented for 8 such evaluations - in correlation with the associated values of discharge current peak amplitude, as recorded on the research mast. Although considerable scatter is evident in this small sample of records, the resultant trend of the measured striking distances (in relation to peak current amplitude) suggests larger striking distances than might be anticipated from the more common empirical electrogeometric relationships - such as that of Whitehead[19], for example.

Building upon earlier work which had been initiated by Anderson[9], an analytical representation of the final stages of a flash to a structure is presented in Appendix 4A. This concept involves the approach of a linearly charged downward leader element, in the vicinity of a structure, and an evaluation of the electrostatic field gradients developed beneath this leader. The striking distance of the downward leader is considered to have been attained when the upward leader ionisation inception gradient is developed at the structure. For a given ratio of the downward and upward leader average velocities, flash termination is defined by the interception of these two leaders.

Application ..... /9

Application of the analytical approach is illustrated by an evaluation of striking distances to the research mast for a range of leader charge magnitudes. The latter, in turn, are correlated with stroke currents amplitudes (using Berger's measured correlations[14]) to yield predicted dependencies of both striking distances and interception distances for flashes to the research mast. The results are found to display trends comparable to those obtained from the measured striking distances.

An important conclusion arising out of this work is that striking distances to a structure are directly dependent upon the degree to which the structure intensifies the prevailing electrostatic field.

Additional aspects examined in this chapter include the implications of leader branching, and the influence of upward/downward leader velocity ratios.

The concept of structure attractive radius is further discussed and evaluation of this parameter in terms of the above analytical concepts is also illustrated. It is concluded that the observed annual incidence of flashes on the research mast is best accountable in terms of a mast "effective" height of about 169 m - in relation to other tall structures.

Finally, in the light of the preceding observations and analyses, the last stages of a flash to a structure are re-examined and three potentially decisive phases are identified, as well as the overall implications regarding the estimation of striking distances and flash incidence.

Chapter 5 - The study of additional lightning and thunderstorm parameters in the Transvaal region

This chapter in particular comprises a virtually independent and self-consistent topic, or field of study, within the general framework of this thesis. The principal objective of the material presented in this chapter is to define the overall background climatology (in the "electrical" context), to the region within which the main research station lightning observations were being carried out.

Three principal aspects relating to the regional thunderstorm and lightning climatology are examined and in each instance, an attempt is made to compare the resultant data with observations from other regions of the world.

Firstly, the incidence and characteristics of multiple stroke flashes are examined - mainly using closed circuit television techniques of observation and recording. After analysis of the resultant data in respect of

multiple ..... /10

multiple stroke flash characteristics, such as interstroke interval and flash duration, it is concluded that the local results are wholly consistent with data from previous work - including observations in several other regions of the world.

The locally observed incidence of multiple stroke flashes depicts a marginal reduction in relation to a "global" trend, however, and the possibilities that this might be the consequence of differing measurement techniques and/or storm and seasonal effects, are examined.

The second main aspect studied in this chapter, involved the measurement of thunderstorm electrostatic field characteristics at ground level - using field mills and computerised techniques of analysis.

A large sample of storm records is evaluated, with the parameters studied including the distribution of maximum field intensities, as well as the durations of persistence of various field levels.

It was found that less than 10% of storms cause ground level fields in excess of 20 kV/m and the resultant median positive and negative storm maximum field intensities were 5,1 kV/m and - 7,3 kV/m respectively.

In comparing the local results with the limited data available from other parts of the world, it was concluded that the characteristics of storm fields in the Pretoria area did not differ substantially from those observed in the other regions.

The third motivation for the work presented in this chapter was to arrive at an objective characterisation of the regional thunderstorm and lightning climatology, using comparatively simple instrumentation. This was achieved by analysing the accumulated registrations of a CIGRE lightning flash counter - having known performance characteristics, and a variety of parameters was examined. These included storm diurnal incidence, storm duration, flash counter registration per storm and average flashing rate. Over 400 storm recordings were accumulated in the course of a 5 year period of study.

Comparisons with data from other regions of the world are illustrated and these indicate that the Pretoria records are characteristic of what might be anticipated from multi-cellular orographic air-mass storms. The overall seasonal mean flash rate was found to be about 6×10^{-6} $km^{-2}s^{-1}$.

In ..... /11

In general, it is concluded that sufficiently consistent data have been accumulated over the period of study, to allow a meaningful characterisation of storm climatology in the Pretoria area - (as expressed in terms of electrically defined parameters) and the expected features of the "average" Transvaal summer thunderstorm are presented.

Seasonal and long term variations (including possible periodicities) are also examined briefly in this chapter. While a pronounced seasonal trend is certainly evident, it is concluded that considerably more data will still be required before this, or any long term variations, may be adequately defined.

Chapter 6 - General discussion and implications.

As the title implies, an attempt is made in this, the final chapter, to re-examine collectively the material presented in the preceding sections and to highlight the implications and possible applications of this work.

There are two main aspects to the overall research which forms the basis of this thesis. The first involves an experimental programme, comprising the acquisition and analysis of field data, while the second is concerned with arriving at a better understanding of the striking process and, (although including experimental measurements also) this is largely based upon analytical concepts.

These two themes therefore provide the basis for the discussions in this chapter.

In the first instance, the material presented in Chapters 2, 3 and 5 is reviewed briefly. It is concluded that the original objectives of the experimental phase of the programme have largely been attained - in the sense that the research station has proved capable of reliable measurement of lightning parameters, and sufficient background field data have also been acquired to provide a meaningful and objective characterisation of the regional storm and lightning activity. The trends of the preliminary data are generally considered to be consistent with what has been observed elsewhere and do not indicate any substantial variations in the characteristics of the downward flash, in relation to observations in other climatic regions. While sufficient local data on lightning parameters have been acquired to justify incorporation in a "global" review of lightning parameters[20], it is accepted that considerably more field data are still required to clarify the preliminary trends, as well as any possible long-term variations.

Thereafter ...../12

Thereafter, the striking distance measurements and analytical concepts presented in relation to the research mast, in Chapter 4, are re-examined, and it is concluded that the preliminary agreement between the experimentally and analytically determined relations is sufficiently encouraging to justify further application of the analytical approach. Appendix 6A therefore, outlines an extension of the earlier analytical model and applies this to the study of a range of structures of varying height - leading to the expression of generalised relations for striking distance and attractive radius (in terms of structure height and prospective stroke current). The trends of these relations are generally consistent with earlier empirically derived estimates - including those of the author's tall structures analysis.[21]

The resultant generalised expression for attractive radius is then applied in a further series of simulations (using Monte Carlo techniques of stochastic analysis), in an evaluation of the protective effect of structures and of the influence of structure height upon the distributions of stroke currents registered in structures.

An important conclusion arising out of this work is that there appears to be no substantial structure height effect upon the frequency distribution of current amplitudes, thereby supporting the author's earlier postulate in this regard.

These analyses also demonstrate consistency with the commonly held concept of a 45° protective cone around structures, but indicate a decrease in this angle, as structure height is increased.

Generalised curves for protective angle, as well as flash incidence and penetration current, are presented in relation to structure height, as a guide in practical engineering applications, but it is recognised that these results should be considered as being indicative of trends only, since the analytical approach includes several important simplifications and assumptions.

The final section of the chapter comprises a restatement of the claims for this thesis and also includes several proposals for future research.

CHAPTER 2

PROVISIONS OF THE RESEARCH STATION

2.1 Introduction

This chapter is concerned primarily with the basic engineering associated with the establishment of the CSIR lightning research station, and, apart from discussions on the choice of site, basic design considerations and instrumentation techniques, mention will also be made of related service aspects, such as the provisions of the earth electrode and the specialised arrangements for the site power supply.

2.2 Considerations on the choice of site

A number of factors were involved in arriving at a decision regarding the location of the research station. These included the following:

(a) Regional ground flash density

It was clearly desirable that the station be situated in an area experiencing a high incidence of lightning. For example, it was known from the results of a related research programme[29], that the Pretoria region experiences a mean annual ground flash density of about 7 ground flashes km^{-2}, which is representative of much of the Witwatersrand or industrialised region of South Africa.

(b) Availability and security

By the very nature of the experiment and in view of the potential hazards involved, it was desirable that the station be situated in a comparatively large and undisturbed area, free from any other structures, buildings or personnel. Similarly, it was preferred that access to the station be controlled.

(c) Nature of the terrain

Although a prime objective of the research programme was that the measurement situation (and the consequent data) be generally representative of practical engineering situations, it was recognised that location of the research mast upon elevated terrain should enhance the strike probability. Accordingly, attempts were made to find a suitably elevated site (upon a small hill or ridge for example), such that a moderate

attractive ..... /14

attractive influence would be exerted upon nearby downward progressing discharges. Bearing in mind that the latter discharge is that most commonly encountered in practical engineering situations, it was hoped that the attractive bias would not be so extreme that a high incidence of upward discharges would prevail, as has been encountered at other measuring stations, such as that on Mount San Salvatore for example, where 84% of the recorded flashes were upward in character.[23]

(d) Logistics

Although the intention was to design an automatic station, it was recognised that effective operation would necessitate frequent site visits for routine data retrieval and equipment maintenance. Hence, subject to the earlier comments on the need for site security, it was clearly very important that the station be readily accessible and reasonably close to the CSIR laboratories in Pretoria.

Accordingly, taking the above factors into account, an optimum site was selected on a small ridge running through the main CSIR property on the Eastern side of Pretoria. This site offered considerable advantages as far as availability, security and the logistics of routine operation were concerned. The site topography (which is shown in plan and cross-section in Figure 2.1) is also representative of the surrounding terrain, which is generally undulating in character.

2.3 Design of the research mast

Budgetary considerations largely determined the choice of mast and that finally adopted for this programme was obtained from the South African Post Office - where it had served as a temporary structure in the course of microwave route planning and surveying.

The available mast (shown diagrammatically in Figure 2.2) was of aluminium triangular lattice construction, being assembled from 24 vertical sections of 2,5 m length, bolted together to make a

total 15

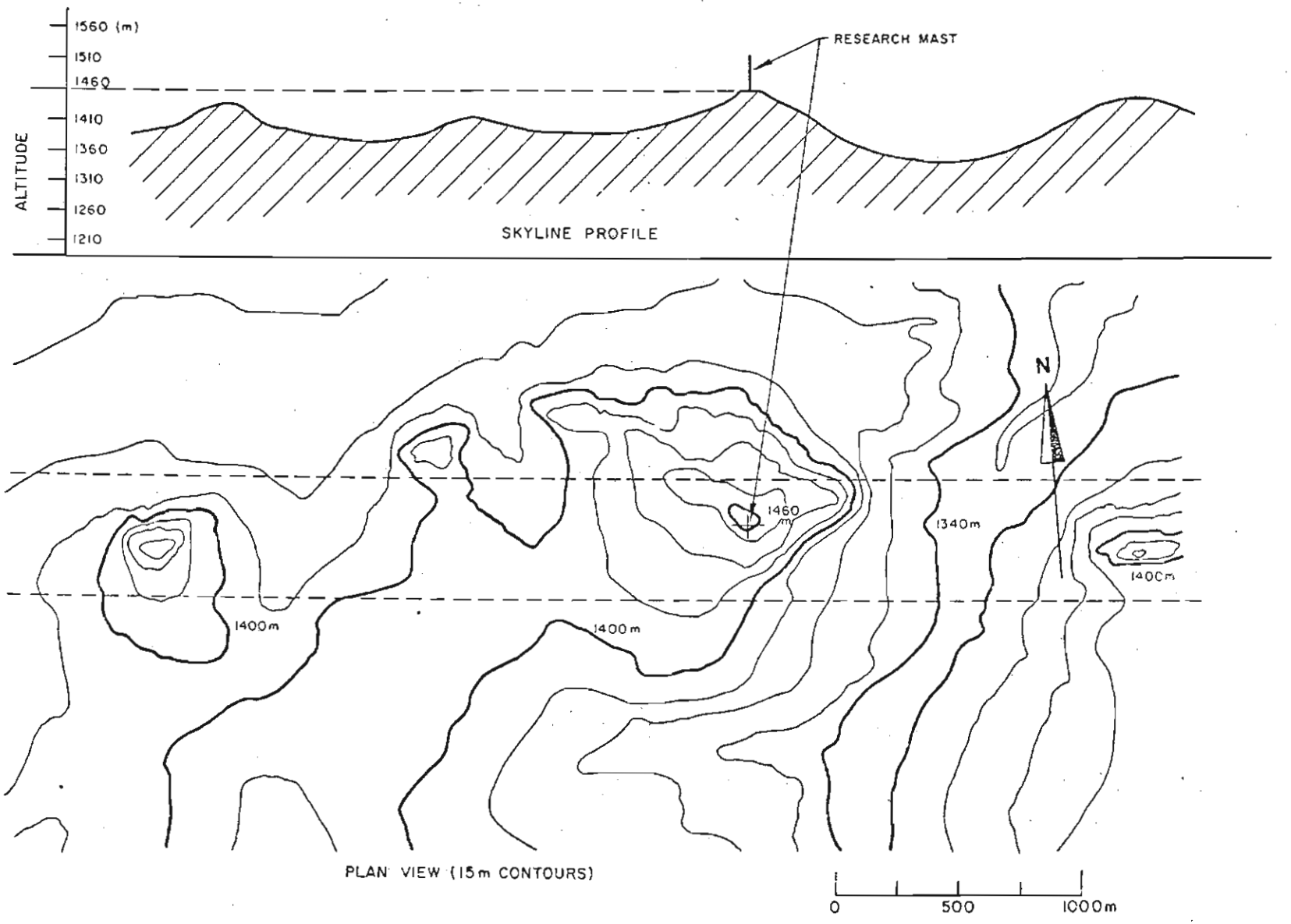

FIGURE 2.1

TOPOGRAPHY OF THE TERRAIN IN THE VICINITY OF THE RESEARCH MAST

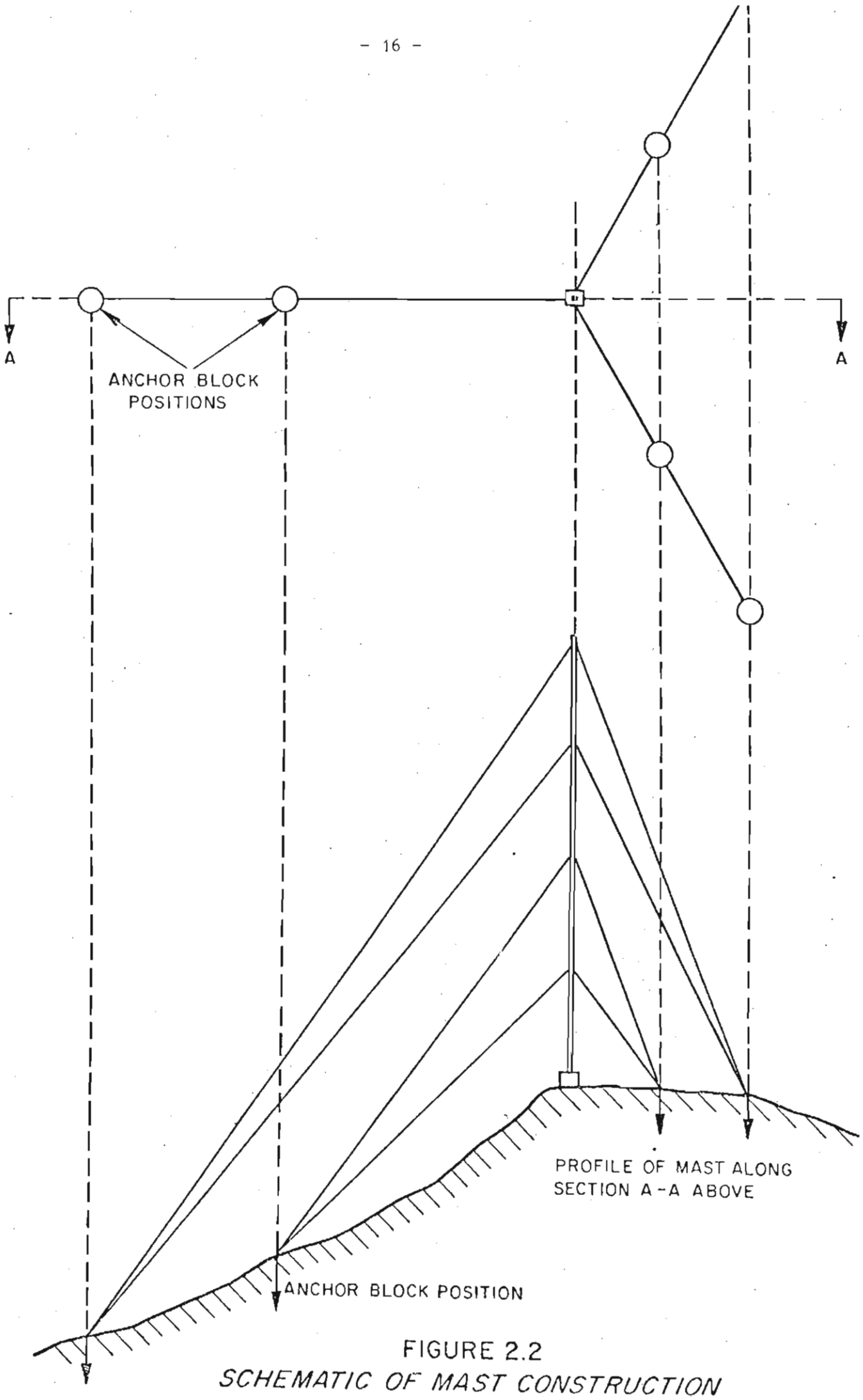

FIGURE 2.2
SCHEMATIC OF MAST CONSTRUCTION

total height of 60 m, and stayed at 15 m intervals. This height, although marginally in excess of those of many engineering structures (such as transmission line towers, which seldom exceed 50 m in height in South Africa), was still considered acceptable, since the little data available at that time suggested that the incidence of upward flashes from a structure of this height should not exceed 10%.

When used as a temporary structure during microwave route surveying, this mast was normally bolted solidly to a steel plate resting upon the ground. In the research application, however, it was considered that considerable advantage would accrue from the incorporation of an insulated base construction. This arrangement has the particular advantage of facilitating the measurement of lightning currents at the base of the mast, where equipment can be readily accessible and also obviates the problems associated with the routing of signal cables up the full length of the mast.

Accordingly, a specially modified base was designed whereby the mast was raised over two metres above the ground and supported upon an arrangement of 4 "stand-off" cap-and-pin porcelain insulators. In view of the more permanent nature of the mast installation, taken together with the comparatively weak shear-strength withstand capabilities of these insulators, this mast base was also designed to incorporate a ball pivot joint - thereby ensuring that the forces experienced by the four insulators were largely those of axial compression. Figure 2.3 depicts the concrete and steel structure which was designed to support the mast and to accommodate the insulators and ball-pivot joint.

Since the mast itself had been purchased as a proven structural design, the mast design was not further examined in any great detail, except with regard to the influences of wind-loading in determining the requisite stay pre-tensions, and in establishing the relevant loads to be provided by the stay anchor blocks. These two aspects are examined briefly in Appendix 2.A, where the relevant design parameters are indicated.

In order 18

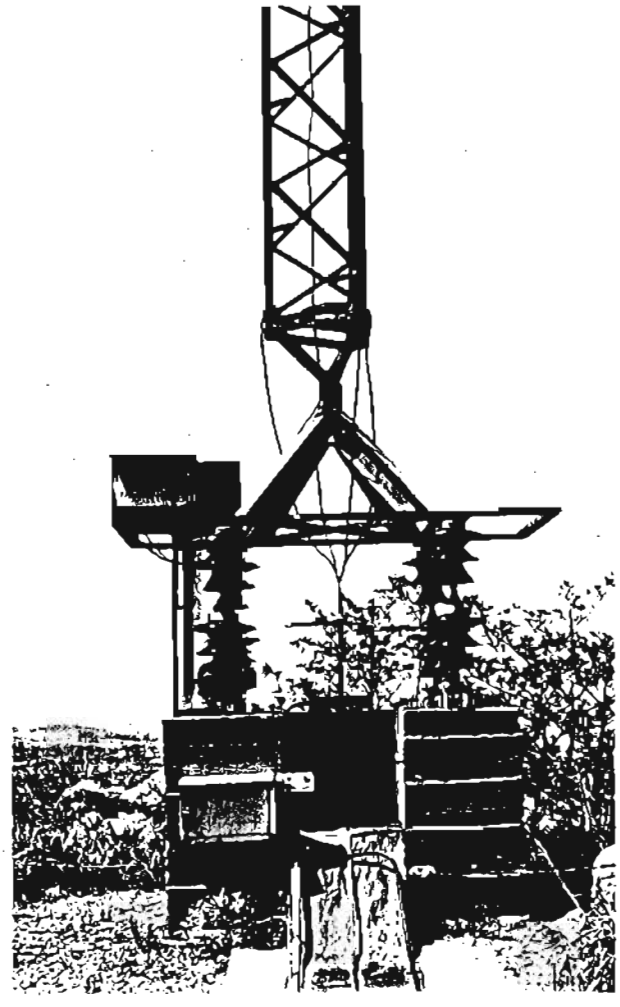

FIGURE 2.3 INSULATED BASE ARRANGEMENTS FOR THE RESEARCH MAST

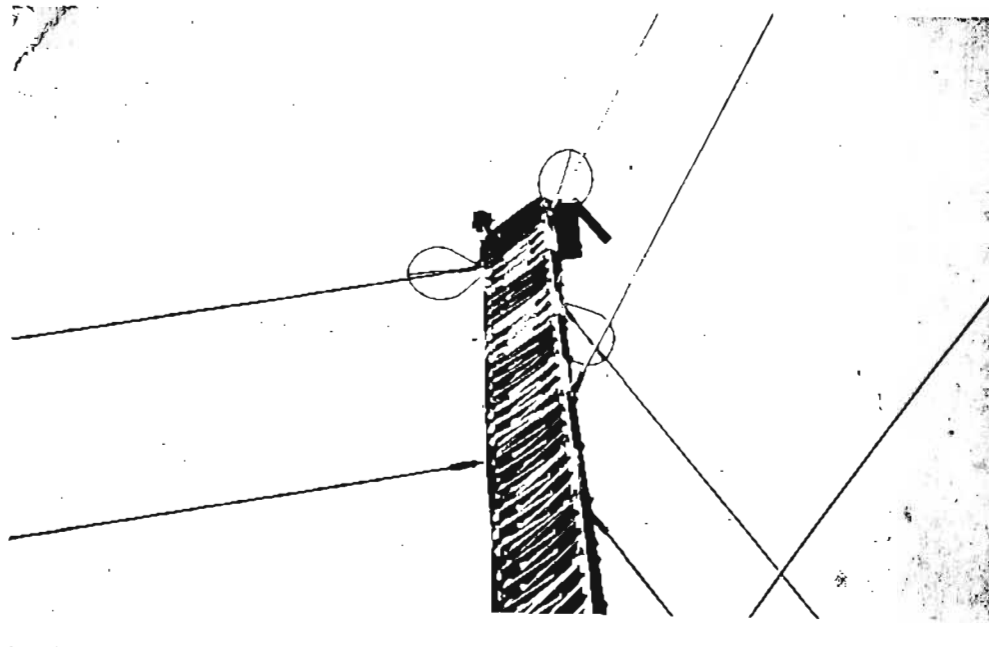

FIGURE 2.4 SHIELDING RINGS FOR THE TOP STAYS

In order to confine any lightning currents (during flashes to the mast) to the body of the mast alone - and thence into the measuring transducers in the insulated base section - the decision was taken to support the mast with fully insulating stays. This also had the advantage electrically of confining the mast geometry to a slender column - in contrast to the more complex geometry which would have ensued had conductive stays with insulating inserts been adopted instead.

Accordingly, when originally erected in 1972, the mast was supported by insulating stays consisting of a fibre-glass rod material, having a diameter of 11 mm and a rated minimum breaking load of about 34 kN. Some four months after erection, however, the top 30 m of the mast collapsed during a severe thunderstorm as a consequence of the delamination and failure of one of these insulating stays. Although similar fibre-glass rod material had successfully been used by the South African Post Office on several installations, it was concluded that this material was not acceptable for the research mast application and an alternative insulating stay material was sought.

The specifications of an imported proprietary terylene fibre rope (having an alkathene sheath for ultra-violent resistance), complied with the mast requirements and the mast was subsequently re-erected in May, 1973, with this material serving for the supporting insulating stays. (The rope-core diameter is 12 mm and the rated minimum breaking load is about 50 kN). The proprietary fittings for attachment of the rope to the mast and anchor blocks did not allow for adjustment and in order to accommodate rope stretching during service (approximately 7% at full rated load), as well as periodic adjustment of the rope tensions, the stays were finished off with 10 m lengths of stranded steel wire rope (cross-sectional area of 75 mm^2) at all the anchor block ends. This also served to protect the synthetic rope material in the possible event of veld fires.

In order also ..... /20

In order also to protect the topmost stays from possible side flash effects in the event of lightning flashes on the mast, the three top stays were attached one mast section below the top of the mast, (i.e. a distance of 2,5 m down). The terminating fittings were also shielded electrically with specially designed stress-relieving rings - as shown in Figure 2.4. (The wet 1,2/50 μs impulse voltage rating of the rope material was in excess of 200 kV/m. With the shortest of the topmost stays having a length of about 85 m, this allowed a short term potential at the mast top of approximately 18 MV (assuming linear grading for simplicity), which, in view of the short surge propagation times down the 60 m length of the mast, was considered an adequate electrical withstand capability).

In operation, the supporting stay tensions are measured regularly (and adjusted when necessary, using the wire-rope terminations), in order to ensure approximate conformity with the design pretensions - as indicated in Appendix 2.A.

2.4 Design of the earth electrode

Figure 2.5 illustrates schematically the general layout of the earth electrode arrangements provided on the research site, while a summary of the relevant design calculations is given in Appendix 2.B, in which it is seen that the calculated electrode resistance is about 1,45 Ω per 100 Ωm soil resistivity.

During the early site construction phase in August 1972, attempts were made to measure the site soil resistivity, using the Wenner method.[32] The resistivity proved to be very high and difficult to measure accurately, but was estimated at about 10 000 Ωm. The rocky nature of the terrain virtually precluded effective burial of the electrode during installation and, accordingly, some 100 m^3 of soil backfill was imported onto the site and was used to cover the electrode to a depth of about 0,5 m. It was anticipated that this backfilling might also improve the effective resistivity encountered by the buried conductors.

In view of the difficulties in obtaining a low value of electrode resistance on the mast site, an additional buried counterpoise, some 210 m in length, was run down the hill from the mast electrode and

bonded ..... /21

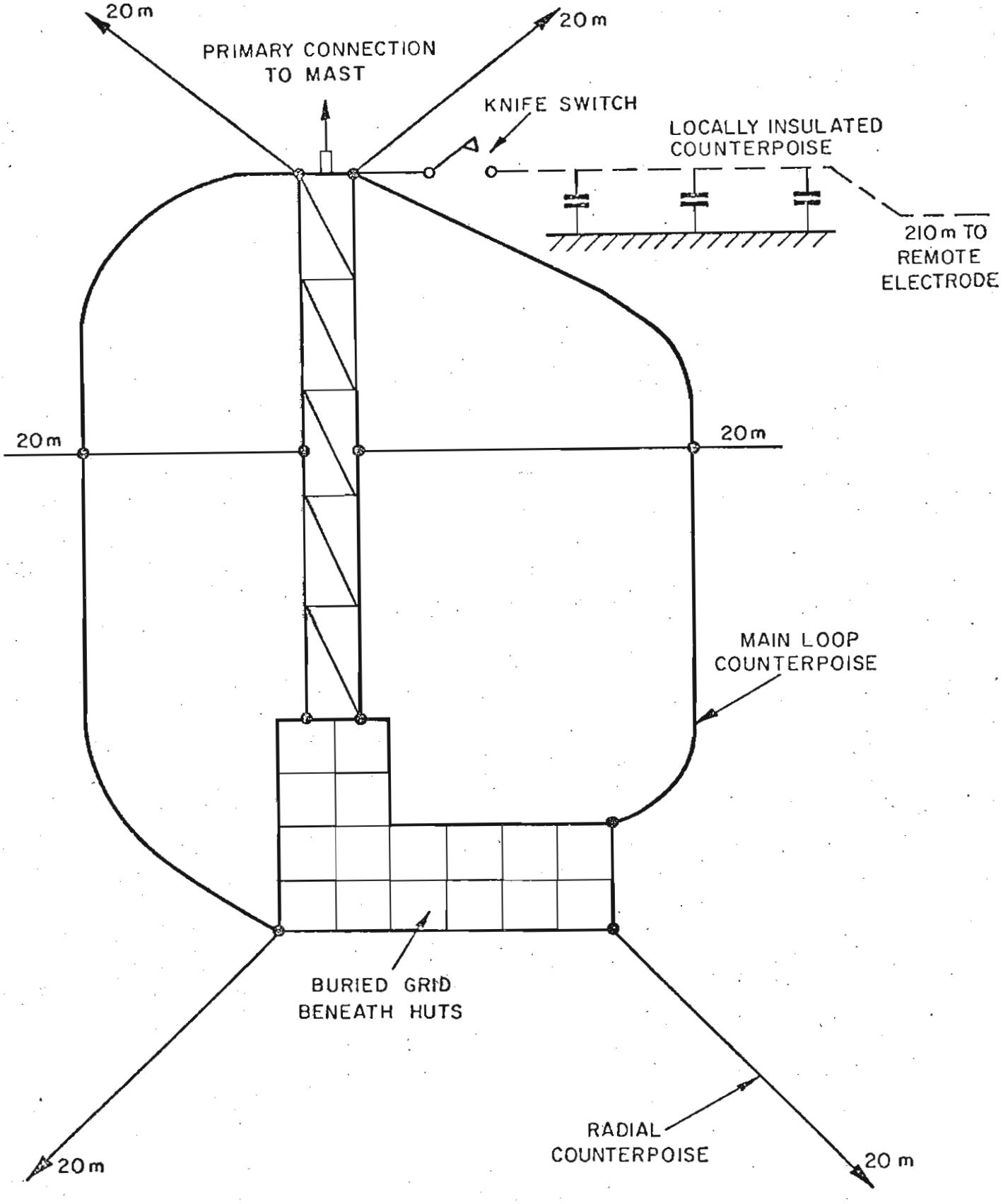

FIGURE 2.5

SCHEMATIC OF THE RESEARCH MAST EARTH ELECTRODE ARRANGEMENTS

bonded to an extensive electrode system beneath a nearby building complex. (The latter electrode had an annual average resistance of about 1 Ω). This counterpoise was supported upon insulators over the last 20 m of its approach onto the mast site in order both to facilitate independent measurement of the mast electrode resistance, as well as to allow the possibility of measuring any current flow down this conductor. The final connection to the mast electrode was achieved via a heavy duty knife-switch, as shown in Figure 2.5.

The mast electrode resistance is monitored regularly throughout the year, as illustrated by the seasonal variations over a sample 13 month period shown in Figure 2.6 (together with an indication of the accumulated rainfall over this period), which depicts an observed resistance range from about 25 Ω up to 115 Ω, with an annual average value of about 65 Ω. In terms of the calculated resistance of the electrode system, this is equivalent to an effective soil resistivity variation over the range 1 700 - 8 000 Ωm, with an average value of about 4 500 Ωm.

Recognising that it would not be economical to provide an electrode system capable of attaining acceptably low values of electrode resistance (say, less than 10 Ω), there were three primary objectives in the design of the buried electrode system:

(a) To ensure safety of personnel on the site. The loop counterpoise was provided therefore, in order to minimise surface potential gradients in the immediate vicinity of the huts and in the area between the huts and the mast. It was anticipated that this would serve to confine lightning currents to the site perimeter (and thence into the radial counterpoises) and to define an equipotential zone across the critical areas of the site.

(b) To provide a well-defined reference point for measurement and for equipment earthing and protection. The two buried grids were installed for this purpose both to define the equipotential zone in the area of measurement and to provide a high degree of capacitive coupling (i.e. a low surge impedance) for the measurement connections between the instrumentation and the reference point - which was the primary mast connection.

(c) To ..... /23

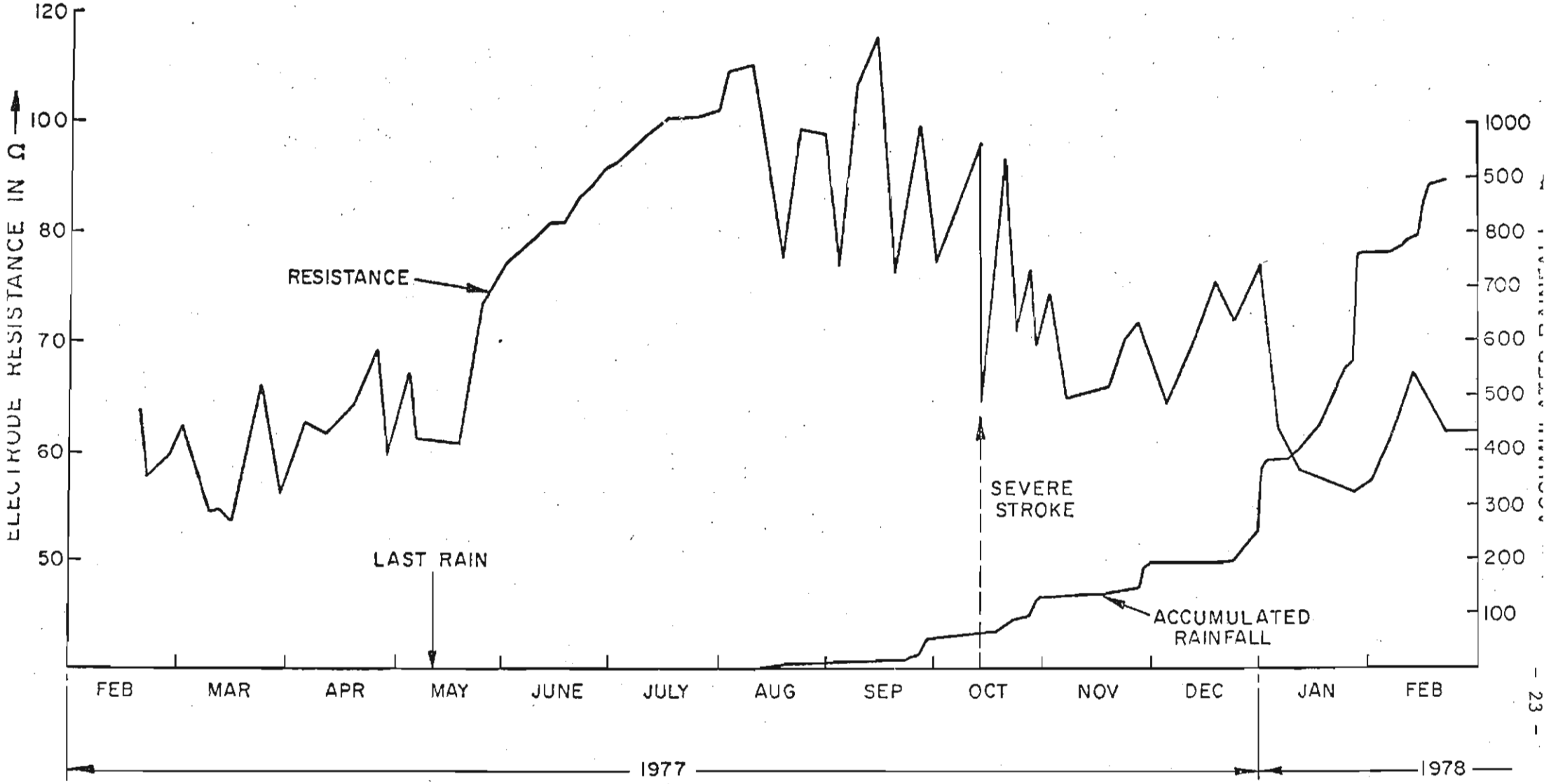

FIGURE 2.6

SEASONAL VARIATION IN TOWER EARTH ELECTRODE RESISTANCE AND THE RESPONSE TO RAINFALL

(c) To provide a well-defined and low surge impedance in the event of lightning currents entering the system.

This aspect is examined further in Appendix 2.B in which surge impedance values in the range 20 - 50 Ω are estimated. These values are still subject to possible reduction due to soil ionisation effects, as also indicated in the appendix and, by way of example, Figure 2.6 illustrates a short term reduction in electrode resistance of about 50%, which was observed after a severe stroke (87 kA). It is possible that this is attributable to local soil breakdown and to the subsequent ingress of moisture into the voids around the conductor.

2.5 Power supply considerations

The preceding analysis indicated that the mast electrode impedance could assume values in the range 20 - 120 Ω for the first 7 μs after the injection of an impulse current into the system. Since it was anticipated that the lightning discharge current waveform could display risetimes of the order of 1 - 10 μs (in the event of flashes to the mast), it was clear that substantial transient surge potentials could develop on the local earth electrode. Any ac power supply connection to the research mast site would itself be referenced to some remote earth connection (i.e. at a remote transformer neutral) and would not share this potential rise. Therefore, the possibility existed of damaging surge potentials being developed between the local mast earth electrode (and anything bonded to it) and an incoming power supply. The incorporation of surge arresters on such a supply in an effort to limit these surges would in turn allow a component of lightning current to enter such a power supply system.

Accordingly, in order to avoid such problems, the concept of an isolated incoming power supply was adopted - as shown in Figure 2.7, which outlines the general power supply arrangements on the research mast site.

The central feature is a motor-alternator combination with an isolating drive shaft. The alternator frame is bonded to the local

mast ..... /25

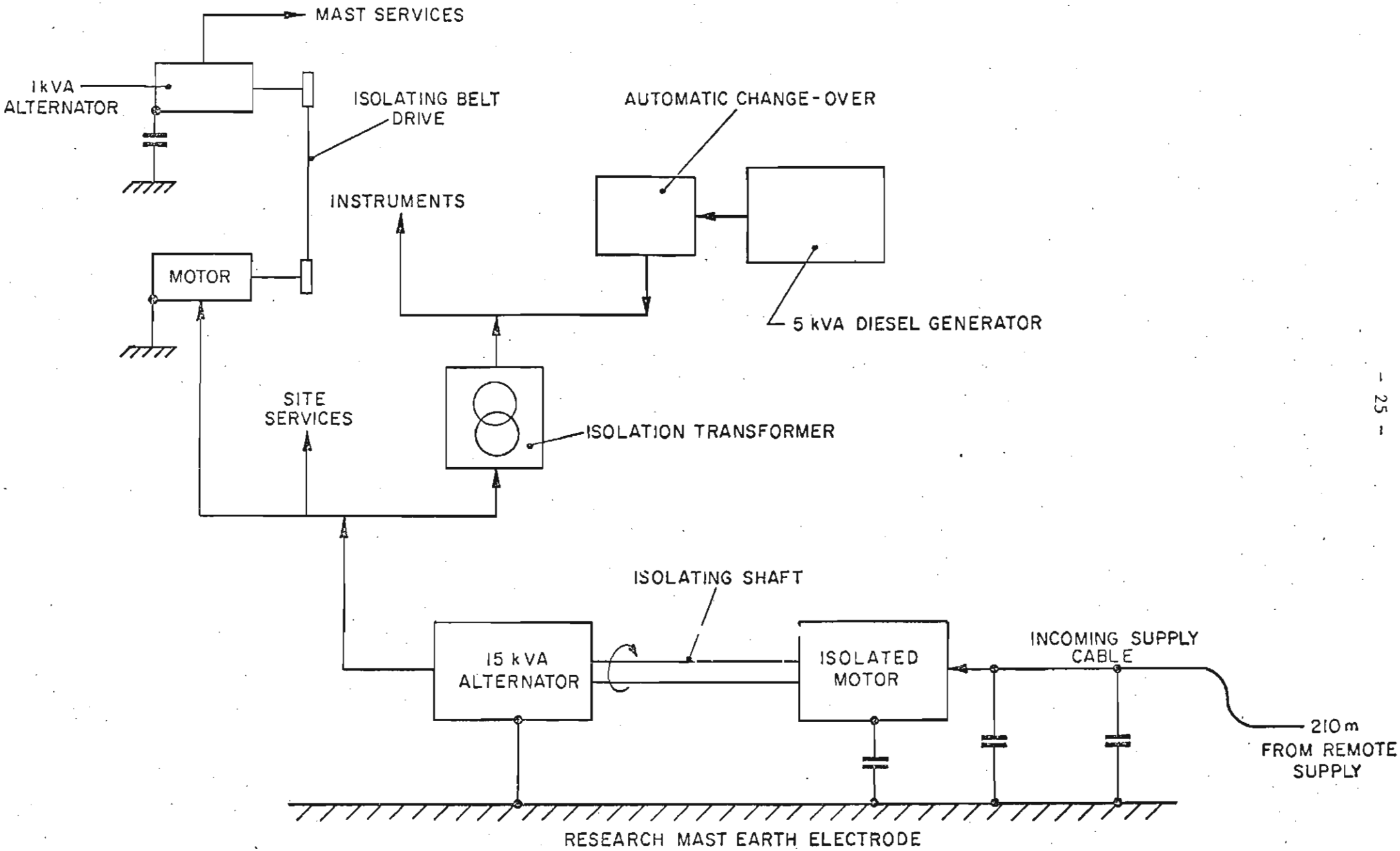

FIGURE 2.7
RESEARCH MAST POWER SUPPLY ARRANGEMENTS

mast earth electrode system, while the motor, which is supplied via a 210 m cable from a remote supply, is mounted upon an insulating frame. The incoming supply cable is also supported upon insulators for the last 50 m of its approach to the research mast site.

The isolating drive shaft is formed from a 1 100 mm length of synthetic resin bonded paper tube and minimum surface flashover stresses in the range 300 - 600 kV/m have been assumed (for both long and short wave impulses respectively). Allowing for the local air-density correction factor of about 0,83, this is equivalent to a minimum long-wave impulse sparkover of about 270 kV. In practice, as indicated in the preceding section, the earth surge potential waveform is likely to be of short duration (i.e. less than about 7 μs). A similar impulse withstand level has been adopted for both the motor and cable supply isolation.

As may be seen in Figure 2.7 therefore, all site electrical load is supplied by the local 15 kVA alternator. In order to ensure a clean supply, however, the instrumentation load is further isolated from the site services via a double wound and screened isolating transformer.

Since several lightning current measurements were missed during the earlier phases of the research program, due to power outages of the primary incoming supply during thunderstorms, a 5 kVA standby diesel generator unit was subsequently installed, together with an automatic control and changeover unit, in order to ensure continuity of supply to the most important instruments. In the event of a sustained power outage, this system restores power to the instruments within 70 seconds.

The concept of an isolated supply has also been applied to the supply of the mast services (primarily structure aircraft warning lights). This was necessary, since the mast structure was mounted upon insulators, as previously described. Accordingly, a 1 kVA motor-alternator combination was also mounted across the mast isolated base structure, and fitted with an isolating belt drive. This system has an impulse withstand level in excess of 250 kV, which is consistent with the flashover characteristics of the mast stand-off insulators.

2.6 Measurement ..... /27

2.6 Measurement technique and instrumentation arrangements

2.6.1 General

Figure 2.8 illustrates the basic arrangement of instrumentation employed for the automatic recording of lightning current waveforms and peak amplitude determination.

In principle, the system involves the use of automatic camera and high speed oscilloscope combinations - together with a special transducer, which provides a voltage analogue reproduction of the discharge current waveform during flashes to the research mast. This transducer is a proprietary unit (Pearson Electronics, Model B-1973), consisting of a specially designed impulse current transformer, and having the following specifications:

Maximum peak current	- 200 kA
Output sensititvity (± 1% over the range < 1 kA - 200 kA)	- 2,5 V/kA
Rise time - typical (10% - 90%)	- 20 ns
Frequency response (3 db points)	- 1 Hz to 10 MHz
Droop (over the range < 1 kA - 200 kA)	- 0,02% per ms
Maximum RMS current	- 1 550 A
Maximum change transfer	- 456 C
Equivalent maximum $\int I^2 dt$	- 9×10^7 A^2S
Output impedance	- 50 Ω
Voltage rating between centre conductor and case (in air - 1,2/50 µs)	- 30 kV peak

The rated maximum measuring errors of this unit are ± 1% over the current range of interest (< 1 kA - 200 kA). A series of performance tests was conducted in the High Voltage Laboratory of the South African Bureau of Standards using this unit, together with a standard impulse current shunt and a conventional impulse generator, and agreement to within 1% on peak impulse current amplitudes was demonstrated over the available range of impulse current amplitudes (i.e. up to about 60 kA).

In ..... /28

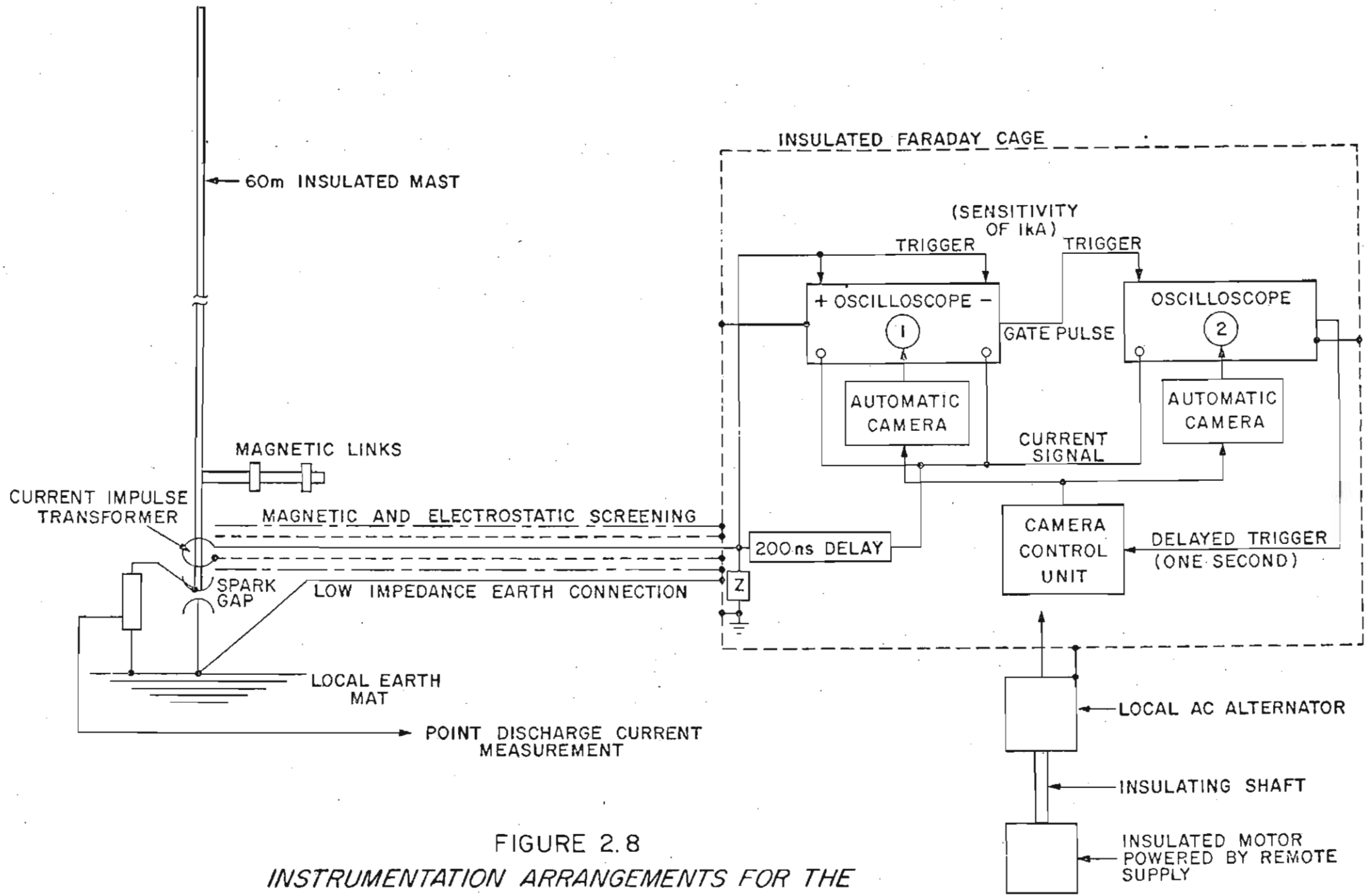

FIGURE 2.8

INSTRUMENTATION ARRANGEMENTS FOR THE MEASUREMENT OF LIGHTNING CURRENTS

In its application, a particular advantage of this impulse transformer (in contrast to more conventional impulse current shunts, such as non-inductive resistors), is that of isolation of the measurement circuit from the current carrying conductor. In the case of the research mast, the latter consists of a 25 mm diameter copper conductor, of 1 m length, which passes through the impulse current transformer and is connected to the base of the mast at one end and to the earth electrode system, via a series spark-gap, at the other end.

As shown in Figure 2.8, the series spark-gap serves to protect a parallel resistive shunt, which was used for the measurement of point discharge currents, and also provided trigger signals for the initiation of oscilloscope deflection, in the event of a lightning flash. This spark-gap was designed as a uniform field gap, having parallel plane disc-electrodes, (which also served as recording electrodes) and was designed to spark-over at 10 kV peak, which was well within the rated withstand capabilities of the impulse transformer isolation.

The oscilloscopes used for recording the discharge current waveforms were the Tektronix dual-beam type 556 (with type 1A1 dual trace preamplifiers). This combination has a signal frequency bandwidth from DC to 50 MHz, at 3 db down. When correctly calibrated (which was checked regularly throughout the course of the measurements), the resultant deflection accuracy, both vertically as well as in respect of the sweeps, is ± 3%. The automatic recording cameras (Robot-type 36E) were operated in the 'shutter normally open mode'; i.e. the shutter was only closed approximately 1 second after a trigger event, whereafter the film was advanced, and the shutter re-opened in readiness for another event.

A variety of system triggering modes was adopted at various stages in the course of the measurement programme. The most commonly used approach is depicted in Figure 2.8 and involves internal triggering of the oscilloscopes from the incoming signal. The equivalent sensitivity in this case corresponded to a current in excess of 1 kA. A 200 ns

interposing ..... / 30

interposing delay cable in the signal path allowed display of steeply rising wavefronts.

An alternative arrangement involved triggering the oscilloscopes with a signal derived from the point discharge current measuring shunt and in this case allowed the adoption of an equivalent trigger level in the current range 40 - 100 A.

2.6.2 Grounding and interference minimisation

Considerable attention was paid to the problem of electromagnetic interference in designing the instrumentation arrangements. The instrumentation hut was constructed from galvanised mild steel sheet sections (with overlapping joints), including the floor and roof - thereby serving as a medium quality screened chamber[26] i.e. providing of the order of 20 - 30 db attenuation in the interfering signal frequency band of concern (normally taken as 1 - 100 kHz for lightning), while the oscilloscopes themselves complied with the interference withstand requirements of MIL-I-6181 D.

A single point nodal grounding philosophy was adopted for the connection of the instrumentation hut to the reference earth point at the base of the mast and a low impedance strap of sheet copper (450 x 0,3 mm^2) was provided for this connection. This strap was run upon hardboard sheets in order to isolate this connection from the body of the earth and to avoid circulating currents. Both the hut foundations and the hardboard sheetings were themselves laid upon a 500 mm deep bed of clean stone ballast (substation grade) in order to ensure a reasonable isolation from the buried earth electrode.

Low impedance grounding for internal signal connections within the instrumentation hut was provided in the form of a copper strap (200 x 0,5 mm^2) mounted around the walls, which served as a 'virtual earth' plane.

Co-axial type screened cables (RG-58 c/u) were used for all signal interconnections. In addition, all signal cables leading from the mast instrumentation to the equipment in the hut, were also run through galvanised mild steel conduit

(having ..... /31

(having a wall thickness in excess of 2 mm) - thereby ensuring in excess of 30 db additional shielding effectiveness over the interfering signal band of concern.[26]

The above measures appear to have been adequate, since stable operation of electronic equipment within the instrumentation hut was experienced and at no time was any damage caused to this equipment. The resultant lightning current oscillograms were also 'clean' in character, being apparently devoid of any indications of interference.

2.6.3 Magnetic links

As a back-up measurement, in the event of site power supply failure and/or the loss of instrumentation, several magnetic links were installed in the proximity of the current path on the research mast - as shown in Figure 2.8.

This is a well-known technique of peak current measurement (having the advantage of being completely passive) and involves the determination of the degree of remanent magnetism observed in a core of high permeability material, following the passage of an impulse current. From prior calibration relations, it is subsequently possible to relate the remanent magnetism to the peak amplitude of the current - provided the distance between the current path and the link position is known.

The principles of calibration are discussed in Appendix 2.C, which includes the determination of the relation applicable to the research mast links.

Since a single magnetic link has a comparatively limited equivalent dynamic range of measurement (before saturation), special brackets were installed on the mast, which allowed the disposition of links over a wide range of distances - thereby allowing a theoretical range of current measurement extending from less than 1 kA, up to about 180 kA.

In addition, by adopting principles of redundancy and employing a minimum of six links (at various distances) in the

estimation ..... /32

estimation of a peak current from measures of the remanent magnetism, the resultant maximum errors are about ± 10%, as demonstrated in Appendix 2.C.

The incorporation of the magnetic links into the measurement arrangements has proved invaluable, especially in the early days of the programme when, on several occasions, back-up measurements of lightning peak currents were still obtained, despite the electronic instrumentation being out of action for various reasons.

2.6.4 Lightning Photography

Two parallel approaches were adopted for photographing lightning flashes in the vicinity of the research mast, viz:

(a) Still Photography

Two automatic 35 mm cameras (Robot Type -36E) were located in outdoor housings just over 2,5 km away from the research mast and viewing it from directions approximately at right angles to each other. The primary purpose of these cameras was to obtain still photographs of each flash to the mast - which could then be analysed for subsequent evaluation of flash geometry and striking distance, as discussed further in Chapter 4.

The resultant flash photographs - especially the degree and characteristics of any branching visible - also served to determine whether the flashes had involved upward or downward leader progression - as discussed later in Appendix 3.A.

Each camera was fitted with a 45 mm lens and the normal exposure aperture was f22. Black and white film (having a speed of ASA 250) was normally used, in 30 m magazines, thereby allowing photography of about 800 frames per film change.

These cameras were operated in the "shutter-normally-open" mode taking short time exposures of the sky in the immediate vicinity of the mast. The exposure periods were

controlled ..... /33

controlled by electronic timers - allowing intervals of 15 seconds, 60 seconds, or 60 minutes. The former two intervals were used during active thunderstorms, (with the choice being determined by the time of day, or ambient illumination), while the latter long interval was found useful at the ends of thunderstorms, or during overnight periods of weak or intermittent activity.

The common field of view of the two cameras was centred on the research mast, and covered an effective ground area of about 2 km^2. Each camera was operated independently (i.e. asynchronously), thereby minimising the chance of a co-incident "dead" period during the automatic film advance at the end of each exposure interval. In fact, this advance period was less than 500 ms and therefore, at the most common exposure interval of 60 seconds, the possibility of both camera shutters being closed at the time of an external event such as a flash to the mast, was less than 1%.

(b) Television video recordings

Closed circuit television video recording techniques have successfully been used for lightning photography by several other workers in the field[33] and have the particular advantage that they allow effective daylight photography - compared to still camera techniques, which require short time exposure intervals or specialised filtering approaches in order to avoid film-fogging problems during high ambient light conditions. An additional advantage of such a video recording system is that the comparatively high framing rate of 50 frames per second provides a good degree of temporal resolution - thereby permitting discrimination of multiple stroke flashes - as discussed further in Chapter 5.

Accordingly, in order to supplement the two still cameras referred to previously, a CCTV video recording system was established toward the end of 1975 at a point

about ..... /34

about 1 km away from the research mast. The TV camera purchased for this purpose has a silicon diode type video tube, which has the capability - as noted for example, by Winn et al[33] - of recording very short duration luminous events. This is a prerequisite for lightning recordings, since many individual stroke durations are only of the order of 100 - 500 μs. Although the individual frame period of the recording system is 20 ms, using a camera tube of this type allows successful recording of such transient events. The silicon diode vidicon also has an enhanced luminous sensitivity which extends into the red spectral regime and is inherently burn proof: both features are attractive for lightning work, since the first allows photography of low illuminosity events such as leaders, and the second prevents damage in the event of nearby bright return strokes.

When played back at normal speed (50 frames per second with a standard 2 : 1 interlace) the overall video recording system had a line resolution of about 300 lines (midscreen) and a total recording time of 65 minutes.

The TV camera was normally focussed upon the research mast and the recording system was operated routinely whenever lightning activity was present in the immediate vicinity.

Examples of flashes recorded successively using this system are illustrated in Appendix 3.A.

2.7 Operation and Remote Control

A feature of lightning research work is the comparatively unpredictable nature of thunderstorms - in respect of their characteristics, as well as in the incidence of ground flashes, in both space and time.

Throughout the development and establishment of the various instrumentation systems employed in this research programme, considerable attention was therefore devoted to achieving reliable and long term automatic operation.

For ..... /35

For certain systems, such as the recording oscilloscopes for obtaining the discharge current waveforms, it was possible (and preferred) to allow continuous operation for the full duration of a thunderstorm season - subject to periodic functional and calibration checks. In other instances, however, due either to the high number of trigger events (on the remote still cameras), and/or to a limited recording capacity (such as the CCTV system, which allowed only 65 minutes), it was necessary to operate these systems selectively whenever lightning activity was in the immediate vicinity of the mast, or was judged to be imminent (i.e. when an active storm appeared to be approaching the mast).

Since many of these recording systems were positioned at different locations and situated several kilometers apart, it was necessary therefore to establish an effective remote control system which would allow selective operation of the relevant items of equipment.

This was achieved with the commission of a VHF radio switching system toward the end of 1975. This comprised a tone-coded system (operating at 152,8 MHz) and involved a central "base-station" transmitter unit, together with switching receivers at each remote location. The tone-coding system allowed the use of unique addresses at each of the receiver stations - as well as control of up to 4 direct functions at each of these points - thereby providing the requisite selectivity and discrimination.

This system proved to be very effective and led to a significant overall improvement in recording success rate - as shown in the general review of results presented in the following three chapters.

CHAPTER 3

DIRECT MEASUREMENT OF LIGHTNING FLASHES TO THE RESEARCH MAST AND RESULTS

3.1 Introduction

The instrumentation arrangements adopted for the study of discharge characteristics during direct flashes to the research mast have been discussed in the preceding section, and this chapter therefore is concerned with a review of the results obtained during the first seven years of operation of the research station.

Although erection of the mast was completed in September 1972, establishment and attainment of satisfactory operation of the remainder of the station, and associated instrumentation, took place over an extended period of time, as outlined schematically in Figure 3.1, which summarises the research mast history. As indicated in this figure, the major items were in operation by early 1974, but additional systems, such as the CCTV and VHF radio control systems, were only introduced in late 1975. As mentioned earlier, the loss of data on several occasions when direct flashes co-incided with power supply outages, also led to the incorporation of an automatic standby power supply unit, and this was commissioned at the commencement of the 1976/77 lightning season.

The problems and consequent experience gained in the earlier years of operation led to various modifications in instrumentation and to an improved success rate as far as measured flashes was concerned. It is ironic therefore, as shown in Figure 3.1, that the incidence of direct flashes to the mast has remained consistently low over recent years (1975 - 1978), compared to that observed over the first three years (1972 - 1975). Of the 28 flash events recorded on the research mast through the whole seven year period of analysis, over 60% occurred before January 1975 and the majority of these took place before fully reliable instrumentation operation was achieved.

Despite these drawbacks, sufficient flashes have occurred since 1975 to allow thorough testing of the instrumentation techniques and to provide preliminary data regarding the major parameters of the ground flash.

2. Flash ..... /37

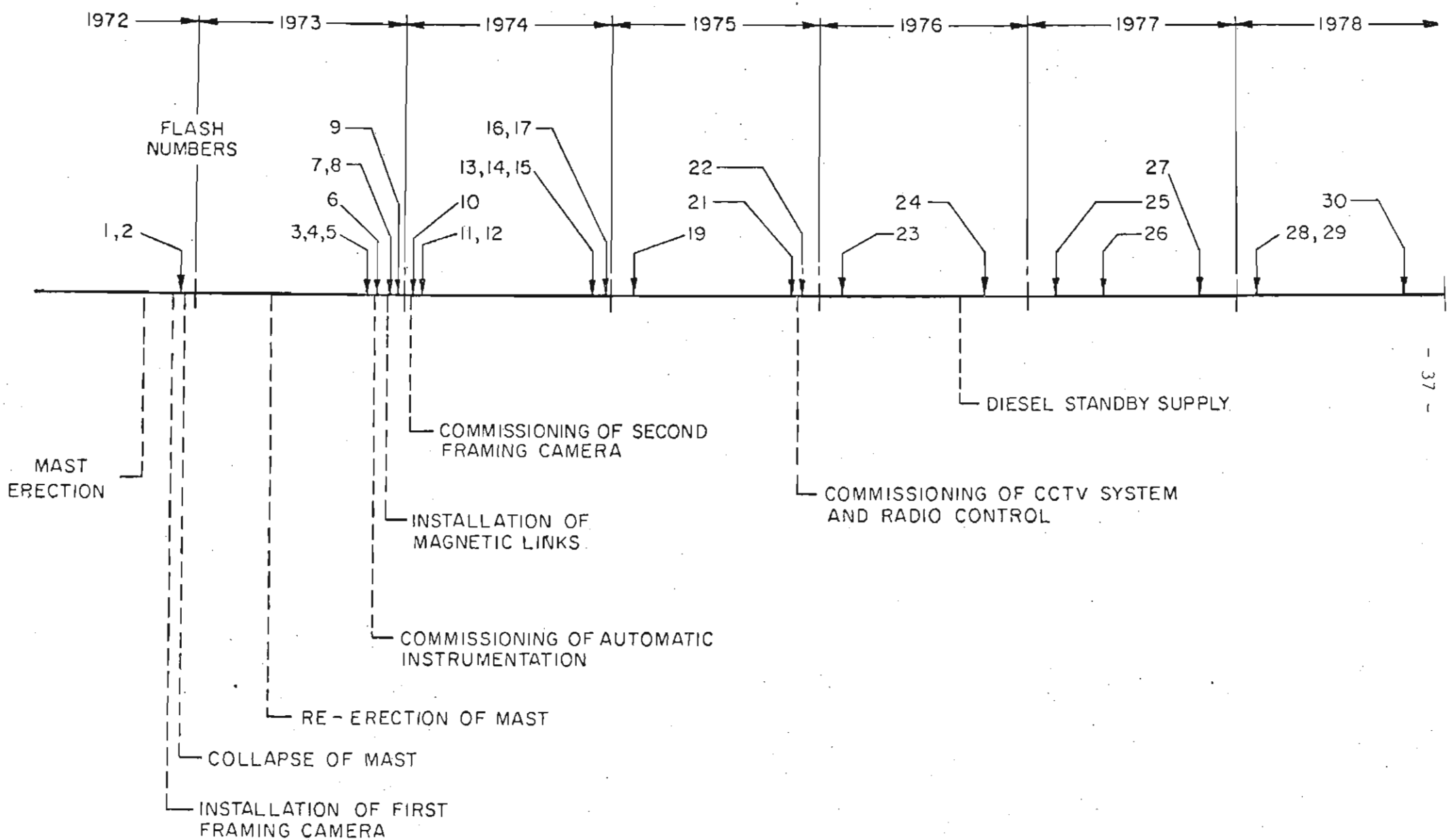

FIGURE 3.1

SUMMARY OF RESEARCH MAST HISTORY

3.2 Flash incidence

As already mentioned, Figure 3.1 depicts a schematic history of the research mast and illustrates the sequence of direct flashes recorded over the past seven years. Table 3.1 gives a summary of the more important characteristics of the recorded flashes (such as direction of progression and discharge polarity), and indicates also what measurements were achieved on each occasion. (The improving measurement success rate is also evident in this table.)

Appendix 3A analyses the circumstances surrounding the occurrence of each flash event and reviews briefly the instrumentation in operation on each occasion, as well as the resultant data. The available flash photographs and associated discharge current oscillograms for each flash are also presented in this Appendix, together with a summary of the relevant waveform parameters and remarks concerning the direction of progression, polarity, storm intensity etc. The results presented in this chapter have therefore been extracted and summarised from the individual flash analyses contained in Appendix 3A.

Figure 3.2 summarises the seasonal incidence of flashes to the mast. Although probably only an artefact arising out of the paucity of records, it is interesting to observe that 9 of the 28 recorded flashes have occurred in the month of November, while the remainder of the flashes are spread approximately uniformly over the period, late September - late February. (The monthly data in Figure 5.14 in Chapter 5 indicates that the maximum monthly storm activity in the region is normally experienced between November and January.)

An analysis of the times of flash occurrence presented in Appendix 3A leads to the summarised diurnal incidence shown in Figure 3.3. This indicates the possibility of there being two times of most favourable probability of flash occurrence - namely, around 03 h 00 in the morning, and 17 h 00 in the afternoon. The latter observation in particular, is consistent with the data given in Chapter 5 for general diurnal incidence in the Pretoria area, (Figure 5.10), where it is shown that the majority of thunderstorms in this region occur in the period between about 15 h 00 and 19 h 00.

Reviewing the available data on dates and times of flash occurrence, a tentative conclusion is that the maximum probability for a flash to the research mast, in any given year, could prevail over the last week of November, with the most favourable time of day being around 17 h 00.

TABLE 3.1: SUMMARY OF LIGHTNING FLASHES ON THE RESEARCH MAST

Number	Direction					Photograph.	Measurements		Polarity
	↓	↓?	?	↑	↑?		Mag. Link.	Oscillog.	
721129/1		X				L	–	–	–ve
721129/2	X					L	X	–	–ve
730929/3			X			–	–	–	?
730929/4	X					–	–	–	?
730929/5			X			–	–	–	?
731015/6	X					L	–	–	?
731126/7			X			–	–	–	–ve
731126/8		X				–	X	–	–ve
731216/9	X					L	X	X	–ve
740104/10	X					L + M	X	X	–ve
740118/11		X				–	–	X	–ve
740118/12		X				–	X	X	–ve
741129/13					X	L	–	–	–ve
741129/14					X	L	–	–	+ve?
741129/15				X		L	–	–	+ve?
741224/16	X					M	X	X	–ve
741225/17			X			–	–	–	?
750227/19	X					L + M	X	–	–ve
751102/21	X					L	X	X	–ve
751114/22				X		L + M + TV	X	X	–ve
760207/23		X				–	X	X	–ve
760928/24					X	L	X	–	?
770222/25		X				L	X	X	–ve
770507/26					X	–	X	–	?
771009/27	X					L + M + TV	X	X	–ve
780128/28					X	L + M + TV	X	–	?
780128/29	X					L + M + TV	X	X	–ve
781018/30				X		L + M	X	–	?
TOTALS	10	6	4	3	5	18*	17	11	

*Photographed by at least one system.

(L = Lynnwood Glen camera)

(M = Murrayfield camera)

Key: ↓ Downward flash

↓? Presumed downward

? Unknown direction

↑ Upward flash

↑? Presumed upward

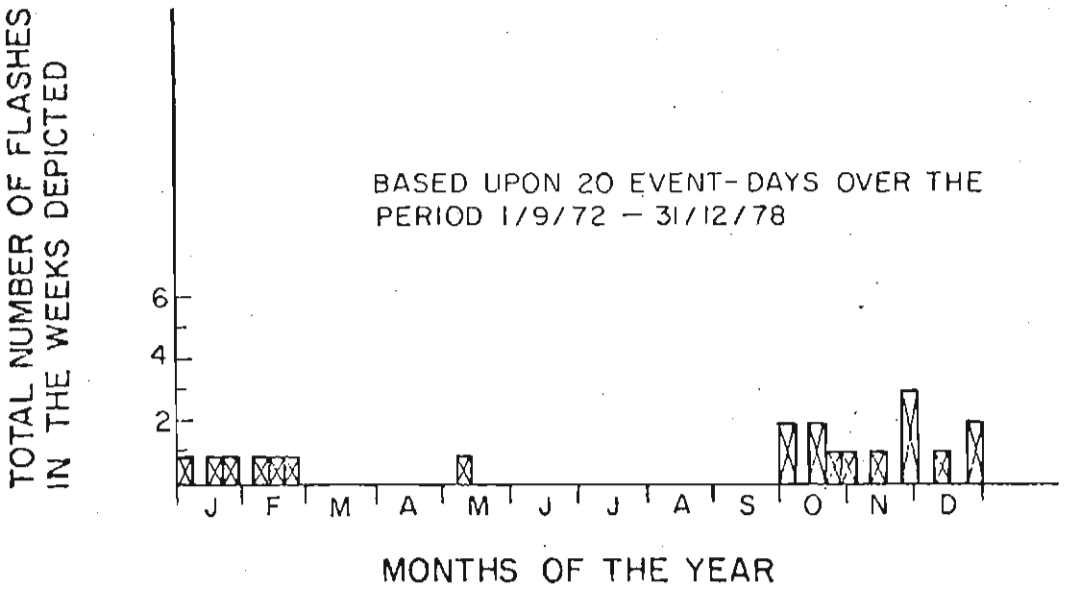

FIGURE 3.2

SEASONAL INCIDENCE OF FLASHES ON THE RESEARCH MAST

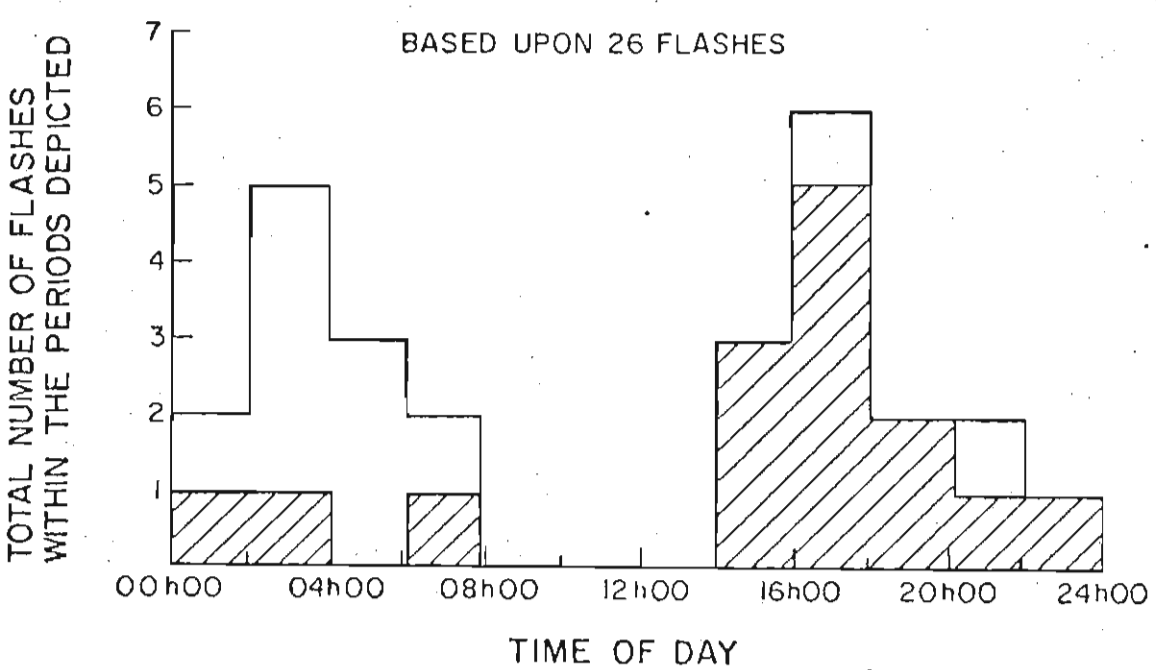

FIGURE 3.3

DIURNAL INCIDENCE OF FLASHES ON THE RESEARCH MAST

3.3. Results and discussion

As seen in Table 3.1, magnetic link measurements were carried out on 17 flashes, while oscillographic records were available from 11 of these. Taking account of 4 upward events which delivered discharge currents having amplitudes less than the measurement sensitivities, (as discussed in Appendix 3A), meaningful data were only obtained from measurements on some 13 flashes. The individual flash and stroke waveform parameters are presented in Appendix 3A and are summarised collectively in Table 3.2.

The following waveform parameters were determined from the recorded current oscillograms:

$\hat{I}$ – maximum peak current amplitude.
(determined either from the magnetic link or oscillographic records)

Q – impulse charge. (The oscilloscope sweep speeds were not slow enough in any instances to record continuing currents.)

$\frac{dI}{dt}$ – maximum rate of rise of current measured on the wavefront. Although the initial "toe" of the wavefront was missed on some occasions, (due to the adoption of comparatively high trigger settings), this did not prevent the measurement of $\frac{dI}{dt}$, since the maximum rate of rise of current on the wavefront usually occurred between about 50% and 90% of the crest amplitude.

$\int I^2 dt$ As in the case of impulse charge Q, this parameter was determined for the impulsive components of the current oscillograms only.

No attempts were made to determine either the wavefront or wavetail times. The latter is of relatively low importance in practical engineering applications, while the former could not be determined in many instances, due to the absence of the wave toe on the oscillograms. In practice, the maximum rate of rise of current is considered to be of more significance than the wavefront time.[20]

The results obtained for each of the above recorded parameters will now be discussed individually.

Table 3.2 ...../42

TABLE 3.2: SUMMARY OF MEASURED WAVEFORM PARAMETERS

Event	F/S	$\hat{I}$ (kA)	Q (C)	dI/dt (kA/ s)	I^2dt (A^2S)	Direction of Progression
721129/1	F	-35	-	-	-	↓
731126/7	F	-73	-	-	-	↓?
731216/9	F	-10	> 1,6	-	> $1,2x10^4$	↓
740104/10/1	F	-41	> 2	-	> $3x10^4$	↓
/10/2	S	> -12	-	-	-	-
/10/3	S	> -4	-	-	-	-
740118/11	F	-50	6,5	> 11,0	$3,2x10^5$	↓?
/12/1	F	-58	12,4	> 4,0	$7,2x10^5$	↓?
/12/2	S	-55	10,4	> 5,0	$5,7x10^5$	-
/12/3	S	-22	5,8	> 7,0	$1,3x10^5$	-
741224/16	F	-53	1,5	> 8,0	$3,7x10^4$	↓
750227/19	F	-26	-	-	-	↓
751102/21	F	-19	0,8	24	$8,4x10^3$	↓
751114/22/1	F	-10	0,9	3,1	$7,3x10^3$	↑
/22/2	S	-16	0,9	22	$9,0x10^3$	-
/22/3	S	-15	0,8	29	$7,0x10^3$	-
760207/23	F	> -100	> 9	> 12	> $9x10^5$	↓?
770222/25/1	F	-83	> 3	20	> $2x10^5$	↓
/25/2	S	-82	> 2	170	> $1x10^5$	-
/25/3	S	-13	> 0,3	27	> $2x10^4$	-
771009/27	F	-87	15	12	$6,8x10^5$	↓

Key: F - first stroke, or flash, value
S - subsequent stroke value
↓ - downward flash
↓? - presumed downward
↑ - upward flash

3.3.1 Peak current amplitude ($\hat{I}$)

As noted earlier, this parameter is of fundamental significance in practical applications, with the data of prime importance being those derived from negative downward flash measurements. Table 3.2 records 12 flashes of the latter type and these therefore comprise the available data sample for analysis.

The resultant cumulative frequency distribution of peak current amplitudes for these flashes is given in Figure 3.4, together with 90% confidence limits which depict a possible spread in the magnitudes of these data in excess of ±30 kA. It is common practice to approximate such cumulative frequency distributions by the log-normal distribution[10]. This has been applied to this data sample, and yields the following values:

$$\bar{I} = 44 \text{ kA}$$

$$\sigma_{\log \hat{I}} = 0{,}30$$

A number of workers have derived similar lightning peak current amplitude distributions from various measurements - as discussed in the recent critical review by Golde[30]. Most such distributions have been approximated by the log-normal form and a comparison of representative results is shown in Table 3.3.[46]

In considering the preliminary results of the research mast study against the perspective of the distributions shown in Table 3.3, several points regarding the latter should be noted:

(i) Those distributions derived from magnetic link measurements on transmission lines (such as those of Popolansky[10], or Anderson[43], or the original AIEE study[44]), are subject to possible inaccuracies regarding the interpretation of the currents recorded in individual towers, or in the separate legs of towers - as discussed, for example by Golde[30]. In fact, this largely prompted Anderson J. to a re-analysis of the original AIEE data and to the subsequent derivation of a considerably higher median value of current, as shown in Table 3.3.

Table 3.3 ..... / 44

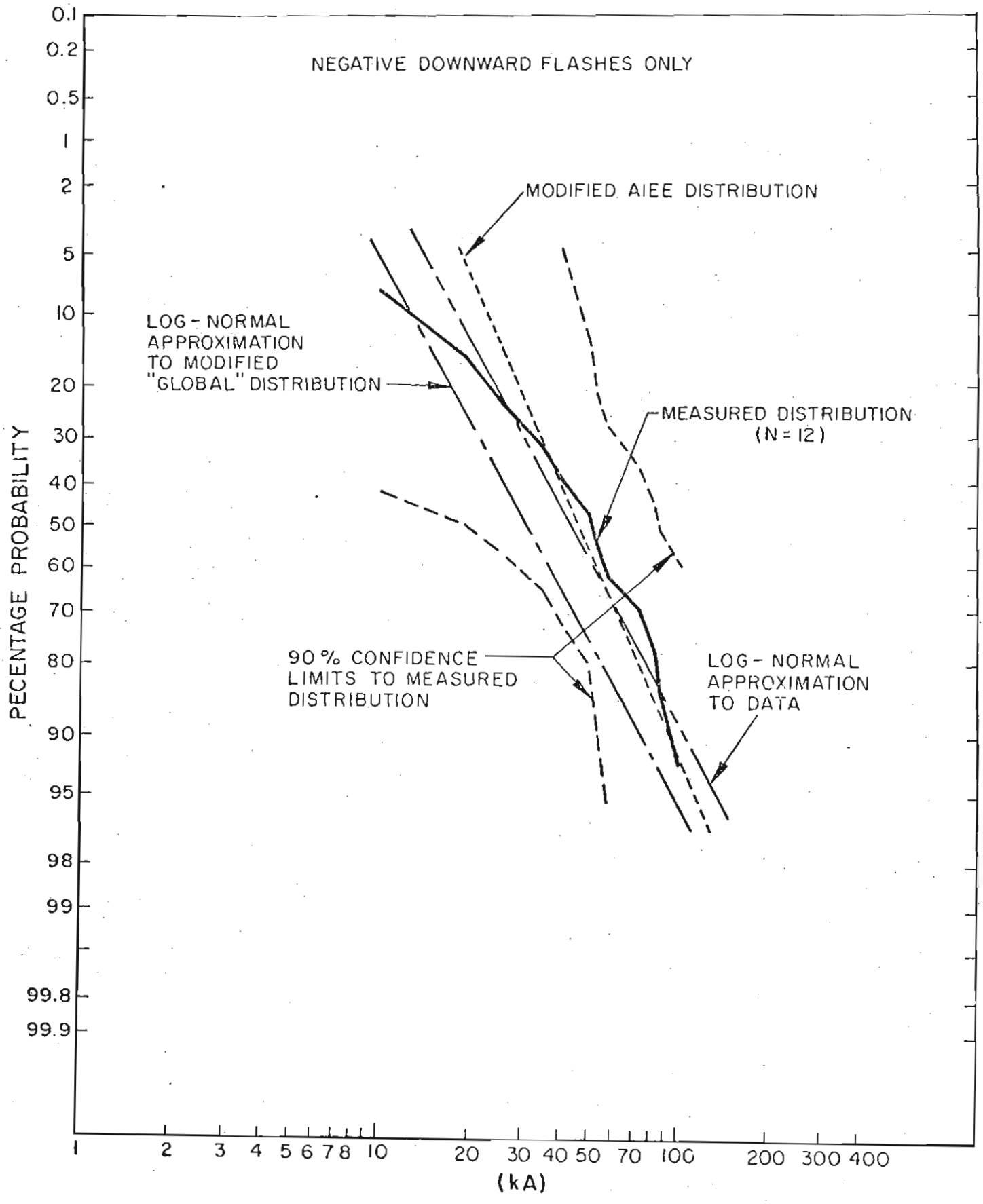

FIGURE 3.4

CUMULATIVE FREQUENCY DISTRIBUTION OF PEAK CURRENT AMPLITUDES

TABLE 3.3: COMPARISON OF PEAK-CURRENT AMPLITUDE DISTRIBUTIONS

Source	Log-normal approximation		Remarks
	Median $(\hat{I})$ - kA	Standard Deviation ($\sigma_{\log I}$)	
AIEE[44] (USA):- lines	15	0,43	"Reference" distribution for performance studies
Berger et al[18]:- masts on San Salvatore (Switzerland)	30	0,26	Negative downward first strokes
Popolansky[45]:- lines (Czech)	31	0,25	
Popolansky[10]:- (combined data)	28	0,39	"Global" distribution from many sources and structures
Anderson, J.[43]:- lines (USA)	46	0,24	Re-analysis of AIEE data
Anderson, R.[15]:- lines (Rhodesia)	40	0,33	
Sargent[17]	13	0,32	Proposed reference distribution for level ground
Anderson and Eriksson[20]	31	0,30	Modified "global" distribution

(ii) ..... /46

(ii) Sargent's reference distribution to level ground [17] has been derived from application of electrogeometric concepts to Berger's measurements, but, as pointed out by the author[16], application of these concepts is generally inconsistent with the observed effects of tall structures on flash incidence. In this case also, it is considered that Sargent assigned an incorrect value of effective height to Berger's measurement station[16].

(iii) Arising out of a consideration of the effects of tall structures, the author has separately re-examined the data comprising Popolansky's "global" distribution[20], to arrive at a modified sample consisting only of negative downward flash measurements, as well as currents recorded on structures of height less than 60 m. The author considers that the resultant modified distribution is the most representative available of the characteristics of negative downward flashes in practical engineering situations.

On the above basis therefore, (and bearing in mind the wide confidence limits applicable to the measured distribution), the preliminary research mast data is generally consistent with the trends of both the modified global, as well as the AIEE, distributions - as shown in Figure 3.4, which includes both the latter distributions.

The measured data suggest the possibility of marginally higher amplitude currents being recorded in South Africa, but the data sample is considered too small to allow meaningful conclusions to be drawn in this regard.

Comparatively few subsequent stroke measurements were obtained in the period between 1972 - 1978 - a total of 19 strokes being recorded from 11 flashes.

In general, these preliminary data are consistent with the results of other multiple stroke current oscillographic measurements, such as those of Berger[18], in that the subsequent stroke peak amplitudes of downward flashes were always less than the first stroke amplitude. The data given in Table 3.2 indicate that the ratio of subsequent stroke/first stroke amplitudes varied from about 0,10 to 0,98, with a mean value of 0,48 - which compares well with the mean value of 0,5 recorded by Berger.

Taking ..... /47

Taking all measured subsequent stroke amplitudes into account, a median value of 19 kA is obtained - which is marginally higher than Berger's value of 12 kA - but again, the present data sample is too small to allow meaningful comparisons.

Figure 3.5 depicts the relationship (or lack thereof) between first and subsequent stroke amplitudes - as determined from the data summarised in Table 3.2 - and no correlation is apparent, which is again consistent with the results from Berger's more comprehensive sample of data.

3.3.2 Impulse charge (Q)

Table 3.2 summarises a total of 16 individual stroke evaluations of impulse charge Q. A median value of 2,5 C was obtained, which may be compared with the values recorded by Berger of 5,2 C and 1,4 C, for first and subsequent stroke data respectively. (The present data sample was considered too small to justify study of the distinctions between first and subsequent stroke distributions.)

The relationship between peak current and impulse charge is shown in Figure 3.6, and although considerable scatter is evident, a measure of correlation is suggested. (In fact, regression using a relationship of the form

$$Q = aI^b$$

yields a coefficient of determination $r^2 = 0,52$, which is just significan at the 95% confidence level in this sample size.)

Berger observed a significant correlation between peak current and impulse charge in his sample[14] and the resultant relationship is shown in Figure 3.6 (for all strokes), together with the trend determined through the research mast data (assuming a relation of the form $Q = aI^b$).

This comparison indicates that the research mast values of impulse charge are generally considerably lower than the magnitudes recorded by Berger. However, as noted earlier, apart from the small sample, the oscilloscope timebases adopted in the present study were frequently shorter than those used by Berger, and in several instances it is clear that the full impulsive component of the wave was not recorded - especially in the case of first stroke waveforms - as shown for example, by the oscillograms recorded for Flash 770222/25, given in Appendix 3A. (Figure 3A-14).

3.3.3 ..... /48

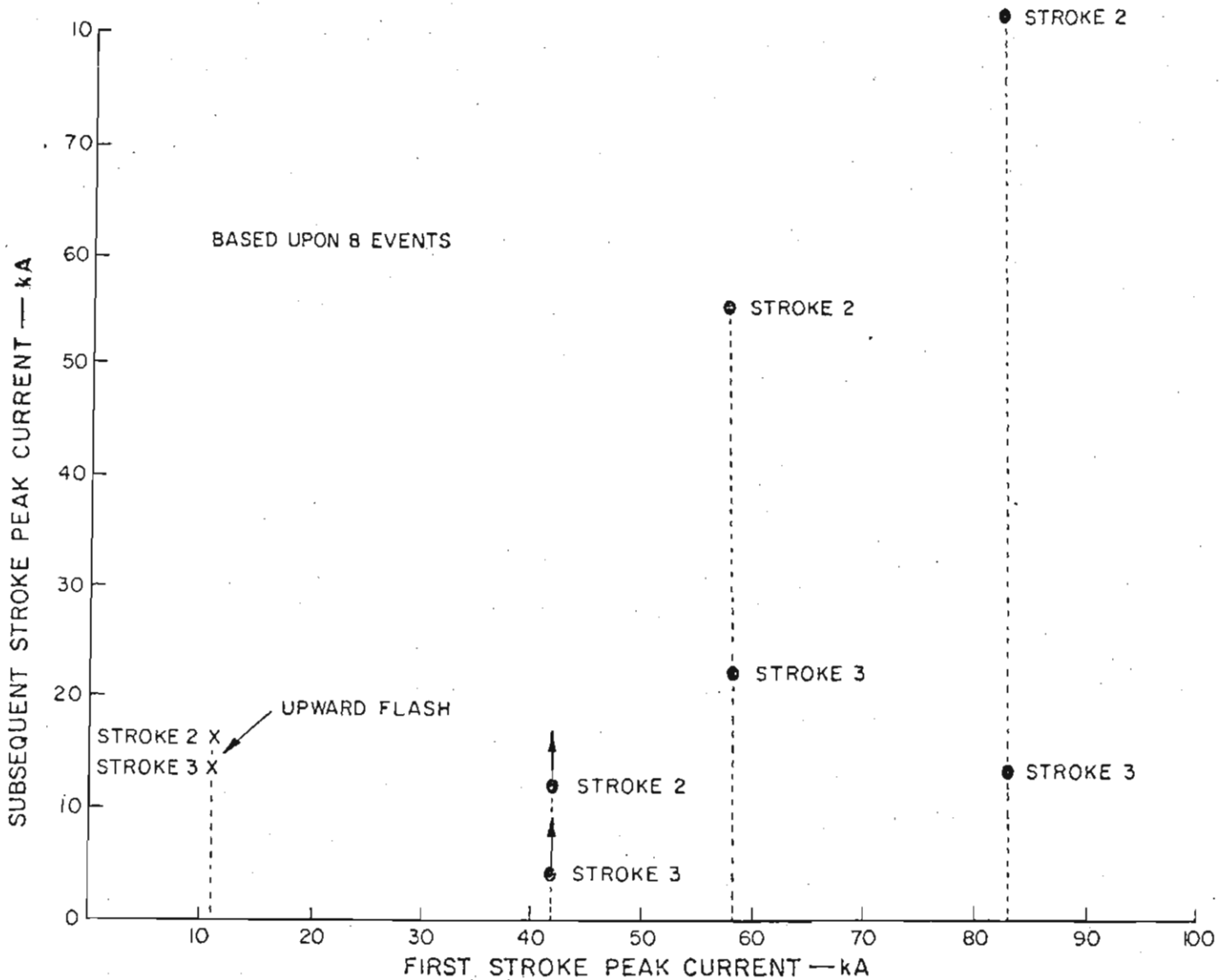

FIGURE 3.5

LACK OF CORRELATION BETWEEN FIRST AND SUBSEQUENT STROKE PEAK CURRENTS

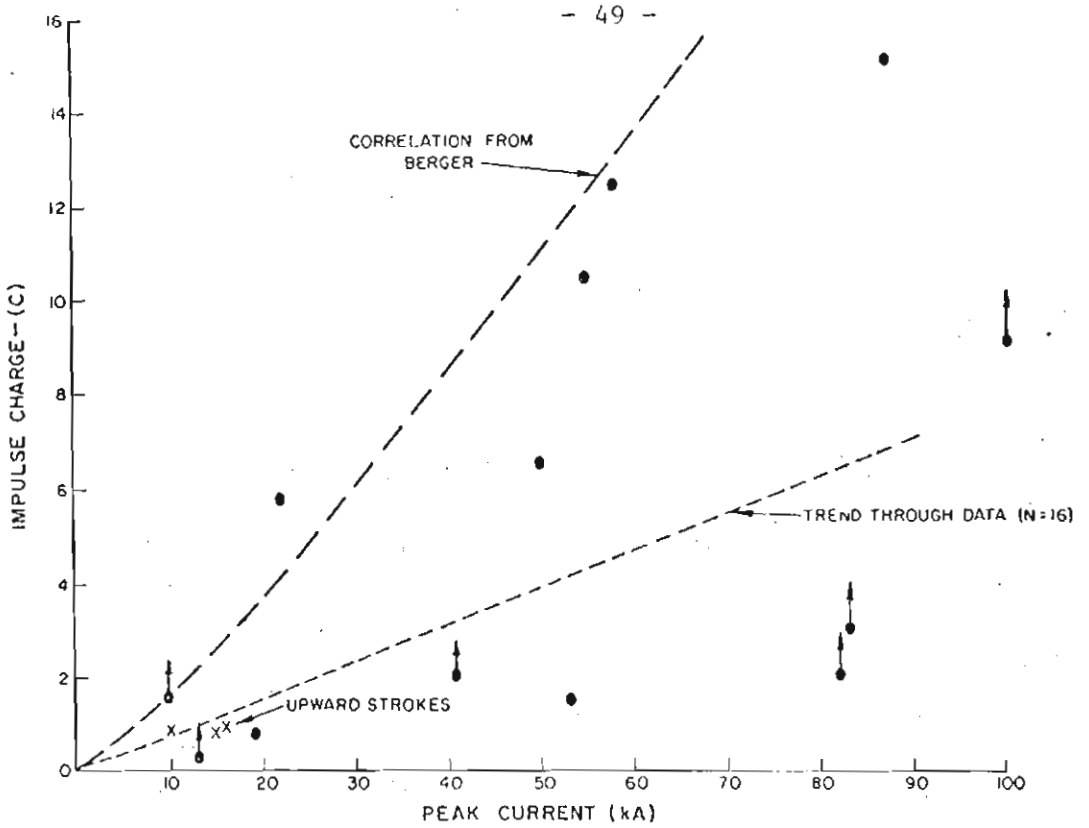

FIGURE 3.6

CORRELATION BETWEEN IMPULSE CHARGE AND PEAK CURRENT - ALL STROKES

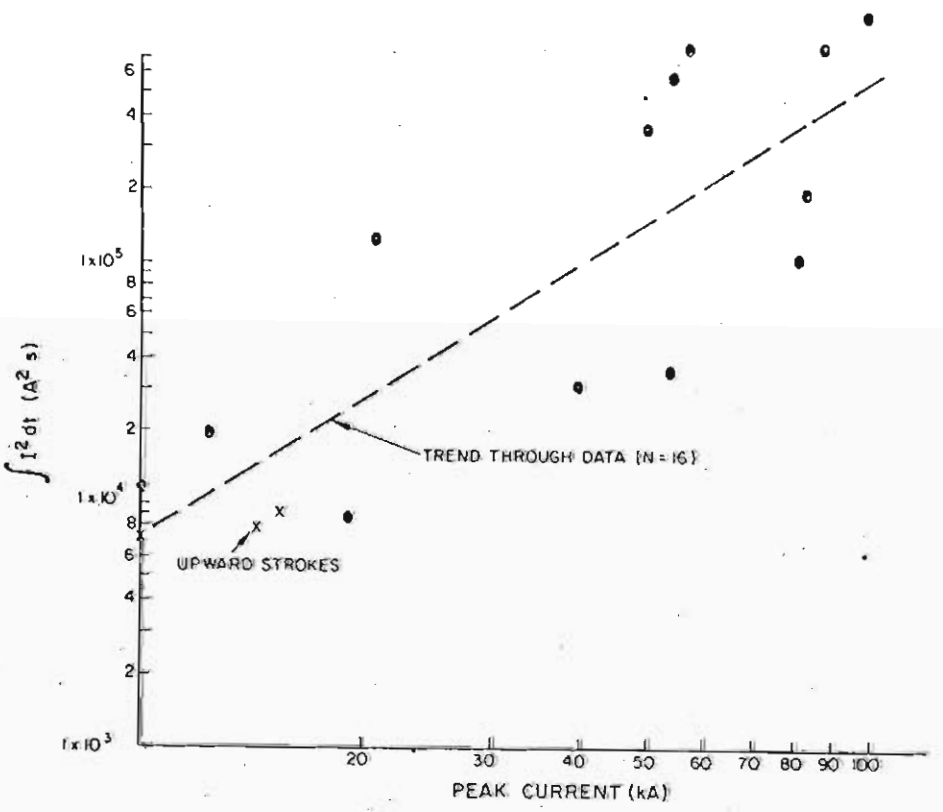

FIGURE 3.7

CORRELATION BETWEEN ACTION INTEGRAL AND PEAK CURRENT - ALL STROKES

3.3.3 Maximum rate of rise of current $(\frac{dI}{dt})$

The available data are shown in Table 3.2 and comprises a sample of 8 first stroke and 6 subsequent stroke estimations of maximum $\frac{dI}{dt}$.

Comprehensive analyses of the wavefront characteristics of first and subsequent stroke discharge waveforms have been carried out by Berger et al[18] and more recently by Anderson and the author[20]. As noted earlier, the most distinguishing feature between first and subsequent stroke wavefronts is the concave form displayed during first strokes. While it is not yet known whether this is characteristic of discharges to tall structures only, the research mast data is generally consistent with Berger's data (which was obtained from a much taller structure), in that the concave form is clearly seen on first strokes, while subsequent strokes display a much faster rate-of rise of current - as shown for example by the oscillograms obtained during Flash 770222. (Figure 3A-14). The maximum dI/dt observed during stroke 2 of this flash was about $1,7 \times 10^{11}$ As^{-1}, which is higher than any value originally recorded by Berger[18]. However, his analysis was truncated at $1 \times 10^{11} As^{-1}$, due to the difficulties of manual evaluation of steep rates of rise. Subsequent computerised evaluation of digitised waveforms from Berger's sample has indicated that values in excess of 1×10^{11} are certainly possible[20] and suggests a 4% probability of occurrence of a value of about $1,7 \times 10^{11}$ As^{-1}.

Previous analyses of Berger's distributions[18] yielded median values of $2,4 \times 10^{10} As^{-1}$ and $3,8 \times 10^{10} As^{-1}$ for first and subsequent stroke data respectively and the research mast data is consistent with this trend, in that mean values of about $1,2 \times 10^{10} As^{-1}$ and $4,3 \times 10^{10} As^{-1}$ were obtained for the preliminary first and subsequent stroke samples respectively.

These samples were considered too small, however, to justify more comprehensive analysis.

3.3.4 Action integral $(\int I^2 dt)$

As in the case of the impulse charge Q, this parameter was evaluated for the impulsive component of the current waveform only; - or, in the case of fast oscilloscope sweep speeds, for the available component observed on the oscillogram.

Table 3.2 ...../51

Table 3.2 summarises 16 stroke evaluations of $\int I^2 dt$ and the general trend is toward higher values for first strokes. (A first stroke mean of 8,6 x 10^4 A^2S, was obtained, compared to a mean of 4,6 x 10^4 A^2S for subsequent strokes, assuming a log-normal distribution). This trend is consistent with the results obtained by Berger[18], but again the sample is too small to justify more comprehensive evaluation.

Figure 3.7 depicts the relation observed between the measured values of action integral and the associated stroke peak current, and a reasonable degree of correlation is evident.

In fact, assuming a regression of the form,

$$\int I^2 dt = aI^b$$

leads to a coefficient of determination $r^2 = 0,7$, which is significant in this size of sample.

(A similar positive correlation between action integral and peak current was observed for both first and subsequent strokes separately, in analysis of Berger's data[18].)

3.4. Classification of observed flashes on the research mast

As noted earlier in Chapter 1, Berger has proposed a classification of lightning discharges[22] (of the ground flash type) into 8 sub-divisions - depending upon flash polarity, direction of leader progression, and the occurrence, or not, of return strokes.

In examining the 28 flashes recorded on the research mast, on the basis of the data and evidence presented in Appendix 3A, it is considered that the majority of flashes (about 82%) may be grouped into 4 of the above classifications. This categorisation is shown in Table 3.4. No evidence was available regarding the balance of 5 flashes and these were asigned an "unknown" classification.

Of the flashes which could be classified, 65% were identifiable as being of the Berger type 1(b) - or classic negative downward ground flash, as originally described by Schonland[1]. The next most common category (22%) was the type 2(a) - or positive upward leader event. This is the most common type of discharge at mountain-top installations such as Foligno[47], or San Salvatore[23], where, in the latter case, the incidence of such flashes was greater than 50% - compared to an incidence of only 11% of type 1(b). In certain of the research mast flashes, the event

was ..... / 52

TABLE 3.4: CATEGORIZATION OF RECORDED LIGHTNING FLASHES (BASED UPON BERGER'S 8 FLASH TYPES[22]

Berger's Type No.	1(b)	2(a)	2(b)	4(a)	Unknown
Description	Negative downward flash	Positive upward leader	Positive upward leader/ Negative multiple flash	Negative upward leader/ Positive following current	
Flash Nos.	1*	13*	22	14*	3
	2	24*		15	5
	4*	26*			8
	6	29			17
	7*	30			23
	9				
	10				
	11*				
	12*				
	16				
	19				
	21				
	25*				
	27				
	28				

Note: *The marked flashes could not be positively categorised, but it was considered that sufficient evidence was available in these instances to support allocation into the designated groupings.

In the absence of any evidence, the remaining flashes were assigned to the "unknown" category.

was considered incomplete, such as flash 780129, which could have led to a flash of the more common type 1(b), had interception of the nearby downward leader taken place.

To date, only one flash of type 2(b) has been recorded on the mast (i.e. the true negative upward flash), whereas this was the next most common event at San Salvatore, being responsible for over 30% of the recorded flashes there.

The remaining two identifiable flashes have tentatively been designated as being of type 4(a) (negative upward leader and positive following current), in view of the apparent polarity of the associated electrostatic field changes - as discussed in Appendix 3A. This represents, therefore, a positive flash incidence of 7% (or about 1:14) but being upward in character, this is not necessarily representative of the incidence of positive downward flashes.

It is also of interest to consider the significance of the above flash classifications in the observed diurnal incidence of flashes on the mast. For example, the cross-hatched areas in Figure 3.3 depict those flashes of type 1(b) (negative downward flashes). It is evident that flashes of this type comprise the majority of events occurring in the afternoon period, when they were generally associated with thunderstorms of the summer "hot" air-mass type. In contrast, the more unusual flashes (i.e. involving upward leaders, or positive discharges etc), tended to be associated more with the anomalous early-morning "cold" frontal thunderstorms.

3.5 Concluding remarks

Although problems were certainly experienced at the commencement of this research programme, it is considered that sufficient good quality data have been obtained to justify the claim that the instrumentation arrangements described in Chapter 2 have proved capable of automatic recording of flash characteristics and discharge current waveform parameters, during direct lightning flashes to the research mast.

In addition, although only comprising a small sample, the preliminary data presented in the preceding sections (and the associated variations of the observed values), appear wholly consistent with the character and trends of results obtained from direct measurements carried out elsewhere; - including especially the results obtained by Berger[14][18], which represent the most comprehensive analyses of waveform parameters presently available.

In ...../54

In particular, although the research mast effective height is clearly less than that of Berger's station, (as evidenced by the differences in the ratios of upward/downward flash incidence) it is of interest to note that first stroke wavefront records still display the characteristic concave form observed in Berger's data[18], while subsequent stroke records have a much steeper rate-of-rise of current - thereby implying that similar "tower-effect" processes (such as the initiation of upward connecting leaders during downward flashes), are probably active at both stations.

The occurrence and relative incidence of other flash types (apart from the normal negative downward flash), indicate that the mast effective height is sufficiently high to exert an influence on the lightning flash mechanism, but the degree of influence is clearly different from that prevalent at mountain-top stations such as San Salvatore. Despite this, it is encouraging to note that the majority of flashes recorded on the research mast were of the negative downward type, since one of the prime objectives of the research program was the study of the characteristics and parameters of this event - being the most important in the majority of practical engineering situations.

An interesting, but in view of the small sample, inevitably speculative feature of the observed data on diurnal flash incidence, is the possibility of a relation between storm synoptic condition and flash type. In fact, similar observations were noted by Bosart et al[48], in a study of San Salvatore flash incidence, who concluded that the relative incidence of upward and downward flashes may be dependent upon cloud thickness and thus upon the related synoptic situation.

Clearly, the research mast measurements will have to be continued for a substantial period of time before sufficient data will have been accumulated to clarify the above preliminary observations.

CHAPTER 4

STRIKING DISTANCE CONSIDERATIONS

4.1 Introduction

In addition to those parameters describing flash incidence and the discharge current waveform, a parameter of fundamental importance in any electrical engineering or lightning protective context is the lightning striking distance - as discussed more generally in chapter 1, (and Appendix 1B).

Implicit in many conceptualisations of the final stages of the downward progression of a charged leader is the attainment of a point at which "discrimination is determined as to where the earth will eventually be struck".[7] The striking distance is akin to the "final-jump" in long-spark terminology[51], and is normally defined as the distance between the stricken point on the ground and this point of discrimination - or more simply, as "that distance over which a lightning leader is attracted to the point about to be struck"[52].

The topic has been received extensively by Golde[31], and an important general conclusion is that the striking distance is determined by the attainment of a critical breakdown gradient across the final air-gap between the downward leader and either the stricken point, or an upward rising leader, (in the event of a connecting leader having been initiated from some point on the ground), during the approach of the downward leader. In turn, it has been shown by many workers[31], including the author, in collaboration with his colleagues[53], that the development and attainment of the requisite breakdown gradients is dependent upon the magnitude and distribution of charges on the leader.

This implies a proportionality between striking distance and charge. Assuming, in addition, a relation between charge and prospective peak discharge current, (as demonstrated by the correlations in Berger's field data[14], leads to a functional dependency between striking distance (D_s) and peak current amplitude (I).

Such relationships have been developed by several workers[19] and these normally take the form:

$$D_s = K(I)^b$$

where K and b are constants, either theoretically or empirically[31] derived.

Relationships ...../56

Relationships of this form have become established components in electrical engineering studies of lightning protection problems and are fundamental to electrogeometrical concepts of analysis[19].

In contrast to these earlier studies, a unique feature of the research programme with which this thesis is concerned is the attempt to measure the striking distances of flashes to the research mast and to relate these to the lightning currents recorded at the base of the mast.

The primary objectives of this chapter therefore are to describe these measurements and to present preliminary results, as well as to consider the concept of striking distance more generally.

4.2 Measurement of striking distances

Based upon Golde's review of the literature[31], there appear to have been very few documented instances of attempts at rigorous measurement of striking distances. Perhaps the best data available are the two results obtained by Berger[22] at the San Salvatore station, derived from rotating-camera photography of the stepped downward leader, with the following values being obtained:

$D_s = 27$ m for $I = 16$ kA

and $D_s = 37$ m for $I = 27$ kA

As noted earlier in section 1.3, striking distances of flashes to the research mast are estimated from a study of bidirectional photographs obtained from the two remotely situated automatic still cameras.

Although stereoscopic photography of lightning flashes has successfully been applied to the study of flash characteristics since at least 1912[54], as far as the author is aware, the initiation of bidirectional photography of flashes to the research mast in 1972 represented the first attempt to apply this technique to the determination of striking distances. (Subsequently, this technique has also been applied to the study of flashes on the Ostakinsk tower[24] and similar bidirectional photography has also recently been initiated on the CN Tower project[55].)

The two remote still cameras mentioned in section 2.6, are each fitted with a calibrated fine-wire graticule mounted upon a frame, which is rigidly attached to the camera housing and is positioned at an accurately measured distance from the camera focal plane.

The ...../57

The general arrangement is shown in Figure 4.1, together with the appropriate geometry, while the Table 4.1 below summarises the relevant values of the geometrical parameters for each camera.

TABLE 4.1: FRAMING CAMERA PARAMETERS

		Camera 1	Camera 2
DC	Distance between mast axis and camera focal plane	2 610 ± 10 m	2 730 ± 10 m
H	Mast height	62 ± 0,3 m	62 ± 0,3 m
ΔH	Difference in altitude between mast base and camera focal point	94,5 ± 0,5 m	97,5 ± 0,5 m
d	Distance between graticule and camera focal plane	697 ± 3 mm	697 ± 3 mm
g	Graticule grid spacing	40 ± 0,2 mm	40 ± 0,2 mm
ϕ	Angle of inclination of camera axis from the horizontal	7,2 ± 0,1°	7,0 ± 0,1°
β	Angle of rotation between the two camera axes	109,4 ± 0,5°	

In all cases the measurement errors for these parameters were of the order of 1% or less.

The ...../58

The grid spacing and its superimposed image upon any photographs taken by a specific camera, (taking account also of the relevant geometry of the situation), provides a scaling factor, which defines the relation between any image dimensions and the actual dimensions of the object being photographed (i.e. in this case, the lightning discharge channel).

In practice, the individual images of a flash, taken by each camera, are projected upon an automatic plotting table and the respective two-dimensional co-ordinates of the flash on each photograph are digitised (with reference to the plotting table frame system). It is assumed that the image of a flash is a straight line between two consecutive points.

A computerised technique of analysis is described below, which combines these two sets of two-dimensional data (taking account of the relevant scaling factors) in a series of geometrical co-ordinate transformations, to yield a three-dimensional "re-construction" of the flash, with reference to the position of the top of the research mast.

The striking distance of a flash, in the course of its progression toward the mast, is then determined from an examination of this three-dimensional flash geometry.

A fundamental assumption in this analysis is that the final stages in the progression of a lightning stroke can be divided into two phases, or progressive processes:

(a) involving the initiation and, on occasion, subsequent deflection of an upward connecting leader from the top of the research mast, and

(b) the subsequent interception of the downward and upward progressing leaders at some intermediate point away from the mast tip.

Subject to these constraints, the striking distance was defined as that distance from the tip of the mast, at which the progression of the lightning channel last assumed a persistent orientation toward the point of interception with the upward connecting leader.

Figure 4.1 ...../59

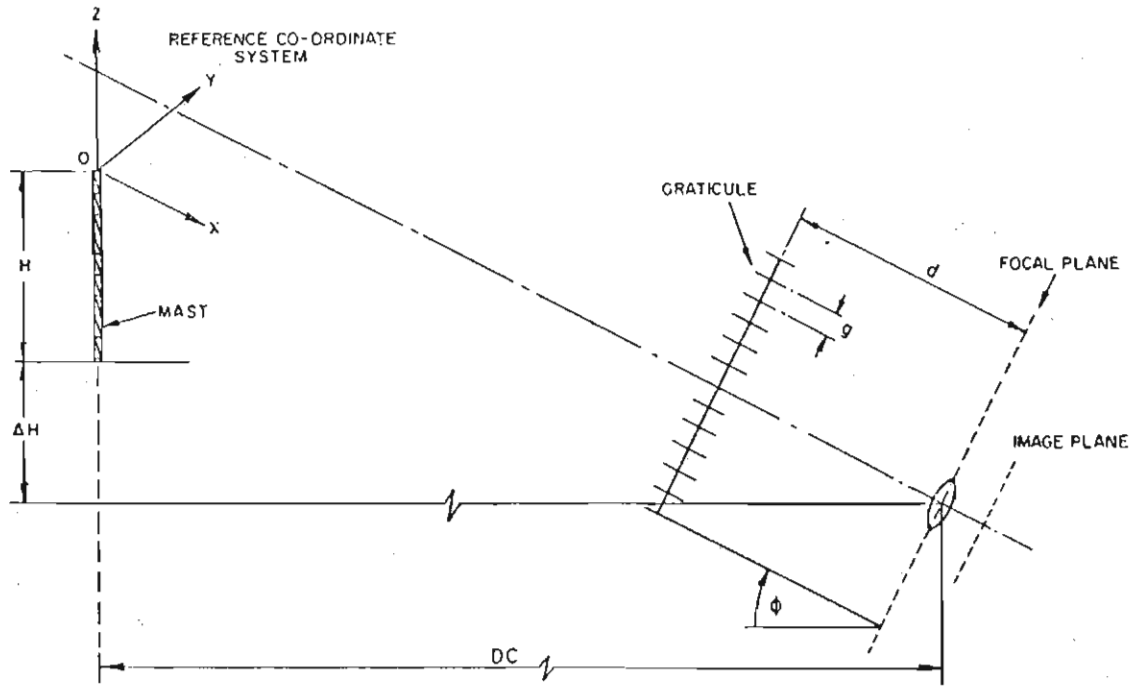

FIGURE 4.1
GEOMETRY OF FRAMING CAMERA UNIT

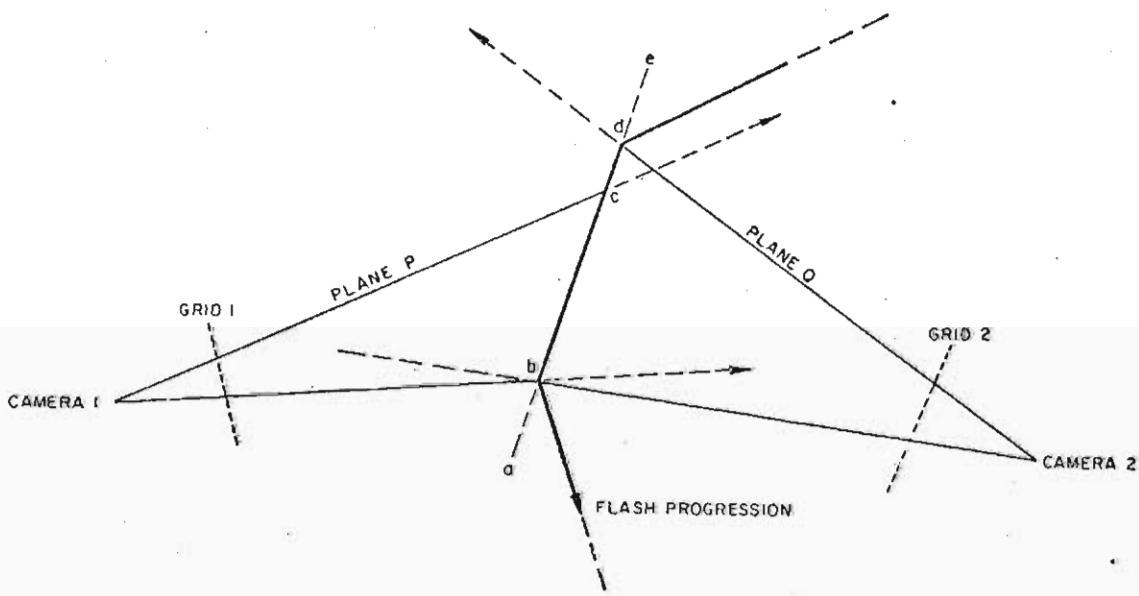

FIGURE 4.2
THREE - DIMENSIONAL RECONSTRUCTION OF FLASH GEOMETRY

4.3 Re-construction of three-dimensional flash geometry

In considering the general geometry presented in Figure 4.1, it is evident that several factors complicate an evaluation of a three-dimensional reconstruction of a flash from analysis of the relevant sets of two-dimensional co-ordinates derived from a pair of photographs. These factors include the following:

(a) the two cameras are at different distances from the research mast and do not view the mast orthogonally, but are separated by an angle of rotation $\beta = 109°$;

(b) the two cameras view the volume of sky above the mast obliquely, being situated at altitudes ΔH below the mast and inclined at angles ϕ with respect to the horizontal.

(c) due to independent digitisation of each flash photograph, the numbers of two-dimensional co-ordinate pairs sampled will differ for two photographs of any particular flash;

(d) similarly, the measured points on the flash channel for the two sets of two-dimensional co-ordinates obtained from the two cameras respectively, will generally not be the images of the same actual points on the flash.

The first two aspects are readily resolved through a series of angular and co-ordinate transformations - in terms of the geometry depicted in Figure 4.1 - but the latter two problems require careful consideration of the elemental flash geometry, as illustrated in Figure 4.2, which shows an element (bd) of the flash channel.

A set of arbitrary points, measured consecutively along the channel and viewed in the grid plane of camera 1, say, define a plane P which passes through the focal point of this camera, as well as the measured points on the grid, and which intersects the flash. Similarly, the correspondin points measured in the grid of camera 2 define a plane Q, which passes through these points and the focal point of camera 2. The two planes intersect in a straight line (abde in Figure 4.2) which must coincide with a segment of the flash channel (bc in this example). The requirement therefore is a determination of the co-ordinates of the two end points, b and c, of this segment.

A method embodying a series of algorithms for carrying out this determination iteratively along the flash channel, was developed by the National Research Institute for Mathematical Sciences - who also prepared a comprehensive computer program (termed Flash) for processing and analysis of the digitised data, in the above manner[56].

Clearly, the accuracy of the overall determination of three-dimensional flash geometry is directly dependent upon the accuracy of the input geometrical parameters - although these had been measured with care, as shown by the relevant measurement errors given in Table 4.1. Accordingly, the effects of these errors were evaluated in a series of sensitivity analyses which were carried out using program Flash, and assuming different measurement errors for the relevant input geometrical parameters. As might be expected, the most important accuracies were those of the distance, or scale factor parameters (namely, DC, d and g, in Table 4.1). The resulting errors in effective flash geometry were found to be almost directly proportional to the input errors, and were thus limited to less than 1%.

However, greater errors arise during the digitisation process, due to the image size of the flash, which is broadened by photographic halation. An overall check of the accuracy of the complete technique of analysis was carried out by applying program Flash to an evaluation of the known height of the research mast from analysis of photographs taken by the two cameras, and the resultant error was about 3% - which was considered acceptable.

4.4 Results

As summarised in Table 3.1 of chapter 3, of the 18 flashes to the research mast that have been photographed by at least one of the above still cameras, only 7 have been photographed bi-directionally and thus are candidates for geometrical analysis of striking distance. The primary concern in this thesis however, is with the more common downward flash event, and only 3 of the above flashes were of this type (Berger[22] classification 1(b)) - namely, flash numbers 10, 19 and 27. (The relevant photographs, as well as those for all 18 flashes, are presented with the review of each respective flash event in Appendix 3A).

The resultant geometrical reconstructions for each of these three flashes are shown in Figures 4.3(a), (b), (c) and the analyses of these are discussed briefly below, based upon the considerations and constraints presented in section 4.2.

Figure 4.3(a) ...../62

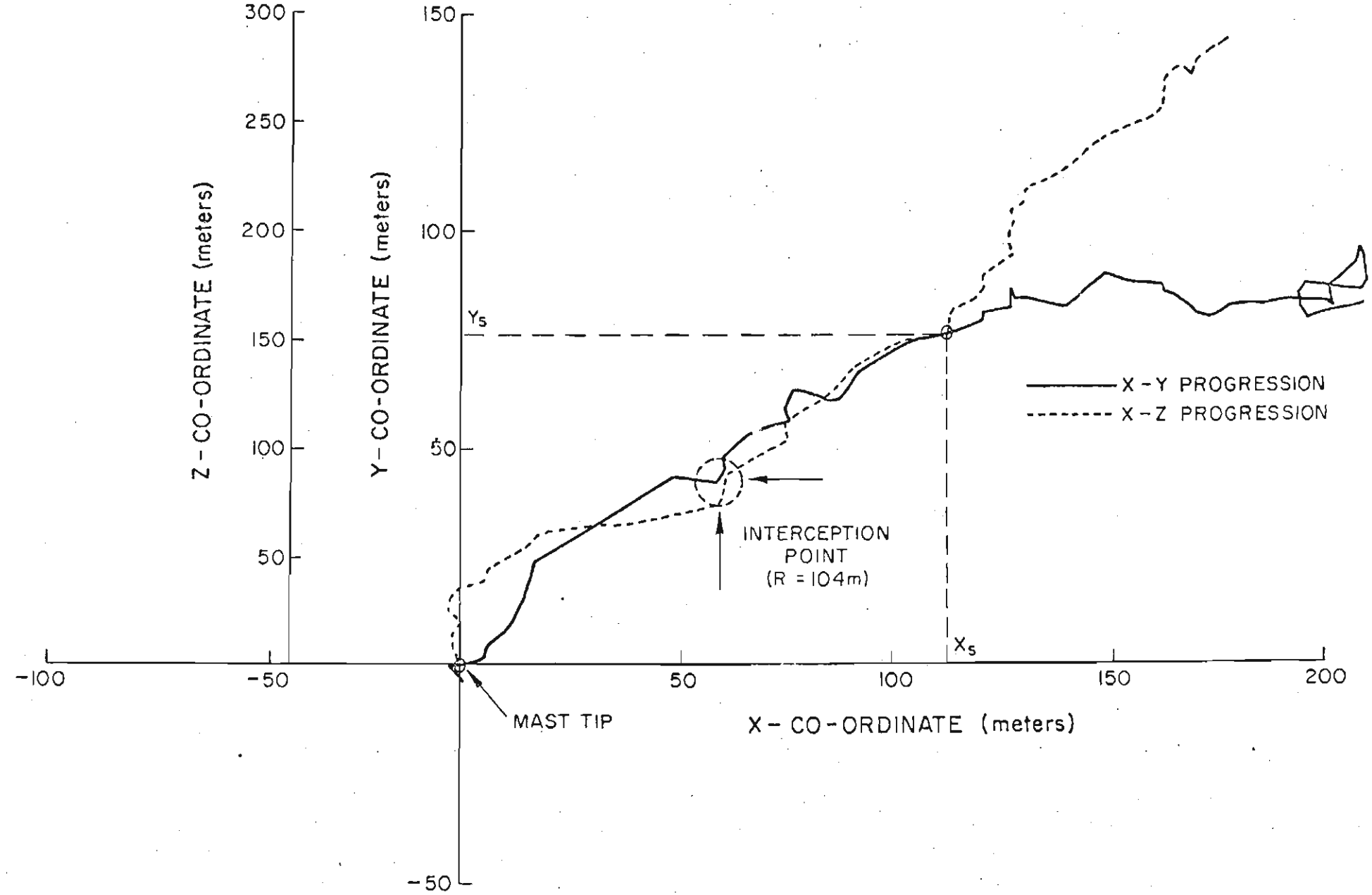

FIGURE 4.3 (a)

RECONSTRUCTION OF FLASH PROGRESSION (FLASH 740104/10) – STRIKING DISTANCE OF 208 m

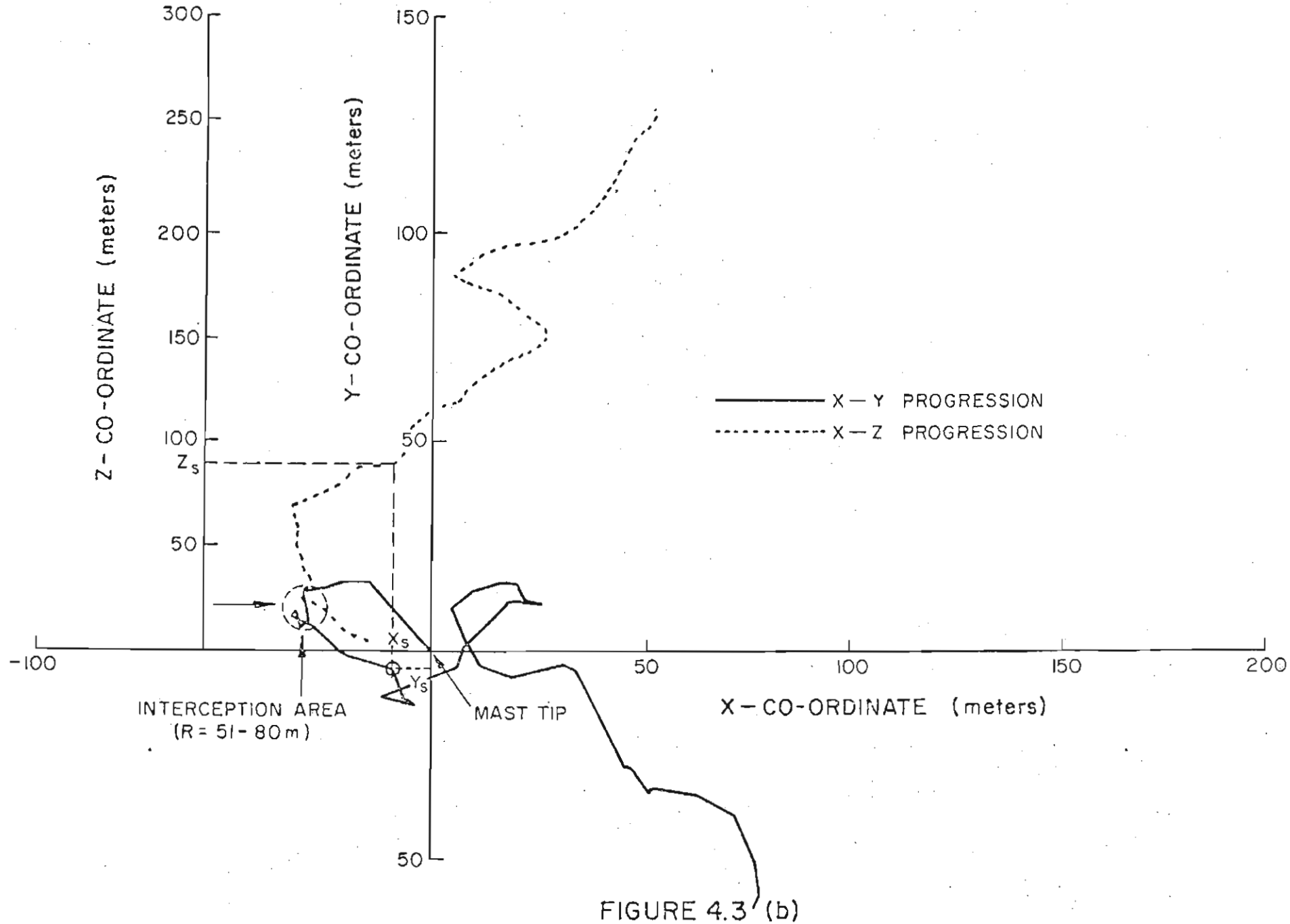

FIGURE 4.3 (b)

RECONSTRUCTION OF FLASH PROGRESSION (FLASH 750227/19) — STRIKING DISTANCE OF 99m

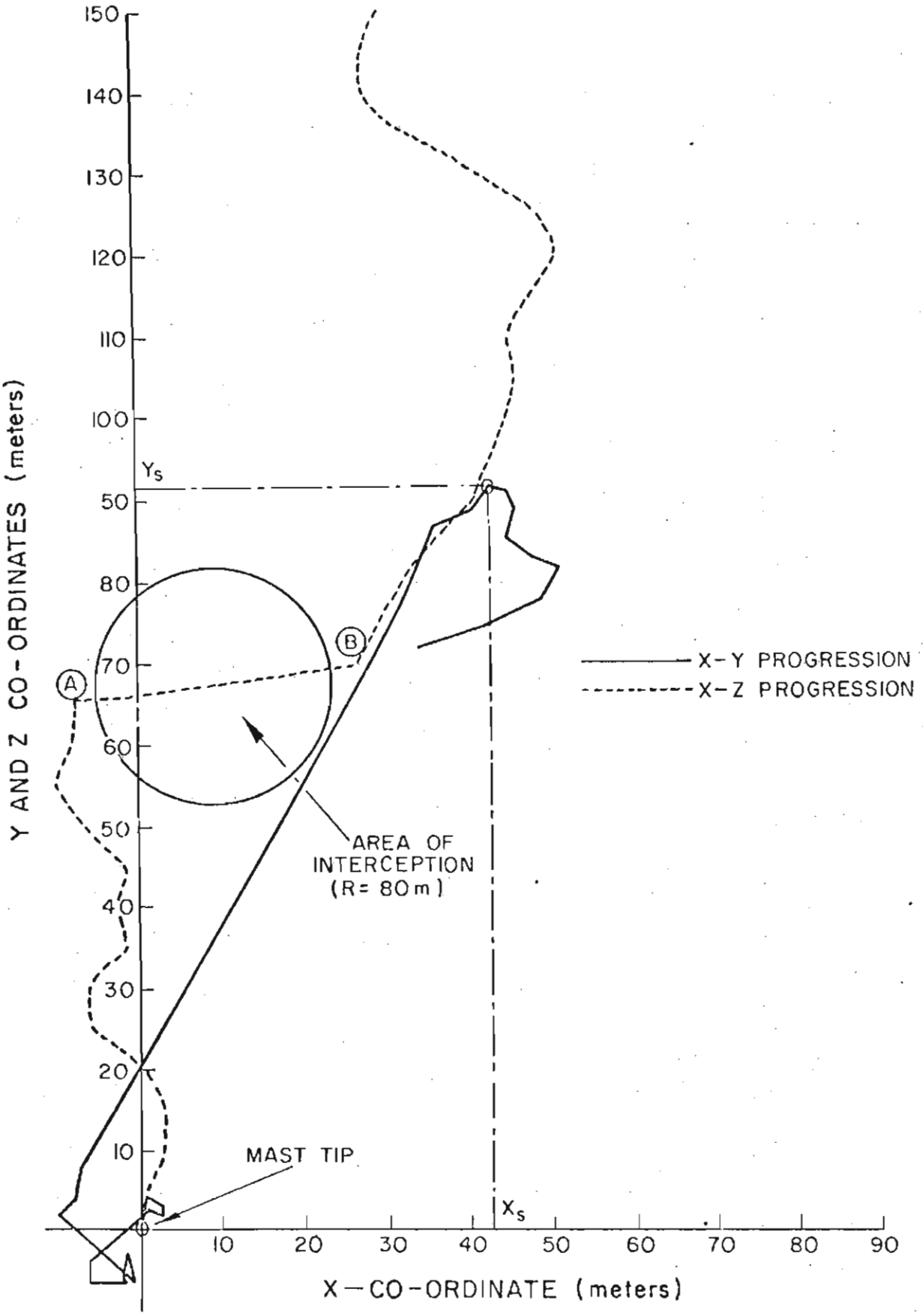

FIGURE 4.3 (c)

RECONSTRUCTION OF FLASH PROGRESSION (771009/27) - STRIKING DISTANCE OF 138m)

Flash No. 740104/10

In reconstruction, a vertical component rising directly above the mast to a height of about 35 m, is clearly evident. This then tracks off almost horizontally, and consistently in one direction, to a prominent discontinuity - labelled "interception point" in Figure 4.3(a). Above meanwhile, the downward progressing leader channel form suggests a random orientation (including a degree of spiralling) until, at a height of about 150 m, a fairly consistent progression starts toward this intersection point.

Although there is also a small "kink" in this progression (at $Z \approx 110$ m), it is felt that the above analysis is consistent in indicating a striking distance given by the co-ordinates, $Z_s = 151$ m, $Y_s = 79$ m and $X_g = 120$ m. This yields a striking distance $D_s = 208$ m, and a distance to the point of interception of about 104 m.

If instead, the "kinked" area mentioned above is used to define the striking distance, a value $D_s = 148$ m is obtained. This therefore defines a possible lower bound to the measured striking distance on this occasion.

Flash No. 750227/19

This flash exhibits a considerably more complex geometry than in the previous instance, but is again amenable to analysis in terms of the intersection of downward and upward progressing leaders.

It is considered that the latter is evidenced by the essentially vertically oriented component which rises from about 20 m, up to 70 m above the tower. This defines the area of interception between the two leaders, while it is suggested that the upward leader process may have been initiated at the discontinuity evident in the progression of the downward leader at a height of about 90 m above the mast, yielding a striking distance of about 99 m.

It is obviously possible, as an alternative, that the striking distance may be defined by the upper discontinuity in the area labelled "interception area". This would yield a lower bound to the measured striking distance of about 80 m, while the distance to the interception point would reduce to about 51 m.

Flash 771009/27

The analysis of the geometry of this particular flash is less ambiguous than in the previous two instances.

Again ..... /66

Again, a vertically oriented element of the channel is clearly evident above the research mast, rising to a height of about 65 m. In this case however, a segment of channel is present which connects this upward leader (as presumed), with the nearby downward progressing leader. The resultant striking distance is estimated to be about 138 m.

In this example, the final interception is thought not to be defined as a point, but rather as an air-gap between the two leaders (e.g. a rod-rod gap), over which the final breakdown takes place - indicated by the points labelled AB in the diagram. In this event, the lower bound to the striking distance is given by the vector OB, corresponding to a distance of about 103 m.

Following this study of the above examples of three-dimensional flash geometry, an attempt was made to estimate the approximate striking distances associated with those flashes which had only been photographed by one framing camera. These analyses were still based upon the presumption of a process involving interception of upward and downward progressing leaders, and therefore attempted to identify these interception points in the flash photographs - in a manner similar to that adopted earlier by Golde[12].

A further 6 flashes could be studied in this manner and peak current amplitude data was available for 5 of these. The resultant estimates of the interception distances are summarised in Table 4.2, together with the above striking distance results from the bi-directionally photographed flashes, as previously discussed. From the study of the latter three flashes it was also possible to determine the ratios of the respective striking and interception distances (D_S and D_I), and these values are given in Table 4.2. A mean ratio D_S/D_I = 1,77 ±0,28 (one standard deviation) is obtained.

This ratio was then applied to the 6 estimates of interception distances derived from the single camera photographs, to yield approximate values of the striking distances that may have been associated with these flashes - as summarised also in Table 4.2.

Table 4.2 ...../67

TABLE 4.2: RESULTS OF STRIKING DISTANCE ESTIMATES

Flash No.	Peak Current (kA)	Interception Distance (D_I) (m)	Striking Distance (D_s) (m)	Ratio D_s/D_I
721129/1	35	78 †	116 - 160	-
731015/6	-	177 †	263 - 364	-
731216/9	10	55 †	82 - 113	-
740104/10	41	104	148 - 208 (3D)	1,42 - 2,00
741224/16	53	151 †	225 - 310	
750227/19	26	51	80 - 99 (3D)	1,57 - 1,94
751102/21	19	23 †	34 - 47	
770222/25	83	169 †	251 - 347	
771009/27	87	65	103 - 138 (3D)	1,58 - 2,12

Note: 3D denotes results obtained from three-dimensional analysis

† denotes values estimated from study of single camera photographs

The resultant correlation between these measured distances and the peak current magnitudes recorded in the research mast on each occasion, is depicted in Figure 4.4 - together with one of the more representative empirical relations commonly used in practical applications. The latter is taken from Whitehead[19] and is given by:

Figure 4.4 ...../68

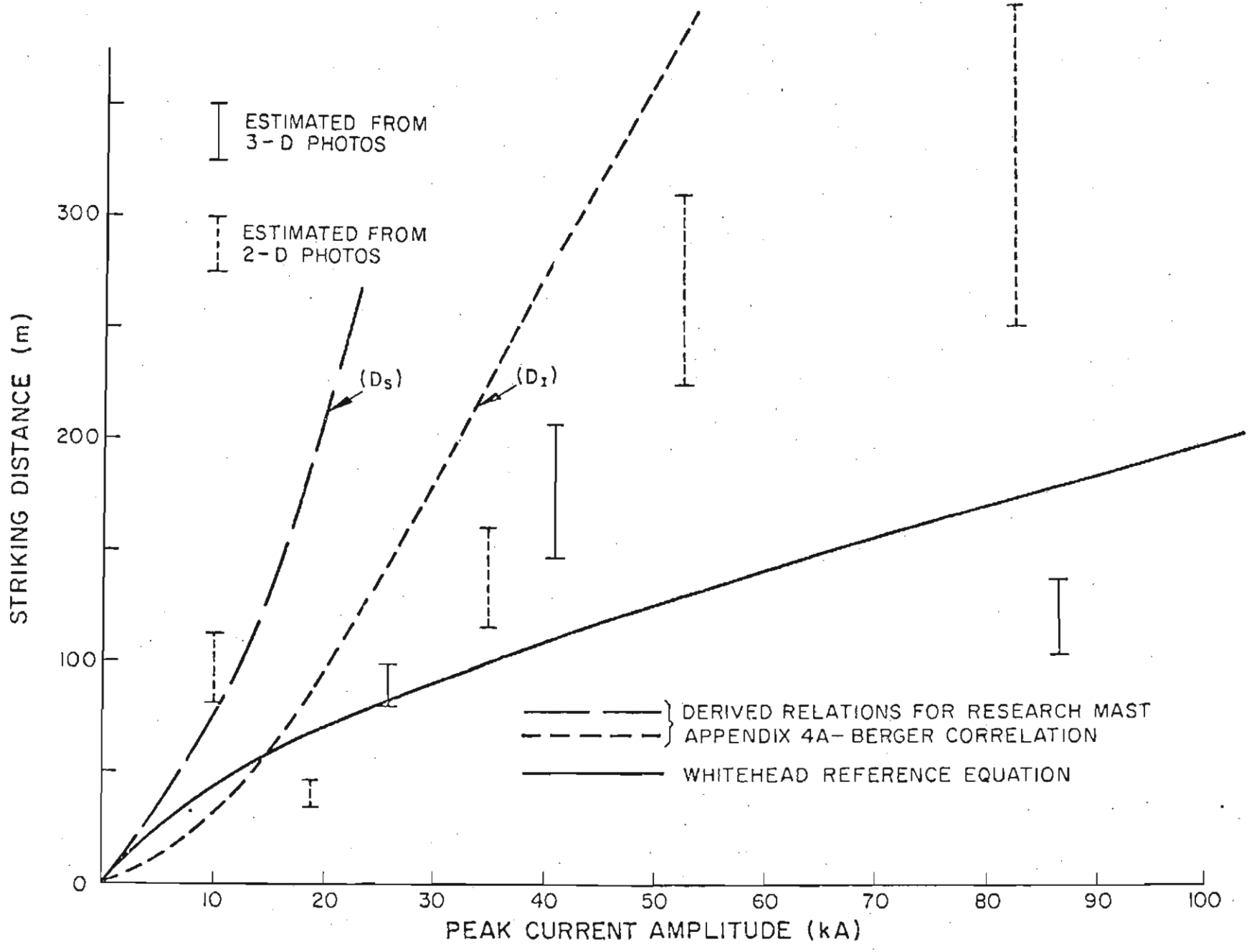

FIGURE 4.4

RESULTS OF STRIKING DISTANCE ESTIMATIONS

$$D_s = 10\ I^{0,65}$$

It is seen to be generally below the measured distances.

This figure also includes two analytically derived relations for striking distance D_s and interception distance D_I - which are based upon Berger's observed correlation between peak current and stroke impulse charge[14].

These analytical relationships and the implications of these results are discussed further in the following sections.

4.5 An analytical approach

This is presented more fully in Appendix 4A and only the salient points and conclusions will be summarised here.

The approach is based upon work originated by Anderson in 1971[9] and subsequently extended by the author in collaboration with Anderson[53][57].

The particular concept involved considers the approach of a model linearly charged line element leader moving downward toward the ground, and evaluates the electrostatic field gradients developed both at the ground, and in the vicinity of a structure.

In this concept, the striking distance is defined as the distance between the downward leader tip and a prospective flash termination point - such as the top of a mast - at that stage in downward leader progression when an upward leader ionisation inception field is attained in the vicinity of such a point. Thereafter, it is considered that the flash will terminate on this point, rather than at the ground, provided the upward leader can traverse the intervening distance to intercept the downward progressing leader, before the corona sheath around the latter has advanced sufficiently to contact the ground. Clearly, this will depend upon the relative velocities of the downward and upward leaders. It is assumed therefore, that the two leaders intercept at some intermediate "interception distance" remote from the stricken point and that the downward leader experiences little deviation in path as a consequence of the approach of the upward leader. (The latter assumption is supported by the fact that the charges raised in the upward leader are substantially less than those lowered on the descending leader - as shown both by Berger's direct measurements[14], as well as by Anderson's earlier analyses[9].)

The application of this approach is illustrated in Appendix 4A, by a consideration of the influence of vertically descending leaders lowering

varying ...../70

varying charge magnitudes in the vicinity of the research mast and a determination of the distances of approach necessary for the attainment of upward leader inception potential gradients at the top of the mast. (For the purposes of this study, these have been defined in terms of corona inception at the surface of an equivalent sphere having a critical corona radius at the mast tip. Account is also taken of the structure field intensification factor and of the relevant air density correction factor.)

The results are shown in Figure 4.5 for a leader of average channel length (5 km). Considering an average leader charge of 5 C for example, these indicate that the approach of such a leader to within a radius of about 440 m of the mast tip is sufficient to cause attainment of upward leader inception gradients at that point. However, interception of the two leaders is determined by an evaluation of the equivalent collection volumes of geometric space around the mast tip, within which the requirement is met that the upward leader traverse the intervening distance before the downward leader reaches the ground. The resulting collection volumes are also illustrated in Figure 4.5 for two values of the relative leader velocity ratio (given as $K_v = v_\ell/v_u$, where v_ℓ and v_u are the velocities of the downward and upward leaders respectively).

From a consideration of the results shown in Figure 4.5, although upward leader inception fields may be attained at quite long distances of approach of the downward leader (i.e. long striking distances), depending upon the relative leader velocities the downward leader is required to enter a comparatively small volume of space surrounding the mast top, before interception by the upward leader is ensured.

As noted in Appendix 4.A, an equivalent attractive radius R_a may therefore be introduced - expressed by the radius of the cross-sectional plan view of the collection volume, for a given leader charge and velocity ratio. For example, for the results given in Figure 4.5, and considering an average leader charge of 5 C, although the so-called striking distance remains constant at about 440 m for a velocity ratio varying between 1,0 - 1,2, the associated attractive radius R_a reduces from 220 m, down to about 90 m, over the same range of velocities.

In order to relate these analytical results - which are expressed as functions of the leader charge q - to the measured striking distances presented in the previous section, it is necessary to make use of the known correlations between stroke peak current amplitude and impulse charge - as derived from Berger's data[14]. This then was the basis of the analytical relations depicted earlier in Figure 4.4. However, as pointed out by Golde[58], and discussed further in Appendix 4A, a consideration of the

Figure 4.5 ...../71

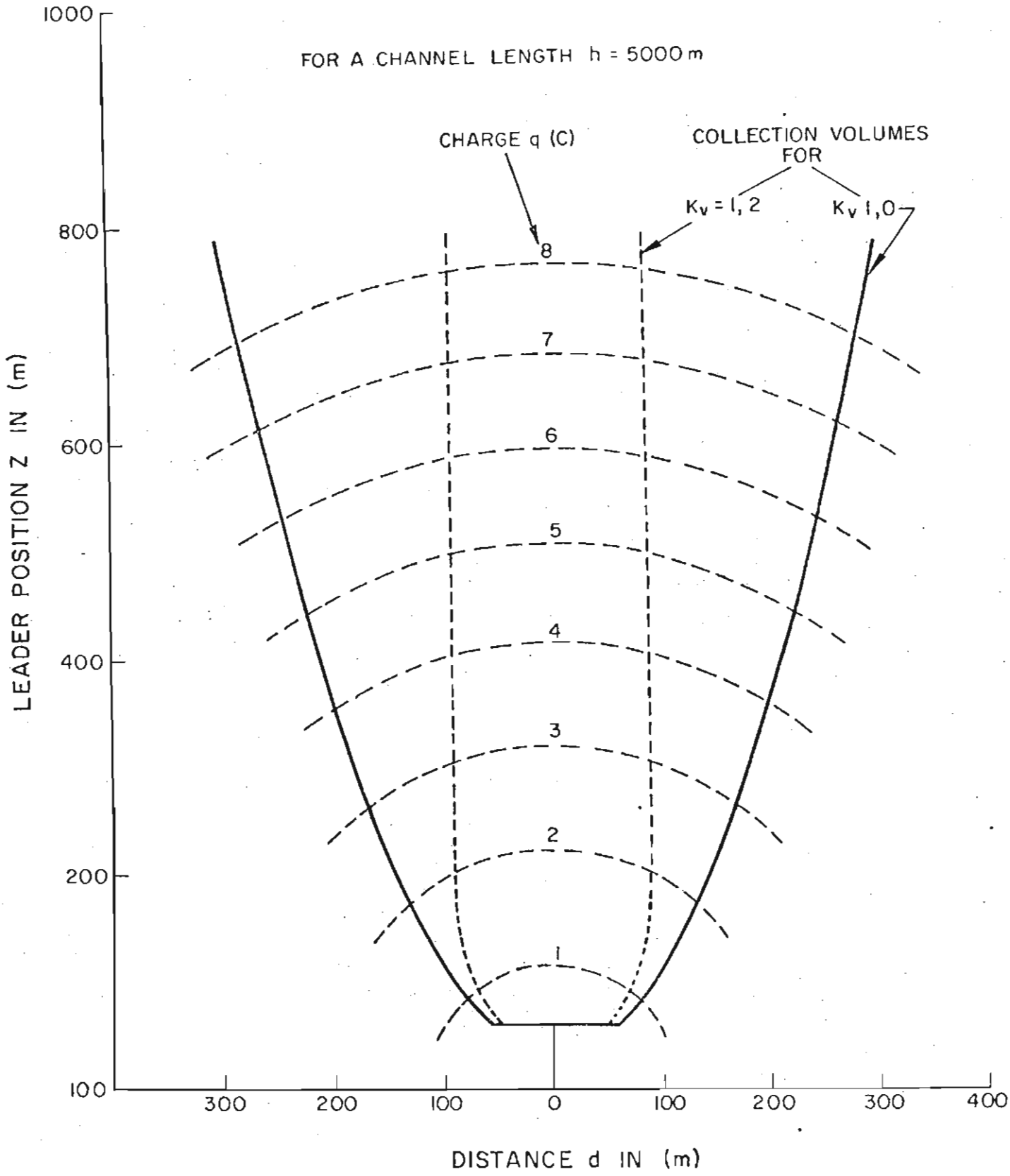

FIGURE 4.5

DOWNWARD FLASH INTERCEPTION BY THE RESEARCH MAST, AS A FUNCTION OF LEADER CHARGE AND VELOCITY

parameters ...../72

parameters of the return-stroke indicates the adoption rather of a relation between peak current and only those charges in the lower portion of the leader.

Berger's observed correlation becomes modified, as shown in Appendix 4A, as;

$$I = 29{,}4\ q^{0{,}7}$$

This relation may be applied to the analytically derived values of striking distance as functions of charge q, to yield an average striking distance relation;

$$D_s = 0{,}6\ I^{1{,}46}$$

In a similar manner, as shown in Appendix 4A and taking a velocity ratio K_v = 1,2, a relation is derived for the interception distances;

$$D_I = 0{,}27\ I^{1{,}46}$$

The above two relationships are shown in Figure 4.6 - in which the mean values of the measured striking and interception distances have also been replotted, together with the related peak current amplitudes. A power curve relation has also been drawn through the measured striking distance data ($S_M = 16{,}5\ I^{0{,}57}$).

Although there is considerable scatter in the measured data (which comprise only a small sample), there is a reasonable measure of agreement between the measured and analytically derived estimates of striking distance. (In general, the measured points tend to lie above the analytical relationships for both striking and interception distances.)

Although this trend toward agreement may only be fortuitous, (due to the small sample size, as well as to the many assumptions involved in the analysis), this does also imply that the basic concepts comprising the analytical approach in Appendix 4A may well be acceptable and could allow application of these concepts to an estimation of striking distances to other structures.

The various conclusions arising out of the analytical study will be discussed further in sections 4.8 and 4.9 below, but one very important aspect that this approach does illustrate is that striking distances depend directly upon the structure field intensification factors. Thus the above derived relationships apply in particular to structures similar to the research mast (i.e. having field intensification factors K_i of the order of 44), and may not be considered as generalised relationships.

Figure 4.6 ...../73

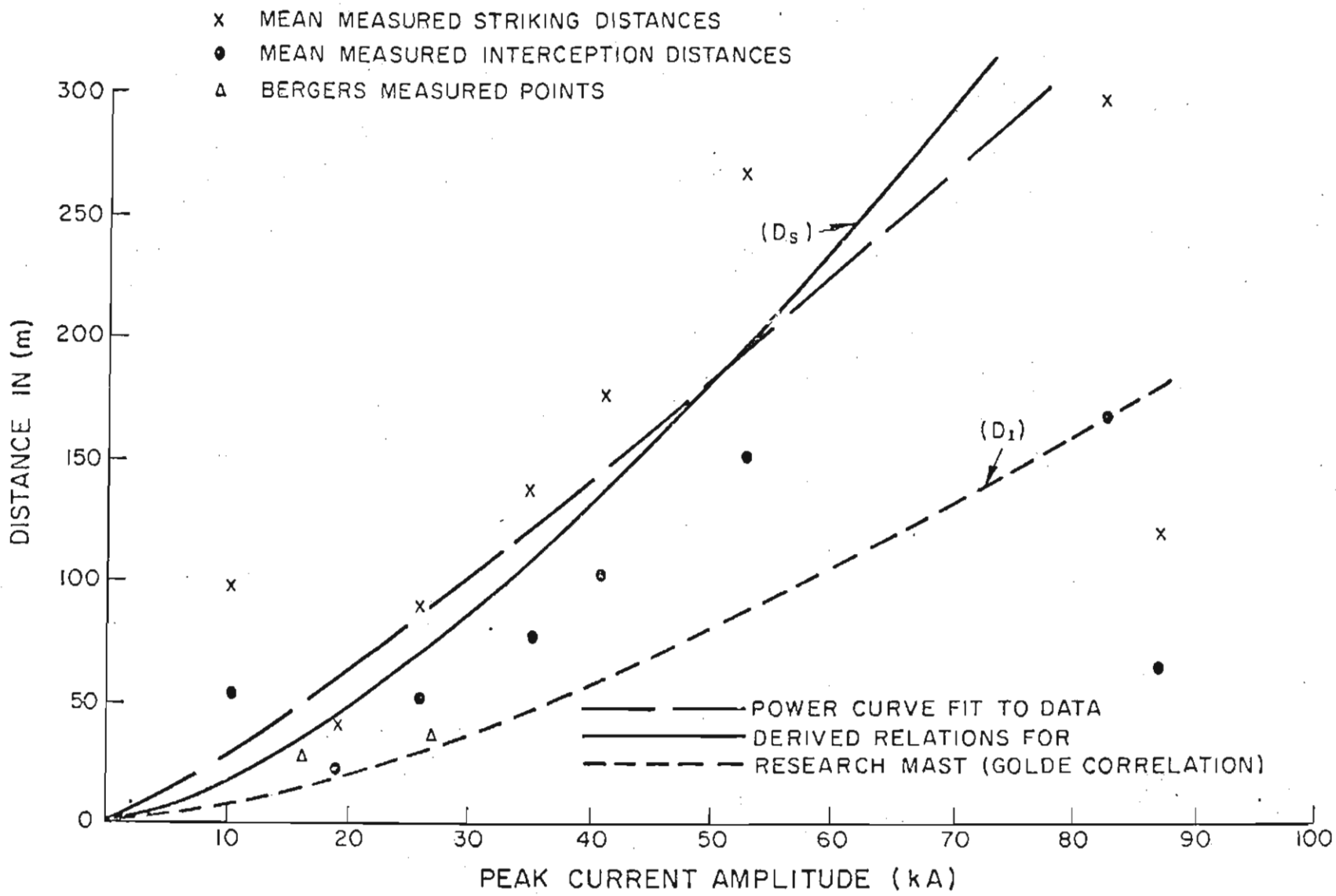

FIGURE 4.6

COMPARISON BETWEEN MEASURED AND MODIFIED DERIVED STRIKING DISTANCES

4.6 The effects of leader branching

In an earlier study of the incidence and characteristics of lightning flashes to tall structures[16] the author concluded that the peak current amplitude distribution of negative downward flashes may largely be independent of structure height. Although data was scarce. this conclusion, if valid, implied that the base assumption of many electrogeometric concepts of analysis (i.e. of a functional relationship between striking distances and peak current), may in turn not be wholly correct. In attempting to account for this observation[21], the author drew attention to the complex branched nature of downward leaders - both on the micro and macro scales geometrically - and suggested that final stages of a flash may still involve the interception of upward and downward leader elements, but that the point of strike termination might be determined more by the approach of one, or more, charged leader branch elements, rather than by the macro distribution of charges along the complete leader structure. In contrast, the resulting discharge current waveform could be influenced by the discharge of charges from adjacent branched leader elements.

This hypothesis would imply that the common practice of representing the downward leader as a single geometrical element, bearing all the prospective impulsive charge - as in fact was the case in the preceding analytical approach (Appendix 4A), could be an over-simplification of the physical situation.

Accordingly therefore, in order to examine these aspects of the problem more fully, a short study of flash branch characteristics was initiated, followed by an examination of the influence of a representative downward branched leader upon the development of the electrostatic field potential gradients at the ground - as discussed below.

Firstly, in order to obtain a meaningful impression of flash branch characteristics, a study was carried out on a sample of downward flash photographs which had been taken by the two remote still cameras. (Although photographic studies of flash tortuousity had been carried out before[59] - there appeared to be little data available on the degree and extent of flash branching - except the early data presented by Schonland[60]).

A sample of 159 flash photographs was examined. These were analysed in respect of the numbers of branches off the main channel, the branching angles in relation to the average direction of progression, and the interval between branches, expressed as a percentage of the visible channel length between cloud base and ground. (In the Transvaal region thundercloud

condensation ...../75

condensation levels normally lie between 1 000 and 2 000 m above ground level).

Some 575 branches were analysed in this sample and the results are summarised in Figures 4.7 and 4.8.

Subject to the difficulties of adequately resolving flash branches and to the possibility that the sample may be non-representative, (although it was based upon several years of recordings) this analysis suggests the following observations.

(a) Unbranched flashes are in the minority - comprising only 12% of the sample.

(b) the average flash has approximately 3 - 4 branches visible (between cloud base and ground)

(c) The most common branching angle is about 45° - measured with respect to the average direction of progression.

(d) The branching interval appears to decrease progressively as the ground is approaching - suggesting that the degree of branching may increase toward the ground. (The latter observation may not be unreasonable since the presence of space charges is known to increase toward the ground due to the effects of point discharge from objects on the ground).

Having completed this exercise, and based upon these observations, a simple model of the lower 2 000 m of a descending leader was derived, having average flash branching features.

This model is shown in Figure 4.9(a) - together with the equivalent single line element model, bearing the same total charge, given in Figure 4.9(b).

The branched model comprises three main branches, together with a minor sub-branch, and all branching angles are chosen as 45°. Branching intervals varying between 400 m and 800 m were adopted, corresponding to intervals of 20 - 40% along a channel length of 2 000 m between cloud base and ground. Any charges above an altitude of 2 000 m were ignored in this analysis, since it is readily shown that their influence upon the fields at ground level is comparatively small. (For example, a point charge of 1 C is required at a height of 2 000 m to cause a field in excess of 4,5 kV/m on the ground.)

Figure 4.7 ...../76

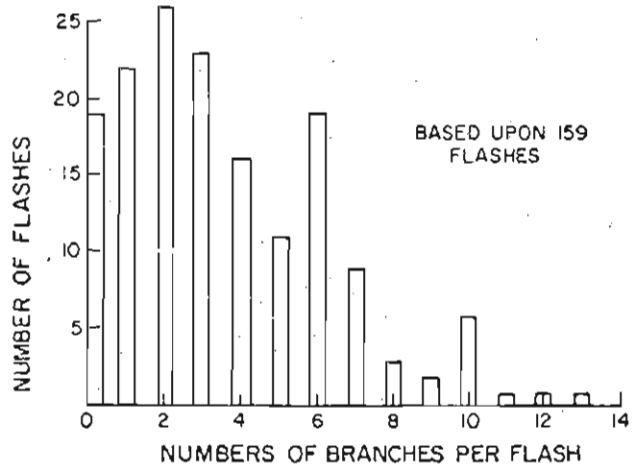

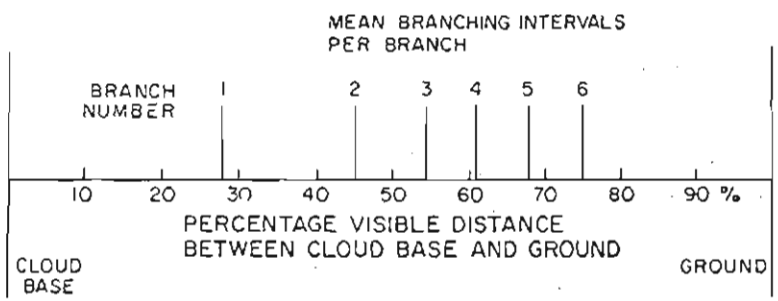

FIGURE 4.7
CHARACTERISTICS OF DOWNWARD FLASH BRANCHING

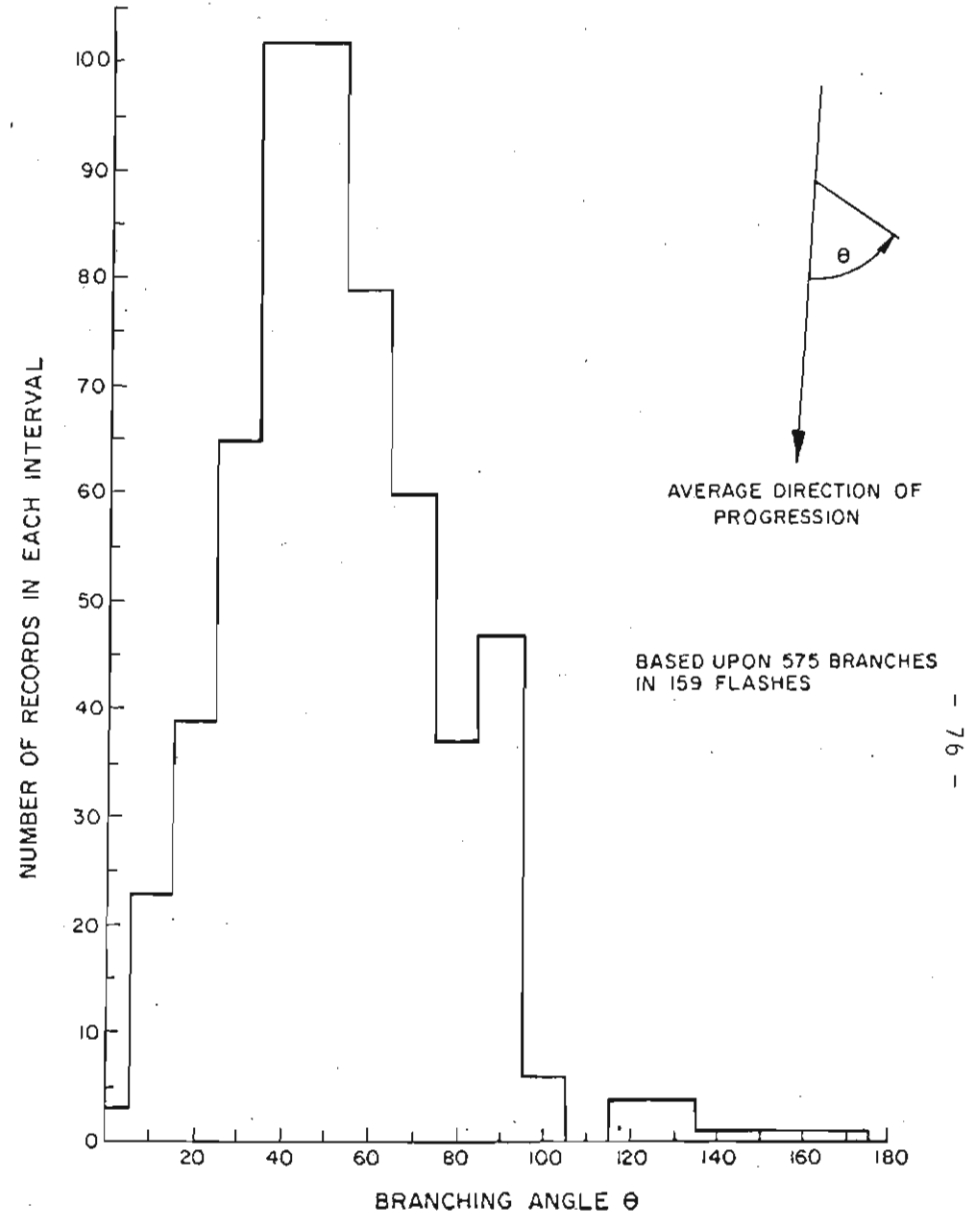

FIGURE 4.8
DOWNWARD FLASH BRANCHING ANGLE CHARACTERISTICS

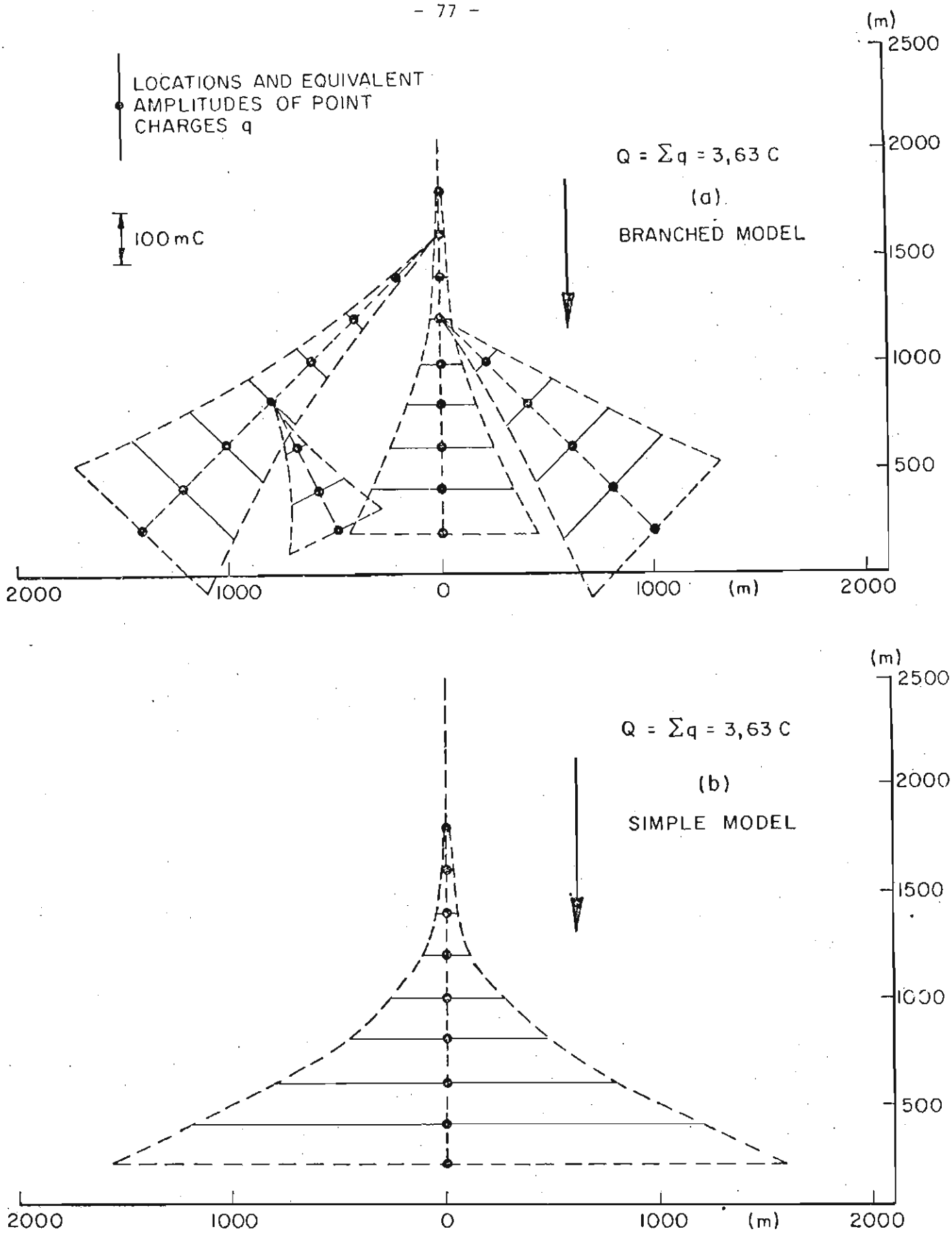

FIGURE 4.9

MODELS OF DOWNWARD LEADER AND CHARGE DISTRIBUTIONS

For ...../78

For consistency with the earlier work, approximate linear charge distributions were assumed along the leader branches and, for ease of calculation in this complex geometry, these charges were represented by varying point charges distributed at about 200 m intervals along the branches - as shown in Figure 4.9. The total charge lowered by the leader when down to an altitude of 200 m above the ground, was 3,63 C - which is close to an average value of impulse charge for first negative downward strokes[18].

The effect of the approach of the downward leader was simulated by repeating the calculation of ground level fields while the leader branch tip positions were advanced at 200 m vertical intervals. In each case, the charges lowered along the branches were increased according to their respective distributions. (Assuming an average downward velocity of 2 x 10^5 m/s, the charges lowered in these step intervals are equivalent to average branch currents varying between 40 - 80 A - which are consistent with various estimates derived from indirect measurements[61]). For each position H of the branched leader above the ground, the integral field strength E was evaluated for a variety of positions along the ground, removed distances D away from the equivalent axis of the leader, using the expression:

$$E = \frac{i}{2\pi\varepsilon} \sum_{i=1}^{n} q_i H \, (H^2+D^2)^{-3/2}$$

The results are summarised in Figure 4.10, which depicts the field potential gradient profiles developed along the ground, for each of the last four positions of the descending model branched leader. (These diagrams also depict the field profiles developed when the branched model is replaced by the equivalent single line element model.)

While it is evident that the single line element model always leads to substantially higher field intensities on the ground vertically below the leader, (i.e. along the leader axis), the wider spatial distribution of the leader charge into the branches leads to the development of comparatively high field levels across a wide extent of the ground beneath the branched model - as might be expected.

Bearing in mind in the case of the research mast, as noted in Appendix 4A, that the upward leader inception field is given by:

$$E' = E_m/K_i = 2,6 \times 10^6/44 = 59 \text{ kV/m},$$

Figure 4.10 ...../79

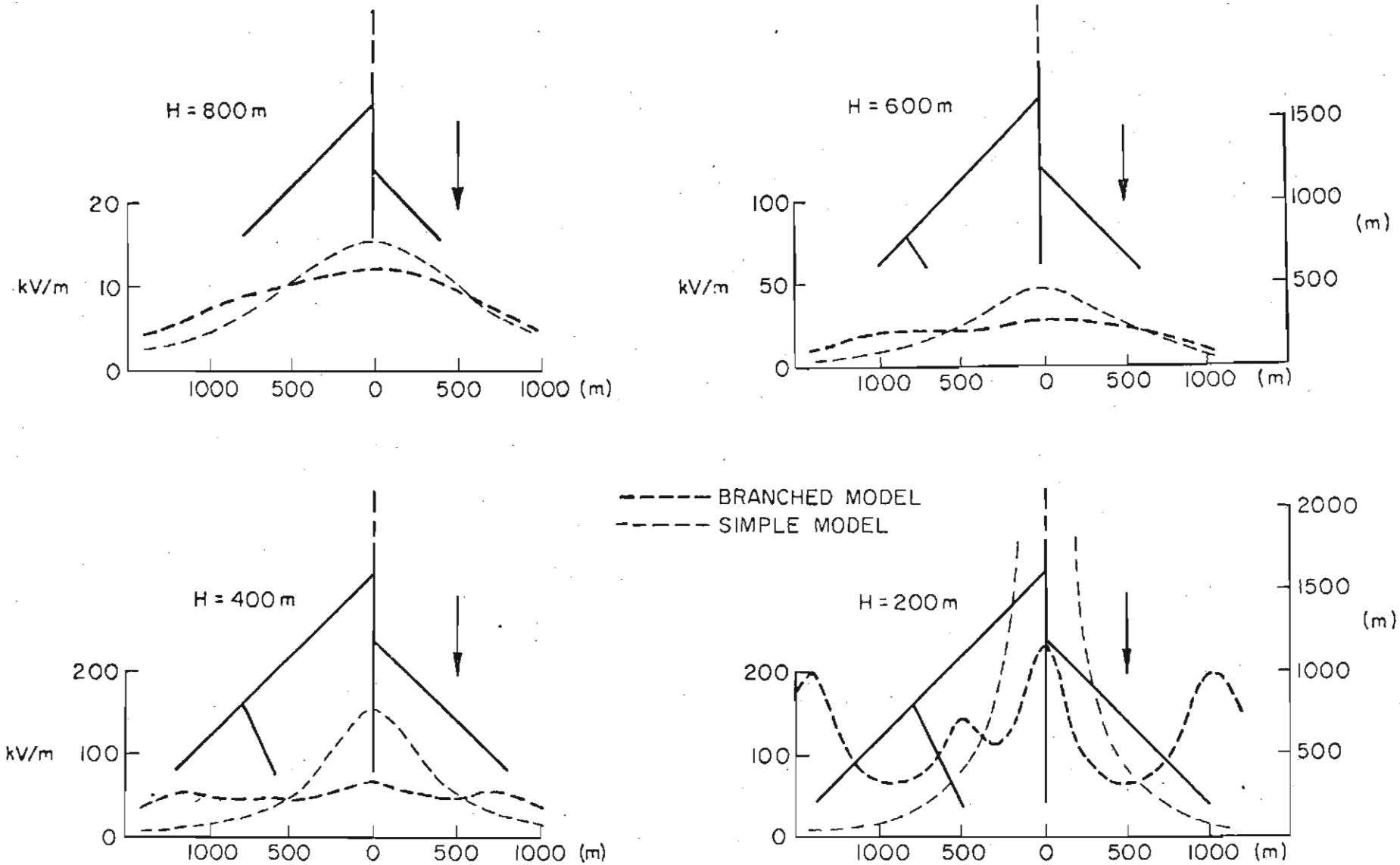

FIGURE 4.10

ELECTROSTATIC FIELD PROFILES AT THE GROUND DURING THE APPROACH OF A DOWNWARD LEADER

Figure 4.10 indicates that fields approaching this level can be developed at several positions along the ground, for a branched leader height of 400 m, and are certainly exceeded at many positions for lower leader heights.

Depending upon the position (and number) of structures on the ground, this would imply the possibility of several potential striking distances being attained during the approach of such a branched leader. The final point of flash termination therefore, might then depend upon which of several competing upward leaders (developing perhaps from several structures in the area), first intercepts a descending leader branch.

In the course of this research programme, two events have been photographed on the research mast which support the above concept of the circumstances surrounding the approach of a branched leader. The two events are described more fully in Appendix 3A - which also includes the relevant photographs (namely Flash Nos. 21 and 28).

In the first instance (Flash 21) - which has been reported elsewhere[50] - the flash presents a good example of the phenomenon originally termed "root-branching" by Schonland et al[60], in that two apparently simultaneous ground terminations are evident in the photograph - each of similar illuminosity, implying at least approximately simultaneous magnitudes of discharge current amplitude.

In discussing the flash[50] the author considered it possible that a short upward leader was initiated from the research mast top during the approach of a descending branched leader, and that this traversed the intervening distance of about 23 m (Table 4.2) to intercept a leader branch, at about the same time as another branched element neared the ground some 300 m away - thereby leading to an instance of simultaneous grounding -a phenomenon which has also be observed by Hagenguth[62].

In the second instance (Flash 28), both remote still cameras photographed a ground flash which struck the ground some 650 m away from the research mast and which exhibited a pronounced branch above the mast. The finely branched lower end of this major branch is clearly evident in the associated CCTV video frame (as shown in Appendix 3A). Of particular interest however, is the presence also of a faintly luminous channel extending about 60 m above the research mast and presumably developing upwards from the mast. In this instance, the author considers that this upward leader was initiated from the mast top during the approach of the charged leader branch (as envisaged analytically in Appendix 4A), but that the relative velocities of the upward and downward leaders were such that interception was not achieved before the remaining leader elements reached the ground and discharged the flash.

In ...../81

In summary therefore, the author considers that the degree and extent of leader branching is an important contributory influence in determining the final point of flash termination - the primary effect being to increase the effective or prospective area of influence over which an upward connecting leader may be initiated, for a given flash.

4.7 A concept of attractive radius

In the course of the analytical approach presented in Section 4.5 (as well as in Appendix 4A), an attractive radius R_a was introduced to represent the effective area over which upward leaders which had been initiated from a given structure during the approach of a descending leader, might intercept that downward leader and cause flash termination upon the structure. The results presented for an analysis of the research mast situation indicated that this attractive radius was sensitive to the relative velocity ratio of the downward and upward progressing leaders, but was comparatively independent of the magnitude of charge present on the descending leader -except for relatively small values of charge.

The concept of structure equivalent attractive radius may also be approached from a different point of view - as in fact has been carried out previously by the author[21], in an examination of flash incidence to tall structures. In this exercise, the incidence of upward and downward flashes was studied separately, together with height dependencies, for a variety of structures in different regions of the world. Although it was found that there was a more dramatic increase in the incidence of upward flashes as structure height was increased, (attaining over 90% upward flash incidence on structures in excess of 400 m), the associated data also indicated a height dependency in the incidence of downward flashes and it was observed that the trend through these data could be approximated by the empirical relation;

$$N_D = 8{,}33 \times 10^{-4} H_s^{1{,}22}$$

in a region experiencing an annual ground flash density $N_g = 1\ km^{-2}yr^{-1}$, where N_D = average annual number of downward flashes to the structure and H_s = structure height in m.

Defining an equivalent effective downward flash "collection area" A for a given structure, as is common practice in lightning protective concepts, and expressing A in terms of an attractive radius R_a, as

$$A = \pi R_a^2$$

it is evident that the average annual incidence of downward flashes N_D

experienced ...../82

experienced by the structure may be stated as:

$$N_D = A.N_g = \pi R_a^2.N_g \times 1 \times 10^{-6}$$

where N_g is the average annual ground flash density in the region of the structure.

Therefore, the above two relations for N_D may be combined to yield an empirical expression for R_a in terms of the structure height H_s, viz:

$$R_a = 16,3\ H_s^{0,6}$$

when R_a and H_s are expressed in m.

A comparison of this expression with the trend of the relation $R_a = 2H_s$, shows reasonable agreement for values of $H_s < 400$ m[21]. (The relation R = 2H has long been adopted as a simple rule in practical implementation of lightning protective concepts[12].)

The above relation for downward flash incidence was derived from an analysis of data describing the average incidence of flashes to a variety of structures of differing heights. In practice, when considering a specific structure, one must take account of the stochastic nature of ground flash incidence over comparatively short periods of analysis. Over such limited periods, the Poisson distribution P(n) has proved effective in accounting for the observed incidence of flashes to small samples of structures - as shown, for example by Golde[12] and Anderson[63].

This may be illustrated by consideration of the observed incidence of downward flashes on the research mast, which, as shown by the data presented earlier in Table 3.1, comprised 15 downward flash events of which 14 finally terminated on the mast - over a 6 year period of recording.

The probability P(n) that a given area A will be struct exactly 0, 1, 2, 3 .... n times over a given period of analysis T, may be expressed by the Poisson relation[63]:

$$P(n) = \frac{z^n}{n!} \exp(-z)$$

where z = average number of strokes to the area, given by $z = T.A.N_g$ and T = period of analysis (in years); N_g = annual regional ground flash density.

Therefore, assuming that the incidence of downward flashes to the research mast may be accounted for in terms of an equivalent collection

area ...../83

area A, having an attractive radius R_a, the above distribution may be evaluated to estimate the possible incidence of flashes, as a function of different values for R_a, over a sample period of 6 years.

This has been carried out - taking a value of $N_g = 7{,}0\ km^{-2}yr^{-1}$, which represents the average ground flash density observed in the Pretoria area over the past 10 years[64]. The results are shown in Figure 4.11 and suggest that the observed incidence is best accounted for (i.e. with maximum probability) in terms of an attractive radius R_a of about 325 m. (It is still recognised however, that there is a very low probability of the mast having behaved as a structure having an equivalent attractive radius of only 100 m, or even 200 m.)

In the earlier examination of the characteristics of flashes to tall structures and the associated influence of structure height, the author also derived the following empirical relations[16][21] for the annual incidence of flashes of all types to structures, as well as for the relative percentage of upward flash events:

$$N_F = 0{,}041 \exp (0{,}015\ H_s)$$

$$P_u = 68{,}2 \ln (H_s) - 315{,}5$$

where N_F is the average annual incidence of flashes of all types - normalised to a ground flash density $N_g = 1\ km^{-2}yr^{-1}$; and P_u is the percentage of upward flash events. H_s is the structure height in meters.

From the data presented earlier in Table 3.1, the following values for N_F and P_u are obtained from the observed research mast performance, over the full period of study, viz:

$N_F = 0{,}6$ (flashes/year per $N_g = 1\ km^{-2}yr^{-1}$)

$P_u = 29\%$

In terms of the above two relationships therefore, this yields values for the research mast effective height H_s of 181 m and 158 m respectively, or an average of about 169 m.

(Note: In the tall structures analysis[16] the author found it necessary to introduce the concept of "effective height" - as has also been used by Pierce[65] for example, to take account of those structures whose performance in terms of flash characteristics and incidence - when viewed against the perspective of the global survey of structures - did not correspond with what might be anticipated from their actual structure height. This was particularly the case for mountain-top structures, or very slender structures, which would have higher field intensification factors than the average structure.)

Figure 4.11 ...../84

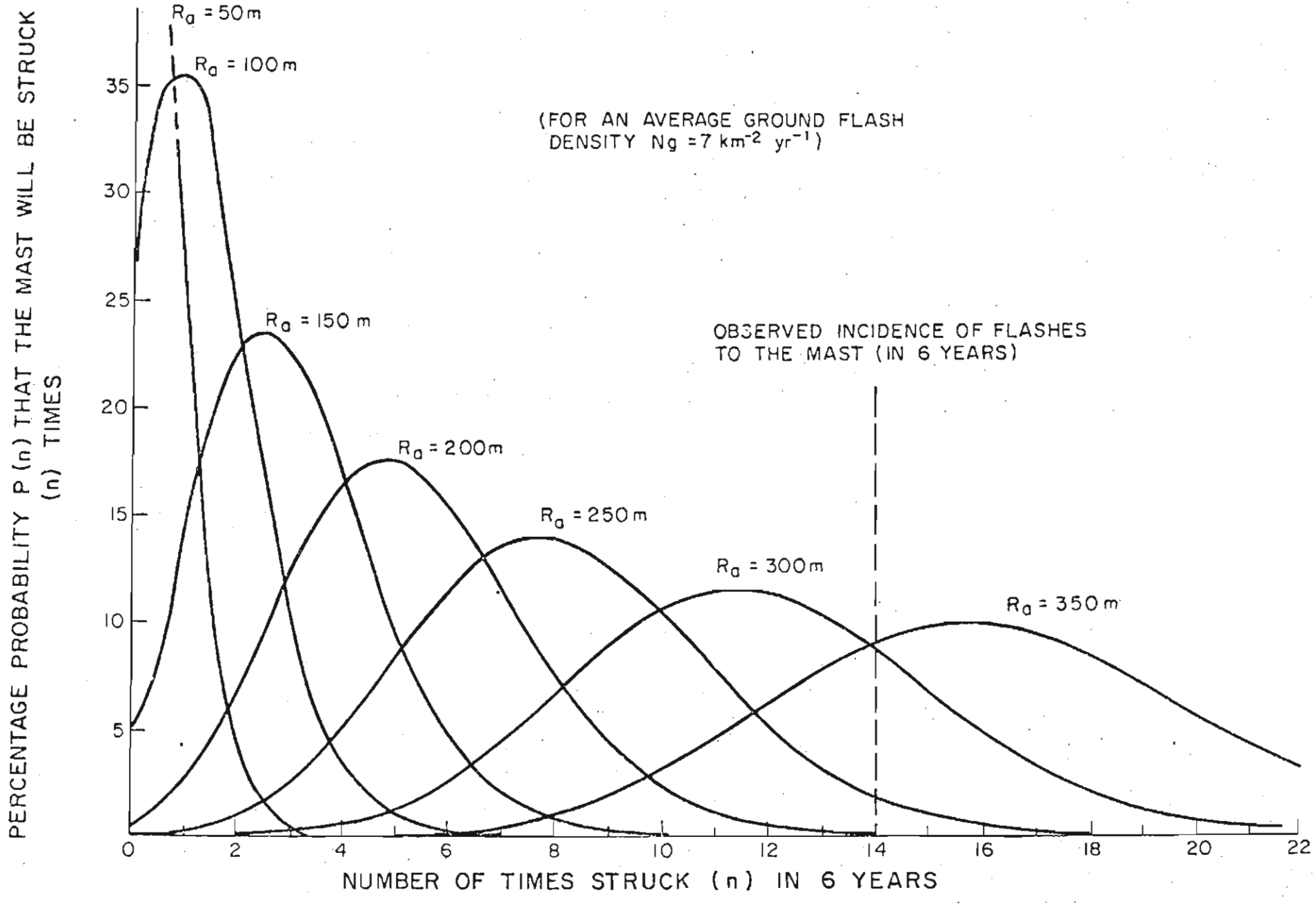

FIGURE 4.11

PREDICTED INCIDENCE OF DOWNWARD FLASHES TO THE RESEARCH MAST

As noted elsewhere by the author[16], it is considered not unreasonable therefore to assign an effective height to the research mast, which is higher than the structural height, since this mast has an unusually high structural slenderness ratio compared to the tall chimneys, or broadcast antennae, which comprise the bulk of structures in the global survey.

This being the case, and taking a value H_s = 169 m for the research mast, the above estimate of effective attractive radius R_a = 325 m implies the relation;

$$R_a \approx 1{,}9\ H_s$$

This result is in accord with the earlier observation that the global trend approximates the relation $R_a = 2H$, and suggests that there is a general consistency in conclusion, as far as the research mast is concerned, whichever approach for estimating attractive radius is adopted.

4.8 Summary and general discussion

In the introduction to this chapter, it was noted that the generally accepted definitions of striking distance are based upon the attainment by the downward leader, of a point of discrimination at which the potential strike point upon the ground is determined. It was also noted that empirical expressions relating striking distance D_s and prospective peak current I are widely assumed as being applicable in electrogeometric techniques of analysis for practical systems; viz:

$$D_s = K(I)^b$$

Thereafter, a photographic and analytical technique was described whereby attempts were being made to measure the striking distances of flashes to the research mast and to relate these to the recorded values of peak current flow in the mast. This technique assumed the initiation of an upward connecting leader from the mast at an interim stage in the descent of the downward leader, and defined the striking distance as that distance at which the progression of the downward leader first assumed a persistent orientation toward the point of interception with this upward leader. This implies therefore, that an element of the descending leader may experience a minor deflection toward the upward rising leader and that the striking distance is determined from this point of deflection.

A clear understanding of the concept of striking distance is further complicated by a consideration of the analytical approach presented earlier

in ...../86

in this chapter. In this analytical study, the striking distance was defined in terms of the distance between the descending leader and the prospective strike point, at that stage when the upward connecting leader is initiated from this point - i.e. on the basis of the required distance of approach of the charges in the leader before ionisation inception field gradients are attained at the prospective strike point.

The analytical approach also showed that attainment of the striking distance (expressed in terms of the above concept) does not automatically lead to flash termination upon the point from which the upward leader developed. This is determined by the relative velocities of approach of the downward and upward leaders and, dependent upon the associated velocity ratio, final termination of a flash upon a structure is determined jointly by the attainment of the required striking distance and by the entry of the descending leader into an equivalent collection volume in the vicinity of the structure. A concept of attractive radius was introduced to express the equivalent area over which the above collection volume was effective (for a particular velocity ratio). This approach also indicated that the analytically determined values of striking distance were proportional to leader charge magnitude and thus, (through a suitable relationship which took account of the discharge current waveform), were also dependent upon the peak current magnitude - in contrast to the values of attractive radius, which remained relatively insensitive to variations in charge magnitude.

Thereafter, the situation was further complicated in an extension of the analytical approach which demonstrated that the effects of the distribution of leader charge into the generally branched structure of the descending leader, could lead to the potential attainment, independently, of several prospective striking distances at a variety of positions (or structures), on the earth in the vicinity of a descending leader. It was suggested therefore, that the final flash termination could be determined by the interception of one (or, on occasion, more) competing upward rising leaders, with branched elements of the downward leader, and it was noted that two recently observed flash events to the research mast depicted features in support of this concept.

The author considers that the above concepts and definitions of striking distance, as well as their possible inter-relationships, may be clarified by a re-consideration of the final stages of downward leader progression toward a structure on the ground.

The ..... /87

The relevant stages are shown schematically in Figure 4.12. (The flash depicted here is derived from a photograph of flash No. 771009/27 to the research mast.)

While in principle the general path taken by a downward leader is broadly determined by the electric field direction between cloud and ground, and, on average therefore, is approximately vertical, it has been shown (by Hill[59], for example) that the detailed channel path is essentially random - being probably influenced mainly by the presence of localised pockets of space charge in the air between cloud and ground. In the final stages of this progression toward the ground, the author considers that three decisive stages may be identified - at least conceptually - as follows:

(a) Point of upward leader initiation

It is known from lightning photography[66] that even flashes to flat ground (such as a sandy beach), involve the interconnection of the descending leader with an upward rising leader. As discussed in the preceding sections therefore, the attainment of a sufficiently close approach of the downward leader to initiate development of this upward leader, represents an important point in the flash process, since it first allows the possibility of determining the prospective point of strike. Since this stage closely resembles the 'point of discrimination' embodied in the general definition, the author proposes that the intervening distance between the leader and the potential strike point be termed the striking distance (D_s). It is clear also from the preceding discussions that the attainment of this distance depends upon many factors, including:

(i) the distribution and magnitude of charge upon the leader.

(ii) the complex branched structure of the leader.

(iii) the presence, as well as geometry, and hence, field intensification factors of structures on the ground; (the analytical approach showed that striking distances to structures are directly proportional to the relevant field intensification factors).

(iv) the critical field gradients required for initiation of a progressive upward leader, which could vary, depending upon the geometry of a structure and/or the occurrence and presence of corona and space charges[58].

It is evident from point (iii) above (and from Appendix 4A) that very tall structures (having high field intensification factors) could

Figure 4.12 ...../88

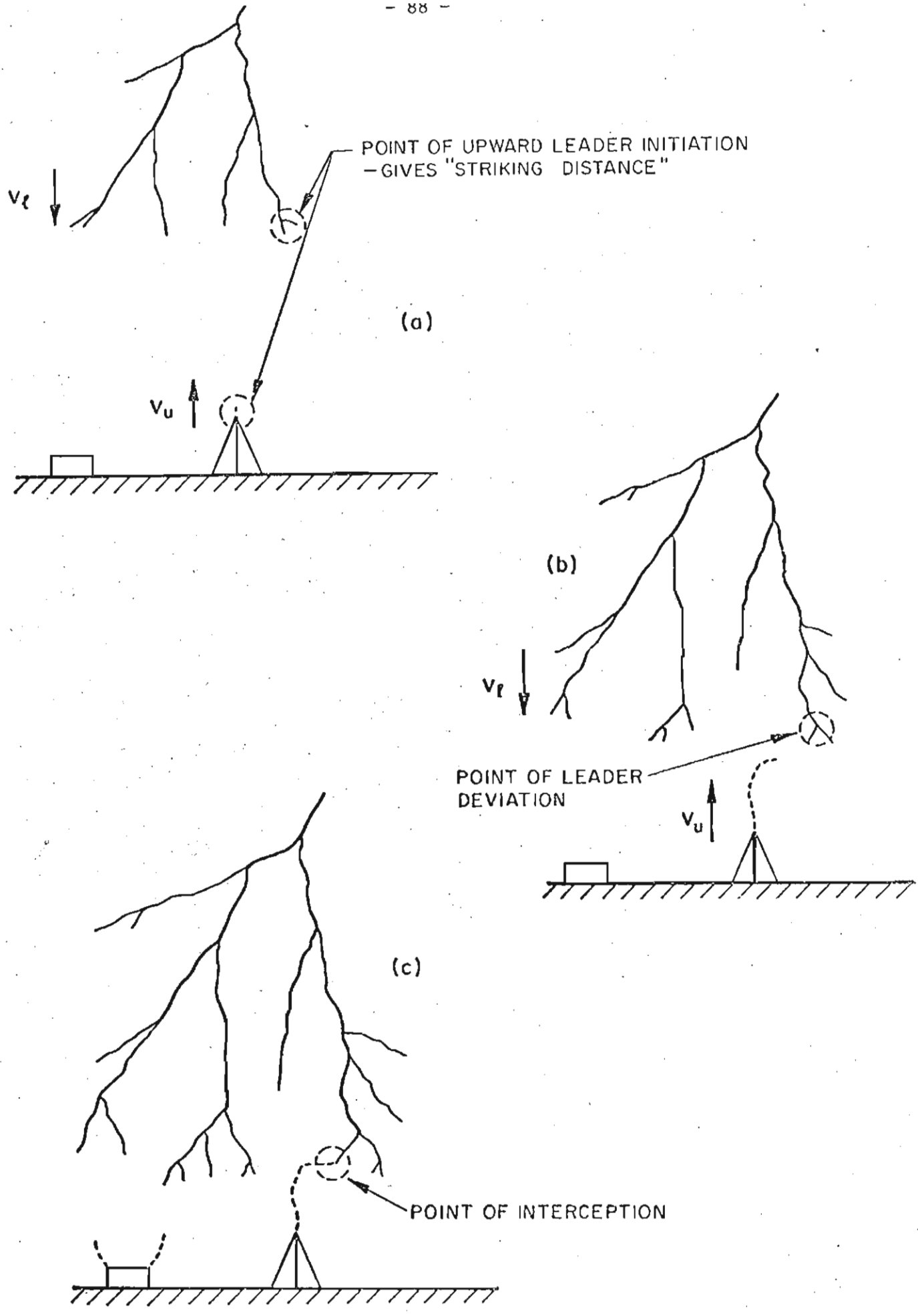

FIGURE 4.12

STAGES IN LEADER PROGRESSION TOWARD A STRUCTURE ON THE GROUND.

be associated with extremely long striking distances (in excess of 1 km) -leading to the initiation of upward leaders from these structures before the descending leader has emerged from the cloud, for example. On very prominent structures, the movement of charges within the cloud (in the form of cloud flashes) may already cause sufficient field enhancement in the vicinity of a structure to initiate an upward leader - as has been found by Berger[23]. Thus it is not unexpected that the observed incidence of upward flash events increases dramatically as structure height increases[16].

A stage has therefore been identified in the progress of the downward leader (advancing at an average velocity v_ℓ), that corresponds with the initiation of one, or more upward rising leaders (having velocities v_u) from structures on the ground. The attainment of this striking distance however, does not represent an exclusive requirement for determination of the potential point of strike, and the advance of the leader must be further examined.

(b) Point of leader deflection

It is considered probable that the initial path taken by upward rising leaders will be determined by the electric field direction in the immediate vicinity of the structure itself - usually highly divergent at the top of a tall structure - and thus will tend to be vertically oriented, as in fact was found for many of the flashes on the research mast.

Thereafter, the upward leader path is likely to become influenced by the intense electric fields developing between the upward and descending leaders. The charge magnitudes raised in the upward leader are small[9] compared to those distributed upon the descending leader and the former is likely to experience deflection before the latter. However, especially in the case of a branched leader, a stage could well be reached when an element of the descending leader becomes deflected toward the rising upward leader. (Preliminary model studies by Dellera et al[67], suggest in the extreme case of an unbranched linearly charged leader, that the intervening distance at which deflection of the downward leader takes place is approximately $7.R_c$, where R_c is the corona radius around the upward leader tip.)

The ...../90

The identification of this point of deflection of the downward leader (or final orientation), was the basic premise of the measurement technique adopted for the study of the three-dimensional geometry of flashes to the research mast - as discussed earlier in section 4.2. The author proposes therefore that the resultant measured values of 'striking distance' be re-defined as deviation distances (D_d).

It is evident that these deviation distances (D_d), will either correspond to, or be shorter than the true striking distances (D_s), and will depend upon the following factors:

(i) in particular, the spatial extent and degree of leader branching.

(ii) the leader approach angle.

(iii) the magnitude and distribution of charges on the relevant leader branches.

(c) Point of interception

Despite attainment of both the striking and deviation distances, it is clear from the earlier discussions that the final point of strike is only determined positively when the upward leader intercepts the downward leader. This then defines a third decisive distance -the so-called interception distance (D_I), which will obviously be less than either (D_s) or (D_d). In physical terms, this act of interception is equivalent to the 'final jump' process observed in long-spark studies and represents attainment of an average field gradient, between the two approaching leaders, in excess of a critical value - considered to be of the order of 500 kV/m[7][31].

4.9 Concluding remarks regarding the concept of striking distance

Based upon the preceding discussions therefore, the author considers that the following conclusions may be noted:

(i) A unique 'point of discrimination' cannot positively be identified in the progression of a downward leader toward the ground or toward structures on the ground. In fact, termination of a flash to a particular point depends upon the dual requirements of approach by the descending leader to within at least striking distance (i.e. leading to initiation of an upward leader), together with entry by the descending leader (or an element thereof) into an effective collection volume within which interception of the two leaders can take place.

(ii) ...../91

(ii) Specific values of striking distance may be estimated for a particular structure. These values are directly proportional to the magnitude and distribution of charge on the leader, and depend as well on the dimensions of the structure (including also its field intensification factor) - being thus specific to the structure and not generally applicable.

(iii) Preliminary expressions have been presented for the research mast, which relate striking and interception distances to the prospective flash peak current amplitudes. These relations show a reasonable agreement with the trend of the first results emerging from measurement of deviation and interception distances for recorded flashes to the research mast. This agreement is sensitive however, to assumptions regarding the correlations between leader charge and peak current amplitude and, in the absence of further data relating these parameters, may only be fortuitous.

(iv) The actual incidence of flashes to structures is not accountable simply in terms of striking distance considerations - due to the dual requirements stated in (i) above - but may on average be expressed in terms of a structure equivalent attractive radius which, for many structures, may be approximated by twice the structure height.

(v) The incidence of flashes to structures - apart from being influenced by the degree of leader branching - is dependent upon the relative downward and upward leader velocities and there is an evident need for additional data in this regard. The scanty available data[68] suggests similar orders of magnitude for both velocities and the estimates derived from consideration of the research mast situation support this possibility, to the extent that an average velocity ratio (v_ℓ / v_u) of about 1,1 is indicated.

The implications of these conclusions for practical engineering studies are discussed further in Chapter 6.

CHAPTER 5

THE STUDY OF ADDITIONAL LIGHTNING AND THUNDERSTORM PARAMETERS IN THE TRANSVAAL REGION

5.1 Introduction

The previous three chapters have concentrated on measurement techniques and the associated results obtained in the course of studying several of the more basic electrical engineering parameters of the ground flash.

In this chapter, work is described which is concerned with a more general characterisation of the local thunderstorm electrical environment - or storm climatology, (defined in terms of electrically measured parameters) - within which the direct measurements of lightning parameters are being carried out.

There are several aspects to this work and the principal objectives of this phase of the research programme were as follows:

(a) Study of the incidence and characteristics of multiple stroke ground flashes.

(b) Study of thunderstorm electrostatic field characteristics at ground level.

(c) Characterisation of the regional lightning and thunderstorm activity using relatively simple instrumentation and analytical techniques.

The above three aspects will be discussed in turn.

5.2 The incidence and characteristics of multiple stroke ground flashes

There were two primary reasons for studying multiple stroke flashes: - firstly, the occurrence of a series of discharges in close succession obviously presents an additional burden to any electrical engineering or lightning protective system, which has thus to be capable of withstanding the effects of such a process. Comprehensive data under local conditions were therefore required in order that the design of protective systems could be optimised; - secondly, several authors had raised the possibility that the incidence of multiple stroke flashes could vary considerably through the various climatic regions of the world[15]. It was considered desirable therefore, that the local situation be defined with comprehensive data, (which could then be compared with results from measurements elsewhere in the world) and that simple measurement techniques be evaluated for obtaining these data.

5.2.1 ...../93

5.2.1 Measurement techniques

In the course of lightning research over the years a variety of instrumentation approaches have been adopted for studying the characteristics of multiple stroke flashes. These have ranged from time-resolved electrostatic field change recordings [73], or high speed photography[22], to direct measurements of lightning stroke currents - as previously discussed.

More recently, the use of closed circuit television (CCTV) video recording techniques, despite some limitations, has also proved effective for recording multiple stroke flashes[33][74]. As noted in Chapter 2, a CCTV system had previously been established for studying flashes in the immediate vicinity of the research mast. Although of necessity this unit had a comparatively restricted field of view, a considerable number of flash recordings was obtained over several thunderstorm seasons.

The limitations of CCTV techniques have previously been discussed by Winn et al[33]. Apart from a relatively poor spatial resolution, (being limited by the line resolution of the camera and tape recorder), the principal disadvantages are the time resolution (which is limited to the system framing rate of 50 Hz - or an equivalent framing interval of 20 ms per frame), and a degree of remanent image persistence which influences the determination of flash durations. In the local system, as observed also by Brantley et al[75], it was found that the decay of image persistence was approximately exponential with a time constant of about 40 ms (or two frames). This had to be taken into consideration therefore, in determining flash durations from video recordings.

The CCTV system was operated routinely (via the radio remote control system) whenever lightning activity was observed within about a 5 km range of the research mast. The resultant video tape recordings were analysed by identifying and recording the number of single stroke flashes, and by noting the number of video frames between stroke images in the event of multiple stroke flashes. In the latter case, flash durations were also estimated by integrating the previously noted interstroke intervals over the whole flash.

However ...../94

However, it was considered that the above approach, in common with most other techniques for studying the incidence of multiple stroke flashes, was inevitably selective, in that the samples of data obtained would normally have been recorded during the most intense periods of thunderstorm activity.

Steps were taken therefore, by the author and his collegues, to develop an alternative technique which would allow measurements of multiple stroke incidence to be continued automatically over extended periods of time - in an attempt to obtain data which would be fully representative over a whole thunderstorm season.

The resultant instrument is termed the multiple stroke discriminator (MSD) and has been fully described elsewhere[76]. (Basically, it comprises the combination of a proven ground flash counter - the RSA10[77] - together with an electronic circuit which classifies subsequent strokes in serial order, as they occur. The unit has a basic subsequent stroke interval resolution of 10 ms.)

A prototype version of the MSD was operated continuously through two storm-seasons (over the 1976/77 period) in conjunction with routine operations of the CCTV recording system in the same area.

5.2.2 Results

The comparative data on multiple stroke incidence obtained using both the above systems, are depicted in Figure 5.1. The two sets of results compare reasonably well, although, apart from flashes having only two strokes, there is a general tendency for the CCTV results to indicate a higher subsequent stroke incidence. The effects of video image persistence after first strokes (which are almost invariably much brighter than subsequent strokes), coupled with a frame resolution of only 20 ms, make the resolution of second strokes on the CCTV system rather difficult and it is believed that this may account for the comparatively low incidence of 2 stroke flashes obtained using this system.

The cumulative frequency distributions resulting from analyses of the CCTV interstroke interval data, as well as total flash duration measurements, are given in Figures 5.2 and 5.3. As found also by Anderson[9], these distributions may be approximated by the log-normal distribution, as shown in these figures. Median values of 50 ms and 189 ms are indicated for interval and duration respectively, while the related 99 percentile limits are about 400 ms (for interval), and 1 500 ms for duration.

Figure 5.1 ...../95

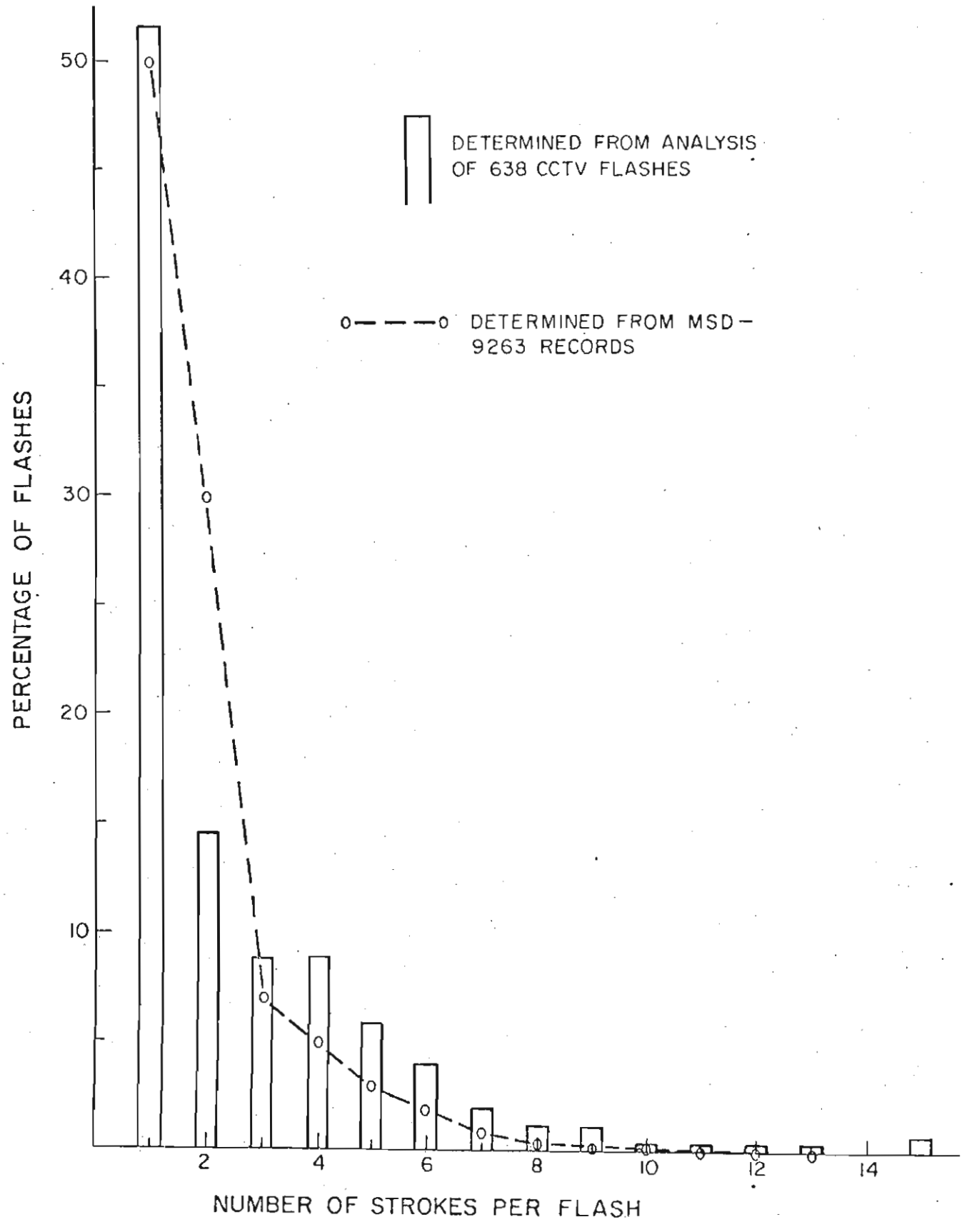

FIGURE 5.1

INCIDENCE OF MULTIPLE STROKE GROUND FLASHES

Figure 5.3 ...../96

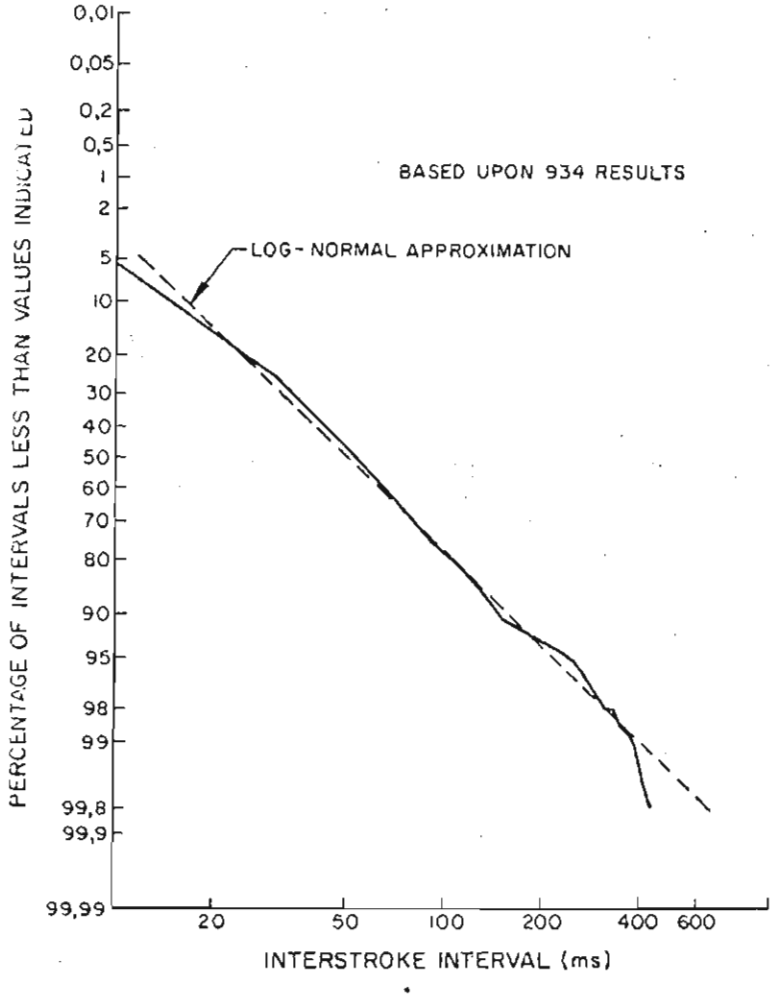

FIGURE 5.2

FREQUENCY DISTRIBUTION OF INTERSTROKE INTERVALS — DETERMINED FROM CCTV RECORDINGS

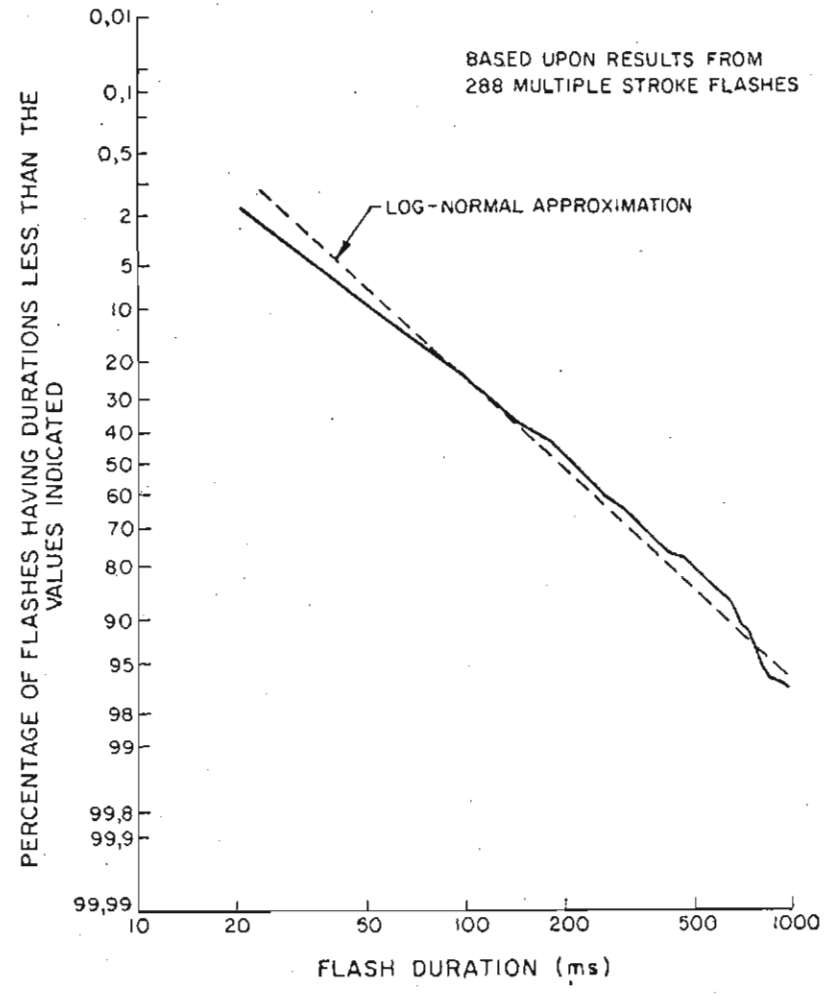

FIGURE 5.3

FREQUENCY DISTRIBUTION OF MULTIPLE STROKE FLASH DURATIONS - DETERMINED FROM CCTV RECORDINGS

5.2.3 Discussion

A variety of data are available from several regions of the world (including some earlier results from South Africa) and these provide a perspective against which the above results may be compared. This is summarised in Table 5.1.

TABLE 5.1: COMPARATIVE DATA ON MULTIPLE STROKE INCIDENCE AND CHARACTERISTICS

(a) Incidence:

Observer	Region	No. of flashes	Mean No. of strokes/flash	Single stroke flash incidence
Schonland[1]	South Africa	1 800	4,2	25%
Anderson[9])	Rhodesia	1 405	3,4	36%
Berger[22]	Switzerland	1 026	1,8	76%
Carte[78]	South Africa	877	1,9	65%
Brantley[75]	Florida	206	2,4	42%
Malan[73]	South Africa	530	3,5	13%
Overall mean results			3,1[1]	45%[2]
Eriksson (CCTV)	South Africa	638	2,5	51%
(MSD)	South Africa	9 263	2,0	50%

Notes

(1) A weighted mean, taking account of the sample sizes.

(2) Determined by combining all the individual cumulative distributions on stroke incidence into a "global" curve. (Figure 5.4).

(b) Interstroke interval

Observer	Region	Interstroke intervals for the cumulative percentage values		
		10%	50%	90%
Anderson[9]	Rhodesia	10 ms	35 ms	150 ms
Berger[22]	Switzerland	10 ms	33 ms	104 ms
Brantley[75]	Florida	-	70 - 80 ms	-
Cianos and Pierce[75]	Global review	10 - 25 ms	35 - 80 ms	90 - 280 ms
Schonland[1]	South Africa	15 ms	45 ms	150 ms
Eriksson	South Africa	16 ms	50 ms	155 ms

(c) ..... /98

(c) Flash duration

Observer	Region	Flash durations for the cumulative percentage values			Remarks on distribution
		10%	50%	90%	
Malan[73]	South Africa	45 ms	200 ms	460 ms	Including single stroke flashes
Kulijew[80]	USSR	125 ms	430 ms	800 ms	All flashes
Anderson[9]	Rhodesia	-	67 ms	453 ms	Including single stroke
Anderson[9]	Rhodesia	20 ms	177 ms	543 m	Excluding single stroke
Berger[22]	Switzerland	0,4 ms	13 ms	400 ms	Including single stroke
Berger[22]	Switzerland	50 ms	180 ms	600 ms	Excluding single stroke
Cianos and Pierce[79]	United Kingdom	-	180 ms	-	Unknown
Eriksson	South Africa	58 ms	189 ms	608 ms	Excluding single stroke flashes

It is notable that the new data on interstroke intervals and flash durations compare very favourably with the trends of measurements elsewhere in the world and there is a general consistency in the resultant median values. (Tables 5.1(b), (c).)

On the other hand, the new data on multiple stroke incidence (from both the CCTV and MSD measurements) suggest a marginally lower number of strokes per flash than has been obtained by several other workers (Table 5.1(a)). Anderson and the author have combined the available data on multiple stroke incidence to derive a "global" cumulative frequency distribution of the number of strokes per flash[20]. This is shown in Figure 5.4, together with the results obtained using the CCTV and MSD systems, and depicts a generally higher multiple stroke incidence than indicated by the new measurements.

The different distributions and measurement techniques employed by various workers have been discussed elsewhere by Anderson and the author[20] and it is considered that the dispersions amongst various sets of data on multiple stroke incidence are at least in part attributable to varying sensitivities amongst the different measurement techniques, (i.e. electrostatic field change studies, revolving camera, or CCTV systems, etc.). Both photographic and CCTV techniques would have

Figure 5.4 ...../99

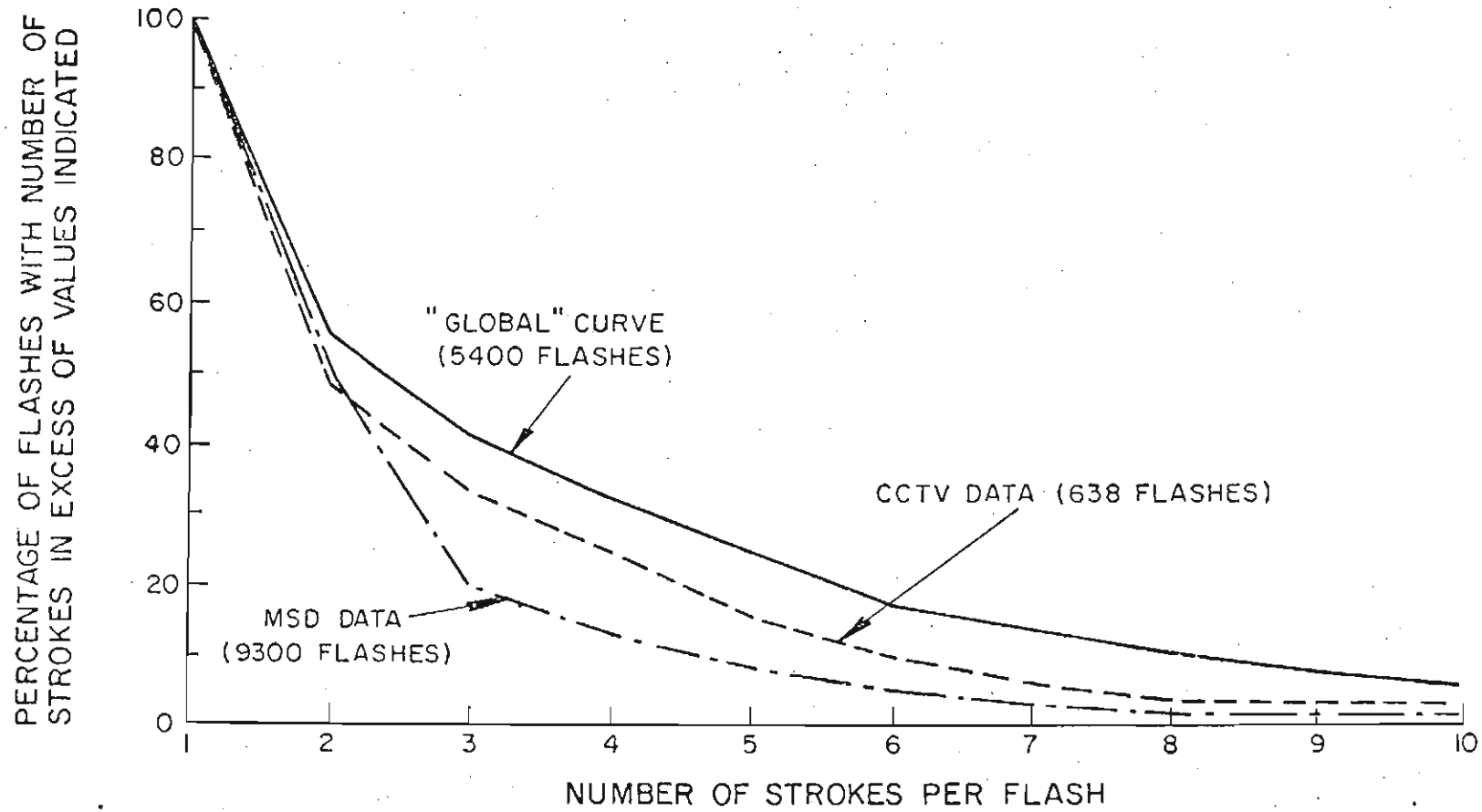

FIGURE 5.4

CUMULATIVE FREQUENCY DISTRIBUTIONS OF THE NUMBER OF STROKES PER FLASH

difficulty ...../100

difficulty in resolving faintly luminous, or distant subsequent strokes, while it is also conceivable that the MSD system may have a different effective range to subsequent strokes[76] (which would involve lower magnitudes of impulse charge transfer), compared to the normally more powerful first strokes.

It is considered probable therefore, that the data on multiple stroke incidence obtained using both the CCTV and MSD systems - as presented in Figures 5.1 and 5.4 - may require adjustment to take account of these differences in sensitivity to first and subsequent stroke events. At this stage however, additional research is required to provide an adequate basis for such adjustments.

It is also possible that the incidence of multiple stroke flashes may vary with the degree of thunderstorm intensity and the author has in fact previously presented preliminary data from the MSD, which suggest a tendency toward a higher incidence of single stroke flashes in storms of reduced activity[81]. It is not unexpected therefore, that the MSD data, being drawn from measurements over a complete season rather than only from selected active storms - such as those providing the CCTV data, may well show a lower multiple stroke incidence, as in fact is the case in Figure 5.4.

In summary therefore, the new data on multiple stroke flash characteristics are wholly consistent with the results of previous work - as far as inter-stroke intervals and flash durations are concerned, - and this suggests that the latter parameters of lightning may vary little through various regions of the world.

The new data on multiple stroke incidence, however, indicates a marginally reduced incidence compared to previous results, but additional research will be required to clarify whether these differences arise only as a consequence of different measurement techniques (having varying sensitivities), or whether global, seasonal, and/or storm effects are also involved.

5.3 Study of thunderstorm electrostatic field characteristics at ground level

5.3.1 Introduction

Measurements of thunderstorm electrostatic fields at ground level were included in the research programme for two main reasons:

(a) ..... /101

(a) in order to provide an additional index of thunderstorm climatology in the area of concern, and

(b) in order to accumulate comprehensive field data characterising local thunderstorm conditions, which could subsequently provide reliable basic criteria for development work on storm warning principles and devices.

5.3.2 Measurement technique

A variety of approaches is available for measuring atmospheric potential gradients - as reviewed for example, by Chalmers[82]. In practice, thunderstorm fields are usually measured with field mills[83], which have the advantages of stability (i.e. absence of drift over long periods), and an effective capability for reliable measurement of slow varying, or d.c. fields.

A prototype field mill of the type originally evolved by Smith[84] and subsequently employed by Berger[85], was under development within the NEERI and this was used for the local measurements. This field mill has an extended equivalent signal frequency range, which is achieved using complementary stator elements and balanced modulation[84], and employs synchronous switching of the clamping circuitry to provide polarity discrimination.

In the form used in these measurements, the inverted mode of operation was adopted, together with a linear scale of sensitivity up to a maximum field strength of ±28 kV/m.

Absolute calibration of the field mill was carried out in a parallel plate capacitor arrangement, while the form factor for the inverted configuration was determined from comparative recordings from a calibrated and flush mounted vertical-facing mill, which was located in the ground plane nearby. The absolute accuracy of these calibrations is estimated to be better than 10%.

Several field mills of this type were deployed at the various NEERI research stations in the Pretoria area, with between 1 and 5 mills being in operation on any particular thunderstorm occasion. The output voltages of these field mills were recorded on continuously operated chart recorders, with chart speeds of 50 mm per hour normally being used. This implies that the emphasis was upon continuous

recording ...../102

recording of the slowly varying thundercloud field strength magnitudes, rather than upon resolution of individual lightning flash field changes.

All field recordings were subsequently digitized upon an automatic plotting table and these data were then processed using a computer program developed by Kröninger[86].

The following parameters were defined and evaluated for each storm:

(i) Start-time and finish-time of storm activity - defined as those times when the electrostatic field strength first exceeded (and last reduced below), an absolute magnitude of 500 V/m.

(ii) Storm duration - defined as the sum of those periods between storm start and finish, during which the field intensity exceeded an absolute magnitude of 500 V/m.

(iii) Maximum positive and negative field intensities attained during each storm.

(iv) For both positive and negative field excursions, the total periods of time that the field exceeded each of the following intensities, 1 kV/m, 2 kV/m, 3 kV/m ..... 14 kV/m, for each storm.

These measurements were continued routinely for three storm seasons over the period 1973 - 1976 and a considerable body of data was accumulated. Individual storm records were evaluated in the above manner and the resultant parameters were collated on a seasonal basis - as well as over the full period of study.

5.3.3 Results and discussion

Typical examples of field recordings for a complete storm were shown earlier in Figure 3A-7. (In terms of a common convention in atmospheric electricity[82], the polarity of the electrostatic field is assumed to be positive when dominant positive charge is overhead.)

The predominating excursions of field during a storm, as shown in this example, may frequently be grouped into two phases of the storm lifetime;

- firstly, a period of intense lightning activity, when frequent reversals of polarity are often observed and,

- secondly ..... /103

- secondly, toward the end of the storm, when lightning activity has mostly ceased, and a period of steady, or slowly varying fields, is observed, during which one or more reversals may also occur.

These features of thunderstorm electrostatic field records have also been observed in American storm studies, (as discussed by Moore and Vonnegut[87] and illustrated in the records presented by Livingstone and Krider,[88]) with the second phase of the storm record often being termed the "end of storm oscillation" or EOSO.

No attempts have been made in the analyses of the local storm records to distinguish between the characteristics of each of these two phases of a thunderstorm, since the primary motivation for this work was to study the statistics of occurrence and the range of magnitudes of storm electrostatic field intensities, as observed at ground level.

The limiting effects of local point discharge currents from grass, bushes etc, on the development of the vertical potential gradient close to the ground are well known[89]. The screening influence of the consequent space charges between the ground and cloud (as discussed, by Moore and Vonnegut[87]), was recognised in this study therefore, and no attempts were made to relate the measured field characteristics to any cloud charge distribution models - even from multi-station measurements (as suggested by Mackerras[90], for example), due to the complexity of the situation.

A total of 461 storm records was obtained over the three years of measurement and the results of this analysis are summarised in Table 5.2.

Table 5.2 ..... /104

TABLE 5.2: SUMMARY OF RESULTS OF THUNDERSTORM ELECTROSTATIC FIELD INTENSITY MEASUREMENTS

Parameter	Seasonal Results			Overall results
	73/74	74/75	75/76	
Number of records	96	215	150	461
Maximum positive field intensities per storm:				
Mean ($\bar{E}$) - kV/m	3,4	6,1	7,1	5,9
Standard deviation (σ_E) - kV/m	1,9	4,1	4,9	4,3
Maximum negative field intensities per storm:				
Mean ($\bar{E}$) - kV/m	5,4	7,8	9,6	7,9
Standard deviation (σ_E) - kV/m	2,8	4,0	5,8	4,7
Storm duration - in terms of field intensities in excess of 500 V/m:				
Mean (hours)	2,9	2,6	1,9	2,4
Standard deviation	1,5	2,1	1,6	1,9

It is evident that the maxima of negative field excursions were generally higher than the positive, with overall mean values of - 7,9 kV/m and +5,9 kV/m being obtained for the distributions of maximum negative and positive field intensities respectively.

The individual distributions of these maxima are depicted in Figure 5.5, in which the tendency for negative field maxima toward higher levels of field intensity is supported.

The numbers of storms displaying field intensities in excess of various levels were separately analysed and the resultant probability distributions are shown in Figure 5.6, indicating a 50% probability of field intensities in excess of about +5,1 kV/m and -7,3 kV/m being attained in any particular storm.

Figure 5.5 ...../105

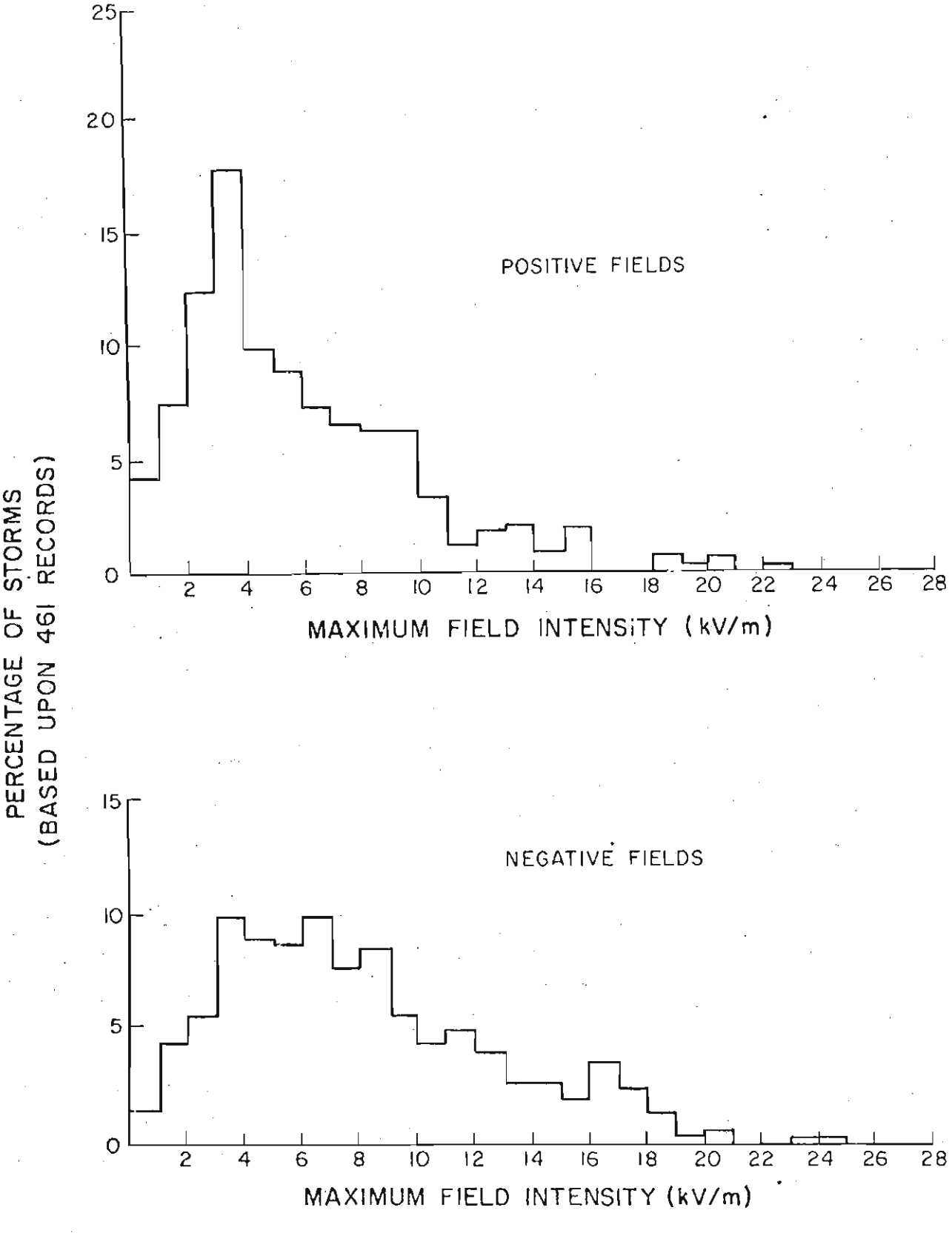

FIGURE 5.5

DISTRIBUTION OF THUNDERSTORM MAXIMUM ELECTROSTATIC FIELD INTENSITIES – AT GROUND LEVEL

Figure 5.6 ...../106

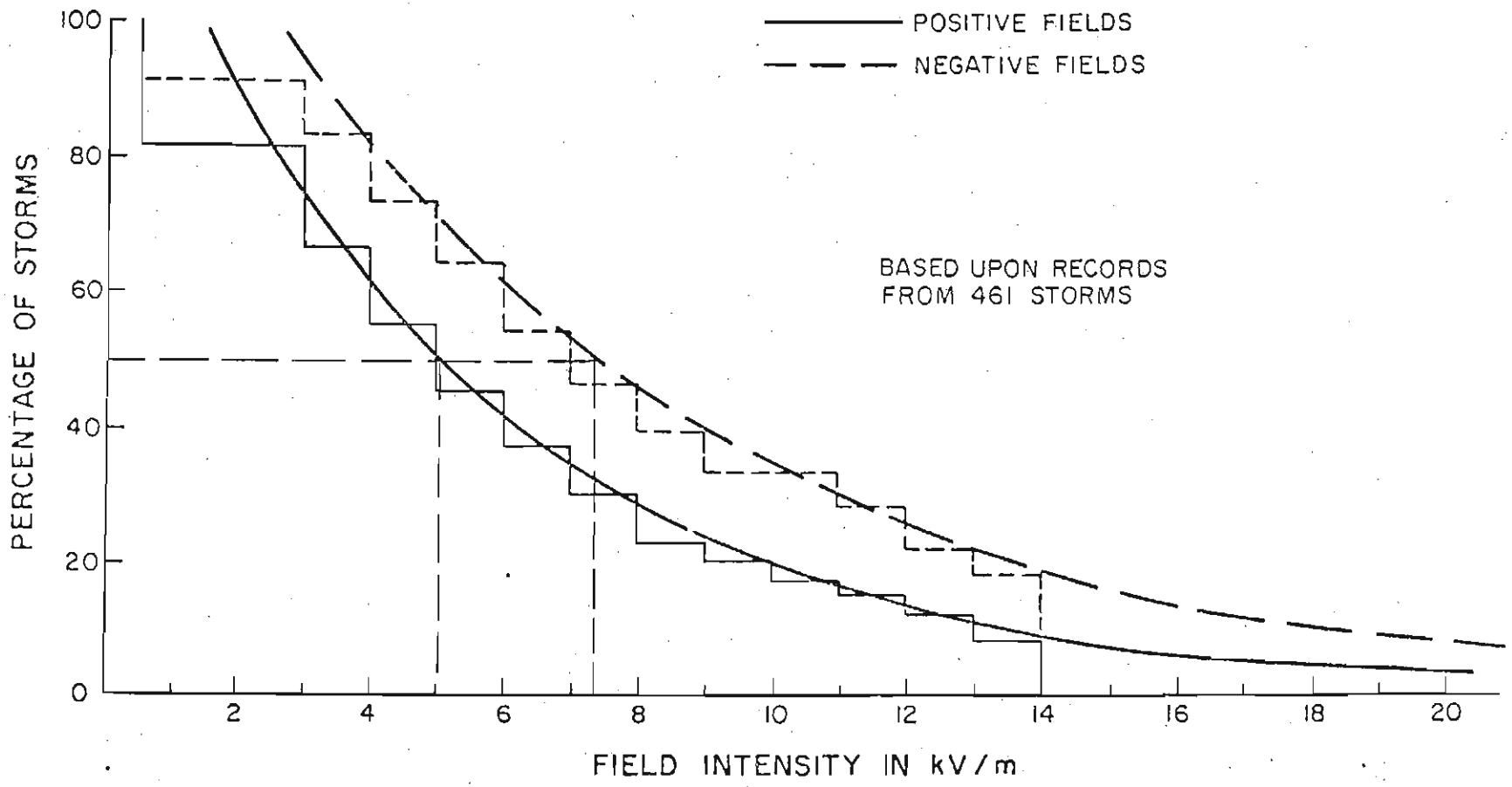

FIGURE 5.6

PROBABILITY OF THUNDERSTORM ELECTROSTATIC FIELDS EXCEEDING VARIOUS INTENSITIES — AT GROUND LEVEL

In ...../107

In general, the range of field intensities recorded is consistent with the results of other measurements[82] [87] [88] and it is apparent that less than 10% of storms attain surface field intensities in excess of 20 kV/m. In contrast with Anderson and Freier[91] however, who reported an almost equal probability of attaining field intensities of both 3 kV/m and 6 kV/m, the results in Figure 5.6 indicate a substantial order of difference in probabilities (about 30%) at this end of the scale.

Although it is recognised that a measurement of surface electrostatic fields is not sufficient to provide an adequate (or reliable) thunderstorm warning, the data and probabilities presented in Figures 5.5 and 5.6, being derived from a comprehensive sample of measurements over several years, provide valuable guidance in arriving at basic warning criteria. (By way of comparison, storm warning field intensity levels in the range 2 kV/m - 6 kV/m have been suggested by other workers[92]).

The summarised data given in Table 5.2 also indicate an overall mean storm duration of 2,4 hours (expressed in terms of the period during which the electrostatic field intensity was above an absolute value of 500 V/m). This value may be contrasted with average American values of 2,0 hours measured in Minnesota by Freier[93] (based on 10 years of data), and 1,8 hours, determined in Florida, by Livingstone and Krider[88], in each case also from using recordings of storm electrostatic fields.

The distribution of thunderstorm durations derived from the local recordings is shown in Figure 5.7 and indicates a low probability of exceeding 5 hours. This is confirmed by the associated cumulative frequency distribution of storm durations, given in Figure 5.8, which indicates that 95% of all storms had durations less than 5 hours.

In fact, it is found that much of the total period of thunderstorm activity involves electrostatic field intensities below 3 kV/m. This is shown by the results given in Figure 5.9, which depict the mean periods per storm during which various levels of field intensity were exceeded. For example, these data indicate that field intensities in excess of 5 kV/m persist on average for integrated periods of only 20 minutes and 32 minutes, for positive and negative fields respectively (i.e. equivalent to only about 14% and 22% respectively, of the average storm duration of 2,4 hours). This implies that storm maximum field intensities which, as noted earlier, have average values of +5,9 kV/m

Figure 5.8 ...../108

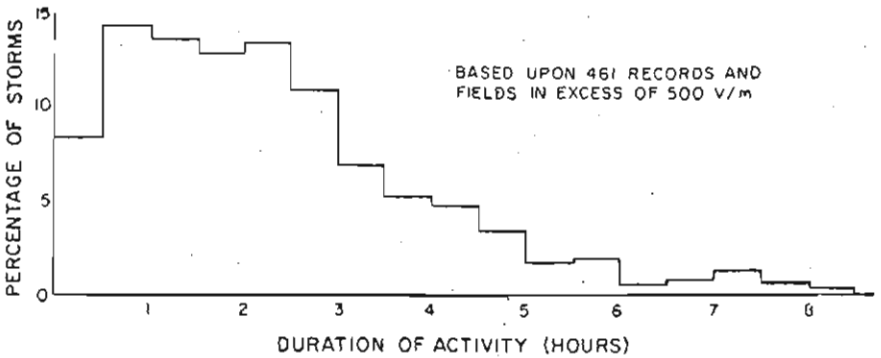

FIGURE 5.7

DISTRIBUTION OF STORM DURATIONS DETERMINED FROM ELECTROSTATIC FIELD INTENSITY MEASUREMENTS

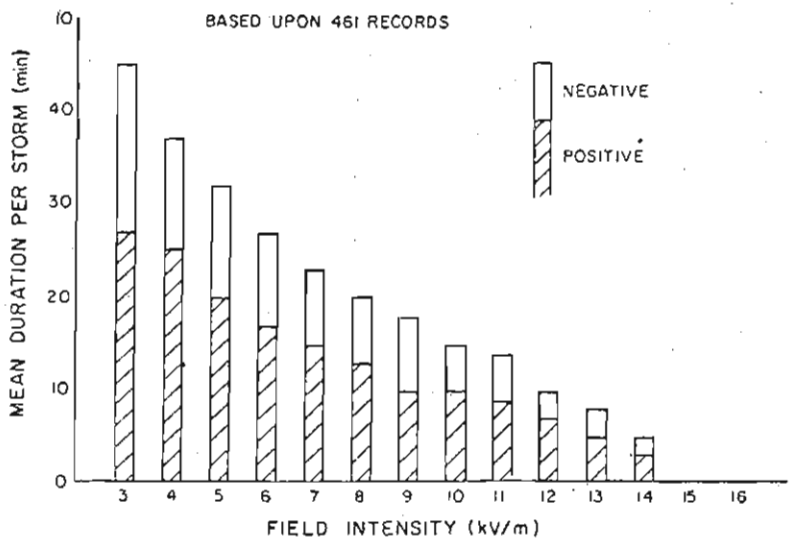

FIGURE 5.9

MEAN PERIODS PER STORM DURING WHICH VARIOUS LEVELS OF ELECTROSTATIC FIELD INTENSITY WERE EXCEEDED

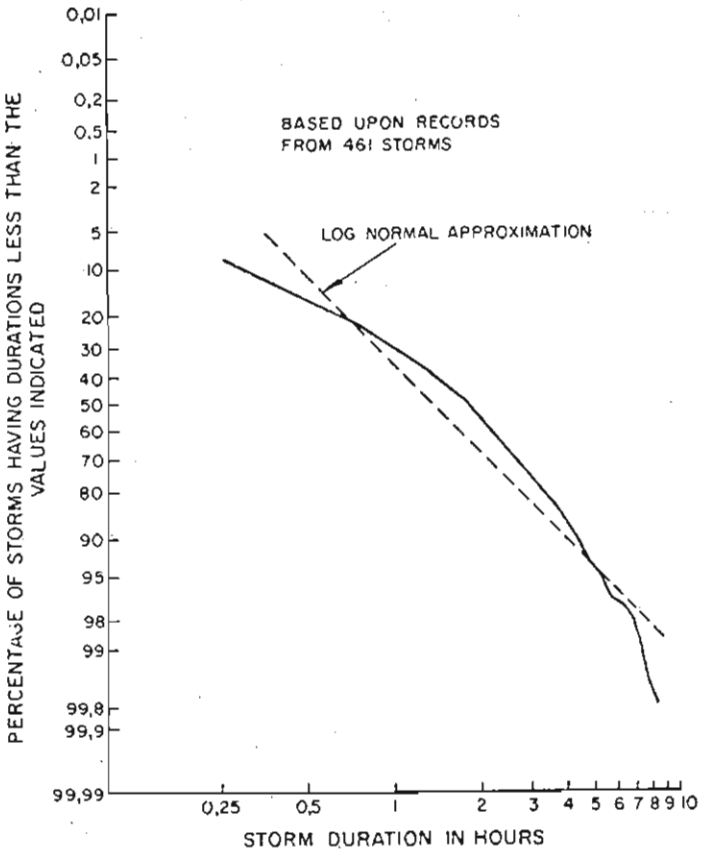

FIGURE 5.8

FREQUENCY DISTRIBUTION OF STORM DURATIONS DETERMINED IN TERMS OF ELECTROSTATIC FIELD INTENSITIES

and -7,9 kV/m, do not normally persist for more than a few minutes.

These data are again consistent with the preliminary observations on Florida thunderstorm characteristics presented by Livingstone and Krider[88]. They found typically that field intensities over the range 1 - 10 kV/m (both polarities) were present for cumulative periods of about 10 minutes or less, during each of the two main phases of storm activity. In addition, they observed a bias toward sustained negative polarity fields having average intensities in the range of 2-8 kV/m during the EOSO phases of the storms studied. This may well account for the fact that in the South African recordings, the negative field excursions generally persist longer than the equivalent positive fields - as shown by the data given in Figure 5.9.

In general, therefore, it would appear that the characteristics of thunderstorm electrostatic fields at ground level in the Pretoria region do not differ substantially from those associated with thunderstorms in several other geographical regions of the world.

Bearing in mind the limited applicability of these data - due to the complicating influences of point discharge and space charge effects, it was considered that sufficient local data was now available for the primary purposes of this exercise: namely, characterisation of the local storm climatology and provision of a meaningful basis for evaluating storm warning criteria. Routine recordings of thunderstorm electrostatic field intensities were therefore discontinued after the 1976 storm season.

5.4 Regional characterisation of thunderstorm activity

5.4.1 Introduction and definition of parameters

The most commonly used index of regional storm activity - as mentioned also in Appendix 1B, is the annual thunderstorm day incidence, or keraunic index, T_D, but as previously noted, this is a very subjective parameter and bears little relation to the actual incidence of lightning in an area of interest, which is more meaningfully expressed in terms of the annual regional ground flash density N_g. The latter parameter has been directly measured by the NEERI on a routine basis in the Pretoria area of the Transvaal for the past 10 years, using lightning flash counters of several types[64].

At ...../110

At the start of the general lightning research programme in 1972, the decision was taken to take advantage of the known characteristics and objective registrations of flash counters in order to study the incidence and degree of lightning activity associated with Transvaal thunderstorms more fully.

In principle, any flash counter having known performance characteristics could be used and the standard CIGRE 500 Hz counter[94], being the most readily available instrument at the start of this programme, was chosen for this purpose. The performance characteristics of this instrument in the Transvaal had previously been determined by the NEERI, from direct calibrations[64]. The CIGRE counter has a statistical effective range to ground flashes of 37 km and a ground flash correction factor of 0,83 - implying that about 17% of its registrations over a sufficiently long period of time would be due to cloud flashes.

The primary data for this study comprised the accumulated registrations of a CIGRE flash counter on a continuously operating event recorder. The latter had a resolution and accuracy of about ±2 minutes over a one-week period of recording. The CIGRE counter itself was located at Silverton, one of the primary NEERI flash counter calibration stations,[64] at a distance of about 5 km from the lightning research mast. This flash counter/event recorder combination was maintained in routine operation and regularly monitored, throughout the year, for a period of 5 years from 1973 to 1978. For the purposes of this study, a thunderstorm was defined in terms of the following criteria:

(a) the start and finishing times of lightning activity were determined by the first, and last five minute periods respectively in which at least two flash counter registrations were noted.

(b) storms associated with less than 25 flash counter registrations were ignored.

(c) flash counter rates of less than one per hour were ignored.

These requirements were arrived at following an earlier study of preliminary data and comparative evaluation of several different criteria - discussed elsewhere by the author[95].

The data sample accumulated over the 5 year period of study included registrations from 434 storms which complied with the above criteria, and the following parameters were adopted for analysis:

(i) ...../111

(i) Diurnal incidence in storm occurrence, expressed in terms of the variations in storm starting and finishing times.

(ii) Storm duration, expressed as the period between starting and finishing times.

(iii) Flash counter registration per storm.

(iv) Average flash rate - expressed by the ratio of the flash counts registered per storm and the associated storm duration.

The primary objective of this programme was to arrive at a more rigorous, or objective characterisation of regional thunderstorm activity, using relatively simple instrumentation and analytical techniques.

The results of the 5-year analysis have been fully presented in a series of reports by the author[81], and are summarised now in Table 5.3, while comparative data from several other regions of the world are presented in Table 5.4. These results, and the variations of these parameters, are examined further in the following sections.

TABLE 5.3: SUMMARY OF THUNDERSTORM ELECTRICAL PARAMETERS RECORDED IN THE PRETORIA REGION OVER THE PERIOD 1973/1978 - USING THE CIGRE FLASH COUNTER

Parameter	Seasonal results					Overall means
	73/74	74/75	75/76	76/77	77/78	
Number of thunderstorm days	84	65	57	70	67	69
Number of thunderstorms	96	89	88	82	79	87
Ground flash density (km^{-2})	6,3	5,9	4,6	7,2	5,5	5,9
CIGRE flash counter total	33 285	33 866	24 332	32 006	20 162	28 730
Flash count per storm						
mean	420	480	348	466	310	402
standard deviation	360	511	403	540	469	466
median	240	180	114	233	121	181
Thunderstorm duration						
mean (hours)	4,7	3,3	3,0	3,5	2,3	3,3
standard deviation (hours)	2,7	2,9	2,2	2,1	1,8	2,5
median (hours)	2,4	1,7	1,6	2,1	1,3	1,9
Average flash count rate per minute						
mean	1,6	1,7	1,9	2,0	2,0	1,9
standard deviation	1,3	2,3	1,9	1,2	1,6	1,7
median	0,9	0,6	1,0	1,5	1,1	1,0

TABLE 5.4: COMPARATIVE REGIONAL DATA ON STORM PARAMETERS

(a) Storm duration

Observer	Region	Keraunic index	Duration (hours) μ	σ	Remarks
Krider et al[88][96]	Florida	91	1,7	1,1	Electric field studies
Popolansky[97]	Czecho-slovakia	30	1,8	-	Observers' data
Mackerras[98]	SE Queens-land	30	1,7	1,3	Observers' data
Eriksson	Transvaal	69	3,3	2,5	Flash counters
Eriksson	Transvaal	69	2,4	1,9	Electric field studies

(b) Flashes per storm

Observer	Region	Keraunic index	Flash/storm μ	σ	Remarks
Hönninger[99]	Austria	40	241	212	Flash counters
Krider et al[88][96]	Florida	91	370	506	Electric field studies
Mackerras[98]	SE Queens-land	30	326	-	Flash counts/storm day
Eriksson	Transvaal	69	402	466	Flash counters

(c) Average flash rate

Observer	Region	Keraunic index	Average flash rate μ	σ	Remarks
Krider et al[88][96]	Florida	91	2,8	2,5	Electric field studies
Lundquist et al[100]	Ontario	20	2,5	3,6	Flash counters
Lundquist et al[100]	Capri	50	2,0	3,8	Flash counters
Lundquist et al[100]	Sweden	10	2,3	5,4	Flash counters
Lundquist et al[100]	Switzerland	50	2,2	3,3	Flash counters
Eriksson	Transvaal	69	1,9	1,7	Flash counters

5.4.2 Diurnal incidence

The 5 year average diurnal variations in storm starting and finishing times over the thunderstorm season (September to April), are shown in Figure 5.10.

The trend in diurnal cycle observed in the Transvaal region is similar to that observed at about the equivalent latitudes in Australia[98] and Florida[88] and indicates a prominent peak probability of storm activity in the mid-to-late afternoon period (local time).

This aspect has been discussed further by Cianos and Pierce[79], who indicate that the above feature is characteristic of air-mass storms caused by local heating and orographic effects, rather than by frontal systems. They indicate also that the amplitude of the diurnal cycle is greatest in continental interiors, and they present data for the mountain and prairie states of the USA depicting a cycle amplitude of about 10%, which is comparable with the 10 - 12% peak amplitudes observed in the Transvaal data.

5.4.3 Thunderstorm durations

The average distribution of storm durations accumulated over the 5 year period of analysis, is given in Figure 5.11 and indicates a significant degree of right skewness, as did the comparative distribution of storm durations determined from electrostatic field measurements, given earlier in Figure 5.7.

Thus, although the average storm duration is 3,3 hours, as stated in Table 5.3, the median duration is much shorter, being only 1,9 hours, which may be compared to the median value of about 1,4 hours obtained from the electrostatic field studies.

Assuming an arbitrary movement of storm activity through the area of observation, this consistent difference in durations determined from the two different measurement techniques, implies a greater effective range of storm registration for the flash counter technique, compared to the electrostatic field measurement approach.

Such differences in measurement technique and definition therefore, are thought partly to account for the variations between Transvaal average storm durations and the values obtained in several other geographical regions - as presented in Table 5.4. (For example, the approximate limiting effective range of storm registration using observers, is known to be only about 15 km[79]).

Figure 5.10 ...../114

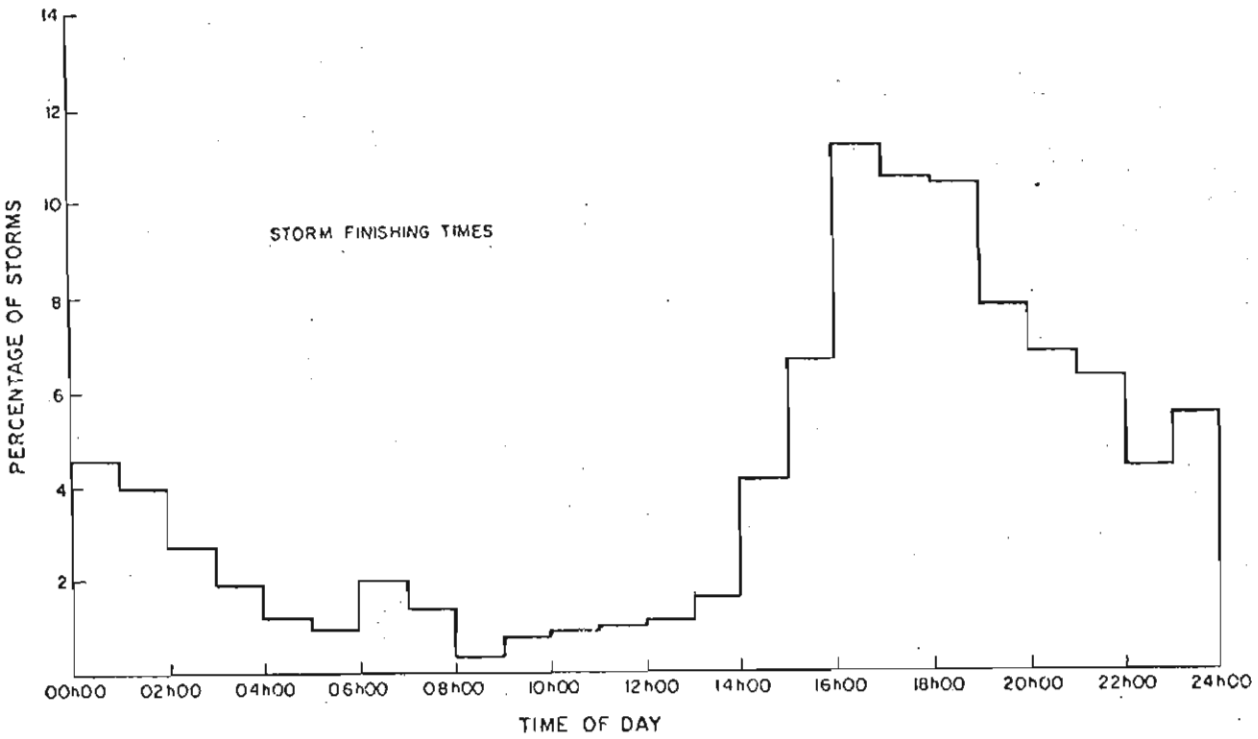

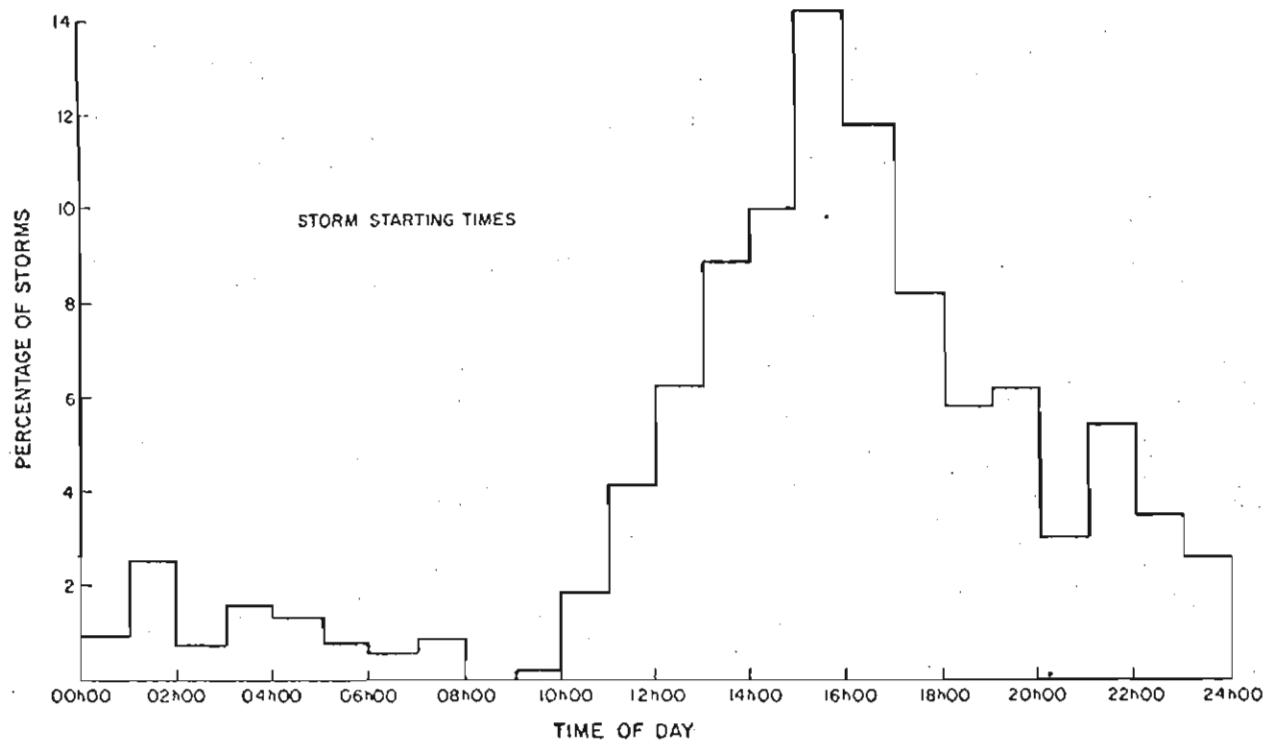

FIGURE 5.10

DIURNAL INCIDENCE OF THUNDERSTORMS IN THE PRETORIA REGION OF THE TRANSVAAL

Figure 5.11 ...../115

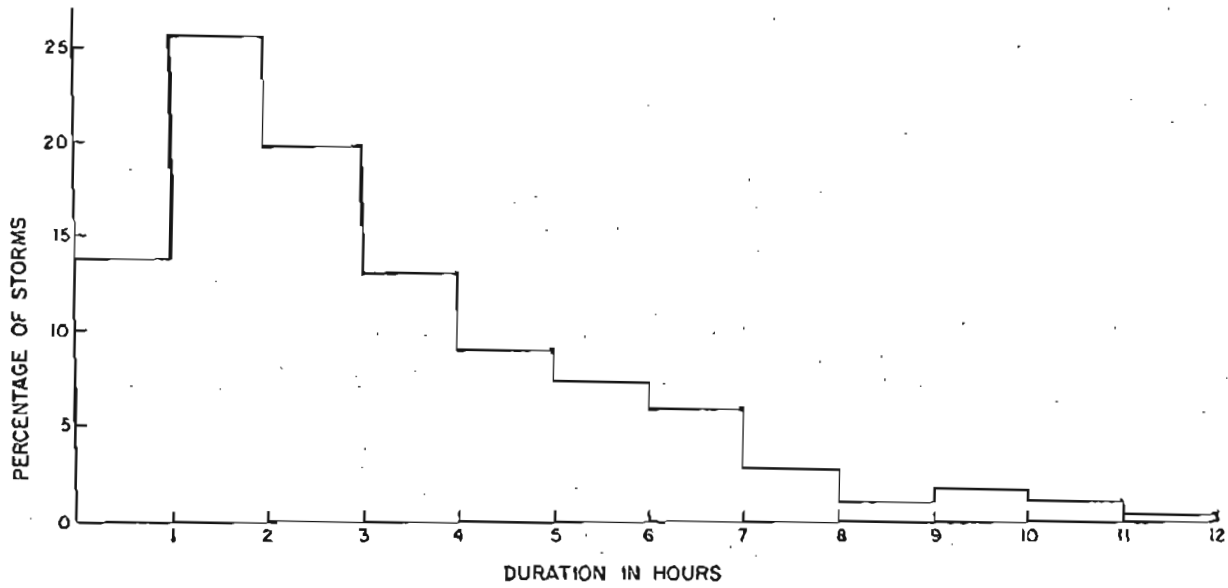

FIGURE 5.11

DISTRIBUTION OF MEAN STORM DURATIONS (BASED UPON 5 YEAR SURVEY USING CIGRE FLASH COUNTER)

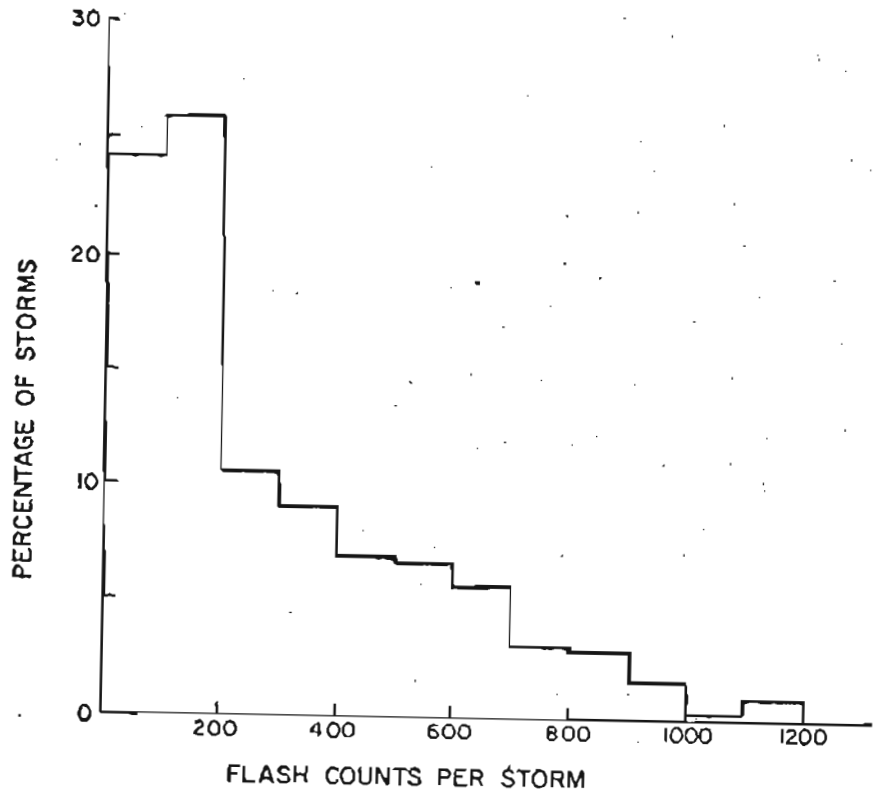

FIGURE 5.12

DISTRIBUTION OF MEAN FLASH COUNTER REGISTRATIONS PER STORM (BASED UPON 5 YEAR SURVEY USING CIGRE FLASH COUNTER)

In a global review of this topic Cianos and Pierce[79] indicate that temperate storms are usually of single-cell nature and have durations of about one hour, while tropical thunderstorms may involve several areas of consecutive cellular activity and have average durations of about three hours - which is consistent with the local measurements.

Bearing in mind that the effective range of the CIGRE counter (37 km) is equivalent to a potential observation area in excess of 4 000 km^2 and that an average storm cell may be only 500 km^2 in extent[79], the possibility in thus very plausible that the Transvaal long duration data may be associated with multi-cellular storm activity - both consecutive and unrelated.

While any determination of storm duration is evidently range dependent, the above average value of 3,3 hours is wholly consistent with what might be anticipated from empirical relationships with the local keraunic index - such as that of Popolansky and Laitinen[101] which gives;

$$D_g = 0,9\ T_D^{0,3} \quad \ldots\ldots\ldots \text{(hours)}$$

where D_g is the average duration of storm activity per storm day (T_D), on an annual basis.

Taking the average T_D value of 69 days over the 5 year period (Table 5.3), the above relation yields a mean storm duration D_g of 3,2 hours -which shows good agreement with the measured result.

5.4.4 Flash counts per thunderstorm

The 5-year average distribution of flash counts per storm, as accumulated seasonally by the CIGRE counter, is shown in Figure 5.11 and again indicates a marked degree of right skewness. This trend is supported by the summarised results given in Table 5.3 where the overall average result of 402 flashes/storm may be compared with the associated median value of 181 flashes/storm. Taking account of the CIGRE counter effective range of 37 km and the ground flash correction factor of 0,83, this is equivalent to an average ground flash density per storm (for the area of observation),

$$N_g = \frac{402 \times 0,83}{\pi \times 37^2} = 8 \times 10^{-2}\ km^{-2} \text{ per storm}$$

The ...../117

The mean value of 402 flashes per storm compares comparatively well with the values for several other geographic regions given in Table 5.4, although tending to be marginally higher. The Florida data[96], however, may not be comparable, being reportedly drawn from a smaller area of observation and apparently equivalent to a ground flash density per storm of about 0,28 km^{-2} per storm - implying a proportionately greater degree of activity than in the Transvaal.

5.4.5 Average flash rate

The lightning flashing rate is perhaps the most direct index of thunderstorm activity and is known to vary considerably through the life-cycle of a storm - with extreme rates approaching 100 per minute being reported - as discussed in a review by Prentice[102].

The author has followed two approaches in studying the characteristics of local storms. Firstly, variations in actual flashing rate were examined by carrying out high speed recordings of electrostatic field changes and analysing the recovery intervals between flashes - in a manner similar to that conducted by Jacobson and Krider[96].

Secondly, as noted in 5.4.1, above the overall average flash rates for individual storms were determined from the ratio of the flash count per storm to the storm duration.

In the first instance, field change recordings were obtained from a horizontal plate-type 'slow' field change antenna,[11] having a discharge time constant of about 1 second. These signals were displayed upon a high speed chart recorder with a resolution of about 5 mm/second. These recordings were taken during the most active phases of thunderstorms and the resultant recovery intervals were then analysed. Over 2 000 flashes were recorded through some 22 storms in this manner, and the ensuing distribution of flash intervals is shown in Figure 5.13 - together with the equivalent flash rates.

These data indicate that maximum flashing rates in excess of 30 min^{-1} are comparatively rare and that the most common recovery interval is about 6 - 8 seconds during the most active phase of the storm cycle; (equivalent to a flash rate of about 8 - 9 $min.^{-1}$.) In an earlier analysis of these data[103], the author found that the median interval was 13 seconds - which is equivalent to a flash rate of about 5 $min.^{-1}$.

As noted previously, the average flash rates were determined from an analysis of corresponding storm duration and flash count data,

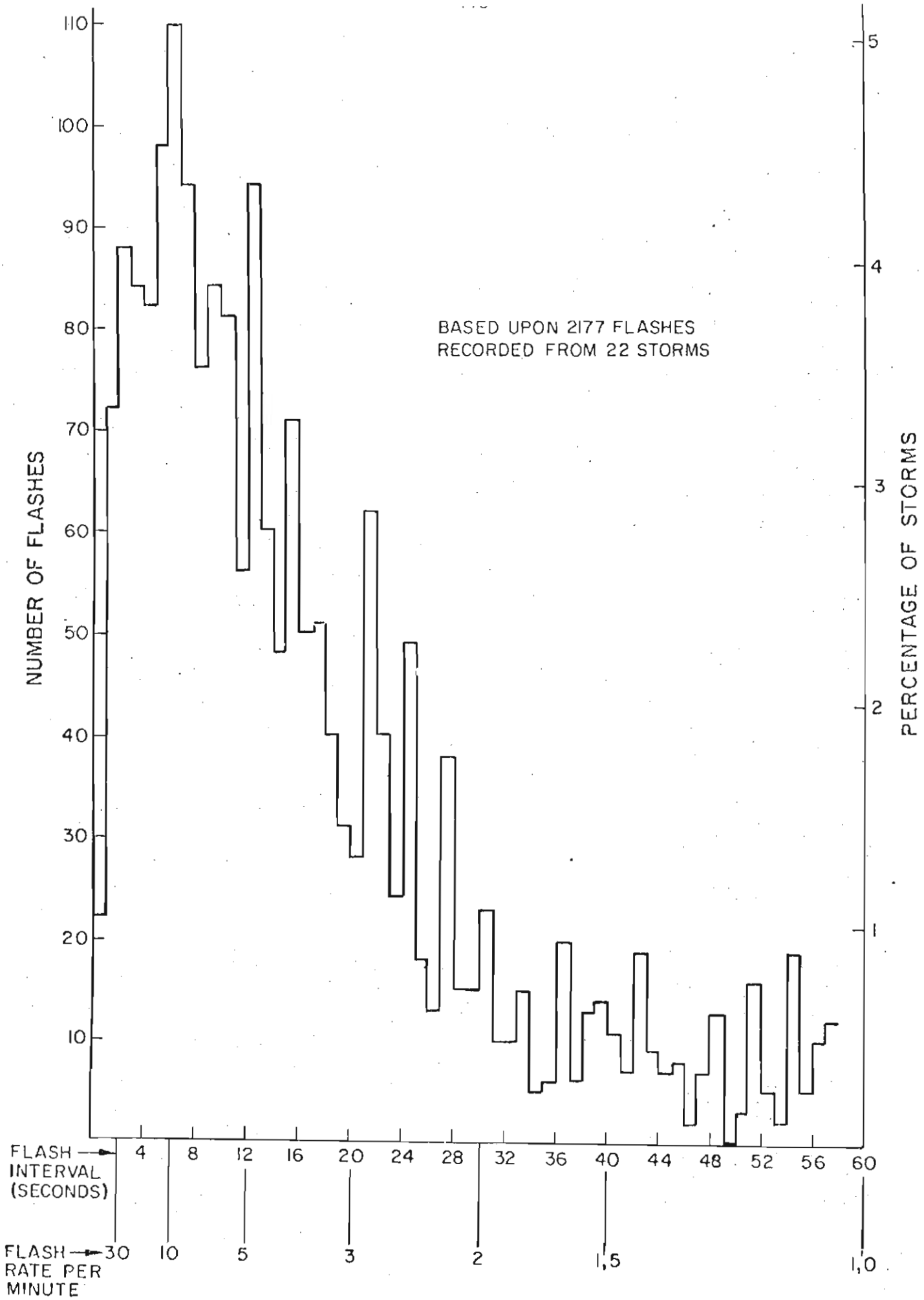

FIGURE 5.13

DISTRIBUTION OF MEASURED FLASHING RATES

on a storm by storm basis. As noted in Table 5.3, the resultant distribution of average flash rates over the past 5 years has an overall mean value of 1,9 $min.^{-1}$, and a median value of 1 $min.^{-1}$. Although Prentice's review of flashing rates[102] indicates that average flash rates may vary from about 1 $min.^{-1}$ to 5 $min.^{-1}$, with rates of the order of 2 - 3 $min.^{-1}$ being common, the comparative data presented in Table 5.4 suggest that the Transvaal result may be marginally lower than has been observed in several other-geographic regions. The author considers however, that the question of definition is again important here and feels that the marginally lower Transvaal flash rate may well be attributable to the large effective area of observation of the CIGRE counter and to the consequent tendency toward the measurement of long storm durations - as discussed in section 5.4.3. In addition, the comparative data presented in Table 5.4 is mostly drawn from small samples (e.g. only 15 storms for Lundquist's data) or from selected periods of storm activity, whereas the Transvaal data includes analysis of activity over complete thunderstorm seasons, comprising many weak as well as major thunderstorms.

Being based upon CIGRE flash counter registrations, the mean flash rate of 1,9 $min.^{-1}$, is equivalent to an average ground flash rate of $6{,}1 \times 10^{-6}$ $km^{-2}s^{-1}$, which agrees well with results obtained from the ratio of the overall mean flash count per storm/mean storm duration, viz.: -

$$402 \times 0{,}83 / 3{,}3 \times 3\,600 \times \pi \times 37^2 = 6{,}5 \times 10^{-6}\ km^{-2}s^{-1}.$$

(It is of interest to note that a similar order of magnitude is obtained when the median values of flash count and storm duration are used, (as given in Table 5.3) namely, $5{,}1 \times 10^{-6}$ $km^{-2}s^{-1}$).

Various other estimates of average ground flash incidence have been suggested by several workers, with typical values varying between 10×10^{-6} $km^{-2}s^{-1}$ and about 100×10^{-6} $km^{-2}s^{-1}$.[79]

The Transvaal result, although on the low side in relation to these estimates, has the merit that it is derived from objective studies of many thunderstorms over several complete seasons, using a flash counter having known performance characteristics, while the earlier estimates tend to be empirically derived from selective studies and involve assumptions about areas of observation and thunderstorm effective areas - as noted for example, in the discussion by Cianos and Pierce[79].

In .....

In summary therefore, while Transvaal thunderstorms may frequently attain peak ground flash rates of about 8 - 9 $min.^{-1}$ (equivalent to a ground flash incidence of about 25 x 10^{-6} $km^{-2}s^{-1}$), the overall average ground flash incidence displayed over a complete thunderstorm season is about 6 x 10^{-6} $km^{-2}s^{-1}$. These results are considered to be generally consistent with estimates from other regions of the world.

5.5 Seasonal variations

A prominent seasonal trend in thunderstorm incidence and characteristics is present in the Transvaal region - as illustrated for example, by the results in Figure 5.14, which depicts the mean monthly variations in several thunderstorm parameters that have been observed over the past few years. These data indicate that the peak activity occurs generally in the months of November and January.

This trend toward a pronounced maximum in thunderstorm activity around mid-summer is a feature of the climate of temperate and sub-tropical regions and is consistent with results that have been obtained in similar climatic regions elsewhere in the world - as discussed by Prentice[102], and Cianos and Pierce[79].

A study of the seasonal trends depicted in Figure 5.14 suggests the following tentative conclusions;

(a) there is an apparent shift in the diurnal cycle toward earlier afternoon storm starting times, as the summer progresses;

(b) there is a tendency for storm durations to be longer during the months of maximum activity (i.e. November - February);

(c) there is also a tendency for those storms occurring in the months of maximum activity to be associated with higher values of flash counts per storm.

The latter feature was also observed by Mackerras[98] in a similar climatic region (SE Queensland) and, taken together with the observation of longer durations during these months, implies the maintenance of approximately the same average flash rate through all storms of the season.

This is reported as a general feature of global thunderstorm behaviour by Cianos and Pierce[79] - who suggest that average lightning flashing rates remain essentially similar throughout the world and that the main differences in flash incidence between storms of different climatic regions arise through variations in thunderstorm duration.

Figure 5.14 ...../121

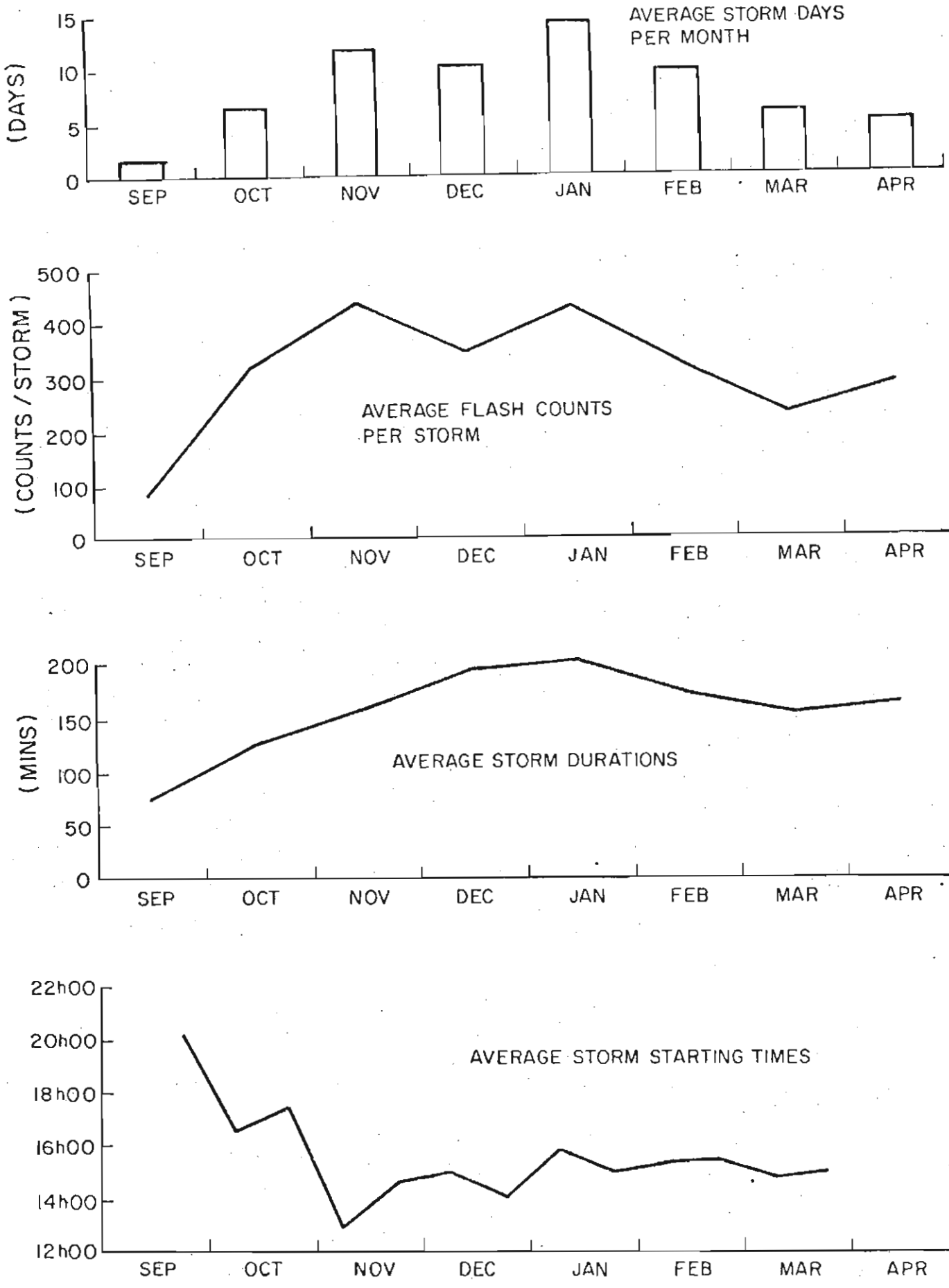

FIGURE 5.14

4 YEAR MEAN SEASONAL TRENDS IN STORM PARAMETERS

The ...../122

The above preliminary seasonal trends therefore appear to be consistent with this observation.

These results are based upon only a few years of recordings, however, and further measurements will clearly be necessary in order that these tentative seasonal trends may be confirmed or modified.

5.6 Long term trends and periodicities

The possibilities of long term trends and/or periodicities in the general incidence of thunderstorms have been discussed by several workers. For example, in the area around Brisbane, Mackerras[98] examined the keraunic index over the past 50 years and found a downward trend after about 1940, while Stringfellow reported data for the United Kingdom[104], which indicated a 10 - 12 year periodicity in lightning incidence and suggested a correlation with the sunspot cycle.

The author has examined this aspect separately,[105] having analysed annual variations in keraunic index for several regions of Southern Africa (including the Transvaal) over the past 33 years. Although the data is considered unreliable, due to the subjective nature of the thunderstorm day as an index of lightning activity, a tentative conclusion of this analysis was that periodicities of the order of 10 - 12 years, or 12 - 16 years, (depending upon the region involved), may be present in the regional annual incidence of thunderstorm days.

The possibility of a downward trend in keraunic index in the Transvaal also exists, as suggested by the data given in Figure 5.15, which depicts annual variations in this parameter for Pretoria since 1939 -based upon Weather Bureau reports[106]. For comparison, variations in ground flash density - which have been measured directly at the Silverton station of the NEERI flash counter development programme over the past 11 years[64], are also included in this figure. The latter parameter is considered far more reliable than the thunderstorm day index, but it is difficult to identify any significant trend over the short period of available data.

Similar comments apply in respect of any annual variations in the other thunderstorm parameters discussed in the preceding sections, for which there is generally only 5 years of data available.

The mean and median values obtained for these parameters each year were summarised in Table 5.3, while Figure 5.16 depicts their corresponding annual variations over the past 5 years, together with variations in keraunic index and ground flash density over the same period.

While ..... / 123

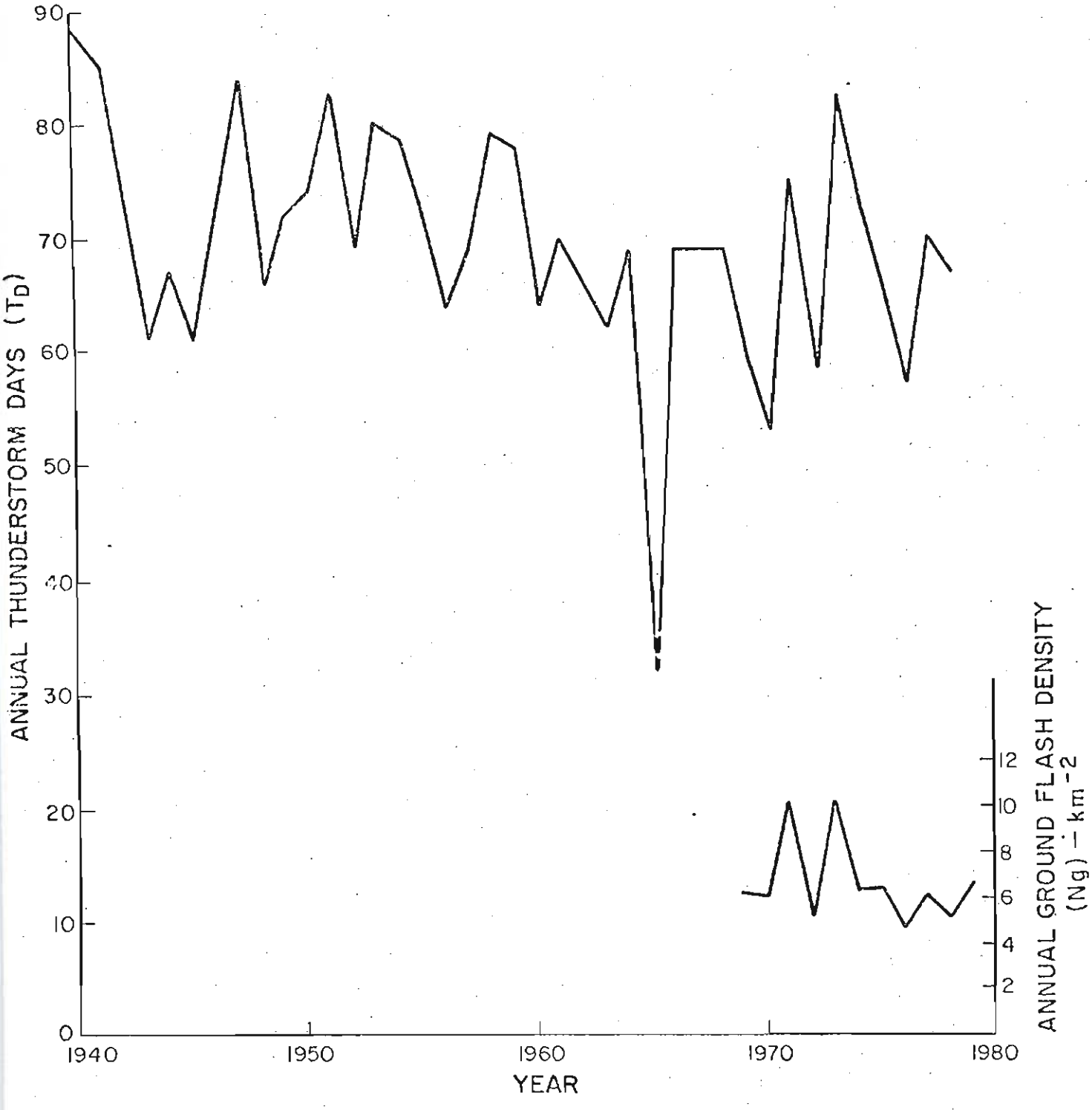

FIGURE 5.15

ANNUAL VARIATIONS IN KERAUNIC INDEX AND GROUND FLASH DENSITY IN THE PRETORIA AREA

Figure 5.16 ...../ 124

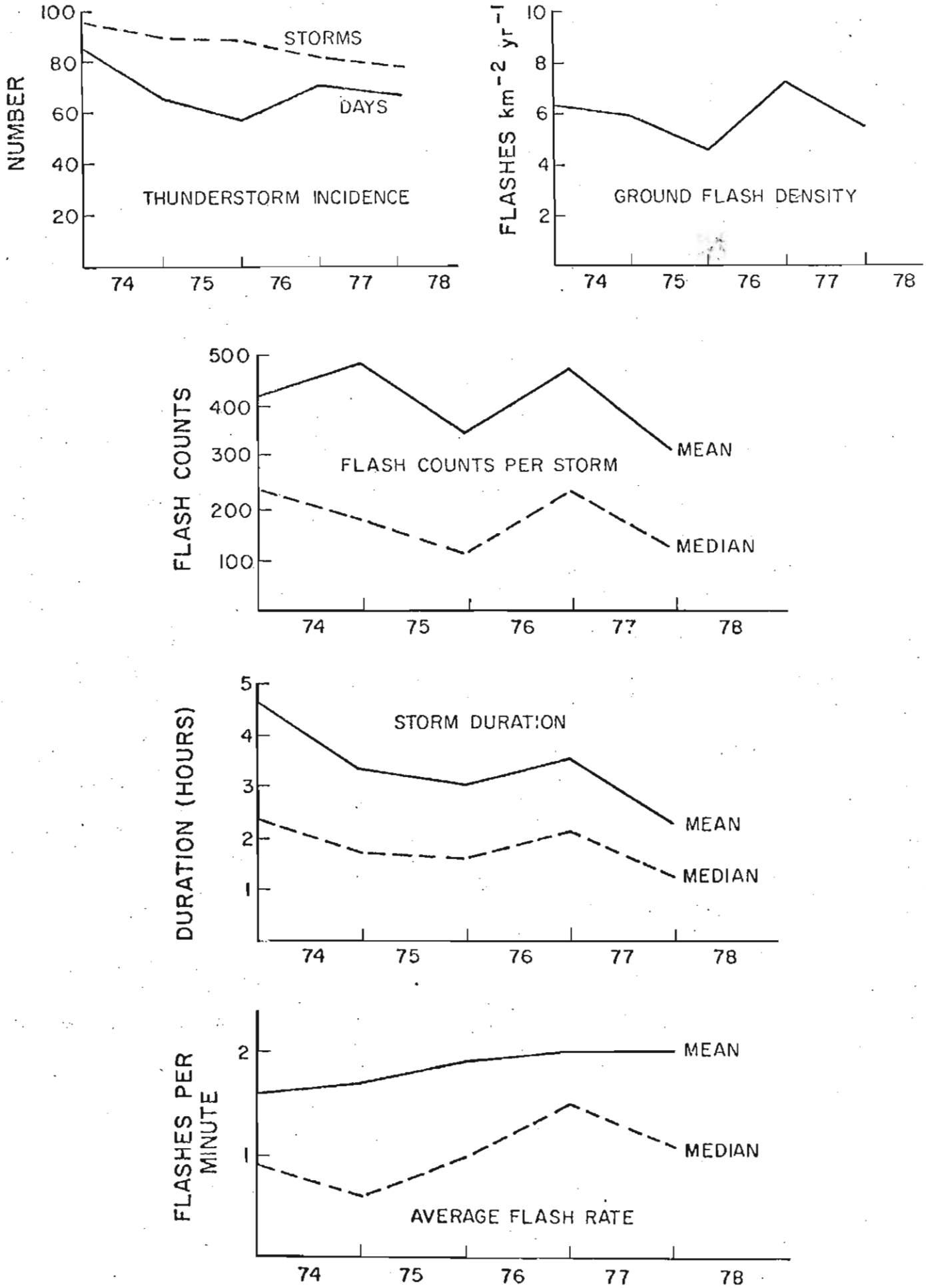

FIGURE 5.16

ANNUAL VARIATIONS IN STORM PARAMETERS OVER THE PERIOD 1973—1978

While there appears to have been a short-term downward trend in keraunic index and storm duration, the effects of this are partly offset by a marginal increase in average flash rate, and the resultant flash incidence, or ground flash density, does not show any significant trend.

Clearly, there is a need for considerably more data over many more years. Any speculations on possible solar related periodicities are thus also premature at this stage.

5.7 Summary on thunderstorm and lightning climatology in the Transvaal region

Based upon the preceding discussions, it is considered that a sufficiently comprehensive sample of data has been accumulated to allow a meaningful statement regarding the electrical characteristics of the "average" Transvaal summer thunderstorm.

Taking account of the data presented in Tables 5.1 - 5.3, this storm would be expected to have the following features:

(a) - the most favourable time of storm occurrence would be around 16 h 00 on a summer afternoon over the period late November - mid March.

(b) - the storm duration would be about 200 minutes (3,3 hours), -as determined by the registrations of a CIGRE flash counter.

(c) - the surface electrostatic field intensities recorded at ground level would be expected to exceed ±5 kV/m and to remain above a level of 500 V/m for about 145 minutes (2,4 hours) of the storm duration.

(d) - in the event of the surface electrostatic fields exceeding ±10 kV/m (about a 20 - 30% probability), such field levels would not usually be present for more than 10 - 15 minutes - or only about 5 - 7% of the storm duration.

(e) - on average, a CIGRE flash counter in the area would be expected to register about 400 flashes - or about 330 ground flashes.

(f) - on average, about 50% of the ground flashes would display multiple stroke behaviour - involving 2 - 3 return strokes per flash.

(g) - less than 50% of the multiple stroke ground flashes would have flash durations in excess of about 180 - 200 ms, while the median interstroke interval would be about 40 - 50 ms.

(h) ..... / 126

(h) - at the peak of the storm activity, the ground flash incidence might attain a flashing rate of about 25×10^{-6} $km^{-2}s^{-1}$ and the storm would be expected to sustain an average flash incidence of about 6×10^{-6} $km^{-2}s^{-1}$, over its full duration.

On average, some 69 storm days and about 1,26 storms per day may be anticipated in the Transvaal region.

Assuming an average ground flash incidence of 6×10^{-6} $km^{-2}s^{-1}$ and an average storm duration of 200 minutes (3,3 hours) the expected average annual ground flash density N_g is given by;

$$N_g = 69 \times 1,26 \times 6 \times 10^{-6} \times 200 \times 60$$
$$= 6,3 \text{ km}^{-2} \text{ yr}^{-1}$$

This compares well with the 11 year average value of 6,6 $km^{-2}yr^{-1}$ measured in Pretoria, during the NEERI flash counter development programme[64].

While it is clear that considerably more data will be required before seasonal or long term annual variations in storm characteristics become clarified, it is considered that the above "summarising" parameters are representative of what might reasonably be encountered in an average thunderstorm in the Pretoria region of the Transvaal.

Of course, as shown by the measured variations in storm parameters depicted in the various figures in this chapter, many of the distributions are non-Gaussian in form - being generally right-skewed - and in practice therefore, average values of parameters may only occur comparatively rarely.

However, for electrical engineering purposes and lightning warning concepts, the above characterisation of thunderstorm climatology is considered to be far more meaningful and comprehensive, than might otherwise be determined from only the prevailing keraunic index.

CHAPTER 6

GENERAL DISCUSSION AND IMPLICATIONS

6.1 Introduction

The preceding chapters have outlined the primary facets of the research project with which this thesis is concerned, namely,

(a) the experimental concept of the local research station

(b) the application of this station to the measurement of the fundamental engineering parameters of the lightning ground flash and a presentation of preliminary results

(c) a consideration of the concept of striking distance, including also an examination of early data emerging from an experimental study of the striking process - together with the introduction of a simplified analytical model, whereby striking distances to structures may be estimated

(d) a characterisation of regional thunderstorm electrical activity in the Transvaal region - based upon a five year study of various thunderstorm and discharge parameters.

It is considered useful to discuss these various facets under two collective headings, namely, "Parameters" and "Striking distance considerations' and the implications of the preceding work in each of these areas will be examined in turn.

6.2 Lightning and storm parameters

The principal objectives of this phase of the work were to establish a research station and to evolve instrumentation techniques whereby the basic engineering parameters of the ground flash could be measured. In conjunction with this, it was to define the prevailing thunderstorm climatology in the region where these measurements were carried out.

In general, the author considers that these objectives have largely been met. The results presented in Chapter 3 have demonstrated the basic effectiveness of the research station and allied instrumentation concepts. The fundamental engineering aspects involved in the original establishment of both the mast and research station also appear to have been adequate, in that the system has operated successfully with minimal problems for over 6 years. The principal problems effecting the measurement success rate have been the loss of power supply on the research site arising from general thunderstorm activity in the area. On no occasions, however, have direct strikes to the mast caused any damage either to the mast itself, or to the

site supporting services, or to the primary instrumentation systems, and it must be concluded that the original protective measures, including the specialised power supply and earthing arrangements, appear to have been adequate.

A total of 28 flash events on the research mast was recorded during the 7 year period of analysis. The circumstances surrounding these events, and the associated measurements, have been fully reviewed in Chapter 3 and Appendix 3A. A summary of the more important features of the recorded flashes is given in Table 6.1.

TABLE 6.1: SUMMARISED FEATURES OF THE RECORDED FLASHES

Total number of flashes recorded (1972 - 1978)	28
Mean number of flashes per year	4
Number of flashes on which measurements were made	17
Total number of strokes recorded during the 11 oscillographically measured flashes	19
(1) Observed incidence of downward flash events	57%
(1) Observed incidence of upward flash events	29%
(1) Observed incidence of negative flashes	61%
(1) Observed incidence of positive flashes	7%
Median current for negative downward flashes	44 kA
(2) Median current for all strokes	19 kA

Notes: (1) i.e. excluding the unknown events in each category

(2) i.e. comprising both upward and downward events, as well as subsequent stroke records.

Although generally, the recorded data samples are too small to permit fully meaningful trends or conclusions to be identified, the following observations may be noted:

(i) Some 65% of the identifiable flashes were of the classic downward negative type (Berger type 1(b)[22] - thereby supporting the original choice of site and mast geometry, since a fundamental objective had been to study the characteristics of those flashes most commonly encountered in practical engineering situations.

(ii) ...../129

(ii) Although the research mast results differ in this respect from those obtained by Berger (where the majority of events were of the positive upward leader type), the preliminary waveform characteristics obtained from the sample of negative downward flash records are generally consistent with those obtained by Berger. This includes in particular, the concave wavefront during first stroke records - thereby suggesting that any tower-effect influences on the discharge process are essentially similar over a wide range of structure effective heights -at least in respect of the initial wavefront development.

(iii) Although the available records comprise only a small sample - and are thus associated with wide confidence limits to the distributions of results - the measured cumulative frequency distribution of peak current amplitudes supports the possibility that flashes in Southern Africa may involve marginally higher amplitudes than have been recorded in more temperate climates. This observation notwithstanding, the general trend of the distribution is consistent with those of several distributions already adopted, or under consideration in modern engineering studies (i.e. the modified AIEE[44] and CIGRE[20] distributions respectively).

While in the past it has been traditional to express the regional thunderstorm activity in an area of interest in terms of the keraunic level (which in the Transvaal, is typically about 70 storm days per year), such a characterisation is totally inadequate in relation to practical requirements, such as the provisions, or criteria for thunderstorm and lightning warning systems, or as the basis for comparative engineering studies.

In an attempt to provide a more meaningful characterisation of lightning and storm activity in the Transvaal region, various measurement concepts and parameters were presented in Chapter 5 - together with results which had been derived over a 5 year period of study of the regional storm climatology. As noted in the discussion of this work, it was considered that a sufficiently comprehensive data sample had been accumulated to allow a meaningful statement of the electrical characteristics of the "average" Transvaal thunderstorm, and the relevant features of such a storm were summarised in 5.7.

In general, when comparing the results obtained from the measurement of various lightning and thunderstorm parameters with data obtained in other regions of the world, an overall consistency in trend was observed. It was concluded that in many respects, the electrical characteristics of

thunderstorms ...../130

thunderstorms may not vary substantially in different regions, and that the distinguishing feature of varying degrees of regional lightning activity may be variations in storm duration.

In particular, the characteristics of multiple stroke flashes showed good agreement with results from many other regions of the world.

Similarly, it was found that the characteristics of thunderstorm electrostatic fields recorded at ground level in the Pretoria area did not differ substantially from those associated with thunderstorms studied in several other geographical regions. It was also concluded that sufficient data had been accumulated on the probabilities of occurrence (and durations), of various electrostatic field intensities at ground level - in relation to storm activity - to allow the development of meaningful criteria for storm warning purposes. This therefore provides a basis for potential future research and application.

The author considers that perhaps the most direct index of regional storm activity (as opposed to lightning incidence or ground flash density), is given by the lightning flashing rate. The data analysed in Chapter 5 indicate that this varies considerably over the lifetimes of Transvaal thunderstorms, with ground flash rates as high as 25×10^{-6} $km^{-2}s^{-1}$ being frequently attained at the height of the storm. On average, however, sustained mean ground flash rates of about 6×10^{-6} $km^{-2}s^{-1}$ were observed over the full storm duration. This value is of comparable magnitude to estimates reported from several other regions.

In discussing the work presented in Chapter 5 and in relating the local data to results from other parts of the world, it was noted that two additional factors could account for certain of the observed differences, namely:

(i) the rigorous definition of several of the local storm parameters (e.g. being determined objectively from the characteristics of proven instrumentation, such as the CIGRE flash counter, or from computerised analyses of field mill records)

(ii) the fact that the local analyses were based upon several years continuous recordings of all storm activity, in contrast to evaluations of selected samples of more active storms - as had been the case in certain of the previous studies.

It is evident that measurements such as those presented in Chapter 5 would have to be maintained for many years in order to clarify both the degree of seasonal variation and the possibility (as well as extent) of long term trends or periodicities. Despite this, it is considered that for

many ...../131

many electrical engineering requirements, the available data and consequent representation of the Transvaal storm climatology demonstrates a far more meaningful and comprehensive characterisation than that expressed by the prevailing keraunic index.

Finally, although the preliminary peak current amplitude data presented in Chapter 4 also comprise only a comparatively small sample, it may be noted that these results, together with some of the parameters reviewed in Chapter 5 (including in particular those relating to the characteristics of multiple stroke flashes), have already found useful application in a general review of lightning parameters for engineering application, which has recently been prepared by the author in collaboration with Anderson[20].

6.3 Striking distance considerations

The concept of lightning striking distance and the relevant implications regarding downward flashes to the mast, were examined both empirically and analytically in Chapter 4, (as well as in Appendix 4A).

The empirical approach involved the introduction of a novel measurement technique whereby the striking distances of flashes to the mast were evaluated from analysis of bi-directional photographs, and 8 such measurements were recorded. It was considered that the resultant flash geometries were best examined in terms of a 3 stage concept of the process of downward leader approach, involving:

(i) the initiation of an upward leader from the mast (thereby defining attainment of the leader striking distance)

(ii) subsequent deflection, or deviation of a branch element of the downward leader

(iii) final interception of the downward leader by the upward leader.

On this basis, values for the leader deviation and interception distances were estimated for each of the 8 recorded flashes and related to the associated measured values of peak current amplitude.

Thereafter, an analytical approach was introduced in which the electric field intensities were evaluated beneath a major branched element of a descending charged leader both at the mast, and on the ground immediately below the leader. The leader was modelled as a linearly charged element, and the striking distance criterion for a given charge was defined by the attainment of a critical upward leader ionisation inception field strength at the mast tip.

In ...../132

In terms of this model, and based upon the above concept of the final stages of the leader, an important conclusion arising out of this work was that attainment of the striking distance (for a given charge on the leader), was not a sufficient condition for flash termination upon the mast. An additional requirement was that the descending leader approach sufficiently close to the mast to allow the upward leader to traverse the intervening distance, (to interception), before the downward leader reached the ground. This in turn was shown to depend upon the relative upward and downward leader velocities. It was also found that interception of nearby leaders was generally only possible over a very limited range of the upward/downward leader velocity ratio (K_v) - typically = 1 ±0,1.

Application of this concept, for a given velocity ratio, allowed definition of an equivalent collection volume within which downward leaders would terminate on the mast. For any particular leader charge Q, a structure equivalent attractive radius R_a was defined as the radius of this collection volume at the striking distance.

In order to relate the analytically derived values of striking distance (which were expressed in terms of leader charge Q) to the prospective stroke current amplitude I, use was made of Berger's empirical correlation between Q and I - based upon direct stroke current measurements[14]. Following a line of approach adopted by Golde[58] however, it was found necessary to take account of the return stroke characteristics in applying this correlation, and to consider only that impulsive component of the leader charge which contributed to the attainment of the current crest in the discharge waveform.

A comparison of the resultant analytically determined relation between striking distance and stroke current with the previously measured results on the research mast, showed on acceptable degree of agreement in trend (as shown in Figure 4.6 in Chapter 4).

In examining the implications of this work, the author considers that the above agreement is sufficiently encouraging to justify further application of the analytical concepts to other structures of varying height, in order to examine the influence of structure height. This is important for engineering studies since there is still considerable speculation in the literature on the effects of structure height upon striking distances and flash incidence, as well as on the distribution of peak current amplitudes in structures - as discussed elsewhere by the author[16].

Accordingly, .../133

Accordingly, the above analytical model has been extended to allow analysis of striking distances and structure attractive radii over structure heights varying over 10 - 200 m. The approach followed is essentially similar to that introduced in Chapter 4 and is outlined fully in Appendix 6A.

As noted in this Appendix, the primary interest was in practical free-standing structures and the critical corona radius concept has again been incorporated, in order to take account of extremity effects - which the author considers may well dominate the electrostatic field enhancement prevailing in the immediate vicinity of practical structures.

Computerised routines were evolved in order to allow analysis over a wide range of varying parameters - as discussed in Appendix 6A - and the resultant variations in striking distance and attractive radius are summarised in Figures 6.1 and 6.2, (for a leader element length of 3 000 m, and a velocity ratio $K_v = 1,0$).

Bearing in mind the calculated dependency of electrostatic field enhancement on structure height (Figure 6A - 1), the resultant substantial variations in striking distance with increasing structure height are not at all unexpected. However, over the normal range of shielding failure current amplitudes (i.e. $I < 25$ kA), the striking distance curves are comparatively insensitive to structure height and it is of interest to note that their trend in this low current range yields striking distance estimates of comparable magnitude to those derived from an established empirical relation[19] ($D_s = 10.I^{=,65}$). This is an encouraging result and may assist in accounting for the fact that previous application of empirical relations of this type in shielding and performance calculations, has often shown good agreement with field experience[19].

The curves in Figure 6.1 imply that this empirical relation may correspond in effect to a compromise, or averaging trend, through several practical structure heights (i.e. about 10 - 50 m) over the range of shielding currents.

Taking structure height into account, the equivalent analytically derived relation (for the curves in Figure 6.1) - as noted in Appendix 6A, takes the form.

$$D_s = (0,4 + 2,1H \times 10^{-2})\ I^{(1,41 - H \times 10^{-3})} \quad (m)$$

The corresponding curves for attractive radius - as depicted in Figure 6.2) also display an encouraging trend, since good agreement is evident with another empirical relation ($R_a = 16,3\ H^{0,61}$), which had previously been derived by the author from a study of the incidence of flashes to tall structures[21]. In the latter instance, the average annual flash incidence

Figure 6.1 ...../134

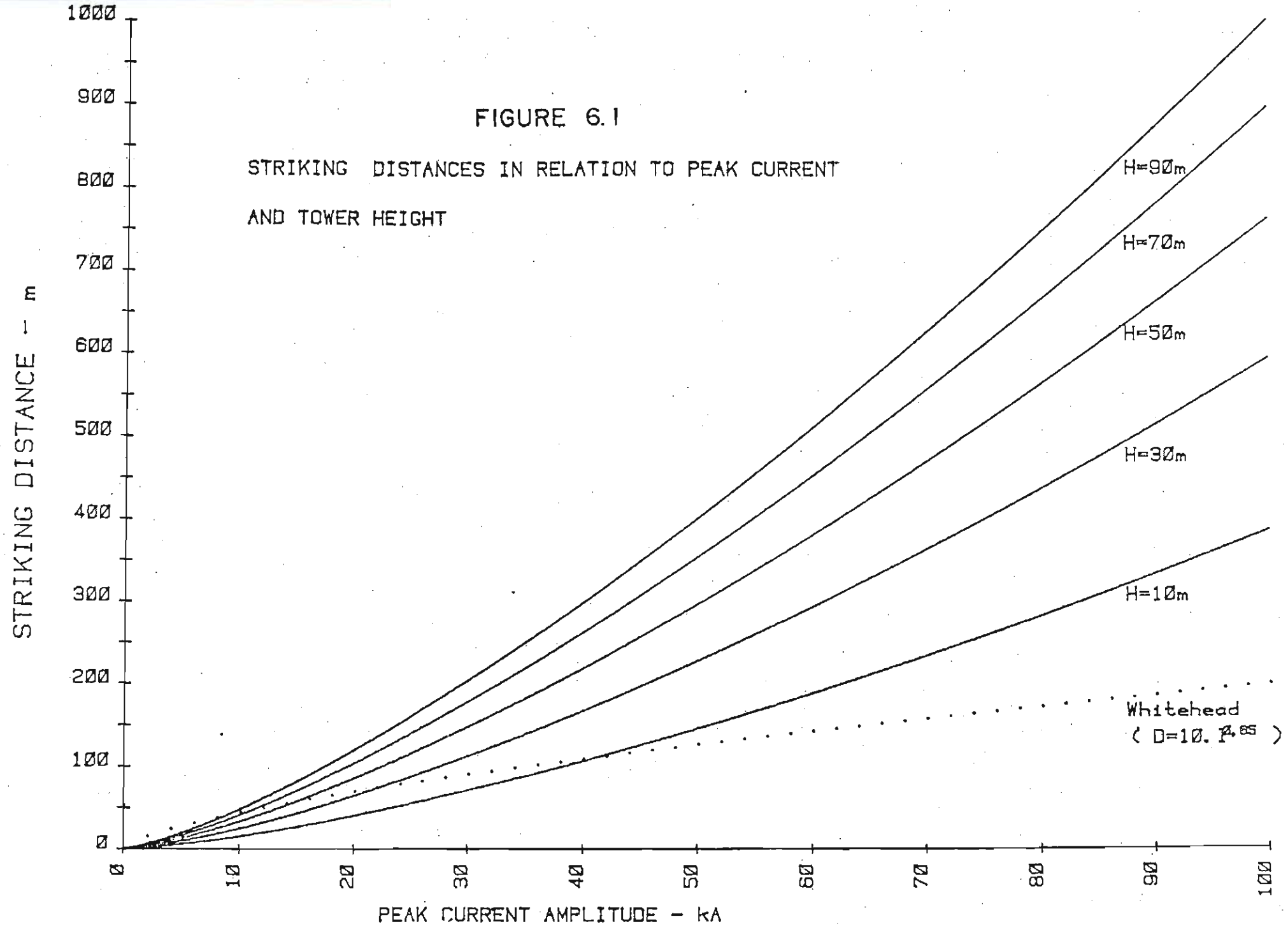

Figure 6.2 ...../135

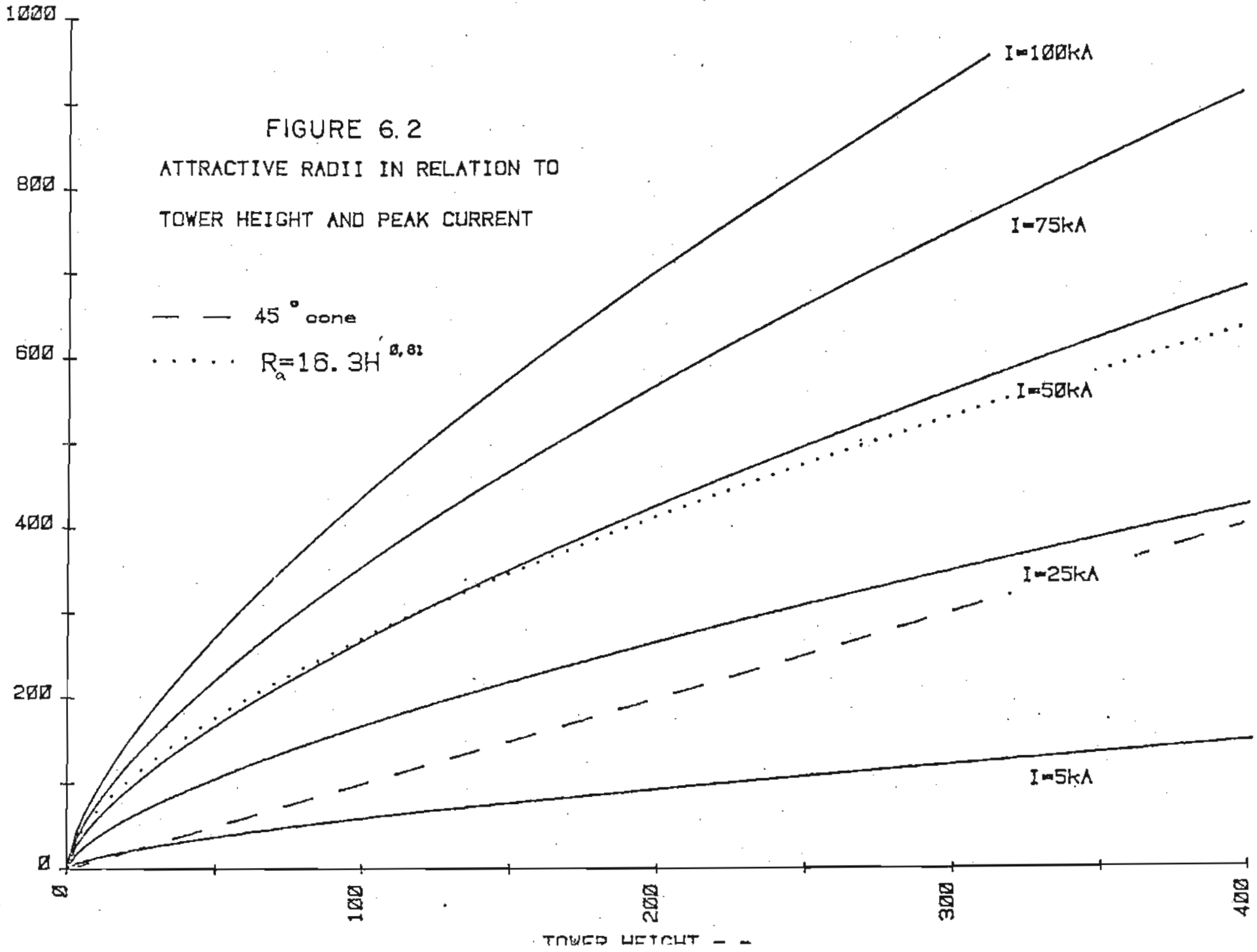
FIGURE 6.2
ATTRACTIVE RADII IN RELATION TO
TOWER HEIGHT AND PEAK CURRENT
45° cone
$R_a = 16.3H^{0,81}$
I=100kA
I=75kA
I=50kA
I=25kA
I=5kA
ATTRACTIVE RADIUS - m
TOWER HEIGHT - m
1000
800
600
400
200
0
0
100
200
300
400

had been analysed, and thus the resultant relation should correspond with the analytically derived curve corresponding to the average value of the distribution of lightning current amplitudes - as in fact is seen to be the case in Figure 6.2, since the average current amplitude is about 45 kA.

A comparison of the trend of the curves depicted in Figure 6.2 with the equivalent protective radius assumed in the empirical 45° cone-of-protection concept (i.e. $R_a = H$), especially over the range of low amplitude currents, indicates an increasing propensity for weak current discharges to penetrate the 45° cone, as structure height is increased above about 50 m.

This observation may account for the fact that the 45° protective concept has commonly proved very effective over the range of structure heights of normal practical interest (i.e. dwelling houses, small masts, etc.), but has been known to fail on much taller structures - such as the 540 m Ostankino mast[24]. These results also provides justification for the adoption of a 30° cone ($R_a = 0{,}58\ H$) in more critical protective applications - as is commonly recommended in many lightning protective codes[12].

The resultant relation fitting the analytically derived curves for attractive radius - as noted in Appendix 6A - is given by,

$$R_a = I^{0,64}\ H(0{,}66 + 2I \times 10^{-4})\ \text{(m)}$$

Although there is thus an encouraging degree of consistency amongst the trends of these analytically derived relations for striking distance and attractive radius, not only in respect of earlier empirical relations, but also with regard to well-established protective concepts, the limitations of the analytical approach must still be recognised. A number of assumptions were adopted in the course of this approach and the subsequent conclusions are therefore subject to the validity of these assumptions. These were discussed previously - mainly in Chapter 4, but also in Appendix 6A, but for convenience, the most important of these are again summarised below, together with relevant comments:

(i) Although other lengths were in fact studied, the specific generalised relations presented above are based upon a linearly charged leader length of 3 000 m. (The attractive radius is comparatively insensitive to this parameter - except for small charge magnitudes - but striking distances depend directly upon the choice of leader element length, as well as upon the form of charge distribution).

(ii) ...../137

(ii) Again, although other velocity ratios were also examined, the above relations are based upon the assumption of equal upward and downward leader velocities. (In this case, the striking distance values are insensitive to this parameter, but the attractive radii vary directly with the choice of velocity ratio, especially for low magnitudes of charge).

(iii) In order to allow practical application of the resultant relations, in both the striking distance and attractive radius analyses it was necessary to relate the original leader charge magnitude Q to the consequent stroke peak current amplitude I. As discussed earlier, this was achieved using Berger's empirically observed correlation between Q and I, but with Q reduced in terms of the average return stroke propagation characteristics, to yield only an impulse component; an approach which was adopted earlier by Golde[58]. In practice however, Berger's data[14] depict considerable scatter between Q and I -as well as in respect of the relevant return stroke parameters (i.e. impulse current and front times, for example). The generalised analytical relations for striking distance and attractive radius, although expressed in terms of the variable I, should therefore be considered as representing only the anticipated average trends for a particular current peak amplitude I, (expressed in kA).

(iv) To a lesser extent, the choice of the criteria determing the critical upward leader ionisation inception field gradient, can also influence the resultant expressions for striking distance and attractive radius. (This relates also to the application of the critical corona radius concept to account for the structure micro-geometric effects upon field profiles). Due to the logarithmic nature of many of the distance terms in the relevant expressions however, (e.g. Eqns. 1 and 2 in Appendix 4A), the relative impact of these assumptions is comparatively small compared to those outlined in (i), (ii) and (iii) above.

As a general comment, in every instance, attempts were made to base these assumptions upon a comprehensive study of the relevant available physical data, but in each case, these data were either comparatively scanty (e.g. velocity ratios), or inconclusive, (e.g. leader charge distribution), and the author considers that there is a very evident need for additional physical data which might clarify these aspects of the discharge process. The primary justification for these assumptions therefore lies in the general consistency in trend between the resultant analytical expressions and other independently derived empirical relations and protective concepts.

For ...../138

For an area experiencing a particular annual ground flash density, N_g, (flashes $km^{-2}yr^{-1}$), the above generalised expression for attractive radius provides a ready means for determining the annual incidence of discharges having a peak current I to a structure of height H (m). This is given by:

$$N_{(I)} = \pi R_a^2 . N_g . \times 1 \times 10^{-6} \text{ flashes per year}$$

This analysis may then be extended over a representative distribution of current amplitudes, to determine the resultant frequency distribution of currents discharged into the particular structure in a sample period of study. One method of carrying out such an analysis is on a stroke by stroke basis, using Monte Carlo techniques of numerical simulation; and a computerised approach employing these techniques is included in Appendix 6A.

In this case, the above methods and relations are applied to an examination of the effects of varying structure height upon both the protective effect of structures, and upon the consequent distributions of peak current amplitudes, over a wide range of structure height.

As was anticipated earlier in the examination of the trend of the attractive radius curves, in relation to peak current amplitude and structure height, the resultant simulations indicate that the 45° protective cones around structures may well be penetrated - as shown by the example presented in Appendix 6A (Figure 6A-4). In addition, both the incidence of such shielding penetrations and the amplitudes of the penetration currents are found to be dependent upon structure height.

This is illustrated by the summarised results of the numerical simulations shown in Figure 6.3. As defined in Appendix 6A, the critical protection angle Θ_c (whose dependency on structure height is illustrated in Figure 6.3) is determined from the closest distance of approach of those flashes which penetrated the 45° cone of protection of any particular structure, (i.e. Θ_c is equivalent to providing 100% protection).

Again, as might be expected from the trend of the attractive radius curves shown earlier in Figure 6.2, these analytically determined results support the adoption of protective angles of about 45° for structures of comparatively low height. An important observation however, is the apparent steady decrease in protective effect as structure height is increased - such that a protective angle of even 30° could be expected to experience shielding penetrations around structures having heights in excess of about 300 m. This in fact is known to have occurred in isolated instances on certain very tall structures - such as the Ostankino mast (540 m high), where an equivalent critical protective angle of about 20° has been observed during a 7 year period of study[24].

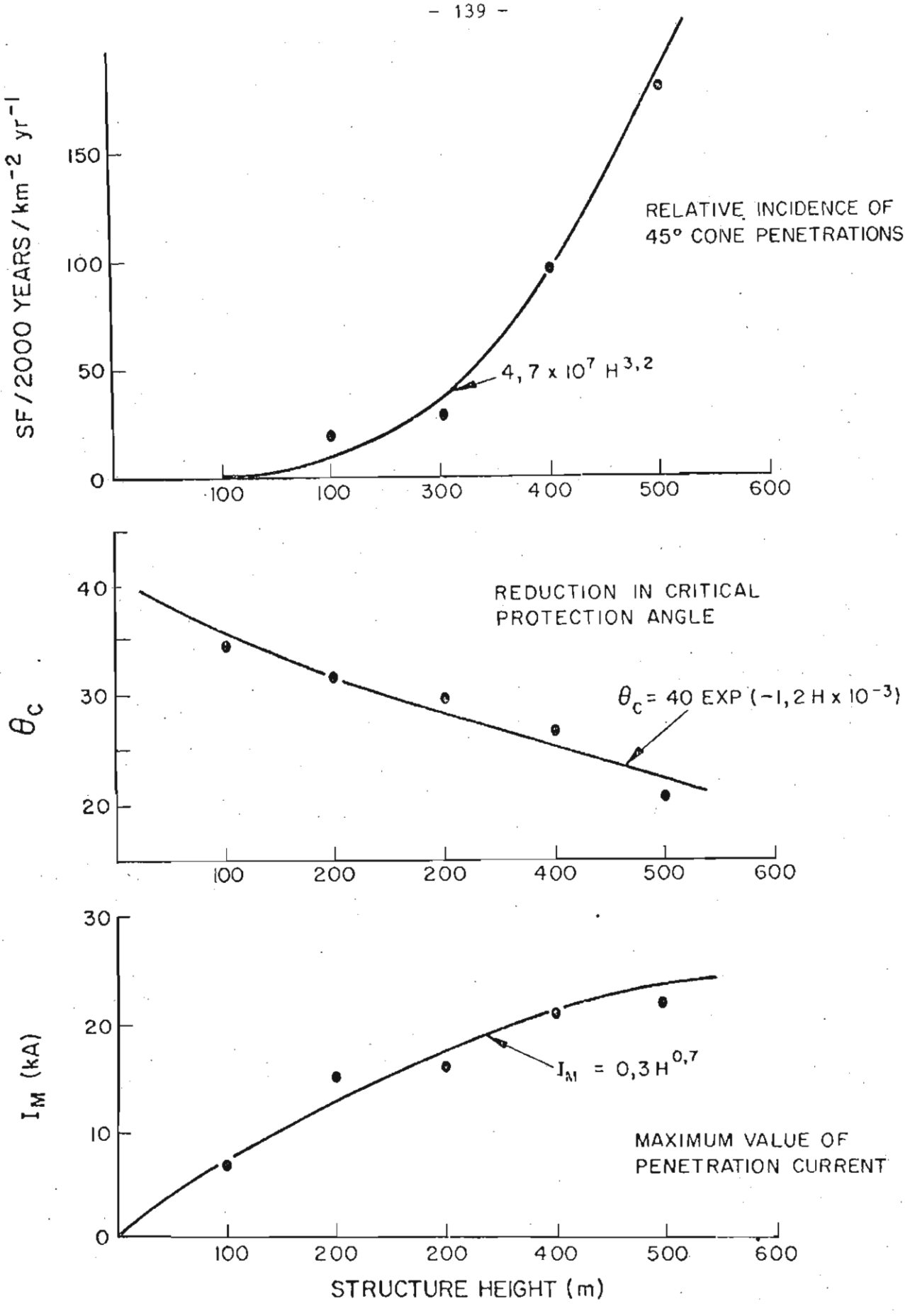

FIGURE 6.3

EFFECT OF STRUCTURE HEIGHT ON THE 45° CONE OF PROTECTION

In ...../140

In practical engineering applications the curves given in Figure 6.3 allow estimation of the effects of structure height upon the incidence of 45° cone penetrations and upon the magnitude of penetration currents - which could have important implications in the systems being protected. In principle provided sufficiently large samples of flashes were studied in the numerical simulations, these curves could be generalised to examine the protective effects of structures in relation to other protective angles, or in terms of varying degrees of protection (i.e. as opposed to the present curve for critical protective angle, which is equivalent to 100% protection - subject to the sample sizes studied is Appendix 6A).

Finally, this Appendix illustrates the application of the analytical approach and numerical studies to an examination of the effects of structure height upon the distributions of peak current amplitudes recorded in these structures.

Typical results are shown in Figure 6.4, together with the CIGRÉ reference distribution[20]. The numerically derived results indicate no substantial height effect upon the frequency distribution of peak current amplitudes.

This is an important observation, since this is contrary to another school of thought - illustrated by the work of Sargent[17] for example -which has suggested that the current amplitude distribution should tend toward higher currents as structure height is increased. The author has examined this concept previously, however, in an independent analysis of experimental field data and, although the latter is meagre, had concluded that there was no significant evidence for such a height dependency -once the effects of upward flashes had been taken into account[16].

Having arrived now at a similar conclusion in these analytical studies, the author is strongly of the opinion that there is little justification for the adoption of any concept of height dependent peak current amplitude distributions. This therefore is the basis of proposals made recently by the author in collaboration with Anderson; namely, that in practical engineering applications the CIGRÉ reference distribution should be adopted independently of structure height[20].

In summary therefore, considering the implications of this work, the analytical approach toward striking distance considerations (as evolved originally in Chapter 4 for the specific example of the research mast, and extended further in this chapter), has yielded generalised relations which accord reasonably well with the early experimental data for the mast studies, but which also corroborate, and, to a certain extent, provide a better basis

Figure 6.4 ...../141

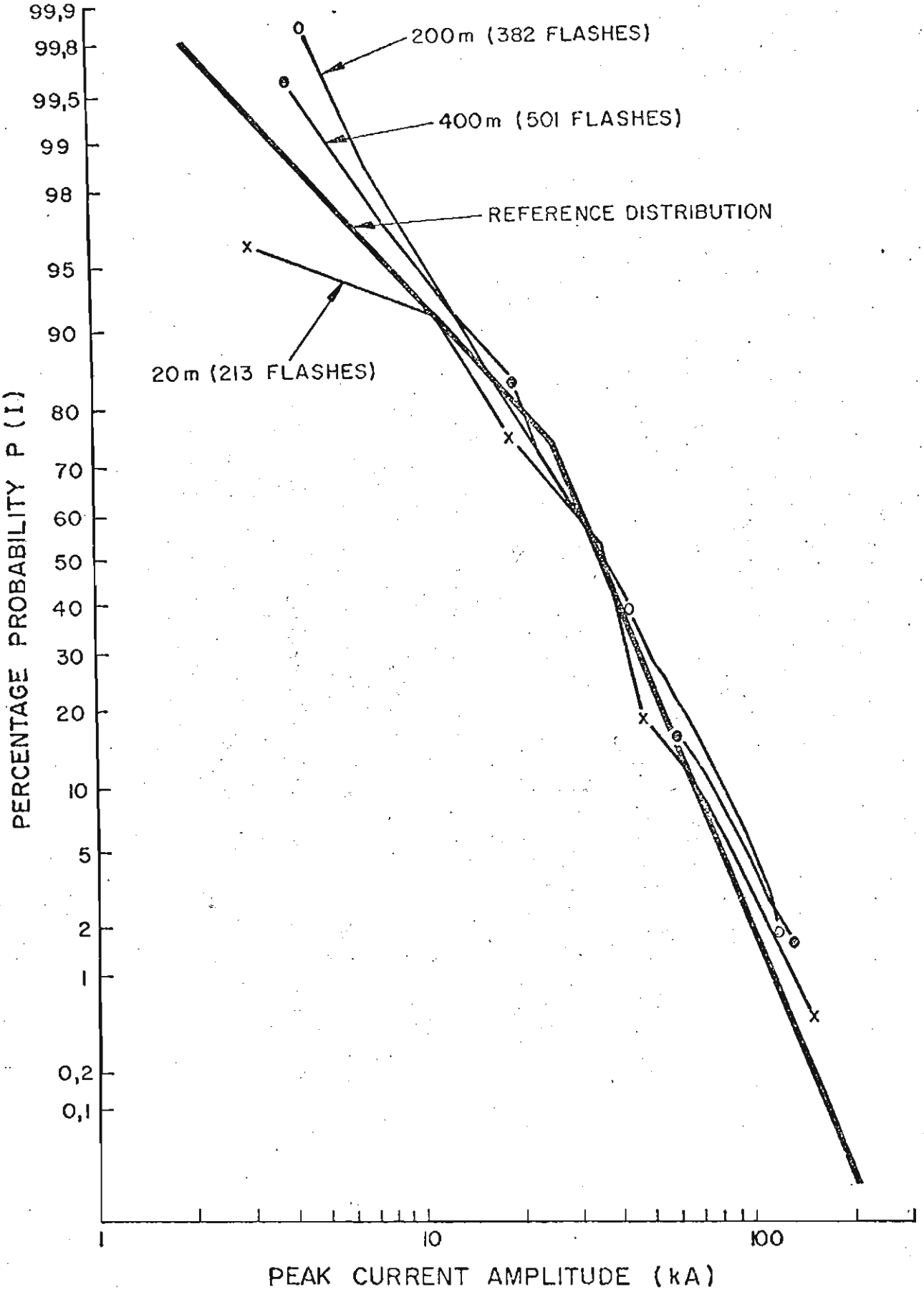

FIGURE 6.4

EFFECT OF STRUCTURE HEIGHTS ON THE NUMERICALLY DERIVED CUMULATIVE FREQUENCY DISTRIBUTIONS OF PEAK CURRENT AMPLITUDES

for, existing empirical protective concepts and relations.

However, having examined the assumptions involved in the analytical approach, the author considers that care should be taken in interpreting any quantitative determinations emerging from the generalised relations, and feels that the primary value of these analytical concepts lies in their expression of a consistent method of approach, whereby protective concepts may be clarified and certain trends delineated, (such as the influence of structure height).

Although considerably more field data are clearly required in order to clarify the assumptions involved in the analytical approach, the author still considers it possible, in the eventuality of better data becoming available, that the methodology is sufficiently consistent that the resultant fundamental trends may thus remain qualitatively unaltered.

6.4 Claims of this thesis

In summary of the preceding discussions, the following claims are noted:

(a) A research station has been established - embodying specialised services and protective arrangements, as well as instrumentation techniques - which has proved capable of reliable operation during thunderstorms and has yielded meaningful measurements of various lightning parameters during direct flashes to a research mast.

(b) The prelimary data accumulated over a 7 year period of observation have justified the original design bases in respect of choice of site and mast height, in that the majority of direct flash events on the mast have involved negative downward progressing discharges. This implies that the resultant measured data should be representative of what might be experienced in most practical engineering situations.

(c) The preliminary measured data describing the discharge current waveform characteristics - although comprising too small a sample to allow meaningful statistical analysis - are generally similar and consistent in trend with the comprehensive data accumulated by Berger in Switzerland. Since the two measurement locations differ markedly both in terms of climate and topographic situation, these observations imply that the characteristics of the downward flash process may possible remain similar over a wide range of structure situations and climatic variations.

(d) Measurement and analytical techniques have been evolved which provide a ready means for characterising regional lightning and thunderstorm climatology - principally in terms of electrical parameters. Subject to the possibility of long term cyclic variations, sufficiently consistent

data ...../143

data have been accumulated in the Pretoria region to allow a meaningful characterisation of storm electrical activity in this area. These data also imply that regional variations in lightning activity may be accountable primarily in terms of variations in storm duration.

(e) A technique involving orthogonal photography of direct flashes to the mast has been evolved, whereby the three-dimensional geometry of the final stages of the discharge path may be determined. Although specific to the research mast, the measured results have allowed the estimation of a unique (but tentative) measured relation between striking distances and peak discharge current amplitudes.

(f) Analytical concepts have been introduced whereby the final stages of a flash to a structure may be represented by a two-stage process, involving the initiation of an upward leader, which subsequently intercepts the downward progressing leader. An analytical approach based upon these concepts has been devised which yields a generalised relation for striking distance - expressed in terms of structure height and prospective stroke current.

(g) A concept for structure equivalent attractive radius has also been introduced and a generalised expression derived from the above analytical approach, which allows estimation of the incidence of direct flashes to a structure of interest.

(h) An application of the above generalised expressions in Monte Carlo techniques of numerical simulation has been illustrated, and yields calculated cumulative distributions of stroke current amplitudes in structures of varying height, which are apparently independent of height. This observation is in support of a postulate to this effect, previously published by the author, which arose out of an earlier empirical study of the influence of tall structures upon discharge characteristics.

(i) Subject to assumptions regarding the leader characteristics in this analytical approach, the results of the numerical study demonstrate a consistent agreement in trend with the results of earlier empirical studies and also corroborate existing empirical lightning protective concepts.

(j) In view of this agreement, it is considered that the above analytical approach - although still qualitative in certain respects - does provide a more meaningful basis for an effective understanding of the ground flash striking process and of the associated influence of structures - thereby demonstrating an improved methodology whereby protective

principles ...../144

principles may be optimised on a more rational basis - compared to earlier more empirical concepts.

6.5 Concluding remarks and future work

The principal objective of this research was to work toward a more comprehensive understanding of the lightning ground flash - both in respect of its characteristics locally in the South African highveld region, as well as in terms of the broader electrical engineering implications of this discharge - and the author considers that the material presented in this thesis may reasonably be claimed to have demonstrated meaningful progress toward this end. Two main directions of approach have been followed:

- an experimental research programme, involving the acquisition and analysis of field data, together with
- an analytical approach, aimed at establishing a better understanding of the striking process and thus of protective principles.

Clearly therefore, several possible directions of future research work may well arise, and, developing out of the discussions of the preceding chapters, the following avenues for further work are suggested:

(a) In the direct measurement of lightning discharge characteristics, it is necessary that the data sample be expanded considerably to allow meaningful statistical analysis. One possibility would be to continue the research mast programme for an adequate length of time, but bearing in mind the observed direct strike rate of only 4 flashes per year (as noted in Chpater 3), this may prove unacceptably long. Alternative possibilities would be to duplicate similar direct flash studies on suitable additional structures, (subject to the constraint that these be not so high as to cause an enhanced incidence of upward flashes), or to examine the possibility of applying indirect measurement techniques, such as those based upon the study of high speed electromagnetic field change recordings. The latter approach is attractive, in that data may rapidly be acquired, but interpretation of such recordings (in terms of the discharge current waveform) is still a matter of some controversy.(107) An interesting possiblity would be to integrate the direct measurements on the mast with remote electromagnetic field change recordings, as a calibration procedure for the indirect technique.

(b) The possibility of long term variations (cyclic, or otherwise) in annual thunderstorm electrical activity, remains an open question and could only be clarified by continuing the local measurement of thunderstorm parameters on a routine basis for an extended period of time. There is

also ...../145

also a need to examine regional and climatic variations in thunderstorm climatology more fully and this could be undertaken by extending the routine registration of thunderstorm parameters into other regions of the country, having markedly different keraunic indices to the Transvaal. An additional aspect of this work could be to study climatic influences on specific lightning characteristics - such as multiple stroke incidence for example, since at this stage it is often assumed that the characteristics and incidence of multiple stroke flashes are essentially similar in different climatic regions.

(c) As in the case of the direct stroke studies, there is an evident need to extend and improve upon the striking distance measurements. This might involve setting up similar orthogonal photographic systems near suitable additional structures, (possibly of different height), but another fruitful area of work could be to extend such studies through the use of high speed photographic techniques - capable of resolving the progression and velocity of leaders, as in the approach followed by Berger.[22]

(d) As far as the analytical concepts are concerned, apart from the necessity for additional physical data whereby the assumptions of the model can be clarified (such as those in relation to leader velocities, or charge distributions, for example), another potential area of further work lies in an examination of the application of the generalised analytical expressions, which are already suitable for application in existing transmission line lightning performance prediction studies and estimating methods. At present, such methods normally involve application of empirical relations for striking distances in electro-geometric techniques of analysis[19] (which do not take account of structure height and also do not include a concept of attractive radius). It is necessary therefore, that the role and implications of both generalised expressions be clarified in relation to existing approaches for line design. A further test of the new expressions would be a comparison between predicted and proven field performance of various systems. This could also lead to more accurate quantitative expression of these generalised relations.

In summary therefore, it is evident from the above that there is considerable scope for future research in the study of engineering aspects of the lightning ground flash.

As is no doubt the case in many other research areas concerned with the study of natural phenomena, one of the more stimulating features of work in the lightning field is the enormous complexity and variability of the phenomenon.

Despite the considerable advances in knowledge that have been gained over many years, the author considers that the lightning ground flash (as only one ramification of the phenomenon), will continue to exercise a considerable influence on engineering endeavours, and thus will also continue to present an intriguing and challenging field of study.

7. ACKNOWLEDGEMENTS

So many persons have contributed toward my progress in this research work that it is difficult to enumerate them all personally.

Firstly, however, I record my gratitude and appreciation to the Council for Scientific and Industrial Research of South Africa, and to my Director, Mr J.D.N. van Wyk, of the National Electrical Engineering Research Institute, for the opportunity to carry out this work and to prepare this thesis. In addition, this research would not have been possible without the substantial support of several of my colleagues in the Power Electrical Engineering Division, notably Dr Ralph B. Anderson (Head of the Division), who first conceived of this project and to whom I am grateful for his support, encouragement, and many hours of discussion, as well as Dave Meal and Margaret Smith, whose unstinting support in the daily operations of the research station and analysis of data I sincerely appreciate. I am grateful also for the assistance of other colleagues in NEERI in the general preparation of this thesis, including the typing and the tracing of the figures.

Secondly, I acknowledge a sincere debt of gratitude to many friends within the lightning "fraternity", whose discussions and contributions I have found invaluable - in particular, Dr. K. Berger, the late Dr R.H. Golde, Prof. E.R. Whitehead, Dr. T.E. Allibone, Dr. F. Popolansky, Prof. M.A. Uman, Mr. A.R. Hileman, and many others. Much of these discussions arose in the course of various overseas visits and in participation in CIGRE working group meetings and again, I record my appreciation to the CSIR for making those visits possible. I have appreciated also the relationship with my supervisor, Prof. H.L. Nattrass, whose encouragement and constructive criticism contributed effectively toward completion of this thesis.

Finally, progress in this research project over the past 7 years would have been impossible without the moral support, patience, and active participation of my wife and family.

8. BIBLIOGRAPHY .....

8. BIBLIOGRAPHY

1. SCHONLAND, B.F.J.; The Lightning Discharge, "Handbuch der Physik", Vol. 22, pp 576-628, Springer-Verlag OHG, Berlin, 1956.

2. MALAN, D.J.; "Physics of Lightning", The English Universities Press Ltd, London, 1963.

3. PIERCE, E.T.; The development of Lightning Discharges, Quart. J. Roy. Meteorol. Soc., Vol. 81, pp 229-240, 1955.

4. BROOK, M., KITAGAWA, N., and WORKMAN, E.J.; Quantitative study of strokes and continuing currents in lightning discharges to ground, J. Geophys. Res., Vol. 67, pp 649-659, 1962.

5. McCANN, G.D.; The measurement of lightning currents in direct strokes, Trans. AIEE, Vol. 63, pp 1157-1164, 1944.

6. HAGENGUTH, J.H. and ANDERSON, J.G.; Lightning to the Empire State Building, pt. 3, Trans. AIEE, Vol. 71(pt. 3), pp 641-649, 1952.

7. WAGNER, C.F.; Lightning and transmission lines, J. Franklin Inst., Vol. 283, pp 558-594, 1967.

8. WHITEHEAD, E.R.; Mechanism of lightning flashover on transmission lines, Final Report of Edison Institute Lightning Flashover Research Project RP-50, No. 72-900, 1972.

9. ANDERSON, R.B.; The lightning discharge, (Pd.D. Thesis), CSIR Special Report ELEK 12, Pretoria, 1971.

10. POPOLANSKY, F.; Frequency distribution of amplitudes of lightning currents, Electra No. 22, pp 139-146, 1972.

11. UMAN, M.A.; "Lightning", McGraw-Hill Book Co., New York, 1969.

12. GOLDE, R.H.; "Lightning Protection", Edward Arnold, London, 1973.

13. "Lightning", Vols. 1 and 2, (edited by R.H. Golde), Academic Press, London, 1977.

14. BERGER, K.; Methoden and Resultate der Blitzforshung auf dem Monte San Salvatore bei Lugano in dem Jahren 1963 - 1971, Bull. SEV, Vol. 63, pp. 1403-1422, 1972.

15. ANDERSON, R.B.; A comparison between some lightning parameters measured in Switzerland with those in Southern Africa, CSIR Special Report ELEK 6, Pretoria, 1971.

16. ERIKSSON, A.J.; Lightning and tall structures, Trans. SAIEE, Vol. 69, pp 238-252, 1978. (See Appendix 8A).

17. SARGENT, M.A.; The frequency distribution of current magnitude of lightning strokes to tall structures, IEEE Trans. PAS-95, No. 5, 1976.

18. BERGER, K., ANDERSON, R.B. and KRÖNINGER, H.; Parameters of lightning flashes, Electra No. 41, pp 23-37, 1975.

19. WHITEHEAD, E.R.; Protection of transmission lines, Chapter 22 in "Lightning" (edited by R.H. Golde), Academic Press, London, 1977.

20. ANDERSON, R.B. and ERIKSSON, A.J.; Lightning parameters for engineering application, Submitted for publication, Electra, 1979.

21. ERIKSSON, A.J.; Reply to discussion on paper "Lightning and tall structures", Trans. SAIEE, Vol. 70, 1979 (See Appendix 8A).

22. BERGER .....

22. BERGER, K.; The earth flash, Chapter 5 in "Lightning", (edited by R.H. Golde), Academic Press, London, 1977.

23. BERGER, K.; Lightning current parameters of upward strokes measured at Monte San Salvatore, Lugano, (C.E. Trans. 7358), from Bull. SEV/VSE 69, pp 353-359, 1978.

24. GORIN, B.N., LEVITOV, V.I., and SHKILEV. A.V.; Lightning strokes on Ostakinsk tele-tower in Moscow, Elektrichestvo No. 8, pp 19-23, 1977.

25. WILSON, G.L. and ZARAKAS, P.; Anatomy of a blackout, IEEE Spectrum, February, 1978.

26. ERIKSSON, A.J., STRAUSS, K.S.G. and VAN NIEKERK, H.R.; A lightning protection guide for electronic installations, CSIR Special Report ELEK 165, Pretoria, 1978.

27. ERIKSSON, A.J.; Lightning overvoltages on high voltage transmission lines - investigation of wave-shape characteristics, Electra No. 47, pp 87-110, July 1976.

28. RUSCK, S.; Protection of distribution lines, Chapter 23 in "Lightning", (edited by R.H. Golde), Academic Press, London 1977.

29. ANDERSON, R.B., VAN NIEKERK, H.R., GERTENBACH, J.J. and MEAL, D.V.; Progress report on the development and testing of lightning flash counters in the Republic of South Africa during 1971/72, CSIR Special Report ELEK 20, Pretoria, 1972.

30. GOLDE, R.H.; Lightning currents and related parameters, Chapter 9 in "Lightning" (edited by R.H. Golde), Academic Press, London, 1977.

31. GOLDE, R.H.; The lightning conductor, Chapter 17 in "Lightning", (edited by R.H. Golde), Academic Press, London, 1971.

32. TAGG, F.G.; "Earth Resistances", George Newnes Ltd, London, 1964.

33. WINN, W.P., ALDRIDGE, T.V. and MOORE, C.B.; Video tape recordings of lightning flashes, J. Geophys. Res., Vol. 78, No. 21, pp 4515-4519, 1973.

34. LAURIE, J.A.P.; Private Communication, NBRI, Pretoria, 1972

35. DONALDSON, G.W. and WILLIAMS, A.A.B.; Private communication, NBRI, Pretoria, 1972.

36. SARAOJA, E.K.; Lightning earths, Chapter 18 in "Lightning", (edited by R.H. Golde), Academic Press, London, 1977.

37. SUNDE, E.D.; "Earth conduction effects in transmission systems", D. van Nostrand Company, Inc., New York, 1949.

38. DEVGAN, S.S. and WHITEHEAD, E.R.; Analytical models for distributed grounding systems, IEEE Trans. Paper T73 182-3, presented at the IEEE PES Winter meeting, New York, 1973.

39. KAWAI, M.; Studies of tower footing resistance on transmission lines, Conf. paper presented at the IEEE Summer power meeting, Detroit, 1965.

40. ERIKSSON, A.J.; Notes on impulse impedance characteristics of earth electrodes, CSIR Special Report ELEK 164, Pretoria, 1979.

41. CANDLER, J.L.; The measurement of lightning currents by means of magnetic links, British Electrical and Allied Industries Research Association Technical Report S/T 31, London, 1940.

42. ANDERSON, R.B. and JENNER, R.D.; Lightning investigation on an 88-kV transmission line in Southern Rhodesia, Trans. SAIEE, Aug./Sept. 1948.

43. ANDERSON .....

43. ANDERSON, J.G.; Lightning performance of EHV-UHV lines, Chapter 12 in "Transmission Line Reference Book - 345 kV and above", Electric Power Research Institute, Palo Alto, 1975.

44. AIEE Committee Report, A method of estimating lightning performance of transmission lines, AIEE Trans. Vol. 69, pp 1187-1196, 1950.

45. POPOLANSKY, F.; Measurement of lightning currents in Czechoslovakia and application to obtained parameters in the prediction of lightning outages of EHV transmission lines, CIGRE Paper No. 33-03, Paris, 1970.

46. HILEMAN, A.R.; Parameters of the lightning flash, private communication to CIGRE WG 33-01, London, 1977.

47. GARBAGNATI, E., GUIDICE, E., LO PIPARO, G.B. and MAGAGNOTI, U.; Survey of the characteristics of lightning stroke currents in Italy -results obtained in the years from 1970 - 1973, ENEL Report R5/63-27, Milan, 1974.

48. BOSART, L.F., CHEN, T.J., ORVILLE, R.E. and ROESLI, H.P.; A preliminary study of the synoptic conditions associated with lightning flashes over Mt San Salvatore, Lugano, Switzerland, Tellus Vol. 26, No. 4, pp 495-504, 1974.

49. KRÖNINGER, H.; Private communication on the computer programme IMPULSE, NEERI, Pretoria, 1978.

50. ERIKSSON, A.J.; An unusual lightning flash?, Weather, Vol. 32, pp 102-106. 1977.

51. ALLIBONE, T.E.; The long spark, Chapter 7 in "Lightning" (edited by R.H. Golde), Academic Press, London, 1977.

52. GOLDE, R.H.; The lightning conductor, J. Franklin Inst., Vol. 283, pp 451-477, 1967.

53. ANDERSON, R.B., ERIKSSON, A.J. and KRÖNINGER, H.; Lightning and tall structures - some preliminary observations, 4th Int. Conf. on Gas Discharges, IEE Conf. Publication No. 143, 1976.

54. WALTER, B.; Stereoskopische Blitzaufnahmen, Physik, Zeitschr XIII, pp 1082-1084. 1912.

55. McCOMB, T.R., LINCK, H., CHERNEY, E.A., and JANISCHEWSKYJ, W.; Lightning research at the C.N. Tower in Toronto, Submitted for publication, 1979.

56. ROLFES, L. and BUYS, J.D.; The three-dimensional representation of a lightning flash, CSIR Special Report WISK 198, Pretoria, 1976.

57. ANDERSON, R.B. and ERIKSSON, A.J.; A preliminary striking distance concept, private communication to CIGRE WG 33-01, Coulommiers, 1976.

58. GOLDE, R.H.; Lightning and tall structures, Proc. IEE, Vol. 125, No. 4, pp 347-351, 1978.

59. HILL, R.D.; Analysis of irregular paths of lightning channels, J. Geophys. Res., Vol. 73, No. 6, pp 1897-1906, 1968.

60. SCHONLAND, B.F.J., MALAN, D.J. and COLLENS, H.; Progressive Lightning VI, Proc. Roy. Soc., Series A, Vol. 168, pp 455-469, 1938.

61. WILLIAMS, D.P. and BROOK, M.; Magnetic measurements of thunderstorm currents (1) Continuing currents in lightning, J. Geophys. Res., Vol. 68, pp 3243-3247, 1963.

62. HAGENGUTH .....

62. HAGENGUTH, J.H.; Photographic study of lightning, Trans. AIEE, Vol. 66, pp 557-585, 1947.

63. ANDERSON, R.B.; Lightning, CSIR Special Report ELEK 32, Pretoria, 1973.

64. ANDERSON, R.B., MEAL, D.V. and SMITH, M.A.; Eleventh progress report on the development and testing of lightning flash counters in the Republic of South Africa during 1978/79, CSIR Special Report ELEK 168, Pretoria, 1979.

65. PIERCE, E.T.; Triggered lightning and some unsuspected lightning hazards, Stanford Research Institute Scientific Note 15, Menlo Park, 1972.

66. McEACHRON, K.B. and MORRIS, W.A.; The lightning stroke: mechanism of discharge, Gen. Elect. Rev., Vol. 39, pp 487-496, 1936.

67. DELLERA, L., PIGINI, A. and THIONE, L.; A tentative model for negative lightning strokes, private communication to CIGRE WG 33-01, Dublin, 1977.

68. ALLIBONE, T.E.; Velocities of leader-strokes to lightning and spark discharges, J. Franklin Inst., Vol. 306, pp 35-39, 1978.

69. ANDERSON, R.B.; Measuring techniques, Chapter 13 in "Lightning", (edited by R.H. Golde), Academic Press, London, 1977.

70. CARRARA, G. and THIONE, L.; Switching surge strength of large airgaps - a physical approach, IEEE Trans. PAS, Vol. 95, pp 512-520, 1976.

71. JONES, B. and WATERS, R.T.; Air insulation at large spacings, Proc. IEE, Vol. 125, No. 11R, pp 1152-1176, 1978.

72. ALLIBONE, T.E. and DRING, D.; Lightning and the long spark; - the significance of leader-stroke velocity, Proc. Roy. Soc., Vol. A357, pp 15-35, 1977.

73. MALAN, D.J.; The relation between the number of strokes, stroke interval and the total duration of discharges, Geofisica Pura & Applicato - Milan, Vol. 34, pp 224-280, 1956.

74. ERIKSSON, A.J.; Video tape recordings of a possible ball lightning event, Nature, Vol. 268, pp 35-36, 1977.

75. BRANTLEY, R.D., TILLER, J.A. and UMAN, M.A.; Lightning properties in Florida thunderstorm from videotape records, J. Geophys. Res., Vol. 80, No. 24, pp 3402-3406, 1975.

76. ERIKSSON, A.J., VAN NIEKERK, H.R., BOURN, G.W. and VAN ZYL, B.B.; Lightning ground flash multiple-stroke discriminator, Proc. IEE, Vol. 125, pp 555-557, 1978.

77. ANDERSON, R.B., VAN NIEKERK, H.R. and GERTENBACH, J.J.; Improved lightning-earth flash counter, Electron Lett., Vol. 9, pp 394-395, 1973.

78. CARTE, A.E. and DE JAGER, J.C.G.; Multiple stroke flashes of lightning, J. Atmos. Terr. Phys., Vol. 41, pp 95-101, 1979.

79. CIANOS, N. and PIERCE, E.T.; A ground-lightning environment for engineering usage, SRI Tech. Report 1, Menlo Park, 1972.

80. KULIJEW, D.A.; Ozillographische Blitzuntersuchengen in der Gebirgsgegend Aserbaidshans, 13th Int. Blitzschutzkonf., Vienna, 1976.

81. ERIKSSON, A.J.; The measurement of lightning and thunderstorm parameters: results for the 1977/78 season, CSIR Special Report Elek 149, Pretoria, 1978.

82. CHALMERS, J.A.; "Atmospheric Electricity", Pergamon Press, London, 1967.

83. GUNN, R.; Electric field meters, Rev. Sci. Instr., Vol. 25, pp 432-437, 1954.

84. SMITH .....

84. SMITH, L.G.; An electric field meter with extended frequency range, Rev. Sci. Instr., Vol. 25, pp 510-513, 1954.

85. BERGER, K.; Methoden und Resultate der Blitzforschung auf dem Monte San Salvatore bei Lugano in den Jahren 1963-1971 - Ozillographische Messungen des Feldverlaufs in der Nähe des Blitzeinschlags auf dem Monte San Salvatore, Bull, SEV, Bd. 63, Nr. 24, Nr. 3, 1972/73.

86. KRÖNINGER, H.; Private communication on the computer programme FIELD, NEERI, Pretoria, 1976.

87. MOORE, C.B. and VONNEGUT, B.; The thundercloud, Chapter 3, in "Lightning", (edited by R.H. Golde), Academic Press, London.

88. LIVINGSTONE, J.M. and KRIDER, R.P.; Electric fields produced by Florida thunderstorms, J. Geophys, Res., Vol. 83, No. C1, pp 385-401, 1978.

89. STANDLER, R.B. and WINN, W.p.; Effects of coronae on electric fields beneath thunderstorms, Quart. J. Reg. Met. Soc., Vol. 105, pp 285-302, 1979.

90. MACKERRAS, D.; Determination of thundercloud charges and related electrical characteristics, CSIR Special Report Elek 44, Pretoria, 1974.

91. ANDERSON, F.J. and FREIER, G.D.; Relation of electric fields to thunderstorm days, J. Geophys. Res., Vol. 78, No. 27, pp 6359-6363, 1973.

92. PIERCE, E.T.; Lightning warning and avoidance, Chapter 15 in "Lightning", (edited by R.H. Golde), Academic Press, London, 1977.

93. FREIER, G.D.; A 10 year study of thunderstorm electric fields, J. Geophys. Res., Vol. 83, No. C3, pp 1373-1376, 1978.

94. PRENTICE, S.A., CIGRE lightning flash counter, Electra No. 22, pp 149-171, 1972.

95. ERIKSSON, A.J.; The measurement of lightning and thunderstorm parameters, CSIR Special Report Elek 51, Pretoria, 1974.

96. JACOBSON, E.A. and KRIDER, E.P.; Electrostatic field changes produced by Florida lightning, J. Atmos. Sci., Vol. 33, pp 103-117, 1976.

97. POPOLANSKY, F.; Correlation between the number of lightning flashes registered by lightning flash counters, the number of thunderstorm days and the duration of thunderstorms, Private Communication to CIGRE WG 33-01. Paris, 1971.

98. MACKERRAS, D.; Subtropical lightning, Ph.D. Thesis, University of Queensland, 1971.

99. HÖNNINGER, E.; Thunderstorms and lightning flash counters in Austria, private communication to CIGRE WG 33.01, Orleans, 1978.

100. LUNDQUIST, S. SCUKA , V. and VEDDA, D.; Some statistical features of discharging processes in thunderclouds, private communication to CIGRE WG 33.01, Le Puy, 1974.

101. POPOLANSKY, F. and LAITINEN, L.; Thunderstorm days, thunderstorm duration, and the number of lightning flashes in Czechoslovakia and in Finland, Studia Geoph. et Geod, Vol. 16, pp 103-106, 1972.

102. PRENTICE, S.A.; Frequency of lightning discharges, Chapter 14 in "Lightning", (edited by R.H. Golde), Academic Press, London, 1977.

103. ERIKSSON, A.J.; The measurement of lightning and thunderstorm parameters: results for the 1975/76 season, CSIR Special Report ELEK 103, Pretoria, 1976.

104. STRINGFELLOW .....

104. STRINGFELLOW, M.F.; Lightning incidence in Britain and the solar cycle, Nature, Vol. 249, pp 332-333, 1974.

105. ERIKSSON, A.J.; Thunderstorm incidence in South Africa, presented at the 21st Annual Conf. of the S.A. Inst. Physics, Johannesburg, 1976.

106. Union/Republic of South Africa - Weather Bureau; Reports on meteorological data of the years 1939-1972.

107. LIN, Y.T., UMAN, M.A. and STANDLER, R.B.; Lightning return stroke models, submitted for publication, J. Geophys Res. 1979.

108. HILEMAN, A.R.; Probability and statistics for power systems engineers (private communication) Pittsburgh, 1979.

APPENDIX 1(A) PHENOMENOLOGY OF THE GROUND FLASH

The material presented in this appendix is not considered to be either original, or even contentious. Much of the content of this thesis is concerned with those facets of the lightning process which relate to practical engineering situations. The engineering characteristics of the phenomenon are therefore of primary interest, rather than the physical attributes or mechanisms of the process. The phenomenology is complex however, and, in the interests of clarity, it was considered that a brief conceptual outline of the relevant aspects of the process could be helpful.

In the following sections the author has attempted to present a consensus view, which has been drawn from a study of the literature, and the interested reader is referred to several comprehensive books in which the subject is more fully reviewed (notably, Golde[13], Uman[11], Malan[2], Schonland[1]), as well as to the work of other researchers (e.g. Berger[22], Wagner[7] and Anderson[9]).

(Note: The terminology used in this thesis is based largely upon that evolved by Schonland[1]).

(a) The lightning flash

The term "lightning" usually embodies a temporary and localised electrical breakdown of the air over distances of several kilometers, leading to the transient passage of a high amplitude electric current. The terms "flash" and "discharge" are commonly used synonymously and imply the complete lightning event.

Several different lightning flash types, or forms, have been classified by Schonland, of which the most important are flashes between cloud and ground, (ground flashes); discharges between clouds, (intercloud flashes); and flashes between charged regions within the same general cloud volume, (intracloud flashes).

The latter two discharge types (often collectively termed cloud flashes), although representing the most frequently occurring form of lightning, are generally of little consequence to most practical engineering situations, (with the exception of aircraft).

The ..... /A-2

The event of direct concern is the ground flash and the remainder of this appendix relates primarily to this form of lightning.

(b) Thundercloud electrification and discharge initiation

Although the mechanisms leading to the generation, separation, and subsequent localised concentration of electrical charges within a thundercloud, are not yet fully understood, it is generally agreed that these involve a complex interaction of water and ice particles in the dynamic medium of the cloud, where these particles are subjected to manifold influences, including complex wind profiles, temperature gradients and gravitational forces. The end result, however, is the development of localised charged regions within the cloud, with different charge polarities being present in different regions. Although this aspect is also not yet fully resolved, evidence is available which indicates a tendency toward a dipole cloud charge structure, with the upper cloud regions being positively charged in relation to the lower negative part of the cloud. Convective thunderclouds in Southern Africa reportedly have typical heights of the order of 10 - 15 kms, with the cloud base being about 1 - 2 kms above ground level in the highveld regions. Typical total thundercloud charges are considered to be of the order of 50 - 100 coulombs.

In a process which is again not yet adequately clarified, the concentration of charges within certain regions of the cloud can, on occasion, allow the attainment of sufficiently high electric field intensities (thought to be of the order of 500 kV/m), to cause localised electrical breakdown and the initiation of the leader process. The initial downward discharge is termed the downward leader and most commonly involves the lowering of negative charge from the cloud toward the ground.

(c) The stepped leader

This term is used to describe the physical mechanism whereby the initial breakdown process in the cloud proceeds toward the ground. The physical process is as yet poorly understood but it is generally agreed that the downward leader displays the following features:

- the ..... /A-3

- the electrostatic field change recorded at ground level during the approach of the leader is comparatively smooth - implying a more or less continuous movement of charge in the leader, toward the ground;
- this downward movement of the leader is associated with a sequence of transitory and weak illuminations of the discharge path - which give rise photographically to the impression of a series of steps. This luminous step process usually takes place within 1 μsec;
- the pause times betweeen steps are of the order of 50 μsec and step lengths (i.e. distance of leader advancement between re-illuminations) are typically about 25 - 50 m;
- the average velocity of progression of the downward leader varies between about 1×10^5 and 2.10^6 m/s with values in the range of $1 - 2 \times 10^5$ m/s being representative;
- the charge lowered along the downward leader is generally considered to vary between about 1 and 10 coulombs with an average value of about 5 coulomb;
- the initial cloud breakdown processes are thought to initiate at heights above ground level of the order of 3 - 7 kms. At an average downward velocity of about 1×10^5 m/s, the leader will therefore require about 30 - 70 ms to traverse this distance - implying that the average current in the leader should be of the order of 100 A, in order to lower charges of about 5 coulomb. This magnitude of current is generally supported by indirect field observations, and is thought to increase momentarily to the order of 1 - 10 kA during the step illumination process.

There is as yet no general agreement regarding the distribution of charge along the leader, although electrostatic field change recordings at ground level suggest that the distribution could lie between uniform and linear forms. Usually, the downward leaders of first strokes exhibit substantial branching and the author inclines to the view that the charge distributions along the individual branches could tend more to the linear (or even exponential) form, due to

the .....

the enhancement of the electrostatic field as the ground is approached. In practice, the spatial extent of these leader branches could then give rise to the effect of a more uniform distribution of charge as far as ground based field change determinations are concerned.

Structually, the leader is generally considered to comprise a central arc-like core filament (of the order of 10 mm diameter or less) in which the leader current flows, surrounded by an extensive corona sheath of the order of 5 - 10 m radius - which provides the main medium for the deposition of the leader charge.

The physical mechanism of the stepping process is still unresolved and a variety of theoretical leader models have been presented. Although by no means exclusive, these often invoke the characteristics of the glow to arc transition to account for the transient illuminations. One school of thought also considers that the visible, and apparently intermittent leader steps, are preceded by a continuously advancing (i.e. ionising) tip region - generally thought to have the attributes of a corona or glow discharge - and often termed the "pilot leader".

In a more detailed study of stepped leader characteristics, Schonland introduced several subdivisions (termed α and β stepped leaders) dependent upon step length, average velocity and degree of branching.

For the purposes of this thesis however, the stepped leader is considered to comprise a randomly oriented and branched system of breakdown channels, propagating downward toward the earth at an approximately uniform velocity. Each major branch is considered to be composed of a filamentary core surrounded by a corona sheath, and the charges deposited along the leader in the course of its propagation, are thought to be distributed in such a manner that the local charge per unit length increases, as the ground is approached, (i.e. corresponding to a linear or even exponential representation).

(d) The .....

(d) The "final jump" and the return stroke

In its path between the cloud and ground, the progression of the stepped leader is considered to be randomly oriented - being influenced primarily by the direction of the electric field between the charged cloud and the induced charges on the ground, as well as by the presence of localised "pockets" of space charge in the intervening atmosphere - the latter being the by-product of point discharge processes from the ground and from surrounding objects.

As the downward leader approaches the ground, the increasing proximity of the charges being lowered along the leader causes a pronounced increase in the electric field between the ground and the tip of the descending leader. Eventually, at a stage in this descent which depends upon the magnitude of these charges and upon the degree of field intensification caused by the presence of any structures on the ground, electrical breakdown conditions are attained at the ground - or on objects or structures - leading to the initiation of an upward progressing discharge - often termed the upward "streamer", or "connecting leader".

It is normally considered that the requisite field conditions involve the attainment of local field gradients of the order of $1 - 3 \times 10^6$ V/m - or, alternatively, as discussed by several authors, the attainment of an average gradient between the descending leader tip and the ground (or a structure), of about 500 kV/m.

Although data are scarce, these upward connecting leaders are considered to be positively charged, and to have average upward velocities in the range $1 \times 10^5 - 1 \times 10^6$ m/s.

The final stages of the process, (termed the "final jump" in the field of laboratory long-spark research), involve the interception of the connecting leader and the downward stepped leader and the resultant initiation of the return stroke - which is observed as a high velocity intensely luminous process propagating from the ground back up to the cloud.

The physics of the return stroke process are as yet largely unresolved and several conceptual models have been presented in the literature. One school of thought considers that the stepped

leader .....

leader is at an extremely high potential immediately prior to the commencement of the return stroke, (effectively given by the cloud potential minus the leader potential drop), and that the return stroke involves the propagation of ground potential up the leader channel. Alternatively, Anderson has suggested that the descending leader tip potential reduces virtually to ground potential as the earth is approached and that the return stroke comprises a re-combination process travelling back up the channel. In the former instance a temporary high potential gradient is considered to exist at the leader/return-stroke interface and to travel upwards as an ionising potential wave. In the course of this process, the charges originally deposited along the leader corona sheath become discharged to earth through the return stroke channel and lead to a rapid rise in the current flowing at the base of the channel into the ground. (In the event of a normal negatively charged stepped leader, this current is made up of electron flow and is therefore negative). Wagner has suggested that the thermalisation energy required for the increase in channel conductivity to allow the transition from leader currents of some hundreds of amperes to the return stroke current (of the order of kiloamperes), gives rise to retarded wave propagation of the return stroke front and has determined relations between the resultant return stroke velocity and the stroke current.

Direct observations (usually based upon high speed photography) have shown that return stroke velocities can vary over the range of about 2×10^7 m/s to $1{,}5 \times 10^8$ m/s, with mean values being typically about 5×10^7 m/s. Return stroke velocities are also found to decrease with increasing channel height (especially for first return strokes), and to display significant reductions in velocity at branch junctions. Optical estimations of return stroke channel diameter have indicated values of the order of 5 - 100 mm.

Theoretical studies of the arc channel physics have suggested that the intense thermalisation of the leader core in the transition to the return stroke arc (involving a core temperature increase from about $3\,000^{\circ}K$ - $30\,000^{\circ}K$), gives rise to a transient channel over-pressure, which in turn generates a supersonic and approximately

cylindrical .....

cylindrical shock-wave. Within a few metres of the channel, the expanding shock-wave relaxes to a sound wave, which, after propagation through the surrounding atmosphere, gives rise to the audible thunder normally recorded at ground level.

The return stroke current flow - as measured at the ground - decreases rapidly in a period of the order of 100 μs - but may on occasion persist as a low current discharge of a few 100 amperes for many milliseconds, in a process termed a "continuing current" discharge. Excluding these comparatively rare instances, the total charge transferred by the return stroke is of the order of 2 - 4 coulombs - or marginally less than the average charge originally lowered by the stepped leader.

In about 50% of ground flashes, the extinction of the return stroke current represents the termination of the flash process - which is then characterised as a single stroke event.

(e) Subsequent strokes

Alternatively, in many instances, following a "recovery" interval of the order of 30 to 50 ms, a second faintly luminous leader traverses the original discharge path between cloud and ground and initiates a subsequent return stroke process. In contrast to the stepped leader, this new leader (usually termed the "dart" leader), does not normally display steps, but moves continually downward at a substantially higher velocity (typically 2×10^6 m/s). In addition, direct measurements have indicated that the resultant subsequent return strokes display marginally higher velocities (about 1×10^8 m/s) and steeper rates of rise of current. Generally, the associated peak current amplitudes are significantly less than that of the first return stroke.

This dart leader/subsequent return strokes process may repeat itself sequentially and multiple stroke flashes exhibiting in excess of 20 subsequent strokes have occasionally been observed. On average however, ground flashes do not usually contain more than 2 - 3 subsequent strokes.

(f) Upward .....

(f) Upward flashes

The preceding sections have discussed the processes involved in the negatively charged downward progressing ground flash - which is the discharge of most concern in the majority of practical engineering situations, due to its frequency of occurrence.

Depending upon the polarity of the originating cloud charges and the direction of progression of the flash leader, four main types of ground flash may be identified:

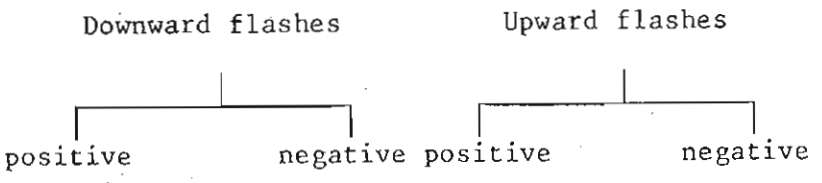

Downward positive flashes occur extremely rarely (displaying an incidence of less than 10% in comparison to negative downward flashes), and in practice are thought to occur mainly toward the end of thunderstorms, when the lower negatively charged regions of the cloud may largely have collapsed, or been discharged.

Upward flashes are found to occur mainly from mountaintop installations, or from very tall structures. In such situations, the upward progressing leader referred to previously (in (d) above), is in fact initiated very early in the discharge process - either following a cloud flash - or, in some instances, when the field gradient developed by the thundercloud charges themselves becomes sufficiently intensified around such tall structures to cause the attainment of upward leader inception conditions.

As in the case of the downward flash process, these upward leaders are initially positively charged, and, if followed by return strokes, lead to the discharge of negative currents, which are generally found to be of comparatively low magnitude. In a detailed analysis of upward flash characteristics, Berger[23] has shown that in many instances such tall structure-initiated upward leaders are in fact not followed by return strokes and he has identified such events as a further sub-grouping of the above four types of ground flash process[22].

In .....

In a separate analysis of the characteristics of flashes on tall structures[16], the author has shown that the incidence of upward discharges is extremely low on structures having heights less than 100 m. Since this applies to the majority of practical engineering structures which may be concerned with lightning protection considerations (e.g. transmission lines, buildings, etc.), the discharge process of primary concern to this thesis is the negative downward flash.

The role of the structure in the discharge process (including the influence of structure height), is further examined in Chapters 4 and 6.

APPENDIX 1(B) PROTECTIVE CONCEPTS AND ELECTRICAL ENGINEERING ASPECTS

(a) Lightning protection

In its modern conceptualisation, lightning protection embodies two interdependent requirements, namely "diversion" and "conduction". The former implies the provision of preferential strike points, which exert a local attractive influence on nearby flashes - in the sense that upward connecting leaders are initiated preferentially from these points - thereby defining the point of stroke termination and simultaneously shielding adjacent installations from the flash. The second requirement involves the provision of adequate means of safely conducting lightning return stroke currents from the point of strike - and thereby away from the installation being protected - and down to an effective earth electrode.

Clearly therefore, in order to achieve effective lightning protection, a comprehensive understanding is required of the striking process and of the influence of structures upon this process, so that shielding principles may be clarified and optimised. Thereafter, information is also required regarding the parameters of the discharge current (for example, peak amplitude and duration), in order that the protective system may be adequately designed.

For practical protective applications, a variety of either empirical or analytical concepts and relations has been evolved over the years - as reviewed for example by Golde[12]. For a structure, these are often expressed in terms of a protective ratio R/H_s, where H_s is the height of the structure, and R a radius drawn around that structure to define the zone within which objects are effectively shielded. Values proposed for this ratio have varied between about 0,25 and 9, with a ratio $R/H_s=1$ being commonly adopted in modern practice. In many lightning protective codes of practice the area shielded around a structure is often represented by a "cone of protection", drawn with the apex of the cone at the top of the structure and an apex angle of 45° is normally adopted - although in critical situations a more conservative angle of 30° is often recommended.

Over .....

Over the years, such empirical concepts have been found to yield quite adequate protective experience in the normal range of structure heights - such as domestic housing, office blocks, or explosive magazines (in the case of the 30° protective angle.)

At this stage little information is available regarding the influence of structure height upon the degree of protection afforded in terms of these concepts, but several workers have noted that on occasion, weakly charged flashes have struck the sides of very tall structures, or have struck the ground within the equivalent radius of the 45° protective cone[24].

Thus, although empirical concepts such as the 45° cone of protection may well have proved adequate in many practical and domestic situations, it is also apparent that the degree of effectiveness may possibly reduce as structure height is increased.

(b) Electrical engineering aspects

The manner and degree to which lightning can effect electrical engineering systems vary considerably, but the disruptive influences of lightning are experienced over the full range of electrical systems - extending from sophisticated and sensitive electronic microcircuitry to major extra high voltage (EHV) power transmission networks. The consequences of lightning in such systems can also vary similarly, ranging from the induction of spurious or disruptive logic pulses in a digital computer system, to sustained interruption of major power supply systems (such as the 1978 New York blackout, for example, where the consequential costs of the disturbance were estimated to be of the order of US $350 million[25].)

In every instance, effective protective or remedial measures require an understanding of the lightning phenomenon and of the range of parameters that may be encountered in practical situations.

Although the problems involved in operating modern electronic systems represent a growing area of concern[26] extending even to the aerospace industry - the field of practical engineering endeavour in which lightning disturbances have the main impact

remains .....

remains the transmission and distribution of electrical power. (For example, in the Transvaal region, the average monthly outage rates of power lines at the height of the summer lightning season varies from about 10 outages per 100 km of line per month at the 11 kV distribution level, down to about 0,5 outages per 100 km of line per month at the 400 kV transmission level.)

The electrical engineering implications of this have been reviewed elsewhere by the author[27] and therefore only the salient aspects will be repeated here.

The primary effect of lightning discharges, as far as power lines are concerned, is the impression of transient overvoltages upon the system. Depending upon the line insulation withstand characteristics (and thus in turn upon the nominal voltage rating of the line), this may, or may not lead to a breakdown, and ultimately to an outage of the system.

There are three mechanisms whereby lightning overvoltages may be impressed upon the conductors of a power line, and, as shown in Figure 1.B-1, these are related to the final paths to earth that a nearby lightning leader may take - as summarised below:

(i) The induced voltage mechanism

This arises when a ground flash does not actually terminate on the line or on the supporting towers, but strikes the ground in the immediate vicinity instead. For a given line, it is readily shown, using classical electromagnetic field theory[28], that the resultant overvoltage amplitude induced on the line is directly related to the crest value of the lightning return stroke current.

A study of the prospective overvoltage amplitude distribution therefore requires knowledge of the distribution of peak lightning current amplitudes during ground flashes.

Practical experience has indicated that the induced voltage mechanism is principally of concern at distribution levels of system voltage.

(ii) The .....

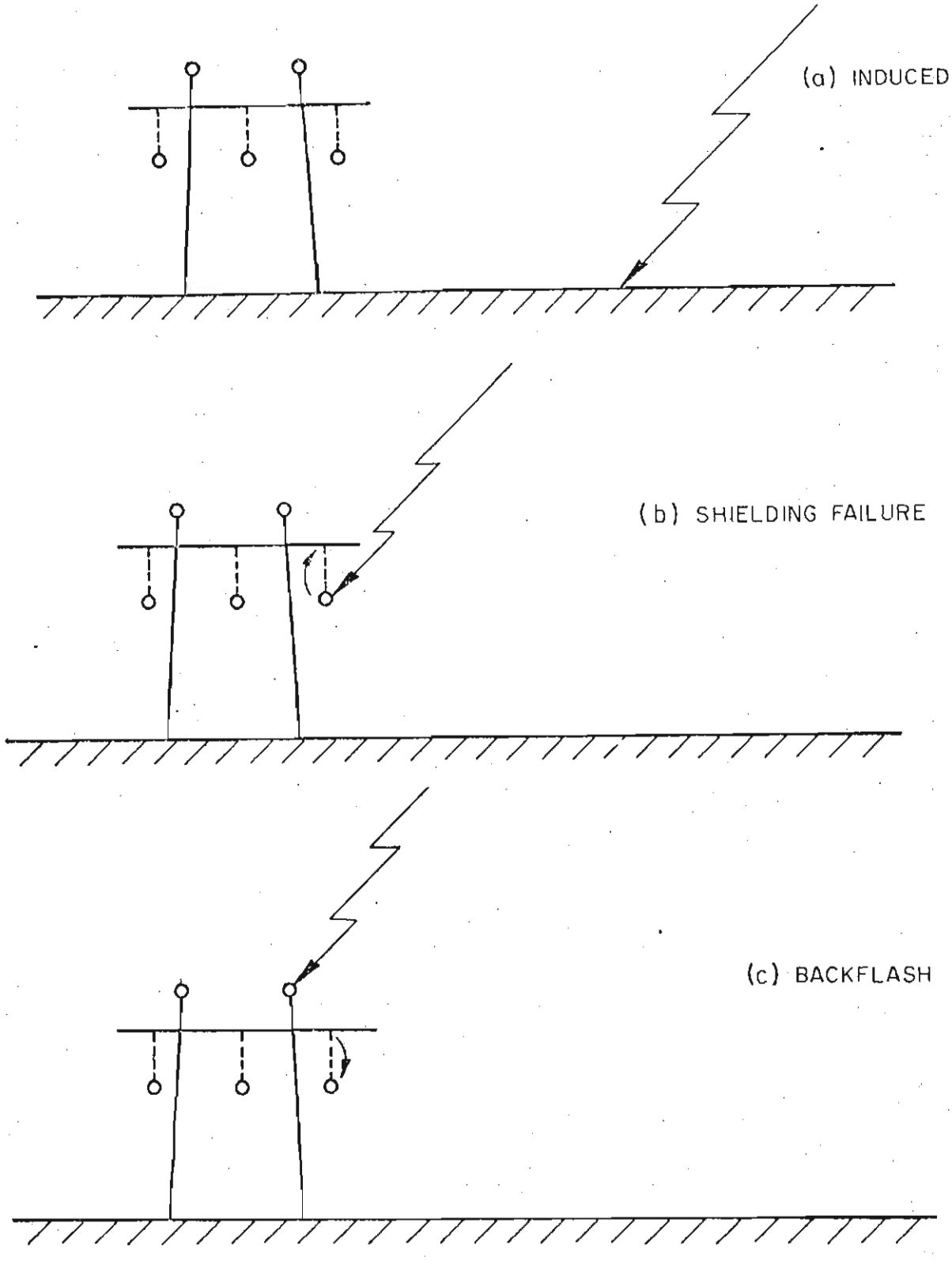

FIGURE IB-1

MECHANISMS WHEREBY LIGHTNING OVERVOLTAGE SURGES MAY BE CAUSED ON A TRANSMISSION LINE

are frequently encountered in the literature

(where D_s = striking distance
I = crest return stroke amplitude
and K and b are empirical concepts).

In consequence therefore, any application, as well as any optimisation of such shielding concepts requires an understanding of the striking process, together with knowledge of possible striking distance dependencies, and of the distribution of peak current amplitudes.

In the event of a shielding failure, the resultant transient overvoltage upon the phase conductor has a crest amplitude U given by;

$$U = I.Z_o/2$$

where I = peak amplitude of the stroke current
Z_o = conductor surge impedance.

In order to assess the probability of a flashover, the overvoltage waveshape U(t) must be related to the voltage-time withstand characteristics of the line insulation system. This therefore implies the need not only to know the probability distribution of lightning current amplitudes, but also the time dependent features of the stroke current waveshape and any likely variations in shape.

(iii) Provided a power-line is adequately shielded, the majority of ground flashes in its immediate vicinity should terminate upon the shield wires, or upon the supporting towers. As the stroke current is discharged to earth via the shield wires and tower elements, the possibility then arises that sufficient voltage may be developed across the series impedances presented along these discharge paths to cause a "back flash-over" across the supporting insulator strings into one or more of the phase conductors.

Analysis of the voltage stresses developed across the line insulation in this situation is complex however, and must take account of several complicating factors, including;

- coupling .....

- coupling effects amongst the phase conductors and shield wires, as well as with the upward leader
- pre-discharge corona effects
- transient impedance characteristics (i.e. as a function of time, or frequency) of the supporting towers and of the terminating earth electrode arrangment at the tower base.

Fundamental to all such analysis however, is again the need for an adequate representation of the lightning discharge current waveshape, and in this case, particularly of the maximum current rate-of-rise characteristics on the impulse wavefront.

(c) Lightning parameters

In summary of the preceding sections therefore, implementation of an effective lightning protective approach (whether this relates to the protection of a dwelling house, or of a broadcast antenna station, or of a major power line), requires a comprehensive knowledge of one, or more, of the following primary aspects of the discharge - and more particularly, in respect of the negative downward flash, since this is most commonly encountered in practical situations:

(i) striking distance characteristics

(ii) probability distribution of stroke peak current amplitudes

(iii) time dependent characteristics of the discharge current waveform.

In certain protective applications it may also be necessary to know the incidence of multiple stroke flashes, as well as the probability distributions of such related parameters as, flash duration, stroke duration, inter-stroke interval, etc.

A fundamental parameter in virtually all lightning protective studies is, of course, a measure of the incidence of lightning in the area of concern. Although historically this is normally expressed in terms of annual thunderstorm day occurrence (or keraunic index), a far more reliable determination is on the basis

of .....

of a measurement of the local ground flash density. This can be carried out using calibrated lightning flash counters. Since a comprehensive long term project involving the development and application of lightning flash counters was already in operation in the Pretoria area[29] at the commencement of this thesis project, the study of ground flash density has not been included in the scope of the thesis work.

As far as available data on the other lightning parameters is concerned, probably the most comprehensive source of information lies in the results accumulated by Berger[14], in a long term study of ground flashes at the San Salvatore research station in Switzerland. These results include considerable data on the impulse waveshape characteristics of the discharge current and several statistical analyses of these data have been published[18].

Over the years, a variety of studies of the distribution of lightning current amplitudes have also been carried out - as reviewed recently by Golde[30], for example. Of the various distributions that have been prepared for practical applications, perhaps the most representative is that compiled by Popolansky[10] - which also includes data from Berger's measurements.

More recently, arising partly out of work carried out in the course of this thesis project, Popolansky and the author, in collaboration, have compiled a modified summarising distribution[20], which is considered to be more representative of practical engineering application situations.

The latter summarising distribution, together with Berger's comprehensive waveform data, will provide the main basis for comparison with the locally measured results presented in this thesis.

As far as striking distance relationships are concerned, the author is not aware of any meaningful measured data. Published expressions relating striking distance to prospective stroke peak currents[31] have normally been derived empirically, or calibrated from field observations of service performance of transmission lines having various shielding arrangments.

The .....

The study of striking distance concepts and relationships therefore represents a major aspect of the work of this thesis, as discussed further in Chapters 4 and 6.

APPENDIX 2.(A) ASPECTS RELATED TO THE RESEARCH MAST STRUCTURAL DESIGN

(a) Wind loading and stay tensions

This analysis was carried out in collaboration with the Structural Engineering Division of the National Building Research Institute[34], and only the salient points will be summarised here.

Since the research mast was considered a temporary structure, the analysis was based upon the maximum 3 second wind gust for a 10 year return period, which is about 33 m/s at an anemometer reference height of 13 m (as predicted from gust records from Jan Smuts airport).

The drag coefficient of the structure and the variations in dynamic pressure exerted by the wind on the mast were calculated by the NBRI from the dimensions of the tower components (taking the exposed position of the mast also into account). The resultant dynamic pressure was found to increase from about 130 kPa at the base, up to about 165 kPa at the top.

On the assumption that each stayed point on the mast (apart from that at the top position), has to cater for the wind forces exerted on the intervening 15 m height of structure, the resultant approximate horizontal reactions are as shown below:

Top (60 m)	–	7,6 kN
Third (45 m)	–	13,7 kN
Second (30 m)	–	12,8 kN
First (15 m)	–	11,4 kN
Base	–	5,6 kN

The stay angles are as indicated below (for the three stays at each position, together with the calculated requisite stay pretensions that would be necessary in order to sustain the above loading:

Position	Stay Angles (NW and NE)	Tension	Stay Angle (S)	Tension
Top	53°	6,1 kN	46°	5,5 kN
Third	35°	7,9 kN	36°	8,1 kN
Second	42°	8,6 kN	40°	8,2 kN
First	35°	6,5 kN	35°	6,5 kN

The .....

The equivalent vertical loading effect on the mast as a consequence of the above stay pretensions is about 105 kN. Taking the mast weight of 10 kN into account, the total vertical loading upon the isolated base structure becomes 115 kN, which is well within the capabilities of the four pedestal insulators which share this load. (Each unit has a compression loading capability in excess of 100 kN).

As a check on the original design assumption of the maximum gust velocity of about 33 m/s, a recording anemometer was installed at a height of about 6 m and approximately 10 m away from the research mast.

Recordings were maintained through three thunderstorm seasons and a total recording period of 310 days was obtained. The maximum gust velocity recorded in this period was 23,7 m/s and the peak gust velocities, when analysed, displayed the distribution shown in Figure 2.A-1. This suggests a very low probability for gusts in excess of 25 m/s (about 0,8% per year) and would indicate that the assumption of 33 m/s as a design parameter (which was based upon a 10 year return period), provides an acceptable margin of safety.

(b) Anchor block loading and design

A total of 6 stay anchor blocks was provided - each serving for the attachment of 2 stays, as shown earlier in Figure 2.2.

In terms of the above stay angles and pretensions the maximum vertical reaction on each anchor point would vary between 10 kN and 12 kN.

The anchor block design adopted is shown in Figure 2.A-2. Basically, it consists of a concrete section comprising a surface slab and a buried cylindrical core. Reliance is also placed on the soil reaction effect which, as a simplification, may be considered as the contribution of a soil frustrum surrounding the concrete core[35]. In soil of the rocky nature encountered on this site a frustrum angle of 8° may be assumed[35].

The .....

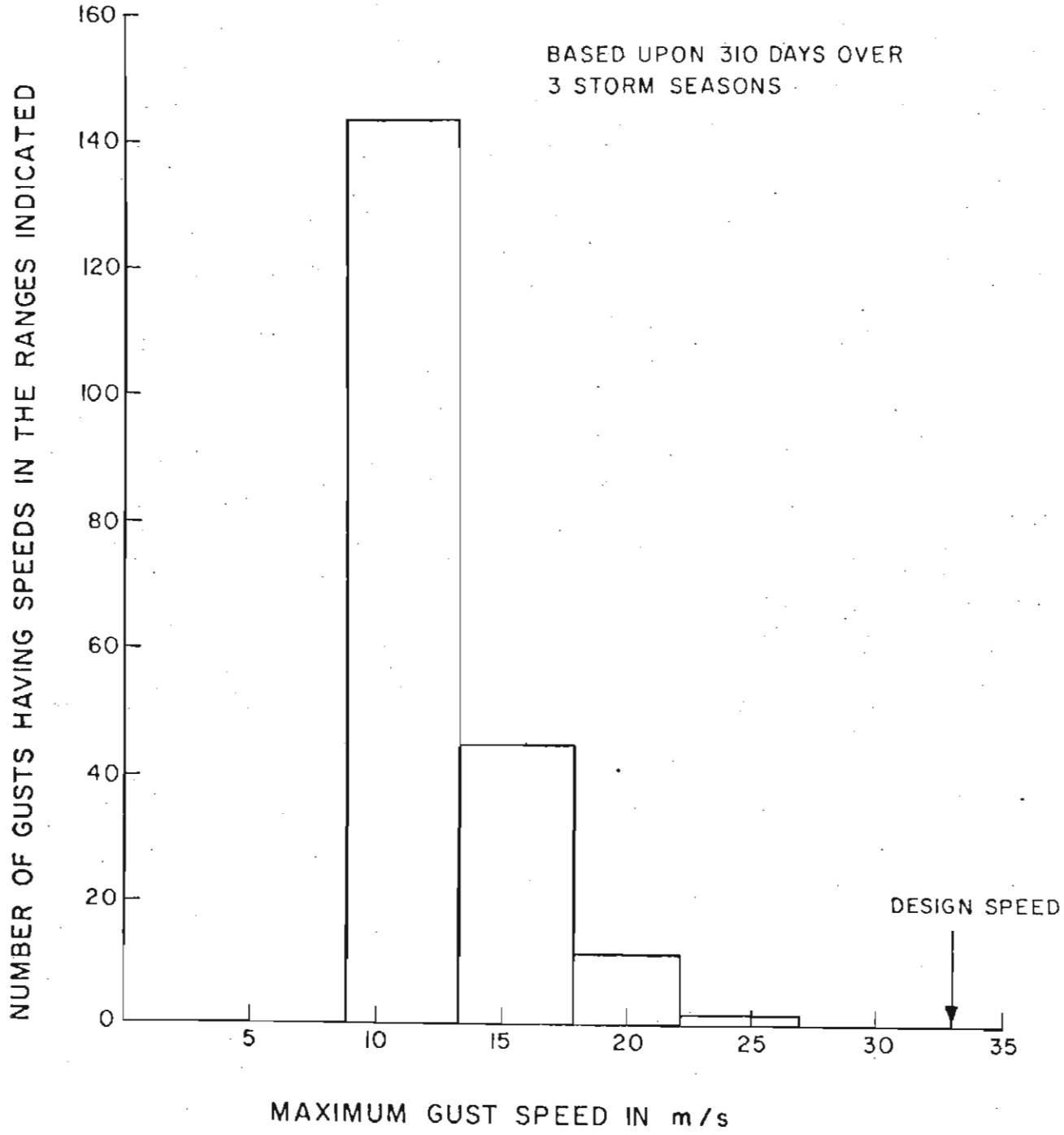

FIGURE 2 A-1
MEASURED DISTRIBUTION OF WIND GUST VELOCITIES

The load effect of this frustrum is readily determined as;

$$L_s = \delta \, (\pi/3 \, \{(R + D \tan \theta)^2 \, (D + R/\tan \theta) - R^3/\tan \theta\} - \pi R^2 D) \quad \ldots \quad (2.A\text{-}1)$$

where L_s = load reaction contributed by the frustrum in kN

δ = density of soil (assumed to be 17,5 kN/m^3)

and R, D and θ are as shown in Figure 2.A-2.

In view of the difficult nature of the terrain it was necessary to optimise the dimensions of the anchor block in order to minimise the amount of digging required.

Accordingly, the anchor block load was estimated for a variety of dimensions, as illustrated by the curves in Figure 2.A-3, (which assume a density for concrete of 23,8 kN/m^3).

As a consequence, an anchor block having a minimum core radius of 450 mm and a depth of burial of 750 mm was adopted, together with a surface slab comprising a minimum concrete volume of 0,3m^3. As may be seen in Figure 2.A-3, this design provided a minimum load of 21 kN which allowed an adequate margin of safety over the anticipated maximum equivalent vertical stay reaction of 12 kN. In practice, with the anchor block dimensions realised on site during construction, it is anticipated that the resultant anchor block loads are in the range of 25 - 30 kN.

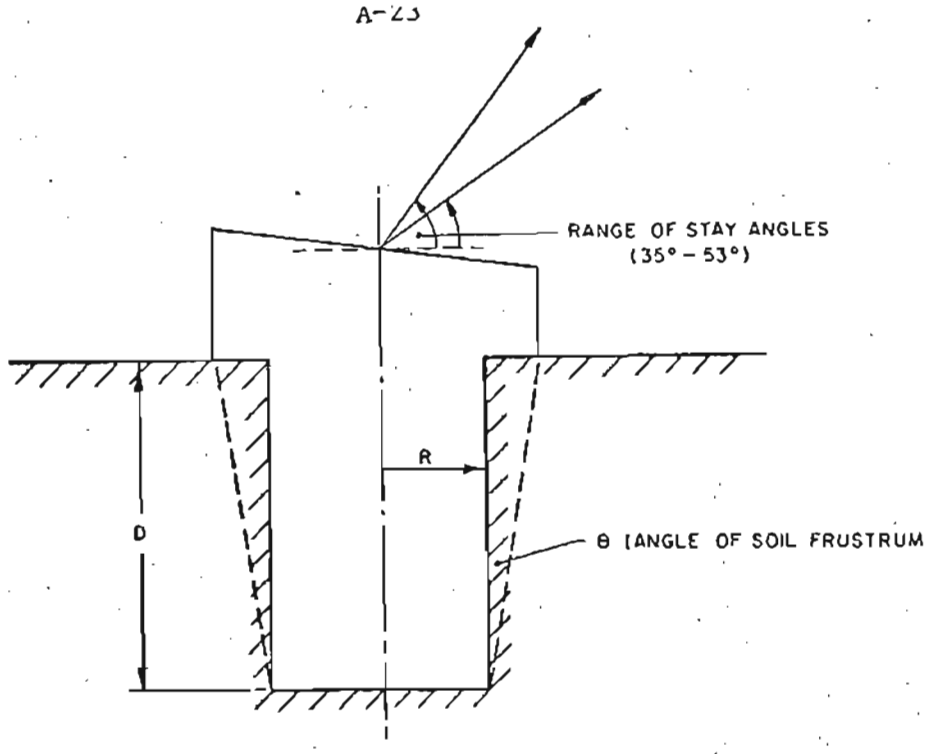

FIGURE 2 A-2
DESIGN OF ANCHOR BLOCK

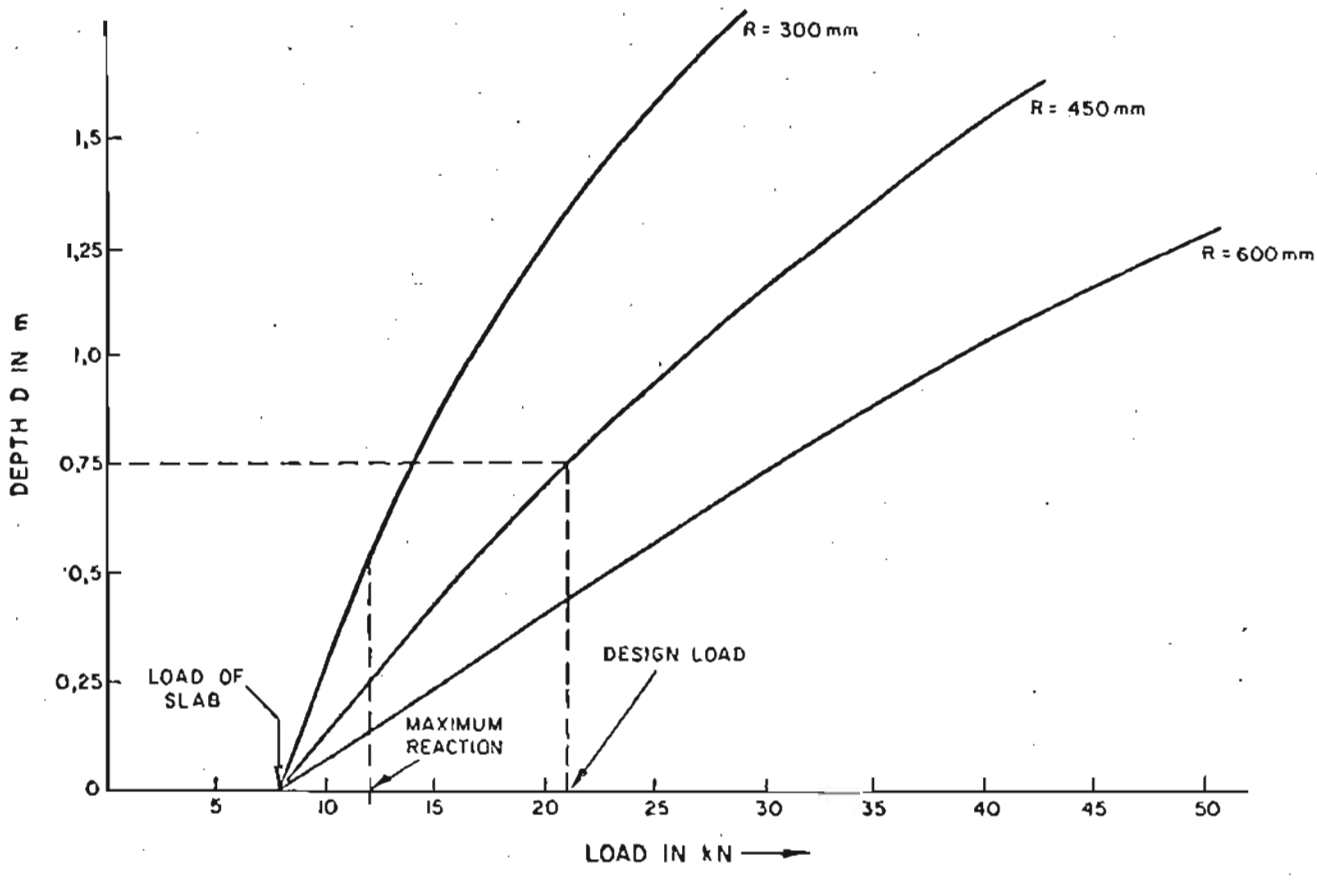

FIGURE 2 A-3

APPENDIX 2(B) EARTH ELECTRODE CALCULATIONS

(a) Electrode resistance

The arrangement shown in Figure 2.5 may be considered to consist of four main elements;

(1) The buried grid beneath the huts.
(2) The elongated grid extending from the huts to the mast.
(3) The loop counterpoise enclosing the site.
(4) The set of 6 x 20 m radial counterpoises extending out from the site.

The following simplified relations have been adopted - based upon standard references[32][36]:

$$R\ (\text{grid}) = \rho\ (\frac{1}{2D} + \frac{1}{L}) \quad \ldots\ldots\ldots\ldots\ldots\ldots\ldots \quad (2.B.1)$$

$$R_{(\text{loop})} = \frac{\rho}{2\pi L}\ \ell n\ (\frac{L^2}{0,167\ h.d}) \quad \ldots\ldots\ldots\ldots\ldots\ldots \quad (2.B.2)$$

$$R_{(\text{6-point star})} = \frac{\rho}{2\pi L}\ \ell n(\frac{L^2.10^3}{9,42.\ h.d}) \quad \ldots\ldots\ldots\ldots \quad (2.B.3)$$

where in each case, ρ = soil resistivity in Ωm
D = effective diameter of the grid in m
L = total length of buried conductor in m
h = depth of burial in m
d = conductor diameter in m

A common depth of burial h = 0,5 m has been assumed.

Accordingly, substituting the relevant conductor dimensions in these relationships, the following values for the corresponding electrode resistances are obtained:

R (two grids combined) = 4,35 Ω/100 Ωm resistivity
R (loop counterpoise) = 1,91 Ω/100 Ωm resistivity
R (6 x radial counterpoise) = 2,69 Ω/100 Ωm resistivity

Paralleling these resistances and allowing an incremental factor of 1,5 in order to accommodate mutual coupling effects, the resultant overall electrode resistance value is;

R = ...

R = 1,45 Ω/100 Ωm soil resistivity ..... (2.B.4)

This calculation excludes the contribution of the insulated counterpoise which is connected to the remote electrode, since this latter electrode resistance only becomes available to the mast electrode once an earth surge has completed propagation and reflection along this 210 m connection.

(b) Transient impedance characteristics

Two main aspects were considered. The first comprises the travelling wave solution for the indicial input impedance of the distributed electrode system, which, for the purposes of this analysis, is considered primarily to consist of six radial counterpoises of 20 m length each. The second aspect is the impulse current response of the electrode as a consequence of soil ionisation effects.

The basic principles followed, (together with the various assumptions involved), are summarised briefly below:

Travelling wave solution

The approach adopted is based upon that originally developed by Sunde[37] and subsequently extended by Devgan and Whitehead[38]:

Assuming initially a buried single counterpoise conductor of length ℓ and unit length parameters L_o, C_o, G_o, ($R_o = 0$), then the general travelling wave solution for the indicial input impedance is;

$$Z(0,t) = Z_o\{\exp(-\alpha t)I_o(\alpha,t) + 2\sum_{n=1}^{\infty} I_o\left(\alpha,\sqrt{t^2-\left(\frac{2n\ell}{v}\right)^2}\; n(t-2n\ell)\right)\}$$

..... (2.B.5)

Here Z_o = surge impedance = $(L_o/C_o)^{\frac{1}{2}}$;

α = decrement factor = $G_o/2C_o$; and

v = velocity of propagation in the soil

This .....

This equation reduces to;

$Z(0,0) = Z_o$ for $t = 0$

$Z(0,\infty) = 1/\ell G_o = R_\infty$ as $t \to \infty$

where R_∞ is the leakage resistance

Devgan and Whitehead, in considering the dielectric nature of the soil, have suggested a simplified four parameter soil model in order to take account of the frequency dependency of this medium, and have produced a three component approximation to the solution of the indicial impedance, using this model;
Namely;

$$Z(0,t) = Z_o \{0,74 \exp(-t/0,9\ T_1) + 0,26 \exp(-t/14T_1)\} + R_\infty$$

$$(1-\exp(-t/T_2) + 2/C_o\omega\ell (\exp(-t/T_3) \sin\omega t) \quad \ldots\ldots\ (2.B.6)$$

where $\omega = (\pi v^2/\ell^2 - \alpha^2)^{\frac{1}{2}}$
and the three component time constants T_1, T_2, T_3 are derived as follows:

$$T_1 = 2C_o/G_o = 2\varepsilon_o(\varepsilon_{r1} + 1)/\sigma_1$$

$$T_2 = C_\infty/G_\infty = \varepsilon_o(\varepsilon_{r2} + 1)/\sigma_2$$

$$T_3 = \varepsilon_o(\varepsilon_{r3} + 1)/\sigma_3$$

where ε_o = permittivity of free space

ε_{r1} = relative permittivity at high frequency

ε_{r2} = relative permittivity at low frequency

ε_{r3} = relative permittivity at intermediate frequency

σ_1 = conductivity at high frequency

σ_2 = conductivity at low frequency

σ_3 = conductivity at intermediate frequency

Devgan .....

Devgan and Whitehead have followed an empirical approach matching theoretical results with the experimental results of Kawai[39] and have derived estimating curves for the above time constants, as functions of frequency and the reference measured value of the low frequency conductivity, ($\sigma = 1/\rho$).

The above method has been followed in estimating the indicial impedance of the mast electrode radial counterpoise system (comprising 6 counterpoises of 20 m length each). In this geometry, the leakage resistance R_∞ and surge impedance Z_o are given by Sunde[37] as:

$$R_\infty (n) = \frac{\rho}{n\pi\ell} \{\ell n\ 2\ell/a' - 1 + N(n)\} \quad \ldots\ldots\ldots\ldots \quad (2.B.7)$$

where n = number of conductors

where a' = effective radius = $(2\ ad)^{\frac{1}{2}}$

and a = conductor radius

d = depth of burial

ρ = soil resistivity

and,

$$N(n) = \sum_{m=1}^{n-1} \ell n\ (1 + \sin m\pi/n)/(\sin m\pi/n)$$

$$Z_o = \{\mu/\ (2\ (n\pi)^2\ \varepsilon_o\ (\varepsilon_{r1} + 1)\} \quad \{\ell n\ 2\ell/a' - 1 + N(n)\}$$

$$\times\ \{(\ell n\ 2\ell/a' - 1 + N_1(n)\}^{\frac{1}{2}} \quad \ldots\ldots\ldots \quad (2.B.8)$$

where $\mu = \mu_o \mu_r$

and μ_o = permeability of free space

μ = 1 (assumed for soil)

and,

$$N_1(n) = \sum_{m=1}^{n-1} \{\ell n\ (1 + \sin m\pi/n)/(\sin m\pi/n)\}\ \cos m\pi/n$$

The relevant conductor dimensions have been substituted into the above equations and two estimations of indicial impedance carried out, using two different values of reference resistivity ρ.

In .....

In the first instance, a value ρ = 5 000 Ωm was assumed (being derived from the mast electrode annual average resistance of about 60 ohms), while in the second case ρ = 1000 Ωm was assumed, being considered the lowest possible value of resistivity that might be achieved on the mast site under excessively wet soil conditions. In the first instance;

$$\left.\begin{aligned} R_{\infty}(1) &= 134{,}6\ \Omega \\ Z_o\ (1) &= 49{,}2\ \Omega \end{aligned}\right\} \text{ for } \rho = 5\ 000\ \Omega m$$

and in the second case;

$$\left.\begin{aligned} R_{\infty}\ (2) &= 26{,}9\ \Omega \\ Z_o\ (2) &= 19{,}1\ \Omega \end{aligned}\right\} \text{ for } \rho = 1\ 000\ \Omega m$$

The estimated indicial impedances in each case are illustrated in Figure 2.B-1, in which it may be seen that the final value of leakage resistance is approached after about 3 µs.

In this context, the connection of the remote electrode (which has an annual average resistance of about 1 Ω), via the 210 m of counterpoise, should also be taken into account.

This counterpoise (in terms of its dimensions) has a surge impedance of about 88 ohms, and the average surge propagation time along its length (for the above range of soil resistivities) is about 3,6 µs.

Therefore, in the event of lightning currents entering the mast electrode, it may be expected that the contribution of the remote electrode will start coming into effect after about 7,2 µs.

In summary therefore, it is considered that the mast electrode impedance behaviour may be illustrated by the simplified model in Figure 2.B-2. Depending upon the prevailing resistivity, R_{∞} could vary from about 20 to 120 ohm (taking the full electrode into account; i.e. including the grids and buried loop), while Z_o could have values between 20 and about 50 ohms.

Impulse .....

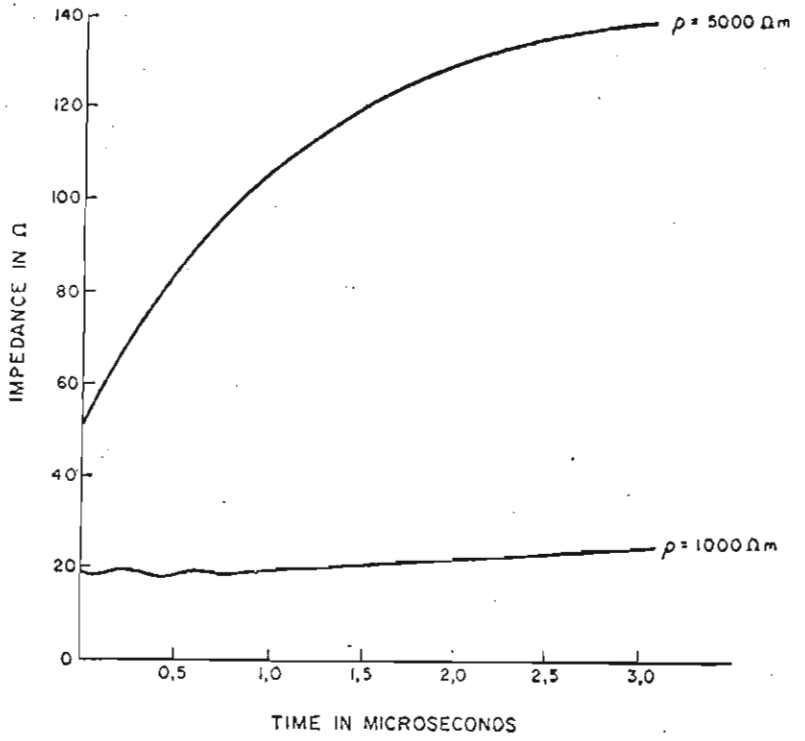

FIGURE 2 B-1

ESTIMATED INDICIAL IMPEDANCE OF 6 x RADIAL COUNTERPOISE SYSTEM

$t < 3{,}6\ \mu S$; $Z = 88\ \Omega$

$t > 3{,}6\ \mu S$; $Z = 0$

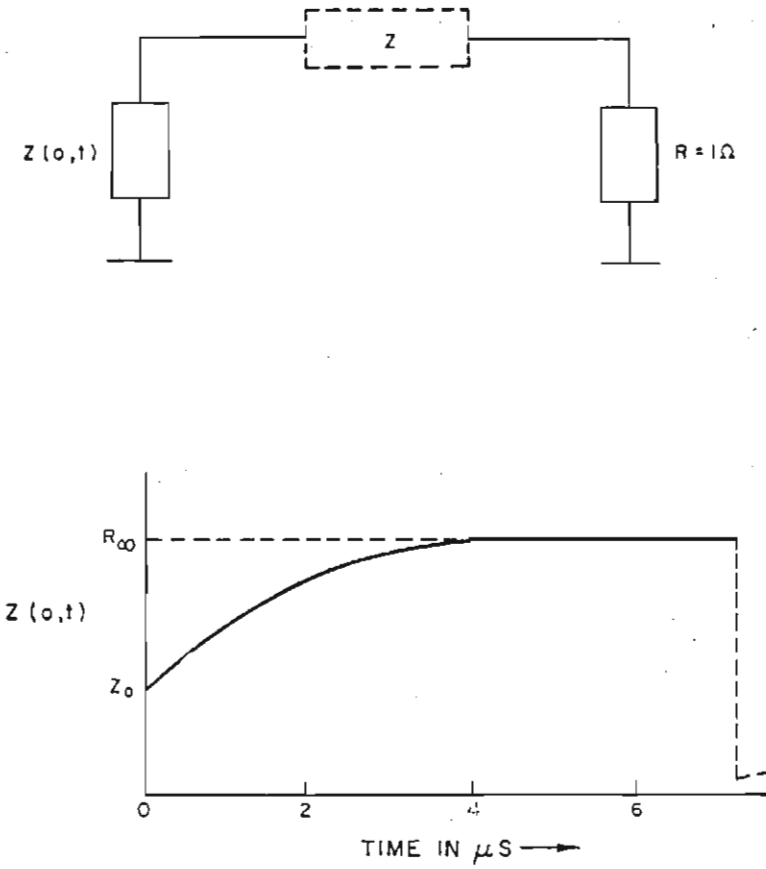

FIGURE 2 B-2

SIMPLIFIED MODEL OF MAST ELECTRODE TRANSIENT RESPONSE

Impulse current response

Several authors have examined the effects of soil ionisation in the vicinity of a buried conductor[40], as a consequence of high currents entering the electrode. In view of the comparatively high impedance of the mast electrode system, it was anticipated that substantial surge potential could temporarily be developed upon the buried conductors during the dissipation of lightning currents, and attempts were therefore made to estimate the corresponding impulse current reduction factor, as a consequence of soil ionisation and the associated increase in conductor effective radius.

For a single conductor of length ℓ, Sunde[37] has derived the relation;

$$a_o = I\rho/2\pi\ell E_o$$

where a_o = conductor effective radius due to soil ionisation (m)

I = current in the conductor (A)

ρ = soil resistivity (Ωm)

E_o = soil breakdown gradient (v/m)

In the absence of soil ionisation, the nominal conductor effective radius is given as;

$$a' = (2ad)^{\frac{1}{2}}$$

where a = conductor radius (m)

d = depth of burial (m)

The resultant impulse current reduction factor is given by Sunde;

$$\eta = (\ell n\ (2\ell/a_o') - 1)/(\ell n\ (2\ell/a') - 1) \quad \ldots\ldots\ldots\ldots \quad (2.B.8)$$

where $a_o' = (2a_o d)^{\frac{1}{2}}$

Soil breakdown gradients have been found normally to vary[40] over about 1 - 4 MV/m. Taking this range, and an assumed variation in soil resistivity over the range 1 000 - 5 000 Ωm, the resultant variation in reduction factor for the buried counterpoise system is

shown .....

shown in Figure 2.B-3 as a function of the current I. (In this case for a single 20 m length).

Although in practice the reduction factors will not be as high as indicated in this figure, (due to the distribution of current throughout the electrode system), it is apparent that substantial impedance reduction factors may well ensue in the event of currents in excess of 50 kA.

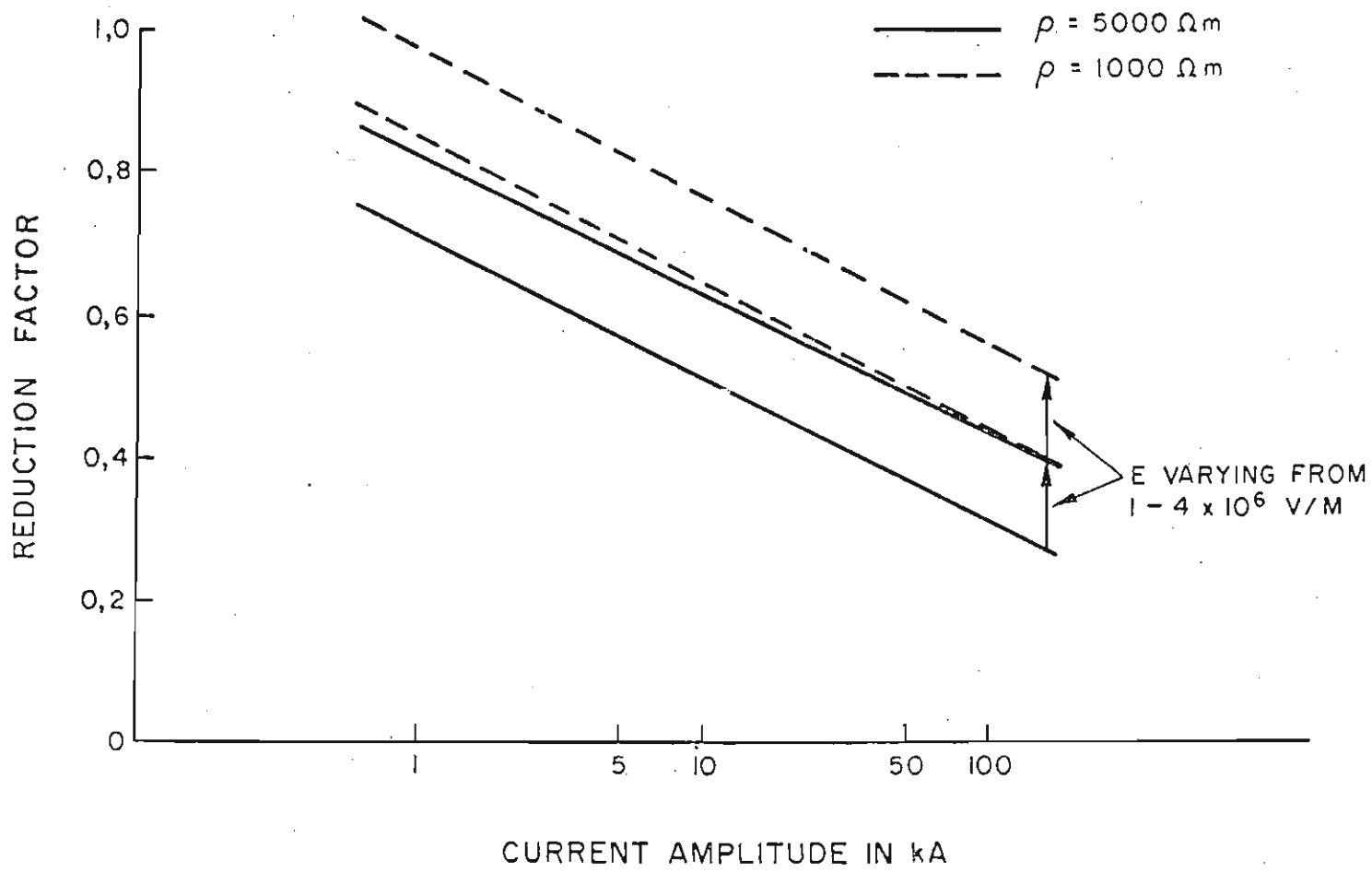

FIGURE 2 B-3

VARIATION IN IMPULSE CURRENT REDUCTION FACTOR FOR BURIED COUNTERPOISES

APPENDIX 2(C) CALIBRATION OF MAGNETIC LINKS

The approach followed is an extension of that originally reviewed by Candler in 1940[41] and subsequently applied by Anderson and Jenner[42].

In principle, in the event of the passage of impulse current in a conductor in the proximity of a magnetic link, the magnetising force H available to produce a given degree of remanent magnetism in the link may be calculated from the following relation:

$$H = \frac{I}{2\pi d} \quad \ldots\ldots\ldots\ldots\ldots\ldots\ldots\ldots\ldots\ldots\ldots\ldots \quad (2.C.1)$$

where I = peak amplitude of the current (A)
and d = distance of the link from the conductor (m)

In practice, the remanent magnetism is often measured using a proprietary instrument termed a surge crest ammeter whose scale has previously been calibrated for the specific links involved to provide a linear relationship between the remanent magnetism and the magnetising force, i.e. for a particular distance d, and assuming no current reversal,

$$R = f(H) = kI \quad \ldots\ldots\ldots\ldots\ldots\ldots\ldots\ldots\ldots\ldots\ldots\ldots \quad (2.C.2)$$

where k = a constant representing the slope of the linear relationship
and R = reading on the surge crest ammeter.

Since the magnetising force H is inversely proportional to distance (as shown in equation (2.C.1)) equation (2.C.2) may be generalised for a variety of link distances, as follows:

$$I = K.\ D.\ R \quad \ldots\ldots\ldots\ldots\ldots\ldots\ldots\ldots\ldots\ldots\ldots\ldots \quad (2.C.3)$$

where D is the new distance to the link (a variable)
R is the corresponding reading on the surge crest ammeter
K is a constant for the particular links and surge crest ammeter

The above relation was not known for the set of links and the particular surge crest ammeter available at the commencement of this programme, and recalibration was therefore necessary.

A number of link brackets was constructed which were suitable for clip-on attachment to a 25 mm diameter conductor and were each capable of mounting up to three links at a variety of distances from the

conductor. .....

conductor. (Distances over the range 20 - 160 mm were possible in this fashion).

These brackets were mounted upon a suitable conductor in the High Voltage Laboratory of the South African Bureau of Standards and the associated links were subjected to a calibration procedure, involving a variety of impulse current magnitudes derived from a standard impulse generator. These impulse currents had the approximate monopolar waveform 3,3/16,5 μs and covered peak currents in the range 10 - 42 kA. (The latter were recorded oscillographically, using an impulse current shunt). By mounting the links at a variety of distances, a number of (D x R) products could be determined over the range of applied current amplitudes.

A corresponding number of estimates for the constant K could be calculated and a mean value derived.

The resultant calibration equation (over the range of distances and currents involved) was derived;

$$I = 4{,}01 \times 10^{-3} (D.R) \quad \ldots\ldots\ldots\ldots\ldots\ldots\ldots\ldots \quad (2.C.4)$$

where I is expressed in kA
and D is the relevant link distance in mm
while R is the corresponding reading on the surge crest ammeter.

Subsequently, in the course of the research programme, a number of additional calibration checks was carried out under lightning current conditions on the research mast, by relating the observed lightning peak current amplitudes (as recorded oscillographically), to the corresponding surge crest ammeter readings obtained for the various links mounted on the research mast.

(Normally, each mounting bracket carried three magnetic links at different distances, and it was usual practice to have at least three brackets of varying dimensions installed on the research mast. In this way it was often possible to obtain several (D x R) link products from a single lightning event and representative mean values could be obtained on each occasion).

The .....

The earlier laboratory calibrations were extended in this fashion to higher current amplitudes, as shown in Figure 2.C-1, which depicts the variations in link (D x R) product as a function of the peak current amplitude. Measurements have now been made over the current range 5 - 87 kA and although considerable scatter is evident where individual links are concerned, the overall trend is consistent, as shown by the regression line. (The latter was derived using least squares regression and a correlation coefficient r = 0,94 was obtained).

The final calibration equation takes the form;

$$I = 4{,}09 \times 10^{-3} \ (D \times R) - 1{,}1 \qquad (kA) \quad \ldots\ldots\ldots\ldots\ldots \quad (2.C.5)$$

In view of the scatter involved, the offset current of 1,1 kA in this relation may well be the consequence of experimental error, but may also possibly be attributable to aging of the link magnetisation characteristic, with corresponding scale errors on the surge crest ammeters.

Although the above calibration procedure suggests the possibility of individual link errors in excess of 40% for single link readings, it is found that the errors are normally below 10% when the mean of more than four (D x R) products is used for a particular measurement.

The above calibration equation has been used for all magnetic link measurements of lightning current amplitudes, (with a minimum of 6 links being involved in each measurement), and errors of $\pm$ 10% have therefore been assumed.

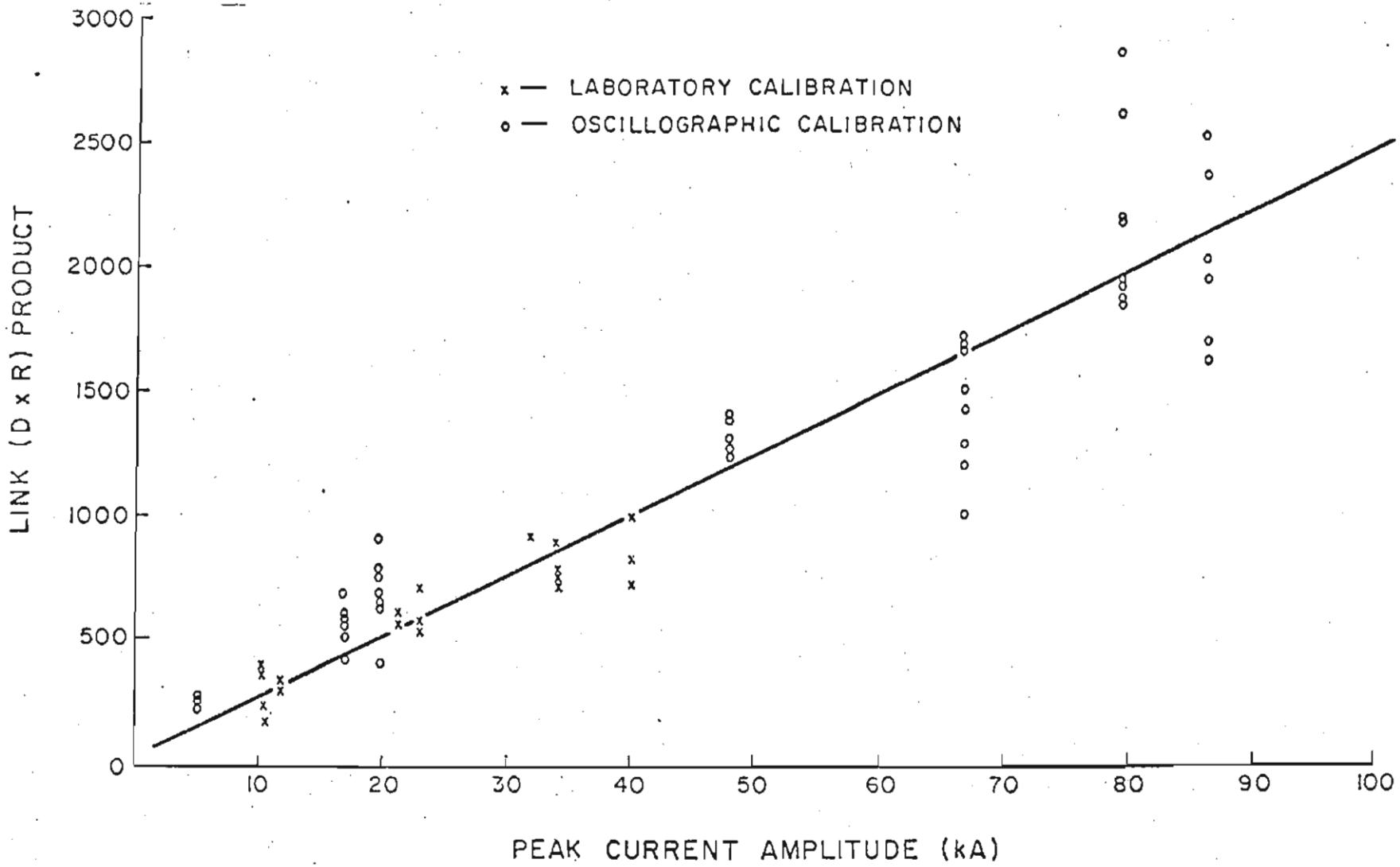

FIGURE 2C-1

CALIBRATION OF MAGNETIC LINKS

APPENDIX 3A: ANALYSIS OF INDIVIDUAL FLASH RECORDS

Introduction

In this section, an attempt is made to present the available data which was obtained on each occasion when a flash occurred on the research mast, and to summarise the salient conclusions regarding flash direction, polarity, discharge current waveform parameters, etc.

Each flash has been assigned a three-catogory number of the form XXX/YY/Z, where the XXX denote the event date, the YY comprise an arbitary serial number, which runs sequentially from the start of the project, and the Z identify the individual strokes in the case of a multiple stroke flash.

(For example, event number 740118/12/2 identifies the second stroke of Flash 12, and records the fact that this flash occurred on 18 January 1974.)

In each case, the circumstances surrounding the occurrence of each flash are briefly reviewed, including which equipment was in operation on that occasion, and what measurements were obtained.

On each occasion also, based upon subjective impressions of the various thunderstorms, an attempt is made to categorise the storms loosely into one of several general types.

When available, the associated flash photographs and current oscillograms are also presented, together with a summary of the various waveform parameters which may have been determined from analysis of discharge current oscillograms.

In most instances, these oscillograms were subsequently digitised on a plotting table and were processed using computerised routines for waveform analysis - as originally evolved by Kröninger[49].

Where-ever possible, the following parameters were evaluated - either manually from the oscillogram, or through computerised analysis of the digitised data:-

$\hat{I}$ - peak discharge current amplitude. (When this parameter was evaluated from the magnetic link registrations, a mean value was determined, together with the standard deviation -σ)

Q - Impulse charge, (subject to the limited oscilloscope sweep times).

$\frac{dI}{dt}$ - Maximum rate of rise of current on the wave-front.

$\int I^2 dt$ - action integral, (again subject to the limited oscilloscope sweep times).

Event ..... /

Event: 721129

Times of occurrence: 721129/1 - 16 h 50
721129/2 - 17 h 05

Circumstances: A very severe thunderstorm lasting in excess of 5 hours, and achieving a ground flash density of 0,9 flashes km^{-2} * At this stage, station recording equipment had not yet been commissioned and only a prototype framing camera was in operation at Lynnwood Glen. The recording spark-gap and a trial set of magnetic links had been installed temporarily on the mast base.

Two direct flashes occurred in short succession during approximately the most intense phase of the storm and both were recorded by the remote framing camera (Figure 3A-1). The second flash is observed to have a downward direction of progression and, in view of its close proximity in time to the first flash, as well as the general high incidence of ground flashes in the vicinity, the first flash is also presumed to have been downward.

The recording spark-gap confirmed the passage of two major discharge components, while the magnetic links indicated a nett current of negative polarity.

(Approximately 20 minutes after the second flash, the top half of the research mast collapsed, due to delamination and failure of one of the top-most fibre-glass stays, and was extensively damaged).

Results

Event	Magnetic links			Processing of waveform data			
			Manual	Digitised			
	$\hat{I}$(kA)	σ(kA)	$\hat{I}$(kA)	$\hat{I}$(kA)	Q(C)	$\frac{dI}{dt}$(kA/μs)	$\int I^2 dt (A^2 s)$
721129/1	-	-	-	-	-	- -	-
721129/2	-35	-	-	-	-	- -	-

General remarks

The peak current reading derived from the magnetic link registration has been assigned to the second flash, since this appeared generally brighter in the photographs.

*Note: On each occasion, the ground flash density was determined from flash counter registrations in the area[29].

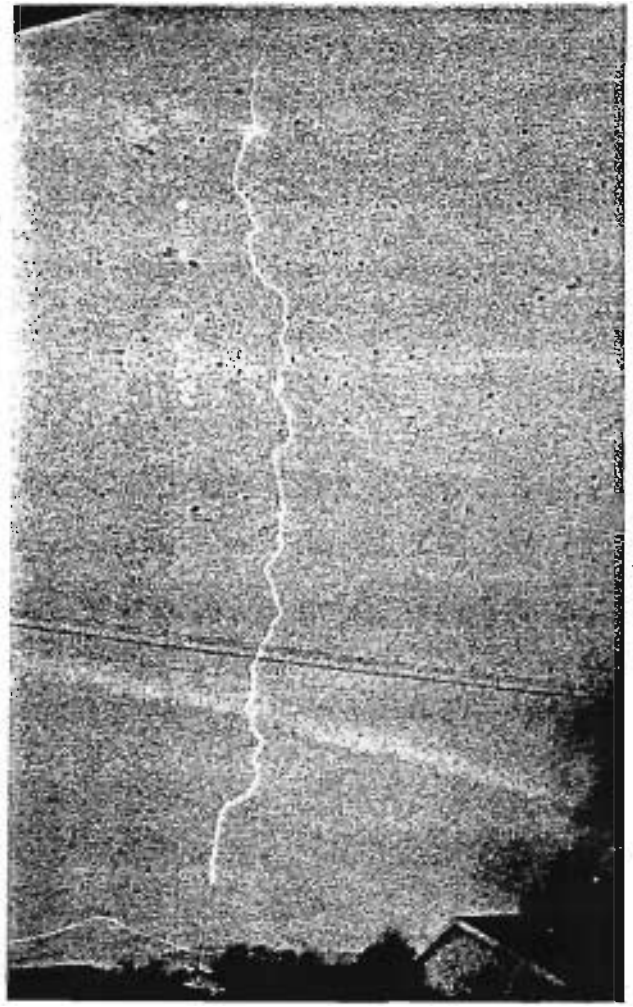

Flash No. 721129/1

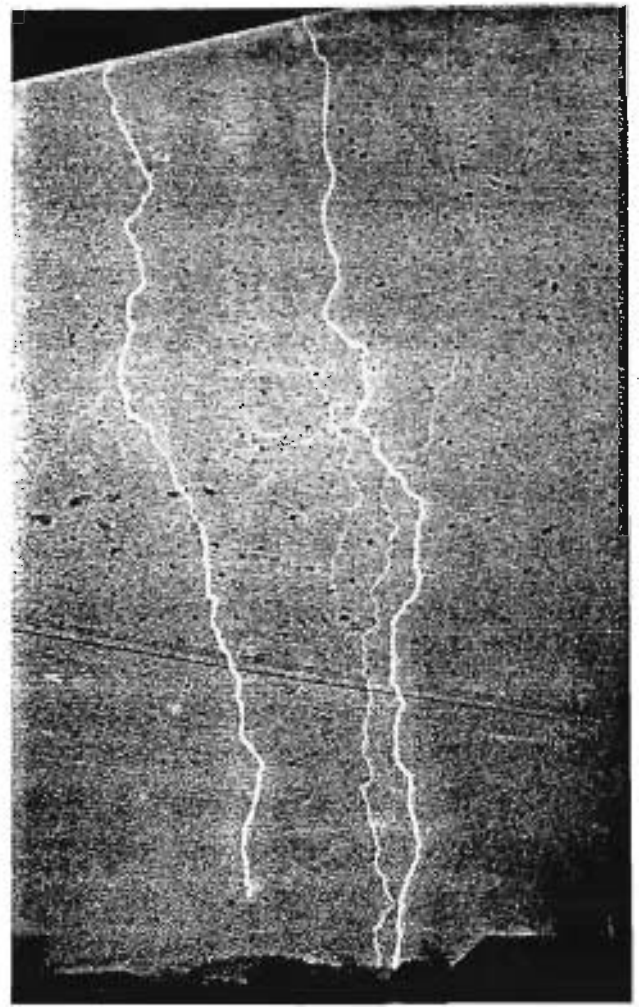

Flash No. 721129/2

FIGURE 3A-1 FLASHES TO THE MAST ON 29TH NOVEMBER 1972
(LYNNWOOD GLEN CAMERA ONLY)

Event: 730929

Times of occurrence: 730929/3 - 05 h 30
730929/4 14 h 45
730929/5 - 21 h 00

Circumstances: These three flashes occurred during periods of very light and isolated electrical activity - associated with the movement of a major frontal system across the area (the total ground flash density recorded over the relevant 24 hour period was only 0,13 flashes km^{-2}.)

At this stage of the season, lightning had not been anticipated and recommissioning of the station equipment after the winter overhaul was not yet complete. Consequently, no recordings or photographs were obtained, but the recording spark-gap confirmed the passage of three comparatively weak discharges.

In fact, flash 4 was observed by the author, who noted a downward direction of progression. The nature of the remaining two flashes is unknown, however, although the arc erosion patterns registered on the recording spark-gap faces are indicative of negative discharges.

Results: No results were obtained on this occasion.

Event: 731015

Time of occurrence: 731015/6 - 17 h 00

Circumstances: This flash occurred at the height of a very active storm (convective, squall-line type). The ground flash density achieved on this occasion was 0,7 flashes km^{-2}.

Although the instrumentation was now in operation, a major power failure in the area some 15 minutes before the flash prevented any measurements being obtained. (Following the earlier trials, magnetic links were on order, but unfortunately had not yet been installed at the time of this flash.) The recording spark-gap indicated the passage of an extremely severe discharge and suggested also the possible occurrence of a second component. The arc erosion was consistent with negative polarity.

The Lynnwood Glen framing camera had been activated prior to the power failure and, being operated in the "shutter-open" mode, had recorded the flash. Special processing was required, however, in order to take account of the excessive film fogging caused during the long exposure period. The resultant photograph (Figure 3A-2) confirms a downward direction of progression.

Results: No results were obtained on this occasion.

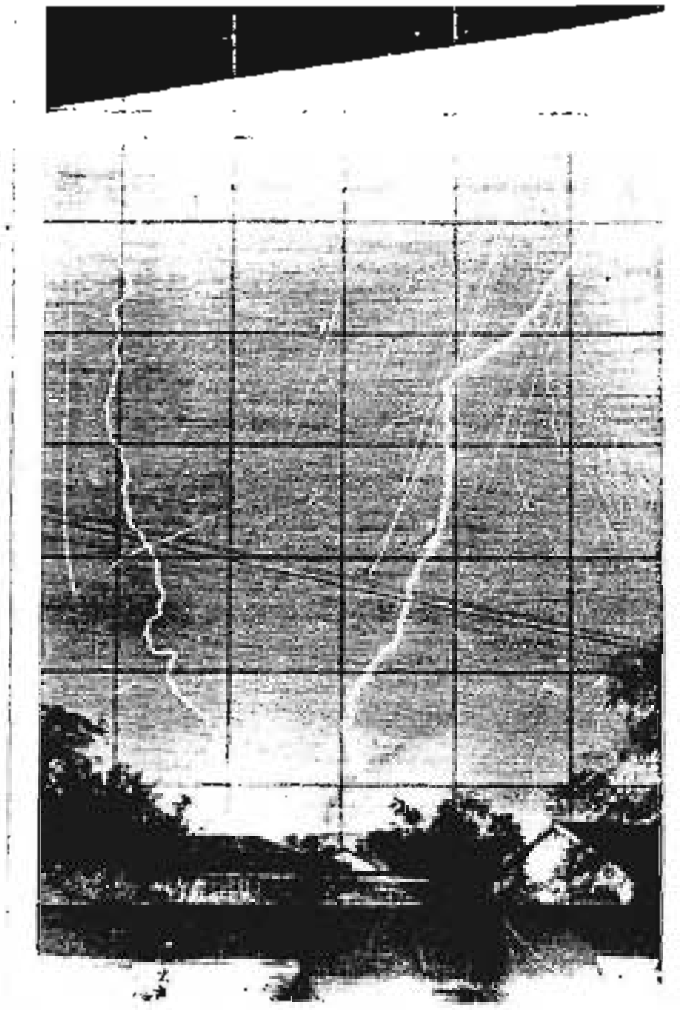

Flash No. 731015/6

FIGURE 3A-2 FLASH TO THE MAST ON 15TH OCTOBER 1973 (LYNNWOOD GLEN CAMERA)

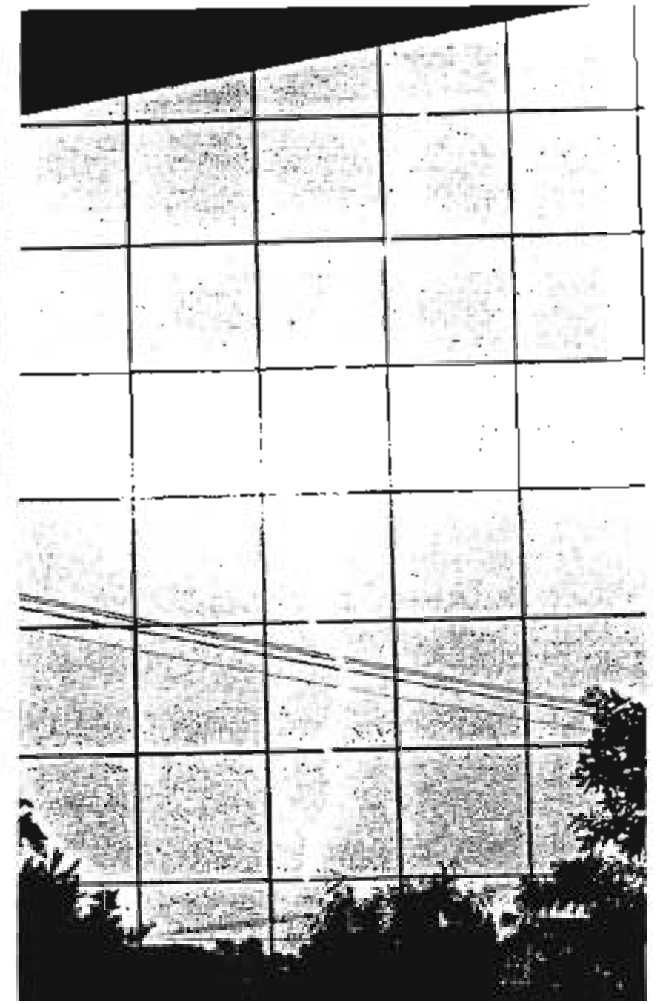

Flash No. 731216/9

FIGURE 3A-3 FLASH TO THE MAST ON 16TH DECEMBER 1973 (LYNNWOOD GLEN CAMERA)

Event: 731126

Times of occurrence: 731126/7 - 06 h 05

731126/8 - 06 h 15

Circumstances: These two flashes occurred in close succession, during a period of light electrical activity, which was associated with the passage of a cold front through the area. The ground flash density noted during the relevant 24-hour period was only 0,09 flashes km^{-2}.

Due to the low activity, the framing cameras had not yet been activated and no photographs were obtained. The station instrumentation was operational and triggered on one of the two flashes, but a defective camera resulted in a spoilt film.

Magnetic links had recently been installed in the base of the mast and the resultant registrations confirmed a nett negative discharge.

Both flashes were observed by the author. The first flash appeared to be very bright and a possible upward direction of branching was tentatively noted. The second flash was much fainter and the direction of progression was not discernible.

Results:

Event	Magnetic links		Processing of waveform data				
			Manual	Digitised			
	$\hat{I}$(kA)	σ(kA)	$\hat{I}$(kA)	$\hat{I}$(kA)	Q(C)	$\frac{dI}{dt}(\frac{kA}{\mu s})$	$\int I^2 dt (A^2 S)$
731126/7	-73	±5	-	-	-	-	-
731126/8	-	-	-	-	-	-	

General remarks

In view of the observed different degrees of flash brightness, the current amplitude derived from the magnetic link registrations has been assigned to the first flash (i.e. No. 7).

Although the observed direction of branching of this flash was thought to be upward, the high magnitude of current is not consistent with the characteristics of upward flashes and consequently, it is suspected that this event was really a negative downward flash.

Event: 731216

Time of occurrence: 731216/9 - 23 h 55

Circumstances: This flash occurred during a comparatively mild squall-line type thunderstorm. (The associated ground flash density was only 0,02 flashes km^{-2}.)

All station equipment was in operation at this time and although problems were experienced with the high speed oscilloscope, a slow-speed negative single stroke oscillogram was recorded. The latter was of poor quality, however, and only the wavetail was readily discernible. The recording spark-gap confirmed the passage of a weak single discharge while the magnetic link registrations indicated negative polarity.

The Lynnwood Glen framing camera was also in operation and recorded a downward branched flash (Figure 3A-3).

Results:

Event	Magnetic links		Processing of waveform data				
			Manual	Digitised			
	$\hat{I}$(kA)	σ(kA)	$\hat{I}$(kA)	$\hat{I}$(kA)	Q(C)	$\frac{dI}{dt}(\frac{kA}{s})$	$\int I^2 dt (A^2 S)$
731216/9	-10	±1	>-7	-	>1,6	_	$>1,2 \times 10^4$

Event: 740104

Time of occurrence: 740104/10 - 17 h 20

Circumstances: This flash occurred early during a severe convective squall-line type storm. (The associated ground flash density on this occasion was 0,22 flashes km^{-2}.)

All station equipment was in operation and three negative stroke oscillograms were obtained. Due to an incorrect choice of oscilloscope settings these records were again generally of poor quality and the wave peaks were not discernible in all three records, although the first stroke rate-of-rise of current could be estimated.

The magnetic link registrations confirmed a negative polarity and allowed an estimation of the true flash peak current amplitude.

The Murrayfield framing camera had also been commissioned by this time and photographs were thus obtained from both remote cameras (Figure 3A-4). No branches are discernible in these photographs, but the flash was also observed by the author (at a distance of only 100 m on this occasion), and a downward direction of progression was noted.

Results:

Event	Magnetic links		Processing of waveform data				
			Manual	Digitised			
	$\hat{I}$(kA)	σ(kA)	$\hat{I}$(kA)	$\hat{I}$(kA)	Q(C)	$\frac{dI}{dt}(\frac{kA}{\mu s})$	$\int I^2 dt (A^2S)$
740104/10/1	-41	±2	>17	-	>2	>2	$>3x10^4$
740104/10/2	-	-	>12	-	-	-	-
740104/10/3	-	-	> 4	-	-	-	-

General remarks: The two flash photographs depicted a comparatively well defined interaction between the downward and upward connecting leaders and thus allowed an estimation of the associated striking distance - as discussed in Chapter 4.

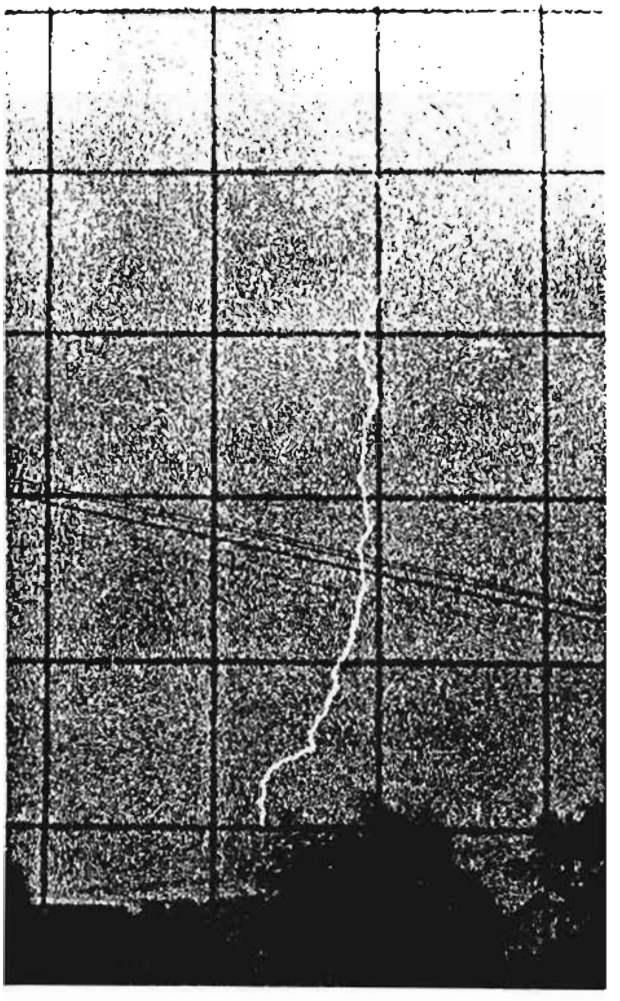

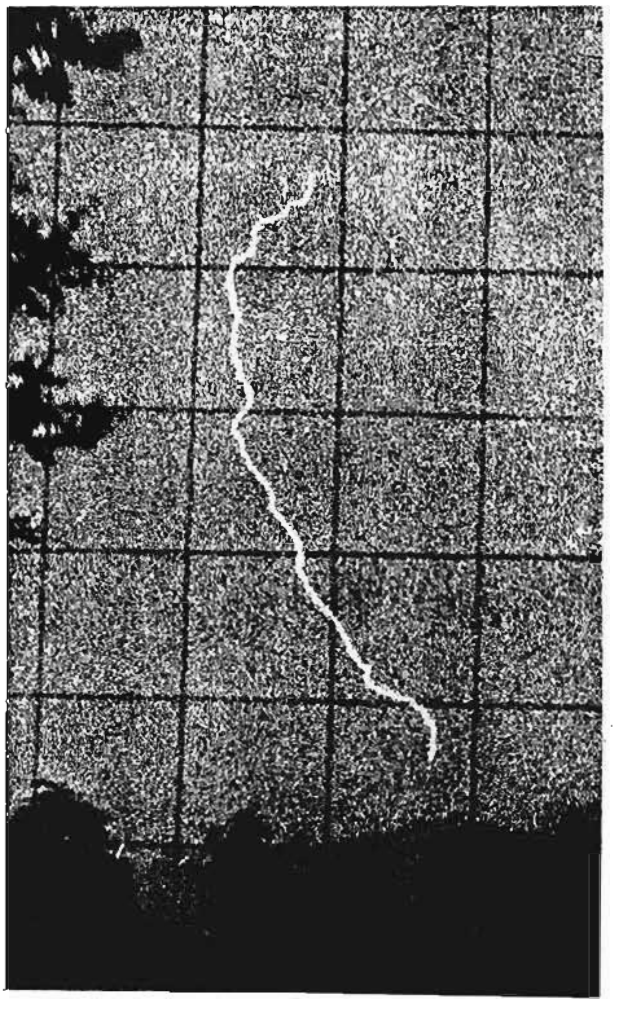

Lynnwood Glen camera

Murrayfield camera

Flash No. 740104/10

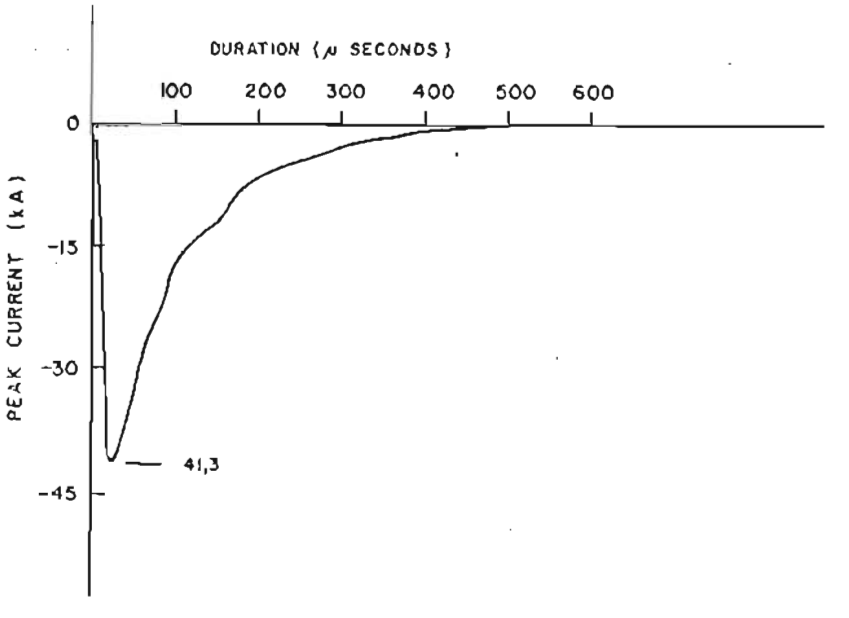

FIGURE 3A-4 FLASH TO THE MAST ON THE 4TH JANUARY 1974 AND RESULTANT OSCILLOGRAM

Event: 740118

Times of occurrence: 740118/11 - 15 h 15
740118/12 - 15 h 50

Circumstances: These two flashes occurred during a short but active squall-line type storm - for which the associated ground flash density was 0,25 flashes km^{-2}.

All station instrumentation was in operation and negative polarity current oscillograms were recorded for each flash (Figure 3A-5). (Flash 11 comprised a single stroke, while Flash 12 involved three strokes). These oscillograms were generally of good quality, although minor problems were experienced with the trigger amplifiers and these may have caused distortion during the initial wavefronts. Magnetic links were also present in the tower base and their registrations confirmed the peak current magnitude and polarity.

On this occasion, it was not possible to activate the remote framing cameras before these flashes occurred and no photographs were obtained therefore.

Consequently, the direction of progression of these flashes is unknown.

Results:

Event	Magnetic links		Processing of waveform data				
			Manual	Digitised			
	$\hat{I}$(kA)	σ (kA)	$\hat{I}$(kA)	$\hat{I}$(kA)	Q(C)	$\frac{dI}{dt}(\frac{kA}{\mu s})$	$\int I^2 dt (A^2 S)$
740118/11	-	-	-50	-	≈6,5	≈11,0	$\approx 3,2 \times 10^5$
740118/12/1	-58	±10	-58	-	≈12,4	≈4,0	$\approx 7,2 \times 10^5$
740118/12/2	-	-	-55	-	≈10,4	>5,0	$\approx 5,7 \times 10^5$
740118/12/3	-	-	-22	-	≈5,8	>7,0	$\approx 1,3 \times 10^5$

General remarks: The value of peak current derived from the magnetic link registrations has been assigned to the first stroke of Flash 12 - since the associated oscillograms indicated that this stroke had attained the highest amplitude.

The oscillograms recorded on this occasion are not consistent with what may normally be expected - especially as far as the subsequent stroke wavefronts are concerned and it is considered that these records have been distorted by the defective trigger amplifiers. The resultant waveform parameters shown above (i.e. Q, dI/dt, etc) should be regarded as order-of-magnitude estimations only.

In view of the recorded current amplitudes, it is thought that these flashes must have been downward in character.

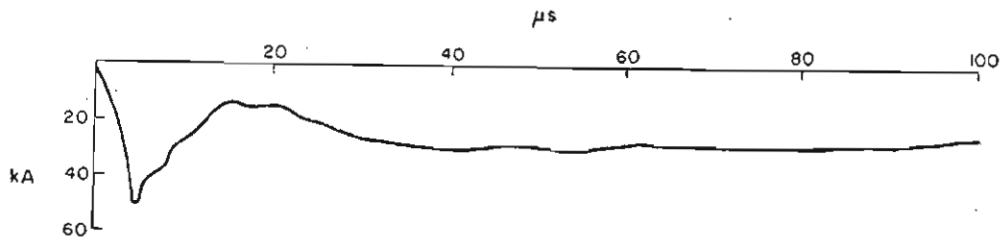

FLASH No. 740118/11

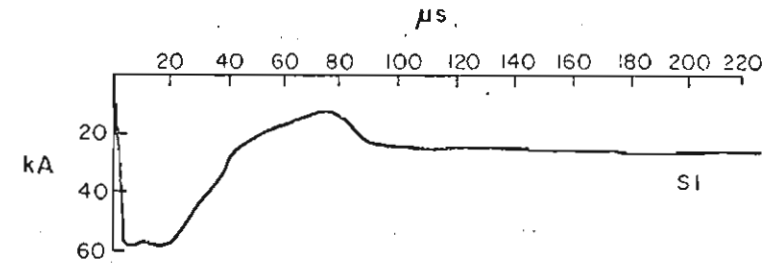

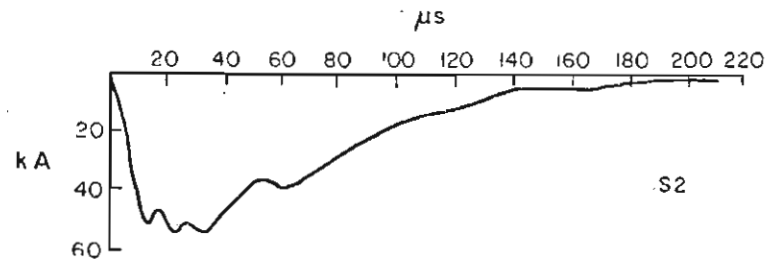

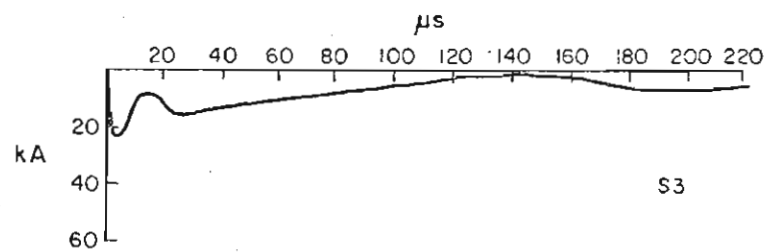

FLASH No. 740118/12

FIGURE 3A-5 OSCILLOGRAPHIC RECORDS OBTAINED DURING FLASHES TO THE MAST ON THE 18TH JANUARY 1974

Event: 741129

Times of occurrence: 741129/13 - 02 h 47
741129/14 - 03 h 02
741129/15 - 03 h 10

Circumstances: These three flashes occurred in close succession during an unusual early morning frontal-type storm. This storm was very mild in character, displaying only minimal electrical activity in the form of isolated cloud flashes. In fact, the only ground flashes observed by the author in the area on this occasion, were the three flashes to the mast. (The associated ground flash density in this 24 hour period was only 0,05 flashes km^{-2}.)

Although all instrumentation was in operation, an open circuit in the measuring cable from the current transformer unfortunately prevented any signals being recorded. The recording spark-gap confirmed the passage of three discrete discharges however, and displayed an unusually intense degree of arc erosion.

The Lynnwood Glen camera had been activated prior to the flashes and photographs of all three discharges were obtained. (Figure 3A-6). No branching is evident on the first two flashes, but Flash 15 is clearly upward in character.

The magnetic link registrations indicated only a marginal degree of remanent magnetisation but this was consistent with a positive polarity of current flow, and was equivalent to a nett current amplitude of about 3 kA.

General remarks: During this particular storm, electrostatic field mills were in operation at the tower site and at a location about 1 km away. The resultant recordings are shown in Figure 3A-7 and are subject to timebase errors of ±2 minutes. At the approximate times of the above three flashes however, significant field changes are readily identifiable, having the following polarities -

741129/13 - positive change (i.e. consistent with negative ground flash)

741129/14 - negative change (i.e. consistent with positive ground flash)

741129/15 - negative change (i.e. consistent with positive ground flash)

In addition, the field mill recording from the mast site (although unreliable as a measure of the absolute field in the vicinity, being subject to the effects of point-discharge space charge above the mast), suggests a marginal negative field level durihg the first flash (Flash 15), which changes to a generally positive field condition during the subsequent two flashes.

Although cloud flashes could have also caused the polarities of the above observed field changes, it is considered that the evidence is generally consistent with the premise that at least one, and perhaps two of the these three flashes involved positive discharges (namely, Flashes 14 and 15).

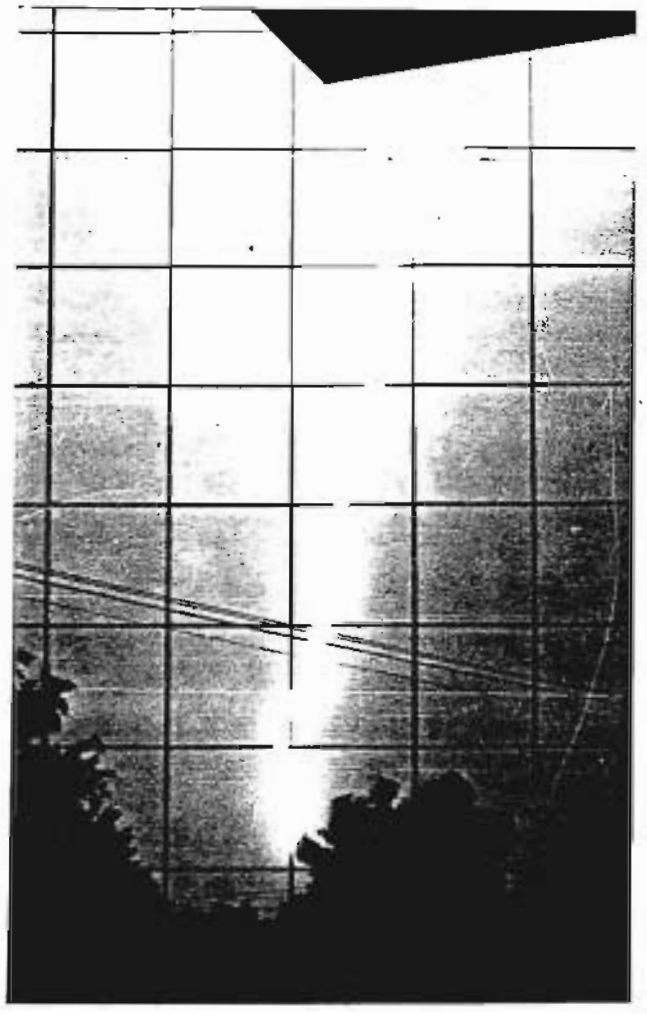

Flash No. 741129/13

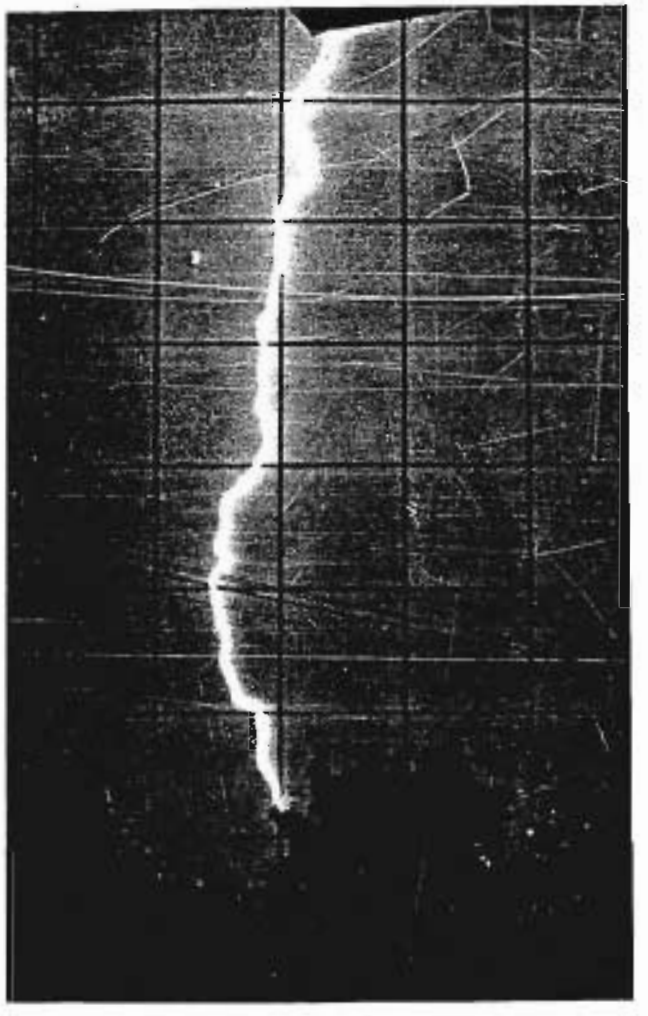

Flash No. 741129/14

Flash No. 741129/15

FIGURE 3A-6 FLASHES TO THE MAST ON THE 29TH NOVEMBER 1974 (LYNNWOOD GLEN CAMERA)

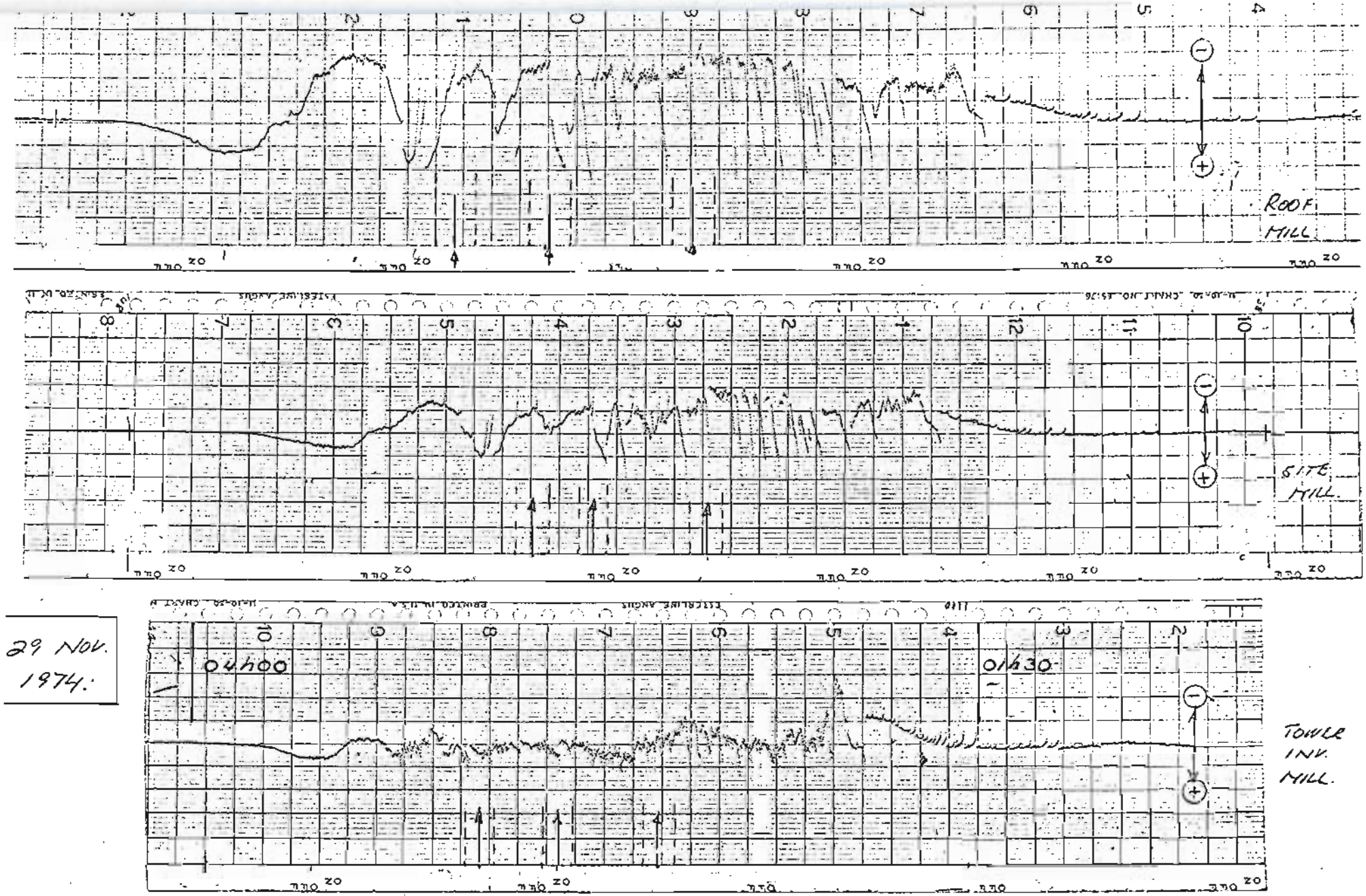

(Note: The amplitude scales vary for each mill, but correspond approximately to 5 kV per major chart division.)

FIGURE 3A-7 ELECTROSTATIC FIELD MILL RECORDINGS ON THE 29TH NOVEMBER 1974

In view of the unusually mild nature of the storm (as far as ground flash activity is concerned), as well as the fact that Flash 15 was confirmed as being in the upward direction, it is thought possible that the earlier two flashes may also have been upward.

Event: 741224

Times of occurrence: 741224/16 - 20 h 25
741225/17 - unknown

Circumstances: The first of these flashes (Flash 16) occurred during a severe thunderstorm - which was associated with a local ground flash density of 0,5 flashes km^{-2}.

All instrumentation was in operation on this occasion and a negative single-stroke current oscillogram was recorded. The Murrayfield framing camera had also been activated prior to the flash and a photograph of a downward branched discharge was obtained (Figure 3A-8). An incorrect setting of the trigger threshhold level resulted in loss of the initial slow part of the wavefront, but apart from this, the oscillogram was of good quality.

The second flash occurred during an afternoon storm on the following day (25/12/1974). However, being a public holiday, and because the station instrumentatio (including the magnetic links), had been cleared of the previous flash data earlier in the day, the station was temporarily out of commission and no results were obtained. Confirmation of this event is provided by the recording spark-gap (which had been replaced after Flash 16), and which indicated the passage of two discharges (i.e. either a two-stroke flash, or two discrete flashes).

Results:

Event	Magnetic links		Processing of waveform data				
			Manual	Digitised			
	$\hat{I}$(kA)	σ(kA)	$\hat{I}$(kA)	$\hat{I}$(kA)	Q(C)	$\frac{dI}{dt}(\frac{kA}{\mu s})$	$\int I^2 dt (A^2 S)$
741224/16	-53	±2	-48	-46	1,5	8	$3,7 \times 10^4$

Event .....

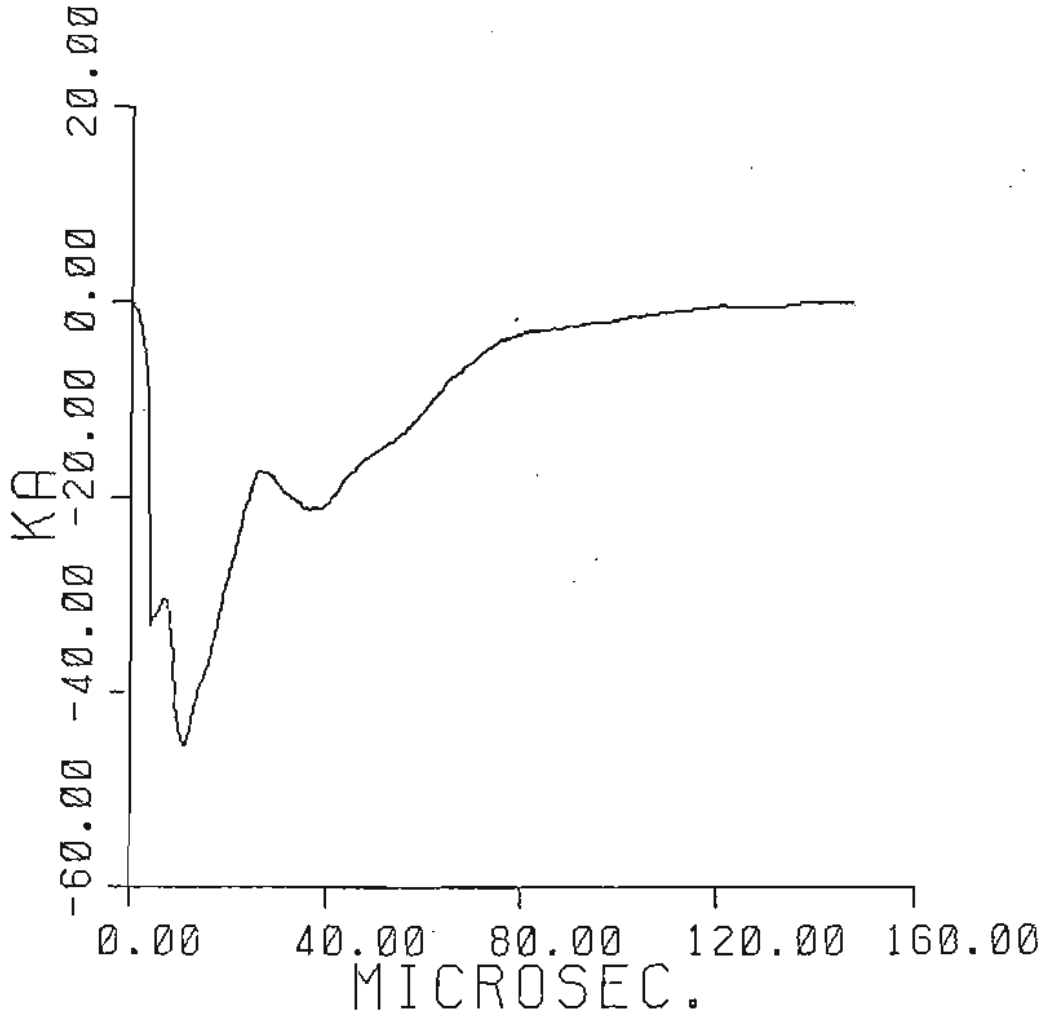

Flash No. 741224/16

FIGURE 3A-8 FLASH TO THE MAST ON THE 24TH DECEMBER 1974
(MURRAYFIELD CAMERA)

Event: 750227

Time of occurrence: 750227/19 - 18 h 55

Circumstances: This flash occurred during a severe convective squall-line type storm, which was associated with a local ground flash density of 0,50 flashes km^{-2}.

All station instrumentation was in operation, but a widespread power supply failure between 18 h 70 and 19 h 05 prevented the recording of any current oscillograms. The magnetic link registrations confirmed the passage of a current of negative polarity, while the recording spark-gap indicated a complex discharge, probably of multiple stroke character.

Both remote framing cameras were in operation at the time of the flash and bi-directional photographs were therefore obtained. (Figure 3A-9.) These confirm a downward direction of progression.

Results:

Event	Magnetic links		Processing of waveform data				
			Manual	Digitised			
	$\hat{I}$(kA)	σ(kA)	$\hat{I}$(kA)	$\hat{I}$(kA)	Q(C)	$\frac{dI}{dt}(\frac{kA}{\mu s})$	$\int I^2 dt(A^2 S)$
750227/19	-26	±1	-	-	-	-	-

General remarks:

Since bi-directional photographs were obtained, this flash was another candidate for computerised analysis of flash geometry and striking distance estimation - as discussed further in Chapter 4.

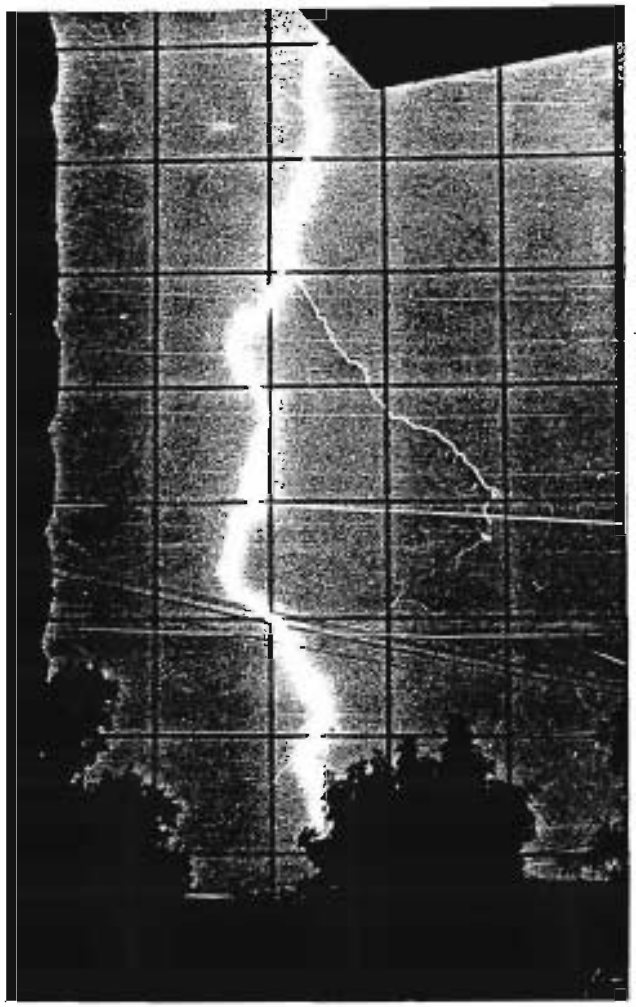

Lynnwood Glen camera

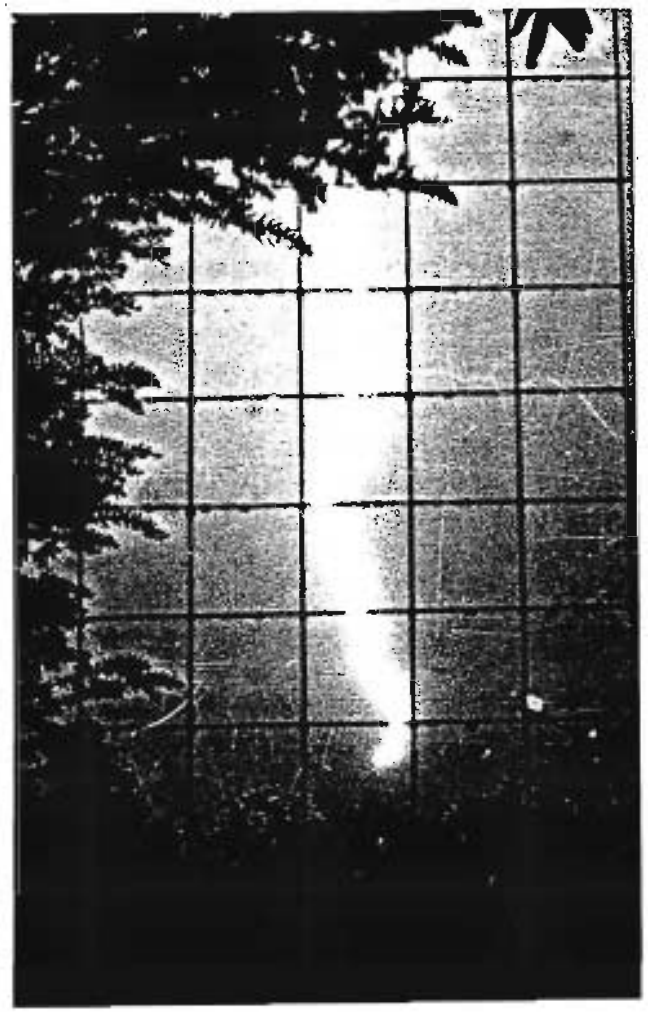

Murrayfield camera

Flash No. 750227/19

FIGURE 3A-9 FLASH TO THE MAST ON THE 27TH FEBRUARY 1975

Event: 751102

Time of occurrence: 751102/21 - 18 h 55

Circumstances: This flash occurred during a short storm of the convective type. The storm was generally mild, but the flash occurred during a short-lived period of localised intense ground flash activity. (The regional ground flash density over this 24 hour period was 0,46 flashes km^{-2}.)

All station instrumentation was operational and a good quality oscillogram of a single-stroke negative discharge was recorded.

The Lynnwood Glen framing camera was also in operation on this occasion and a photograph of a downward branched discharge was obtained. This photograph (Figure 3A-10) is comparatively unique in that it comprises a graphic example of the phenomenon of "root-branching".

Results

Event	Magnetic links		Processing of waveform data				
			Manual	Digitised			
	$\hat{I}$(kA)	σ(kA)	$\hat{I}$(kA)	$\hat{I}$(kA)	Q(C)	$\frac{dI}{dt}(\frac{kA}{\mu s})$	$\int I^2 dt (A^2 S)$
751102/21	-26	±5	-20	-19	0,8	24	$8,4 \times 10^3$

General remarks: This flash is of particular interest in view of the root-branched nature, and has been reported upon separately by the author[50].

The role of leader branching effects in the striking process is discussed further in Chapter 4.

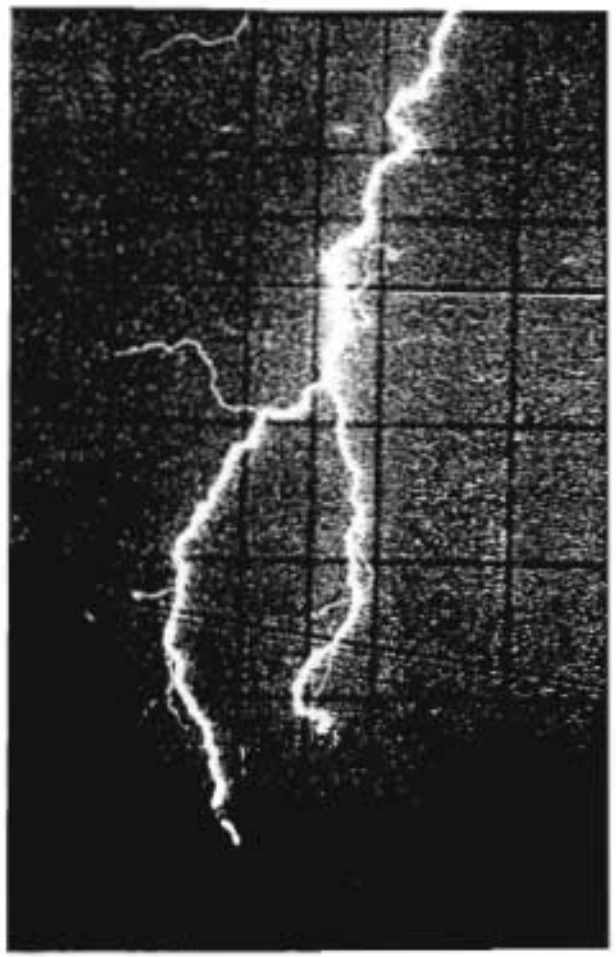

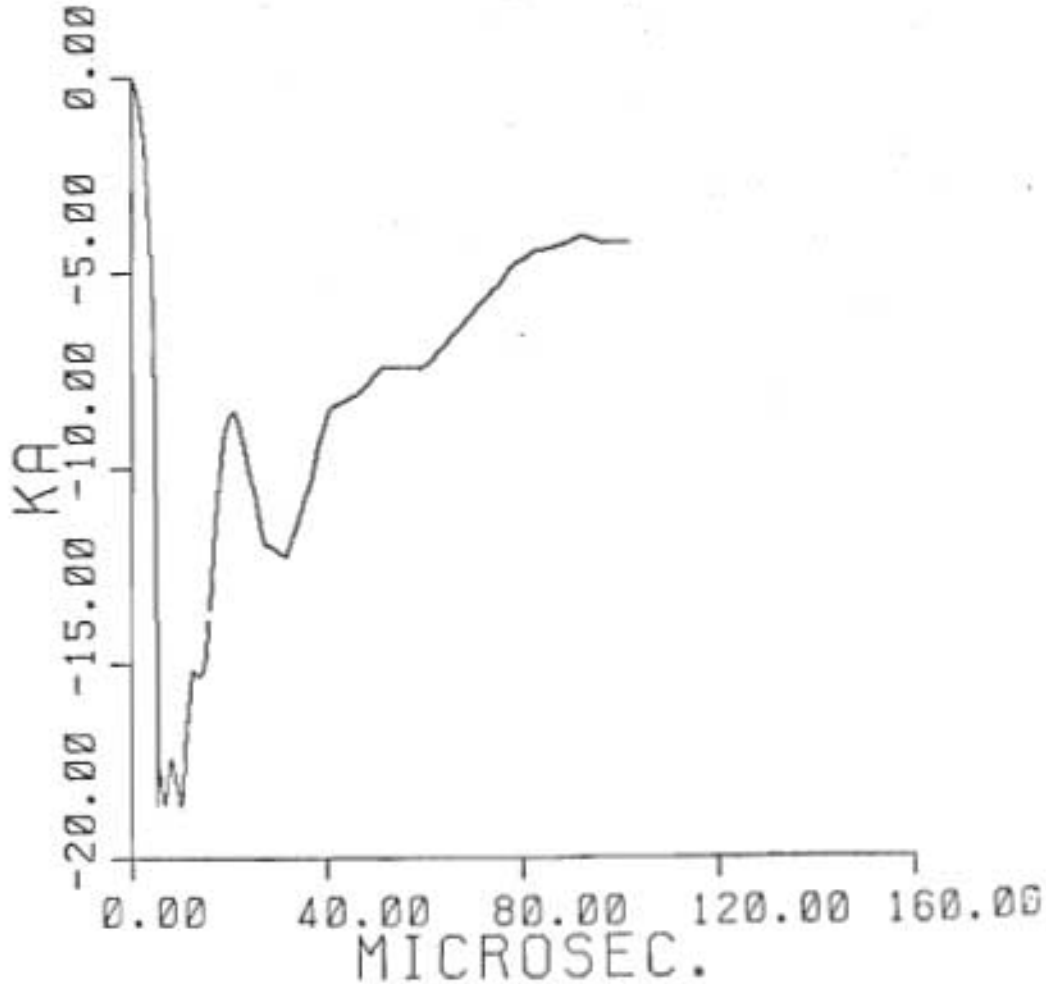

Flash No. 751102/21

FIGURE 3A-10 FLASH TO THE MAST ON THE 2ND NOVEMBER 1975 (LYNNWOOD GLEN CAMERA)

Event: 751114

Time of occurrence: 751114/22 - 16 h 40

Circumstances: This flash occurred at the end of a rapidly moving and active squall-line type storm and, in fact, took place when all ground flash activity in the area had already ceased. (The regional ground flash density recorded on this occasion was 0,69 flashes km^{-2}.)

All station instrumentation was in operation and a negative three-stroke set of current oscillograms was recorded. An excessively high trigger threshhold resulted in loss of part of the initial wavefront.

Both remote framing cameras were also in operation and bi-directional photographs were therefore obtained. (Figure 3A-11a.) These indicate an upward direction of branching. This is confirmed by the recordings obtained from the CCTV video system, which was also in operation at this time, and which clearly shows the development of the initial upward progressing leader. The full video sequence is given diagrammatically in Figure 3A-11(b) and depicts some 8 channel re-illuminations over a total flash duration of 900 ms. The recording oscilloscope camera had an exposure period of only 400 ms on this occasion and thus current oscillograms were only obtained for the first three strokes.

Results

Event	Magnetic links		Processing of waveform data				
			Manual	Digitised			
	$\hat{I}$(kA)	σ(kA)	$\hat{I}$(kA)	$\hat{I}$(kA)	Q(C)	$\frac{dI}{dt}(\frac{kA}{\mu s})$	$\int I^2 dt (A^2 S)$
751114/22/1	-	-	-8	-10	0,9	3,1	$7,3 \times 10^3$
751114/22/2	-22	±3	-17	-16	0,9	22	$9,0 \times 10^3$
751114/22/3	-	-	-16	-15	0,8	29	$7,0 \times 10^3$

Event .....

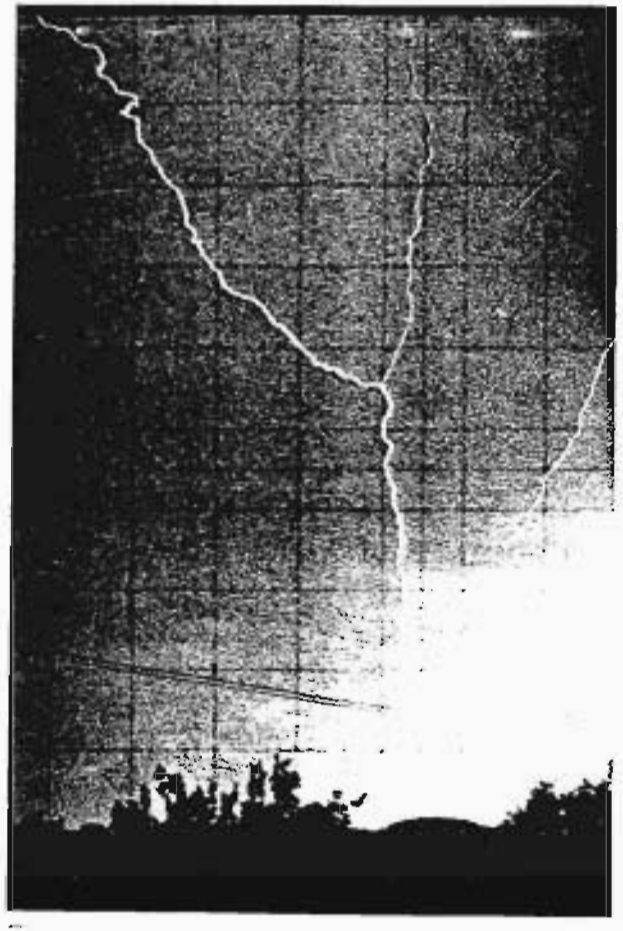

Lynnwood Glen Camera

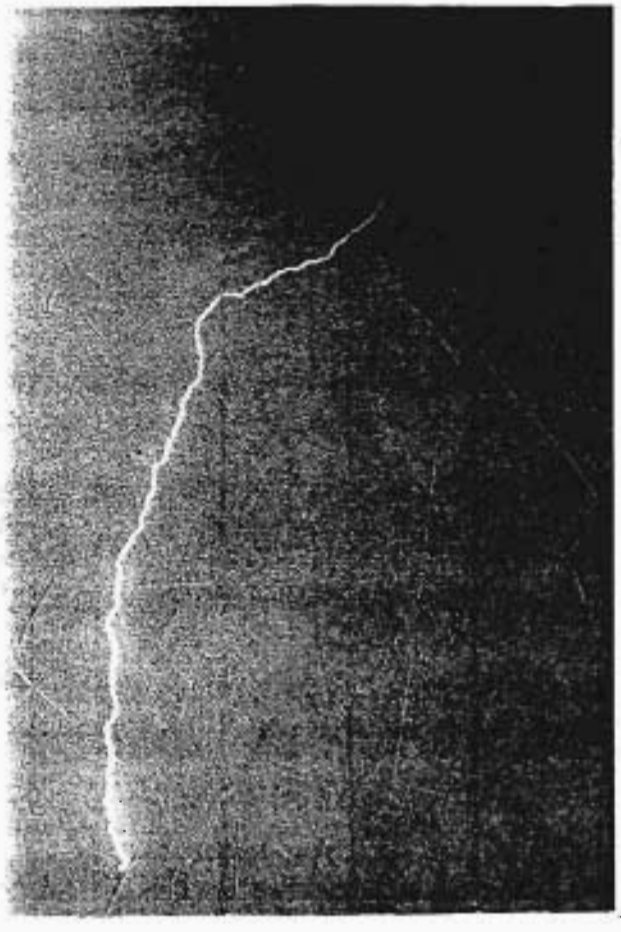

Murrayfield Camera

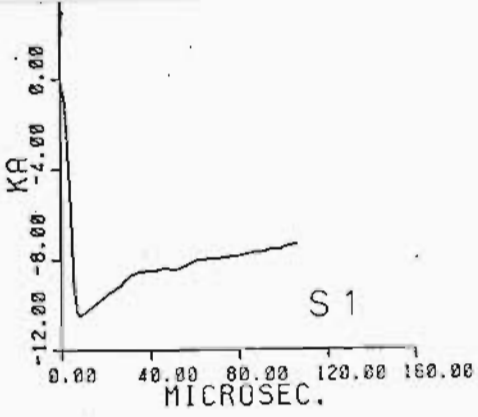

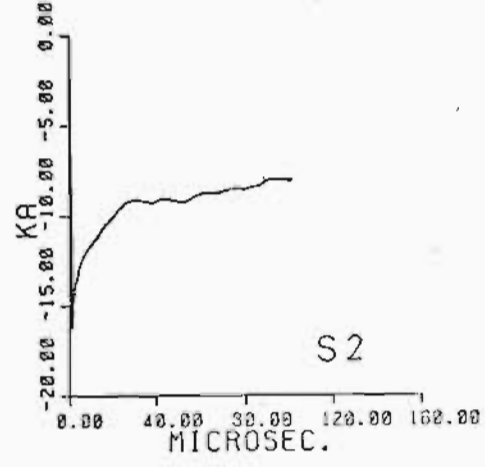

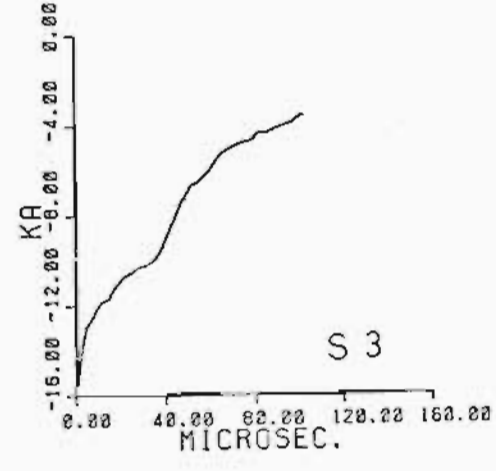

Flash No. 751114/22

FIGURE FA-11(a) FLASH TO THE MAST ON 14TH NOVEMBER 1975

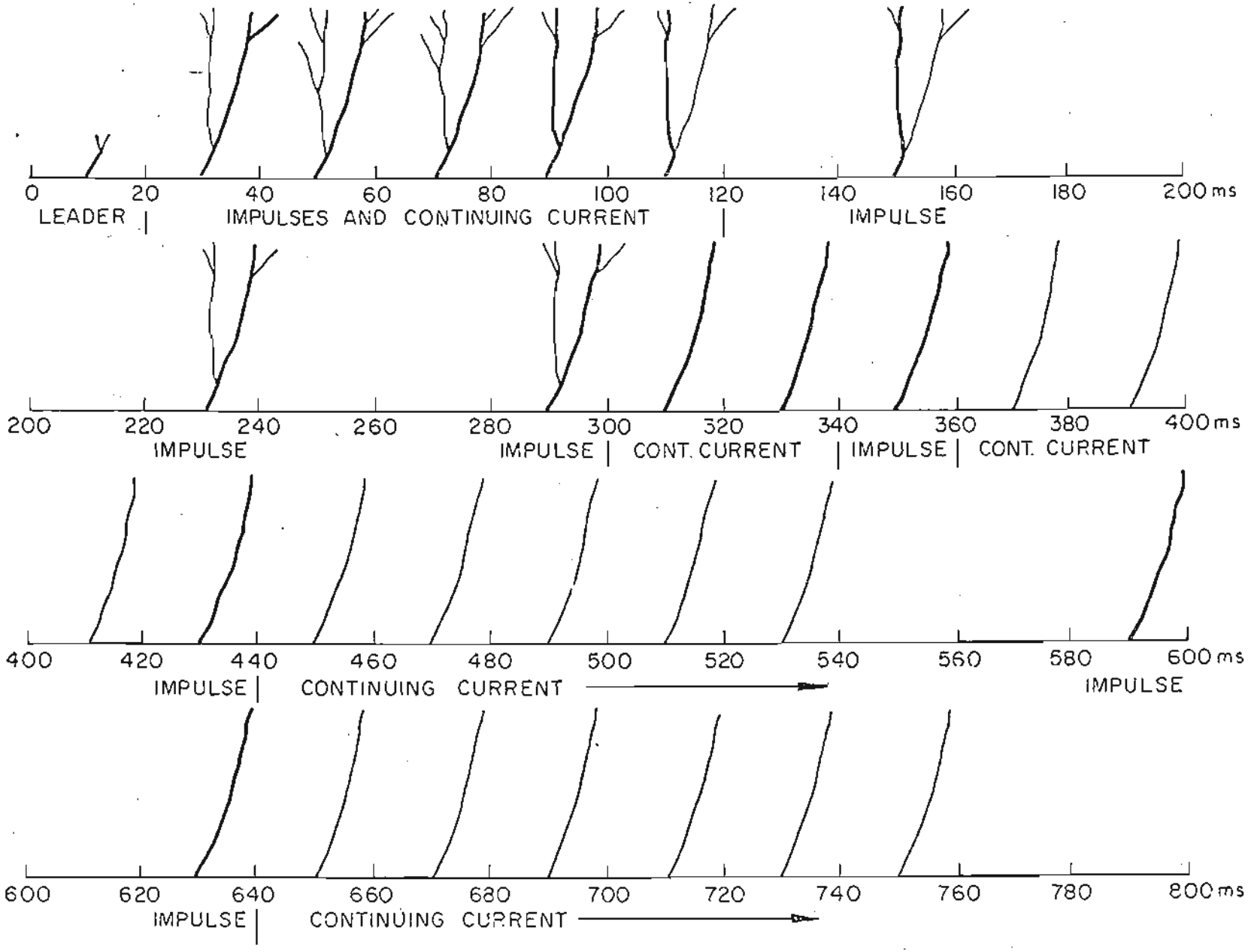

FIGURE 3A-11 (b)

DIAGRAMMATIC REPRESENTATION OF VIDEO RECORDING OF FLASH ON 14 NOV. 1975

Event: 760207

Time of occurrence: 760207/23 - 05 h 00

Circumstances: This flash occurred during a major early morning frontal storm system. The associated ground flash density in the area over the period of concern was 0,34 flashes km^{-2}.

All station equipment was in operation and a current oscillogram was obtained. This is of complex character (Figure 3A-12), but indicates a discharge of negative polarity and suggests an off-scale magnitude. This is borne out by the magnetic links, which were found to have been driven into saturation.

A power failure covering the sites of the two remote framing cameras, prevented any photography of the flash and the CCTV video recording system (which was still in operation), was found to have been obscured by driving rain and the flash geometry and direction of progression could not be discerned.

A possible interpretation of the current oscillogram is also shown in Figure 3A-12 and is consistent with an extremely severe discharge - including a possible upward leader step pulse-current of about 7 kA.

Results

Event	Magnetic links		Processing of waveform data				
			Manual	Digitised			
	$\hat{I}$(kA)	σ(kA)	$\hat{I}$(kA)	$\hat{I}$(kA)	Q(C)	$\frac{dI}{dt}(\frac{kA}{\mu s})$	$\int I^2 dt (A^2 S)$
760207/23		-	-	>100	>9	>12	$>9 \times 10^5$

General remarks

The above analysis of waveform parameters is based upon the interpretation of the oscillogram shown in Figure 3A-12 (excluding the "leader" component). This interpretation must remain speculative, however, and therefore the above derived parameters should be regarded with caution.

Event

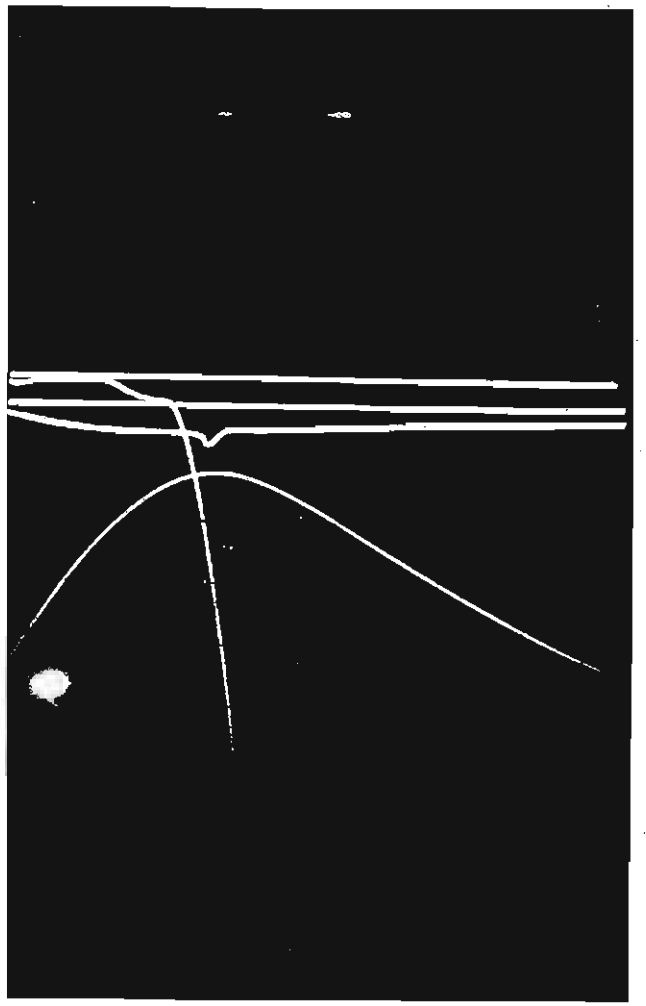

Oscillographic record
(100 μs sweep)

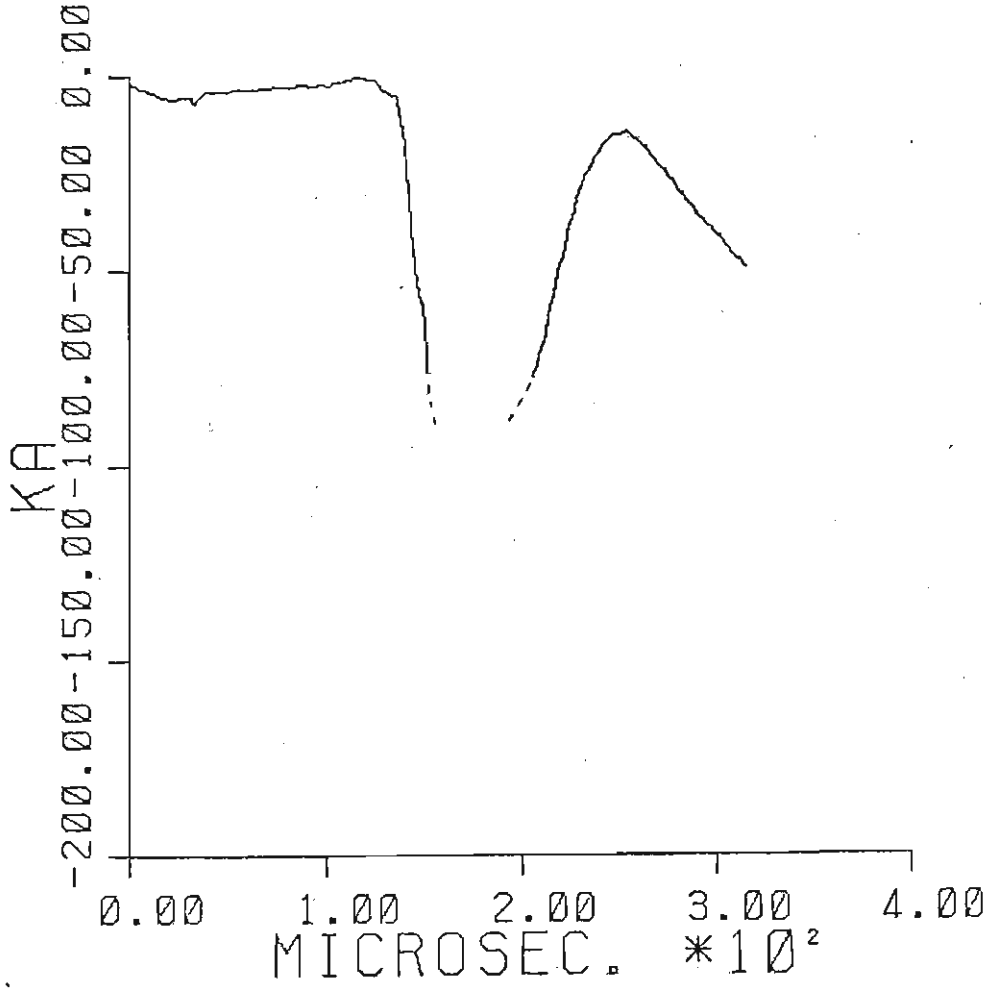

Possible interpretation

Flash No.: 760207/23

FIGURE 3A-12 OSCILLOGRAMS ASSOCIATED WITH FLASH ON 7TH FEBRUARY 1976

Event: 760928

Time of occurrence: 760928/24 - 05 h 24

Circumstances: This flash occurred toward the end of a weak frontal-type early morning storm - during which ground flash activity was minimal. (The associated ground flash density was only 0,05 flashes km^{-2}.)

All station instrumentation was in operation on this occasion, as well as the Lynnwood Glen camera. However, no station trigger was registered, and the magnetic links remained unmagnetised, although the recording spark-gap confirmed the passage of a weak discharge. (The magnetic-link system equivalent sensitivity is about 2 kA.)

The remote framing camera photograph (Figure 3A-13) depicts a weakly illuminated discharge, together with a cloud flash in the background - which must have occurred within the same exposure period (60 seconds).

Results: No results were obtained on this occasion.

General remarks: In view of the low amplitude of current (which must be presumed to have been less than 2 kA), this flash is thought to have been a weak upward discharge - probably triggered by the electrostatic field changes associated with the nearby cloud flash.

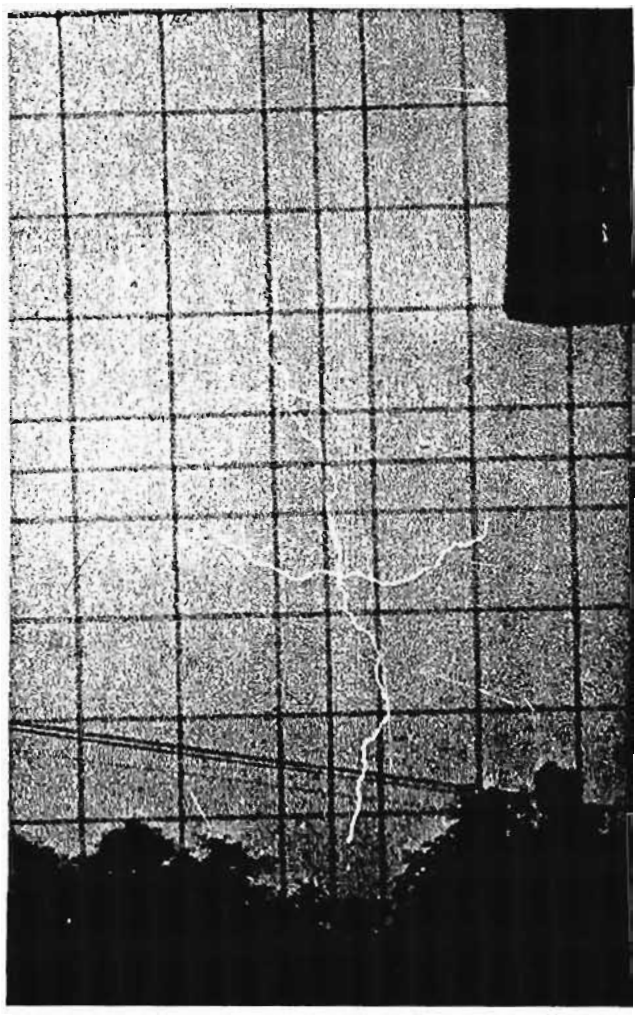

Flash No. 760928/24

FIGURE 3A-13 FLASH TO THE MAST ON THE 28TH SEPTEMBER 1976 (LYNNWOOD GLEN CAMERA)

Event: 770222

Time of occurrence: 770222/25 - 17 h 15

Circumstances: This flash occurred early during a short-lived, but active convective squall-line type storm. (The associated ground flash density was 0,06 flashes km^{-2}.)

All station equipment was in operation and a good quality set of current oscillograms was obtained depicting a three-stroke negative discharge.

The Lynnwood Glen framing camera had also been activated and photographed the flash successfully (Figure 3A-14), but, being partly obscured by rain, no branching is discernible and the direction of progression is unknown.

On this occasion a slow sweep oscillogram was also obtained and analysis of the inter-stroke intervals resulted in values of 32 ms and 21 ms for the second and third strokes respectively.

Results

Event	Magnetic links		Processing of waveform data				
			Manual	Digitised			
	$\hat{I}$(kA)	σ(kA)	$\hat{I}$(kA)	$\hat{I}$(kA)	Q(C)	$\frac{dI}{dt}(\frac{kA}{\mu s})$	$\int I^2 dt (A^2 S)$
770222/25/1	-88	±14	-87	-83	>3	20	$>2x10^5$
770222/25/2	-	-	-80	-82	>2	170	$>1x10^5$
770222/25/3	-	-	-14	-13	>0,3	27	$>2x10^4$

General remarks

A faster sweep speed had been used on the high speed oscilloscope on this occasion and as a consequence, although the wavefronts were well resolved, the wave durations were not fully depicted and the resultant estimations of charge (Q) and action integral ($\int I^2 dt$) given above, represent minimum values only.

In view of the high current magnitudes obtained, this flash is presumed to have been downward in character.

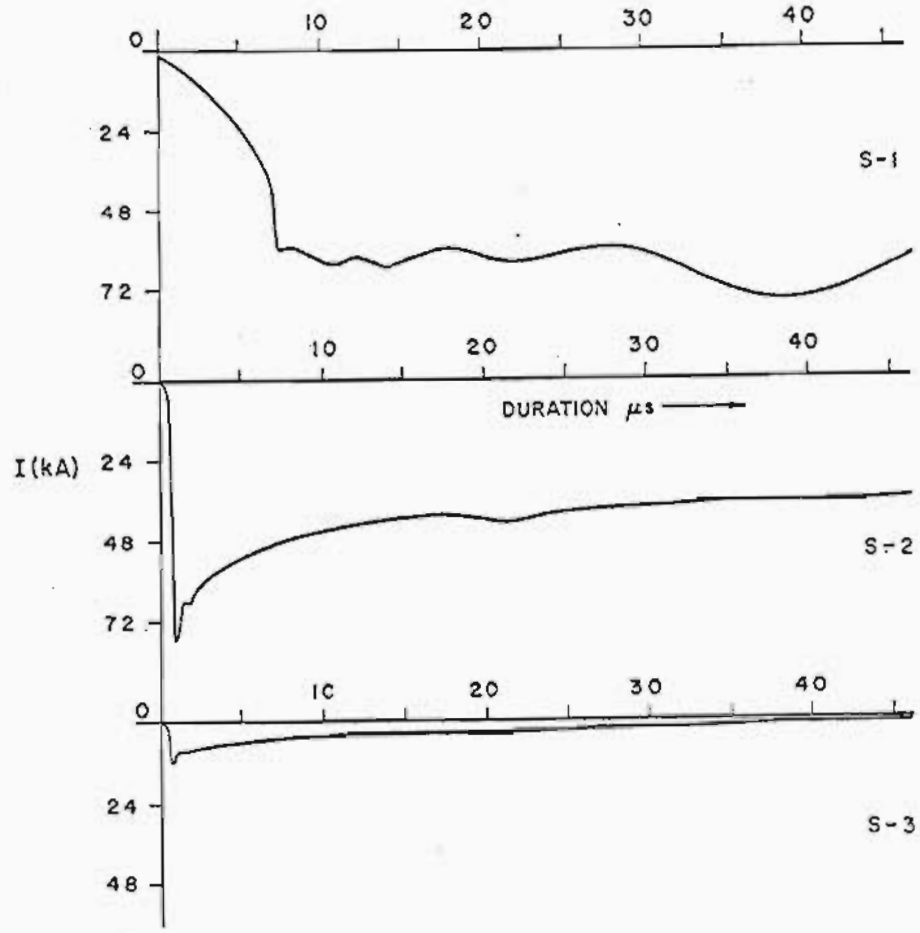

Flash No. 770222/25

FIGURE 3A-14 FLASH TO THE MAST ON THE 22ND FEBRUARY 1977
(LYNNWOOD GLEN CAMERA)

Event: 770507

Time of occurrence: 770507/26 - unknown

Circumstances: This flash occurred during an unusual autumn storm of the frontal type. This storm was short-lived and mild in character, being associated with a ground flash density of only 0,02 flashes km^{-2}.

The recording station had already been shut down for the winter recess, but the magnetic links were still present on the mast. These remained unmagnetised however, indicating a current amplitude below 2 kA. The occurrence of a discharge was confirmed by the recording spark-gaps, whose arc erosion was consistent with a low intensity event.

The remote framing cameras were not in operation on this occasion.

Results: No results were obtained.

General remarks

In view of the nature of the storm and the presumed low current magnitude of the discharge, this flash is thought to have been a weak upward discharge, or perhaps an incomplete upward leader.

Event: 771009

Time of occurrence: 771009/27 - 03 h 20

Circumstances: This flash occurred during a short-lived, but very active early morning storm. (The associated ground flash density was 0,32 flashes km^{-2}.)

All station instrumentation was in operation and a good quality single-stroke negative current oscillogram was obtained.

Both remote framing cameras had previously been activated and bi-directional photographs of the flash were successfully recorded. (Figure 3A-15(a).) These depict a downward progressing discharge with unusually extensive branching.

The CCTV video system was also in operation on this occasion and indicates clearly the probable interception of the downward and upward interconnecting leaders (Figure 3A-15(b)).

Results:

Event	Magnetic links		Processing of waveform data				
			Manual	Digitised			
	$\hat{I}$(kA)	σ(kA)	$\hat{I}$(kA)	$\hat{I}$(kA)	Q(C)	$\frac{dI}{dt}(\frac{kA}{\mu s})$	$\int I^2 dt (A^2 S)$
771009/27	-83	±14	-87	-87	15	12	$6,8 \times 10^5$

General remarks

As in the previous instances when bi-directional photographs were obtained, these records were again subjected to computerised analysis of flash geometry - as discussed in Chapter 4.

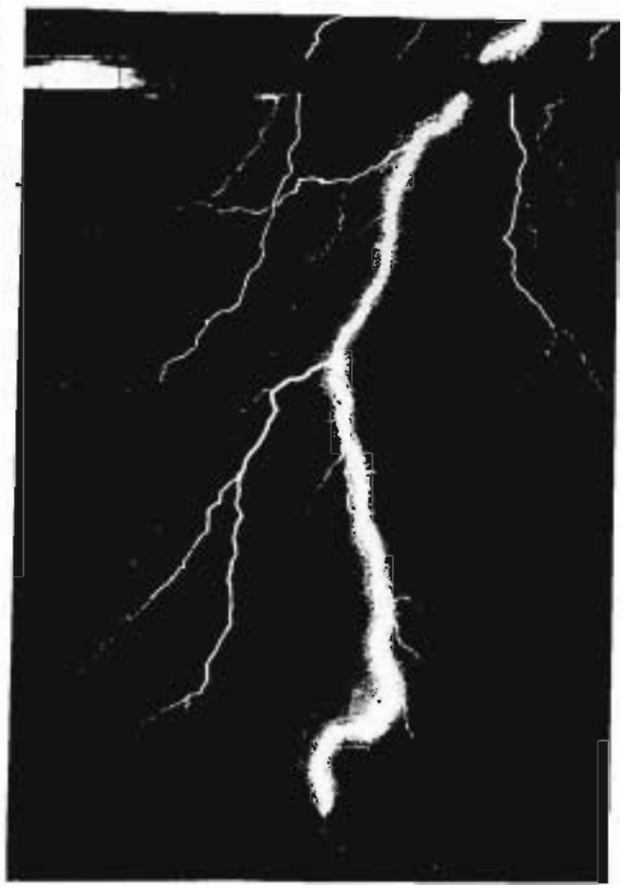

Lynnwood Glen camera

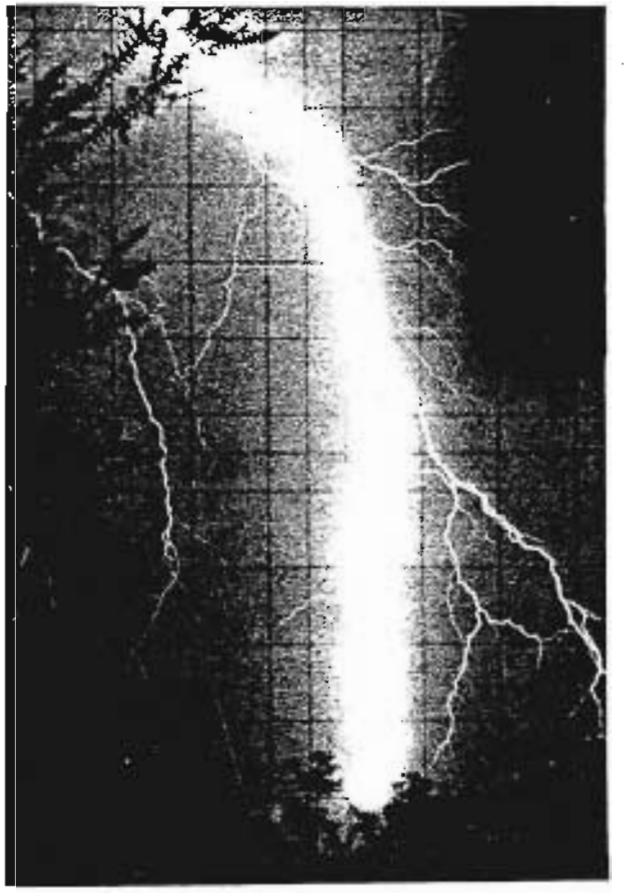

Murrayfield camera

Flash No. 771009/27

FIGURE 3A-15(a) FLASH TO THE EAST ON THE 9TH OCTOBER 1977

CCTV Frame (Flash No. 771009/27)

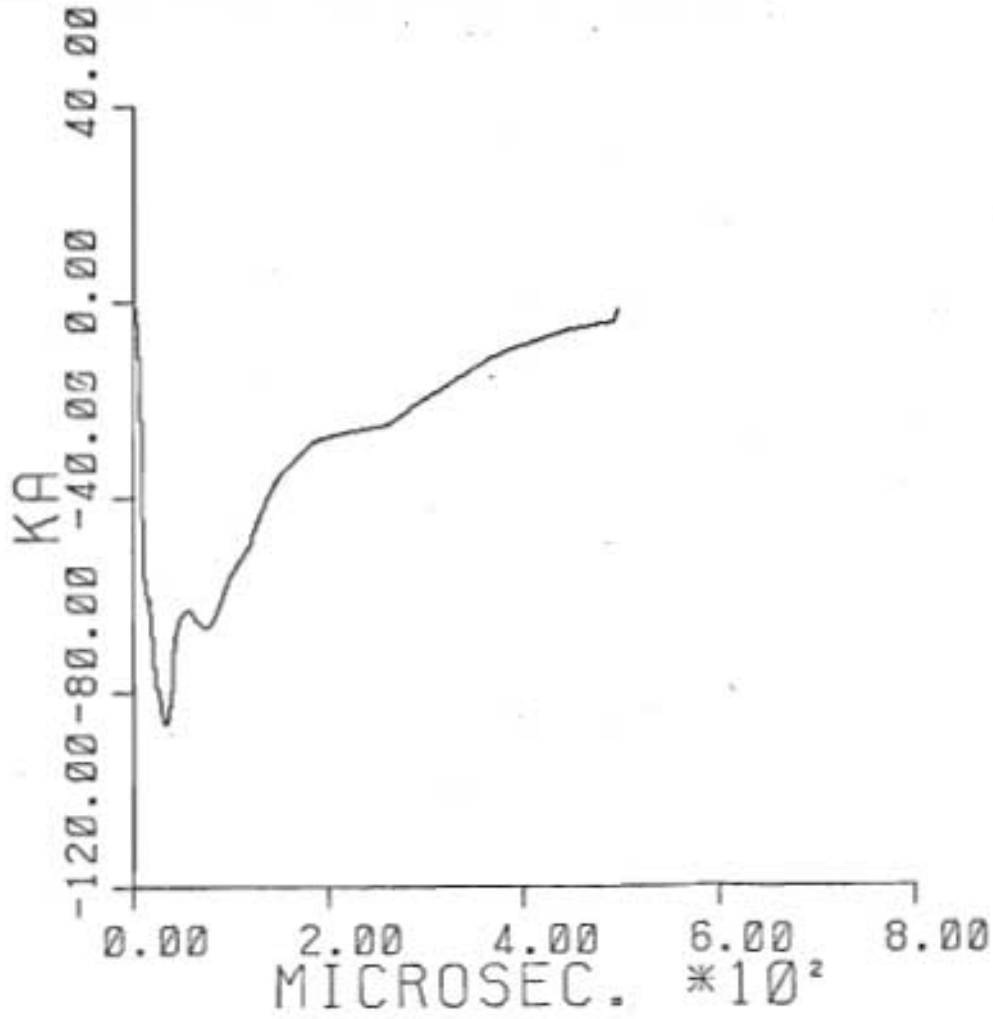

FIGURE 3A-15(b) FLASH TO THE MAST ON THE 9TH OCTOBER 1977

Event: 780128

Times of occurrence: 780128/28 - 00 h 23
780128/29 - 00 h 30

Circumstances: These two flashes occurred during a major and extensive storm which persisted for over 11 hours and was associated with a local ground flash density of 0,62 flashes km^{-2}.

All station instrumentation was in operation throughout the storm, with only one trigger being noted, co-incident with Flash No. 29. (An enhanced trigger sensitivity of 100 A was in use at this time.) The resultant oscillogram is devoid of any signal except a small positive pulse of current of about 800 A - which is barely discernible at the deflection sensitivity adopted.

Both remote framing cameras were also in operation on this occasion, but at the times of the above two events the resultant bi-directional photographs showed flashes to ground about 615 m and 950 m away from the mast, respectively. In each case, however, weakly illuminated branches were apparent in the sky immediately above the mast.

These are seen in greater detail in the CCTV video tape recordings obtained at the same times, as shown in Figure 3A-16. In the first instance, (Flash 28) the approach of the downward branched leader element has apparently initiated an upward leader from the mast, but the two leaders have failed to intercept each other. In the second instance, the interception of the downward branched element has apparently been completed but has not resulted in the passage of any substantial return stroke current - as evidenced by the weakly illuminated channel.

The passage of a small discharge current through the mast is confirmed by the arc erosion caused on the recording spark-gaps and by a low degree of magnetisati of the magnetic links - which indicate a nett negative peak current of about 3 kA.

Results: No further data were obtained on this occasion.

General remarks

It is presumed in the second instance (Flash 29) that passage of substantial return-stroke current may have been inhibited by the approximately simultaneous discharge of the main channel to ground some 950 m away. It is suspected however, that the recording oscilloscope may have triggered too early on this occasion (due to the sensitive setting), and thereby have missed the main pulse of current.

Flash No. 780128/28

Flash No. 780128/29

FIGURE 3A-16 FLASH EVENTS ON THE MAST ON THE 28TH JANUARY 1978
(CCTV FRAMES)

Event: 781018

Time of occurrence: 781018/30 - 03 h 20

Circumstances: This flash occurred toward the end of a major storm, during which the associated ground flash density was 0,57 flashes km^{-2}.

All equipment was in operation on this occasion, including the two remote framing cameras, but although a trigger was recorded (at 100 A sensitivity), no deflection was apparent on the resultant current oscillogram - which had a vertical resolution of 1 500 A/mm. The magnetic links were also not magnetised above their threshhold sensitivity of 2 kA, but the recording spark-gap confirmed the passage of a weak discharge.

The bi-directional photographs obtained from the two remote cameras (Figure 3A-17) depict a weakly illuminated upward branching flash, and a nearby bright ground flash is also evident in one photograph - implying its occurrence within the same exposure period (60 seconds).

Results: No results were obtained on this occasion.

General remarks: It is suspected that this upward flash, or incomplete upward leader, may have been initiated by the electrostatic field changes associated with the nearby ground flash.

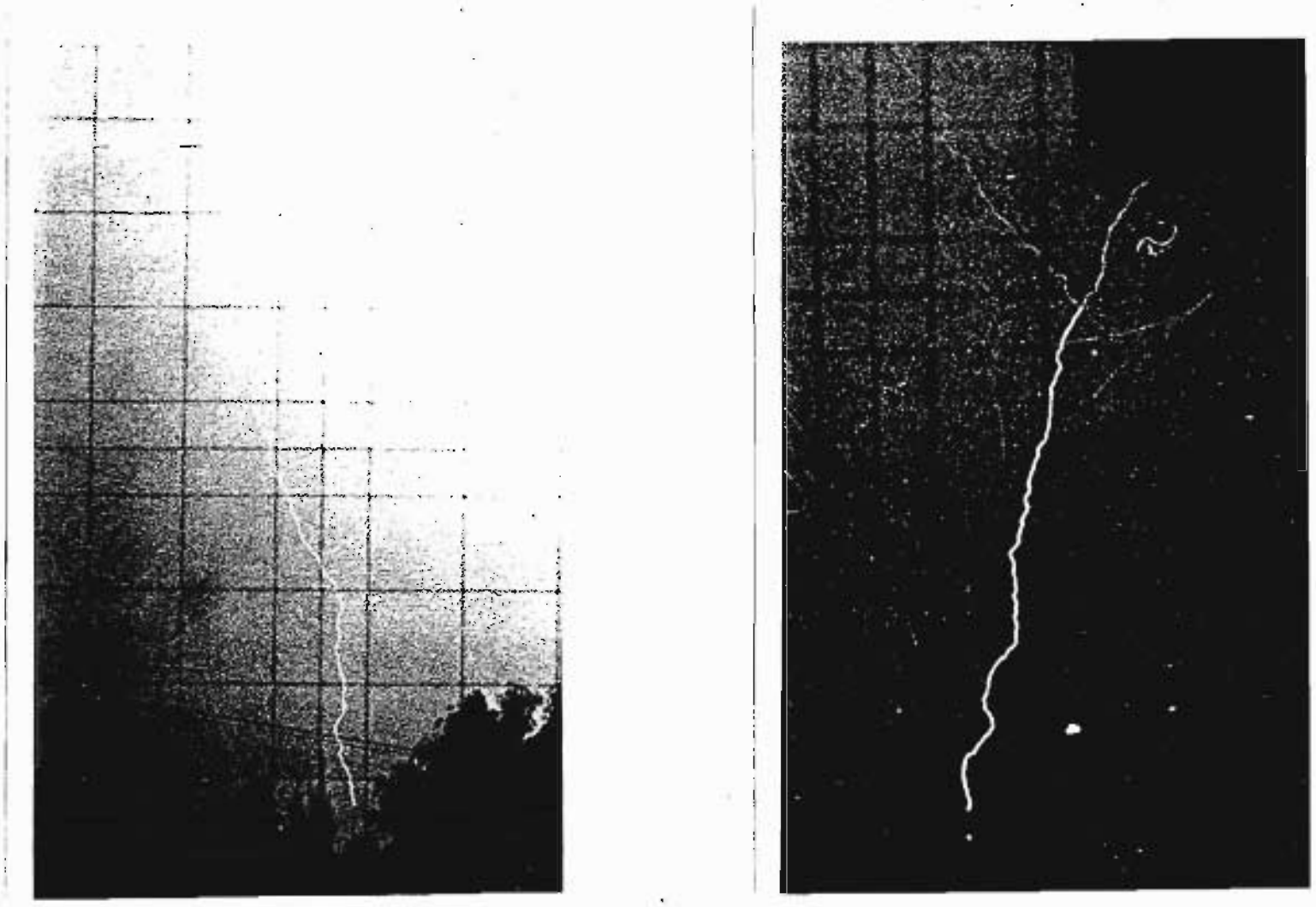

Lynnwood Glen camera

Murrayfield camera

Flash No. 781018/30

FIGURE 3A-17 FLASH TO THE MAST ON THE 18TH OCTOBER 1978

APPENDIX 4A: AN ANALYTICAL APPROACH TO STRIKING DISTANCE RELATIONSHIPS

INTRODUCTION

This approach is based directly upon work originally initiated by Anderson[9] and subsequently extended by the author in collaboration with Anderson - as outlined elsewhere[53][57].

In 1971[9], Anderson devised an analytical model of the negative downward progressing leader - based upon fundamental electrostatic principles - and applied this to a determination of the electrostatic field intensities at ground level during the approach of such a leader, as well as to the influence of a protruding conductor in estimation of lightning striking distances. These were defined as the distances between the corona sheath of the descending leader tips and earth (or the structure), at the moment when an upward leader was initiated from the earth (or structure). He also showed that these striking distances depended upon the charge on the leader, its distribution, and upon the relative ionisation inception potential gradients in the intervening air gap. A fundamental aspect of these analytical studies was the concept of a vertical cylindrical leader model, comprising a single charged line element - i.e. unbranched.

In a related analysis[69], Anderson has also shown that the electrostatic field strength E_t at the top of a structure of length L and radius R, when placed in a uniform field E_o, may be calculated from a field intensification factor K_i, which is given by the ratio of these two fields, viz:

$$K_i = E_t/E_o$$

K_i is in turn a function of the structure dimentional ratio , L/R, (for simple cylindrical structures) - as shown in Figure 4A-1, where L and R are the structure length and effective radius respectively.

Consider now the geometry shown in Figure 4A-2, which depicts the approach of a model leader toward a plane earth (assumed conducting), and assume the location of a cylindrical mast of height L and radius R at the point A. In terms of this geometry, it is readily shown[53] that the potential gradient in the vicinity of the ground may be taken as uniform over the equivalent distance L above the earth (in the absence of the structure), provided that;

$$Z \gg L \text{ and } L \leq d$$

In this eventuality, assuming a linear distribution of the leader charge q, the field strength E_a at the point A (in the absence of the structure) may be calculated from [9][57];

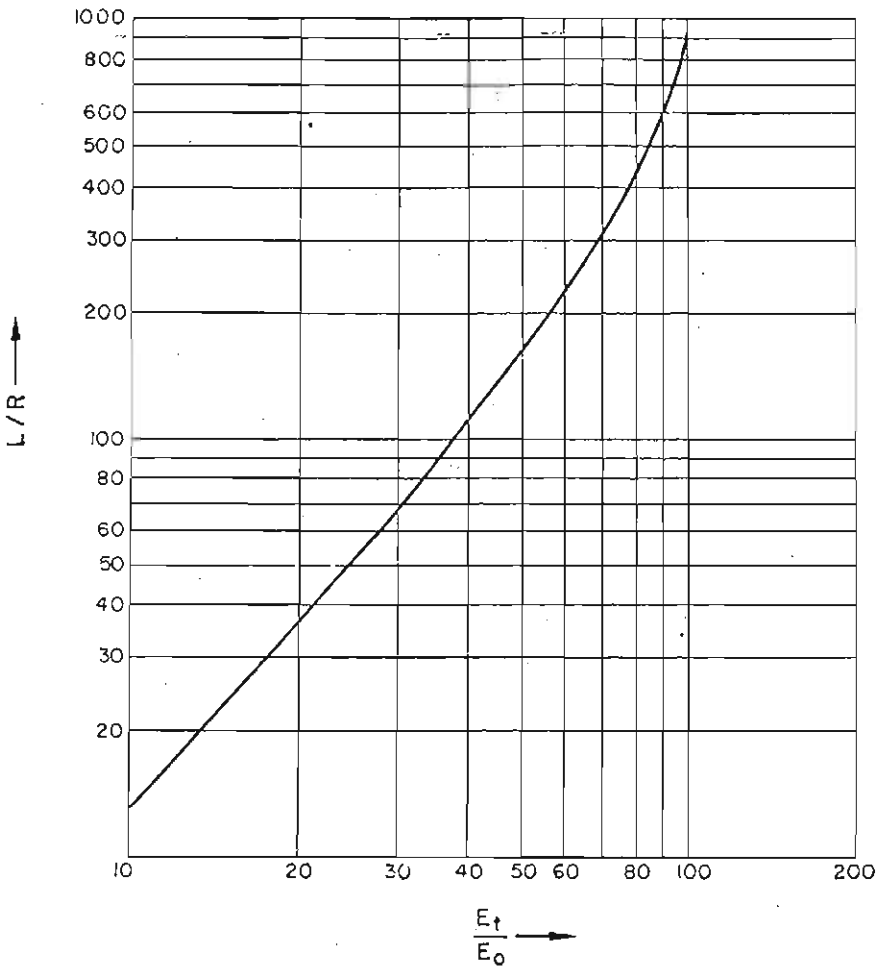

FIGURE 4A-1

RATIO OF RESULTANT FIELD STRENGTH E_t AT THE TOP OF A STRUCTURE TO THE INDUCING FIELD STRENGTH E_o FOR GIVEN RATIOS OF STRUCTURE DIMENSIONS L/R

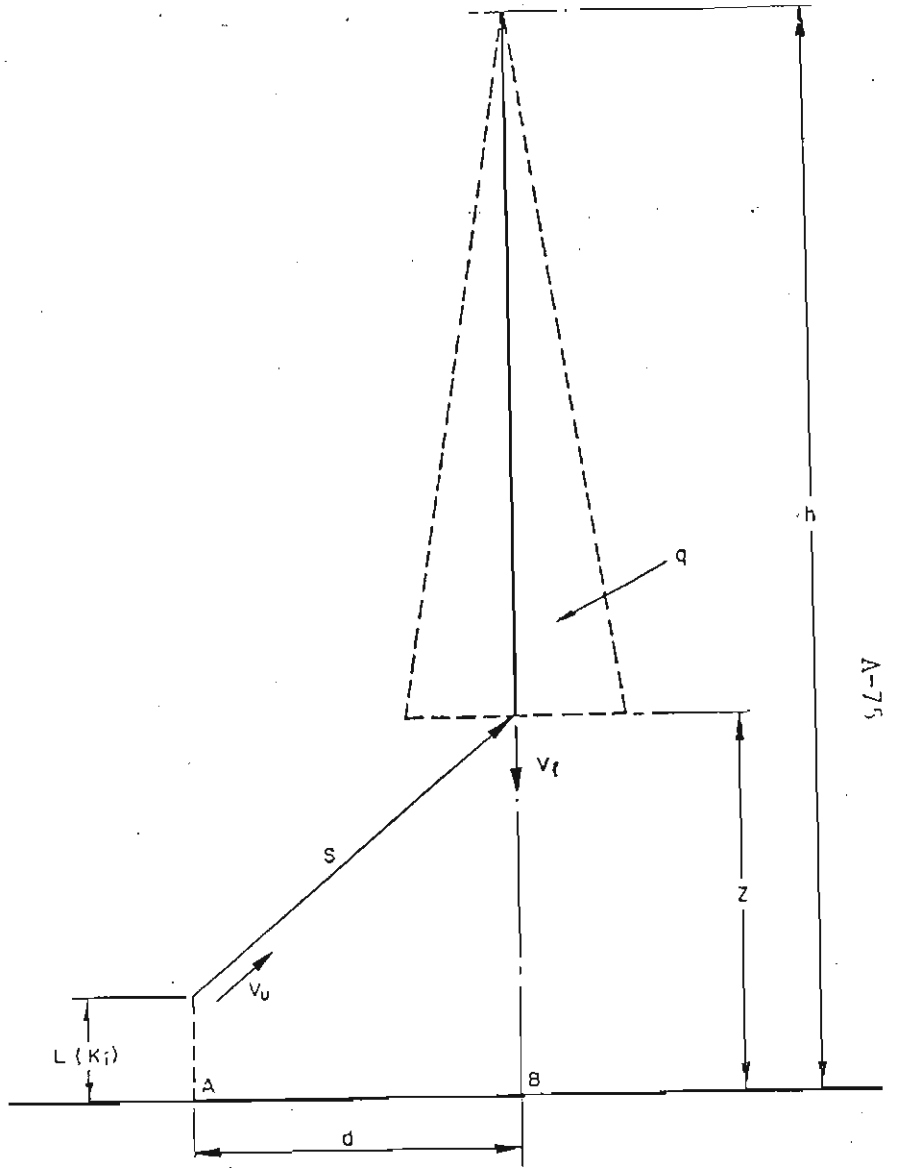

FIGURE 4A-2

STRIKING DISTANCE GEOMETRY

$$E_a = \frac{q}{\pi\varepsilon d^2 (h/d - z/d)^2} \left\{ \frac{(h/d - z/d)}{(1+(z/d)^2)^{\frac{1}{2}}} + \sinh^{-1}(z/d) - \sinh^{-1}(h/d) \right\} \quad \ldots (4A\text{-}1)$$

On the above basis therefore, the field strength E_t at the tip of the mast may be determined from

$$E_t = K_i E_a$$

where K_i is the relevant structure intensification factor.

At the same time, (again assuming a linearly charged leader model), the field strength E_b at the point B on the earth immediately below the descending leader may be expressed by[9][57]:

$$E_b = \frac{q}{\pi\varepsilon(h-z)^2} \left\{ \frac{h-z}{z} + \ell n(z/h) \right\} \quad \ldots (4A\text{-}2)$$

Defining E_m as the requisite leader ionisation inception gradient necessary for initiation of an upward leader from either the earth, or the structure tip (i.e. assumed equal in both instances), it is evident that a stage in leader progression could be attained when either the field E_a, or E_b, could exceed E_m and an upward leader could develop from one, or the other locations, thereby determining the point of strike.

Define also, z_m, to be the value z when $E_b = E_m$. In this case, however, Anderson[9] has shown that z_m is in fact equal to the corona radius around the leader. Thus, in terms of the geometry given in Figure 4A-2, the criterion for the flash to terminate on the structure is that the upward leader from the mast should traverse the distance $(s-z_m)$ to intercept the leader, before the leader has advanced the distance $(z-z_m)$ toward the earth.

Defining upward and downward leader velocities as v_u and v_ℓ respectively, this criterion reduces to:

$$(s-z_m)/v_u \leqslant (z-z_m)v_\ell \quad \ldots (4A\text{-}3)$$

On this basis therefore, for a particular leader channel height h and a specific structure, the equation (4A-1) may be solved to define that volume of space in the vicinity of the structure within which the above criterion is met; (as well as the requisite leader charges q), i.e. the breakdown potential gradient is achieved at the structure tip before the leader corona radius meets the ground.

In subsequent work[53][57], the author and his colleagues have applied these concepts in several analyses of specific numerical examples.

The approach is illustrated now by application to the research mast situation.

ESTIMATION OF STRIKING DISTANCES TO THE 60 m RESEARCH MAST

(a) Field intensification factor K_i

The mast height is known; i.e. L = 60 m.

The mast is of triangular section, and, in an earlier analysis[53], a cylindrical equivalent radius r_{eq} was calculated as r_{eq} = 0,29 m.

Golde has subsequently pointed out[58] however, that allowance should be made for the development of a corona sheath around the mast tip. Accordingly therefore, as is commonly the case in long spark work, the "critical corona radius" concept[70] may be introduced, whereby leader inception on electrodes having dimensions smaller than a particular "critical radius", may be expressed in terms of corona inception on an electrode having the critical radius. The latter is dependent upon the electrode geometry, but in large gaps and for spherical electrodes an empirical expression has been determined as[70]

$$R_c = 0,38\ (1-\exp(-D/5)) \quad \ldots\ldots\ldots\ldots\ldots\ldots\ldots\ldots\ldots\ldots \quad (4A-4)$$

where D is the gap length in m.

In very long gaps therefore, this reduces to R_c = 0,38 m and this value is assumed as the relevant effective radius of the research mast at the tip. This yields an equivalent structure dimensional ratio $L/R = 60/0,38 = 158$.

Applying this value in Figure 4A-1, gives a field intensification factor for the mast,

$$K_i = E_t/E_a = 44.$$

(b) Determination of corona-inception gradients and corona radius

Considerable data are available regarding corona inception gradients and these are shown to vary depending upon the nature of the gap, electrode geometry, and in some instances, on the rate of rise of voltage.

However, in a review on long gaps under switching impulse conditions, Jones and Waters[71] present surface gradients ranging between about 2,8 and 3,3 MV/m for an electrode equivalent radius of 0,38 m, with a mean value of about 3,1 MV/m.

Introducing ..... /A-78

Introducing an air-density correction factor of 0,84 to allow for a 1 400 m altitude at the research mast site and an ambient temperature of 25°C, yields a corona inception gradient E_m at the critical radius of 2,6 MV/m.

For ease of calculation, this is assumed to be the field strength necessary for ionisation inception both at the mast tip and at the earth below the leader. In the latter instance, the corona radius z_m around the leader tip is derived from equation (LA-2), for the field E_b below the leader, viz.:

$$E_b = E_m = 2{,}6 \text{ MV/m} = \frac{q}{\Pi\varepsilon(h-z_m)^2}\left(\frac{h-z_m}{z_m} + \ell n(z_m/h)\right) \quad \ldots\ldots\ldots \quad (4A\text{-}5)$$

As discussed in Appendix 1-A, downward leader breakdown processes are known to initiate at altitudes over the range of 3 to about 9 kms, with average channel lengths being about 5-6 kms, while the charge deposited on the downward leader is found to vary between about 2 and 20 coulombs, with an average value of 5 coulombs.

The above values therefore, define the relevant ranges of parameters applicable to solution of equation (4A-3) and the resultant variations in corona radius z_m are shown graphically in Figure 4A-3. In his earlier analysis of the leader model[9] Anderson pointed out that the corona radius z_m could also be approximated by the expression

$$z_m = q.(\Pi\varepsilon E_m h)^{-1} \quad \ldots\ldots\ldots\ldots\ldots\ldots\ldots\ldots\ldots\ldots\ldots\ldots \quad (4A\text{-}6)$$

This expression has been evaluated for the above range of values of q and h and the results are also plotted in Figure 4A-3 - showing generally good agreement with the values derived from solution of equation (4A-5).

(c) Determination of striking distances in the vicinity of the research mast

As noted earlier, equation (4A-1) defined the field intensity E_a, at a point A on the ground, for a given position of the descending leader tip and assuming a particular magnitude of charge q distributed linearly along a line element model of the leader. In turn, assuming a uniform potential gradient close to the ground, it was shown that the field intensity E_t at the top of the mast could be expressed in terms of the field E_a, viz:

$$E_t = K_i E_a$$

where K_i is the field intensification factor and, for the research mast,

$$K_i = 44.$$

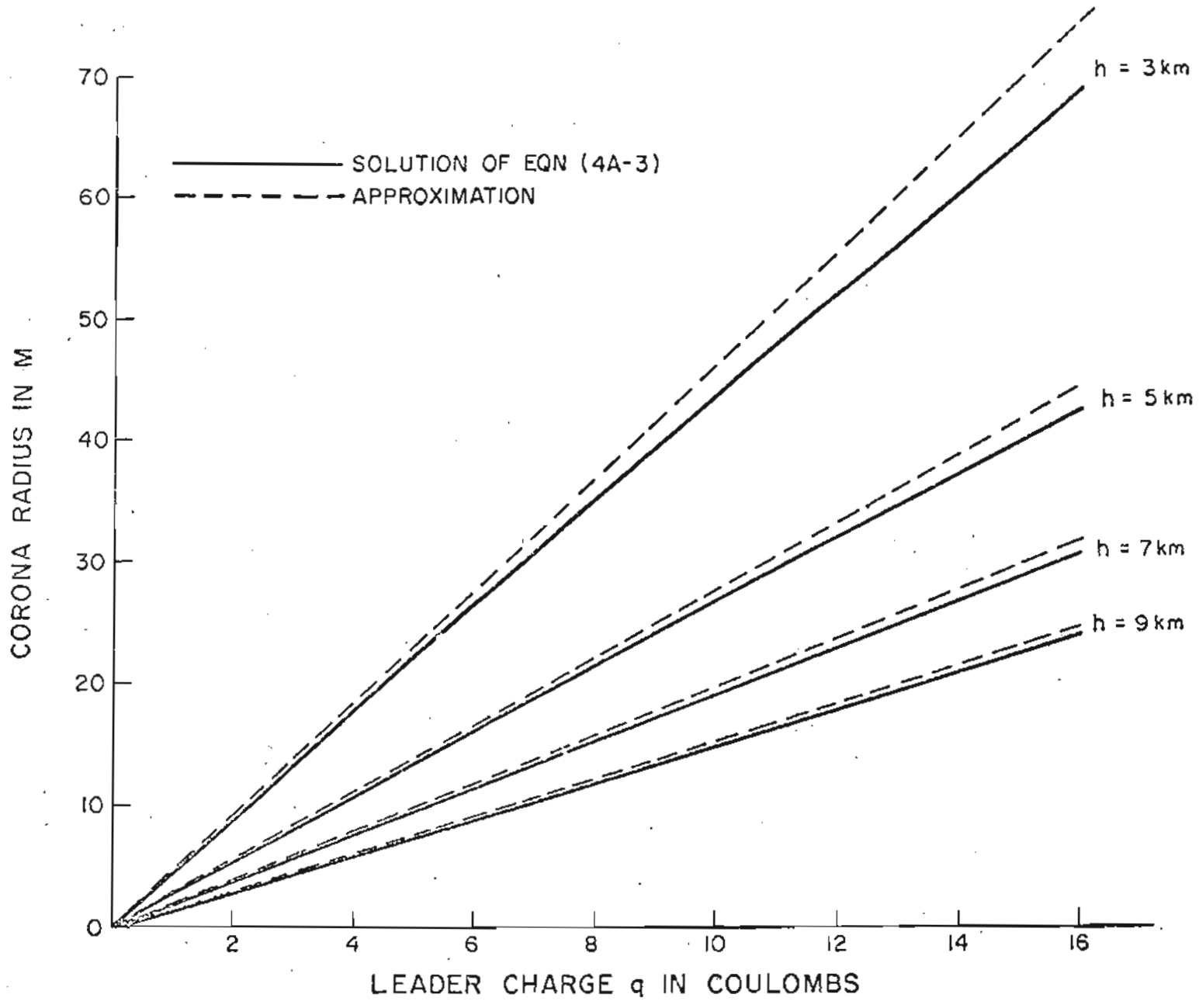

FIGURE 4A-3

VARIATION IN LEADER CORONA RADIUS AS A FUNCTION OF LEADER CHARGE AND CHANNEL LENGTH.

Thus, defining the corona inception gradient E_m = 2,6 MV/m, this approach indicates that upward leader inception at the mast tip (i.e. over the corona critical radius R_c), would occur when the descending leader has approached sufficiently close to cause an equivalent field at the mast position; $E_a \geqslant 59,1$ kV/m, i.e. in the presence of the mast, $E_t = E_a K_i = 2,6$ MV/m = E_m

On the above basis therefore, adopting the parameters d and q in equation (4A-1) as the dependent variables, this equation may be solved iteratively, to yield the relevant heights z_m of the leader tip when the gradient $E_a \geqslant 59,1$ kV/m is attained at the mast equivalent position.

This process has been carried out over a range of values of q and d, (assuming an average channel length h = 5 000 m), and the results are shown in Figure 4.5 - where the dotted curves denote the loci of the relevant positions of the charged leader tip.

The criterion for a flash to be intercepted by the mast was defined by equation (4A-3), viz:

$$(s-z_m)/v_u \leqslant (z-z_m)v_\ell$$

where v_u and v_ℓ are the velocities of the upward and downward leaders respectively and s is the resultant striking distance.

On the trial assumption that $v_u = v_\ell$, this criterion reduces to;

$$s \leqslant z$$

and, from Figure 4A-2, s may be expressed as

$$s = \{d^2+(z-L)^2\}^{\frac{1}{2}}$$

the above equality may be restated as

$$s = z = \frac{d^2+L^2}{2L} \qquad \text{..... (4A-7)}$$

For the research mast height L = 60 m, the points (z,d) solving this equation trace out a parabolic "volume" above the research mast, which defines the limits of compliance with the above criteria, i.e. the volume within which the descending leader would be intercepted by the upward leader, and the flash would terminate on the structure. This "volume" is also shown in Figure 4.5, and the interceptions of the curve s = z with the various loci of the requisite charges q, define the relationship between striking distance s and charge q.

The resultant values of striking distance, together with the associated values of corona radius z_m, are summarised in Table 4A-1 (for an average channel length h = 5 000 m).

TABLE 4A-1: ANALYTICALLY DERIVED VALUES OF STRIKING DISTANCE FOR THE RESEARCH MAST

(For a leader channel length of 5 km)

Charge q (c)	Corona radius z_m (m)	Striking distance s (m)	
		for K_v = 1,0	K_v = 1,2
1	2,8	82	75
2	5,5	172	168
3	8,3	262	260
4	11,1	355	353
5	13,8	441	441
6	16,6	555	555
7	19,4	612	612
8	22,2	694	694
9	24,9	775	775
10	27,7	854	854

These results indicate that for the case of the research mast (with its high field intensification factor K_i = 44), the corona radius z_m does not exceed 4% of the striking distance s, and thus may be neglected in the criterion expressed in equation (4A-4), which thus reduces to;

$$s/v_u \leqslant z/v_\ell$$

Data on the comparative magnitudes of downward and upward leader velocities are comparatively scarce. Of particular relevance here are the velocities of downward negatively charged leaders, together with those of the upward positively charged leaders, and especially any possible relation between these two parameters. In recent review studies, Allibone and Dring[68][72] found values for the former varying between $0,5 \times 10^5$ - 13×10^5 m/s, while positive upward leaders from masts were marginally slower, covering the range $1,3 \times 10^5$ - $9,7 \times 10^5$ m/s.

This would imply that the earlier trial assumption of equality between v_u and v_ℓ is not grossly in error. However, in terms of this model approach, the effect of any variations in the ratio v_ℓ/v_u can be quite significant.

In ...../A-82

In more general terms, defining

$$K_v = v_\ell / v_u$$

the limiting criterion expressed in equations (4A-3) and (4A-7) may be restated as;

$$d = \{2zL - L^2 - z^2(1 - {}^1/K_v{}^2)\}^{\frac{1}{2}}$$

For example, considering $K_v = v_\ell / v_u = 1{,}2$, (i.e. an upward leader velocity some 20% slower than that of the downward leader), leads to a substantial reduction in effective "collection volume" - assuming that all downward leaders are effectively vertically oriented - as shown schematically in Figure 4.5. The effect of the changed velocity ratio on striking distance is comparatively small however, as shown by the results given in Table 4A-1.

(d) Estimation of equivalent attractive range

The preceding analyses have demonstrated (for the assumption of a linearly charged leader model), that with the approach of a given charged leader to within a distance s of the mast-top, the field strength in the vicinity of the mast equivalent corona sheath is sufficiently intensified to attain the field intensity requisite for upward leader initiation.

Thereafter, the possibility of the flash being deflected to the mast depends upon the interception of the downward continuing leader by the upward progressing leader and thus, in turn, is dependent upon the respective leader velocities - as shown by the two prospective "collection volumes" given in Figure 4.5 for two values of the ratio $K_v = v_\ell / v_u$.

In terms of this concept, vertically descending leaders traversing paths outside these collection volumes will reach the ground before being intercepted by the upward leader developing from the mast. Thus, for a given charge magnitude q and velocity ratio K_v, the cross-section through this collection volume (when defined in plan-view), is equivalent to an attractive area A, over which flashes bearing that charge q will be diverted to the mast; A may be stated as;

$$A = \pi R_a^2$$

where ..... /A-83

where R_a is an equivalent attractive radius for the charge q and velocity ratio K_v. Dependent upon the velocity ratio, this attractive radius may be relatively insensitive to leader charge magnitude, as shown for example in Figure 4.5, in which it is evident that the attractive radius is essentialy independent of charge values in excess of 2 coulombs.

The resultant values of attractive radius for the two ranges of velocity ratio considered in the preceding analyses are summarised in Table 4A-2, as functions of the associated charge magnitudes.

TABLE 4A-2: VARIATIONS IN EQUIVALENT ATTRACTIVE RADIUS

Charge	Attractive radius in m	
	K_v = 1,0	K_v = 1,2
1	79	68
2	130	88
3	168	89
4	198	89
5	223	89
6	246	89
7	265	89
8	283	89
9	300	89
10	316	89

(e) Relationship with equivalent peak current amplitude

As previously noted, most practical applications of striking distance relationships require expressions of the form;

$$D_s = K(I)^b$$

while the preceding analyses have related all derived parameters to the leader charge q. For convenience therefore, a relation between charge q and the associated peak current amplitude I would be preferred.

The earlier analyses of Berger's discharge current waveform data (18) - as discussed in Chapter 3, have established that a significant correlation is present between peak current and impulse charge for negative discharges, and the relevant regression relation for negative first strokes is given as (14);

$$I = 10,6\ Q^{0,7} \quad \ldots\ldots \quad (4A-8)$$

Accordingly, this relation may be used to relate the analytically derived striking and interception distances (assumed to be half the striking distance for $v_\ell = v_u$), to peak current amplitude. The resultant curves are shown in Figure 4.4 as (D_s) and (D_I) - (labelled 'Berger correlation').

However, Golde[58] has pointed out that the relevant charges are those in the lower portion of the leader channel.

In fact, considering that return stroke velocities normally lie in the range of 20 - 100 m/μs and that first stroke current waveforms have median times to crest (as opposed to wavefront risetimes[18]) of about 10 - 20 μs, (as noted in Appendix 1A) leads to the conclusion that the charges in the lower 200 - 2 000 m of the channel are principally involved in determining the peak currents. For example, for an average linearly charged leader length of 5 km, it is readily shown that about 36% of the total leader charge would be present in the lowest 1 000 m. The latter estimate accords well with Golde's proposal[58] that a peak current of about 25 kA should be associated with a charge of only 1C - which implies a shift in the relation expressed in equation (4A-8), by a factor of about 3.

Accordingly, the mean measured values of striking and interception distances are again depicted in Figure 4.6, together with modified relations between these distances and peak current which have been derived from the preceding analyses, but modified in terms of Golde's correlation between charge and current - and a better measure of agreement is evident than was present in Figure 4.4.

The modified relation between charge and current takes the form;

$$I = 29{,}4\ Q^{0{,}7}$$

Applying this relation and fitting a power-curve expression through the resultant analytically derived values of striking distance as functions of peak current, yields the striking distance relation;

$$D_s = 0{,}6\ I^{1{,}46}$$

Similarly, assuming a velocity ration $K_v = 1{,}2$, a relation for the interception distance d_I may be derived; viz.

$$D_I = 0{,}27\ I^{1{,}46}$$

These ...../A-85

These then are the two relations plotted through the measured data in Figure 4.6.

In general, although both curves appear to follow the trend of the measured points, both curves also tend to lie below the measured data - as shown by the power curve fit through the striking distance data - which takes the form;

$$S_M = 16,5\ I^{0,57}$$

where S_M are the measured values of striking distances.

APPENDIX 6 A A GENERALISED APPLICATION OF THE STRIKING DISTANCE MODEL

Fundamental relations

In Chapter 4 (together with its related Appendix 4A) a simplified analytical model was presented whereby striking distances to the research mast could be estimated, as well as their functional dependency upon prospective peak stroke currents. A comparison of the predicted distances with the experimentally determined estimates (for various values of peak current amplitude), suggested a reasonable degree of agreement - to within about 20% - as depicted in Figure 4.6.

In this section therefore, an attempt is made to demonstrate a more general application of this analytical model to an estimation of striking distances and attractive radii over the range of practical engineering structure heights.

The following steps are embodied in the conceptualisation of the model:

(a) It is assumed that the structures concerned may be regarded as free-standing and capable of approximate representation by cylindrical geometry; e.g. broadcast antennae, lightning protective masts, tall chimney stacks, and transmission line towers. (In the latter instance, the assumption is considered valid in at least the two dimensions transverse to the line itself.)

(b) Following on the examination of the effects of leader branching in 4.6, the downward leader is represented by a vertically descending linearly charged element 3 000 m in length. (Although channel lengths up to 7 000 m were in fact studied, the above length was adopted, since it was considered that the attainment of prospective strike points upon the ground is principally determined by the approach of one or more major leader branches - as illustrated earlier in Figure 4.10, for example.)

(c) In a manner similar to that followed in 4.5, the prospective stroke peak current is considered on average to be related to the leader charge by assuming Berger's experimentally determined correlation between peak current and impulse charge, but modified to take account of return stroke parameters. For simplicity, Golde's relation was taken as a guide, leading to the following result,[58]

$$I = 25\ Q^{0,7}$$

where I = prospective peak stroke current in kA

Q = leader charge in coulomb.

(d) ..... /A-87

(d) In principle, as discussed in Chapter 4, the field enhancement at the structure top is determined by the structure dimensional ratio (for cylindrical type geometries). In this instance, however, bearing in mind the practical structures envisaged in this study (such as transmission line towers, for example), it is felt that allowance should also be made for the micro-geometry at the structure extremities. This could prove excessively complex and a useful engineering approximation is again available in the form of the critical corona radius concept - as applied previously in Appendix 4A. In this study therefore, it is assumed that the varying degrees of field enhancement associated with varying structures and heights H_i, may be represented by considering equivalent structures, having the same heights H_i but having effective radii given by the critical corona radius R_c - as expressed earlier in Appendix 4A. Although this assumption is critical to this study (since the resultant striking distances and attractive radii are directly proportional to these field enhancement factors), the impact is reduced, since Figure 4A-1 shows that field enhancement factors are comparatively insensitive to moderate variations in structure dimensional ratio (due to the logarithmic dependencies), and quite large errors in the assigned values of effective radius can thus be tolerated. On this basis therefore, field enhancement factors have been determined over the range of structure heights of practical interest, as shown by the summarising curve in Figure 6A-1.

(e) Standard atmospheric conditions have again been assumed, and the criterion for the initiation of an upward leader from a particular structure has therefore been defined as the attainment of a critical field intensity of 3×10^6 V/m at the structure extremity (i.e. over the critical corona radius).

The above factors outline the basis of this model study. Thereafter, the approach followed is identical to that presented in Appendix 4A - i.e. embodying the estimation of the electrostatic field intensities developed below the descending charged leader and defining the termination of the stroke in terms of the initiation and subsequent interception of an upward leader from a structure, with the downward leader.

Iterative routines were developed for carrying out these calculations over a comparatively wide range of the various parameters involved and the resultant programs were executed upon a Hewlett Packard 9825S desk computer system.

The ..... /A-88

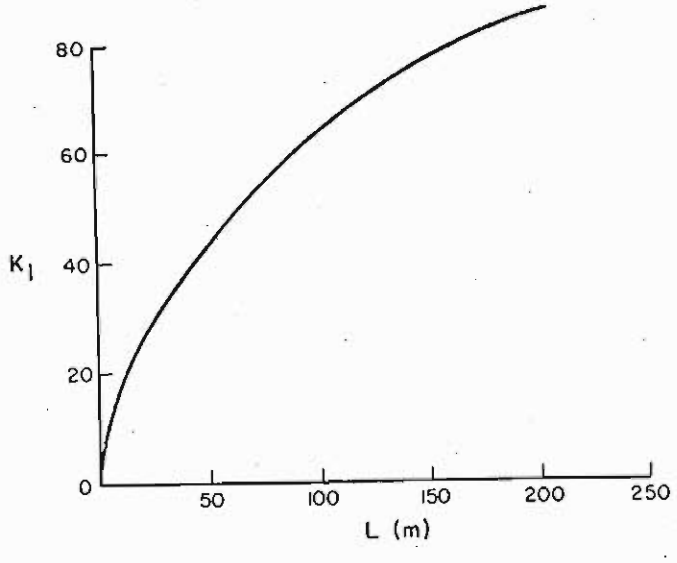

FIGURE 6A-1

FIELD ENHANCEMENT FACTOR vs TOWER HEIGHT

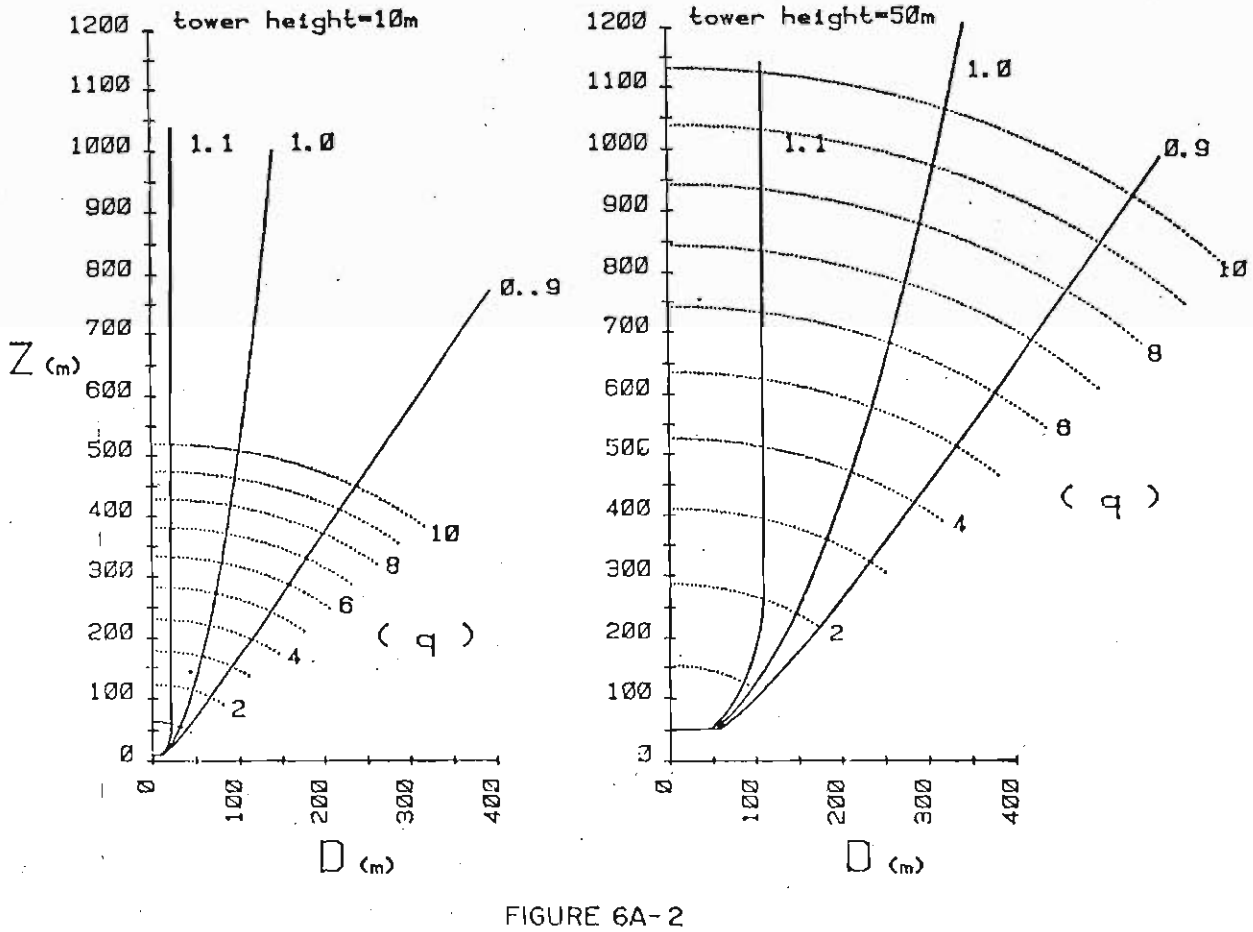

FIGURE 6A-2

COMPARATIVE STRIKING DISTANCE ANALYSES FOR 10m AND 50m

The following parameters were examined:

(i) Leader channel lengths of 3 000 m, 5 000 m, and 7 000 m were studied, although, as previously noted, the final solutions were based upon a 3 000 m leader "branch".

(ii) Structure heights over the range 10 m, 30 m, 50 m, 70 m, 90 m, 150 m, and 200 m.

(iii) Leader charges over the range 0,5, 1, 2, 3, ----- 10 coulombs (i.e. equivalent to currents up to about 125 kA).

(iv) Three values of the relative upward/downward leader approach velocity ratio were considered, namely - 0,9, 1,0 and 1,1.

Typical examples of the results are shown diagrammatically in Figure 6A-2 (in this case illustrating a comparison between structure heights of 10 and 50 m).

As in the previous analyses, striking distances to a structure (for a given leader charge), were defined in terms of the distance of approach of the leader at the point when the critical field of 3×10^6 V/m was attained at the structure tip. It is readily seen from the examples in Figure 6A-2 that these distances are essentially independent of the value of the velocity ratio.

This is in contrast to the estimates of attractive radius - which were again defined by the radius of the cross-sectional plan view of the collection volume (for various values of leader charge).

In this manner, and applying the expression relating average leader charge and prospective peak current ($I = 25Q^{0,7}$), it was possible to generate curves depicting the variations in striking distances and attractive radii, with respect to peak current and structure height - as given in Figures 6.1 and 6.2.

As already mentioned, the striking distance estimates were independent of the choice of the velocity ratio parameter. However, in considering the attractive radius results, a velocity ratio of 1,0 was adopted, since then the resultant trend of attractive radius with structure height showed best agreement with an empirical relation derived earlier from a study of the average incidence of flashes to tall structures[21]. This relation ($R_a = 16,3H^{0,61}$) is also depicted in Figure 6.2 and shows good agreement with the analytically derived trend of attractive radius corresponding to an average current of about 45 kA. (Although the median of the reference peak current amplitude distribution is about 34 kA, being of log-normal form the average value is higher and is given by about 45 kA.)

Having ..... /A-90

Having arrived at these results, numerical least-squares techniques of curve fitting were used to arrive at generalised "best-fit" expressions relating both striking distance and attractive radius, to peak current amplitude and structure height. The resultant expressions are given below:

$$D_s = (0,4 + 2,111 \times 10^{-2})\ I^{(1,41 - H \times 10^{-3})}$$

$$R_a = I^{0,64}\ H^{(0,66 + 2I \times 10^{-4})}$$

where D_s = striking distance in m

R_a = attractive radius in m

and H = particular structure height in m

I = relevant peak current amplitude of interest - in kA.

It should perhaps be re-emphasised that the above dependencies of both D_s and R_a upon peak current I, are in turn derived from Berger's experimentally observed correlation between I and impulse charge Q[14] (modified to take account of the return stroke characteristics). Berger's data show considerable scatter however, and the above relationships should therefore be considered as being indicative of average trends only.

This point is examined further in the following sections.

The protective effects of tall structures

The above generalised expressions for striking distance D_s and attractive radius R_a, provide a ready means for examining the influence of structure height upon the incidence of flashes to structures, and thus the degree to which tall structures may protect the surrounding terrain.

For a given structure, the stochastic nature of lightning may be simulated over periods equivalent to many years of thunderstorm activity, using Monte Carlo techniques of numerical analysis[108]. Figure 6A-3 shows an organisational diagram of a program prepared by the author, which was run upon an HP 9825S system and which employs Monte Carlo techniques of numerical simulation, together with the above relations for attractive radius, to study flash incidence in structures of varying height.

An area of 6,25 km^2 was examined, with the structure of interest being located at the central origin. For convenience, an annual ground flash density of 10 $km^{-2} yr^{-1}$ was adopted. Flash locations within this area were randomised and their associated stroke parameters (i.e. peak current amplitude), were randomly sampled from the CIGRE reference current amplitude distribution[20]. For each flash, the possibility of a strike to the structure was evaluated from a comparison between the applicable attractive radius R_a (as determined from the above relations), and the distance D to the randomised prospective stroke termination point. In the event that $R_a \rangle D$, the flash was considered to have struck the structur

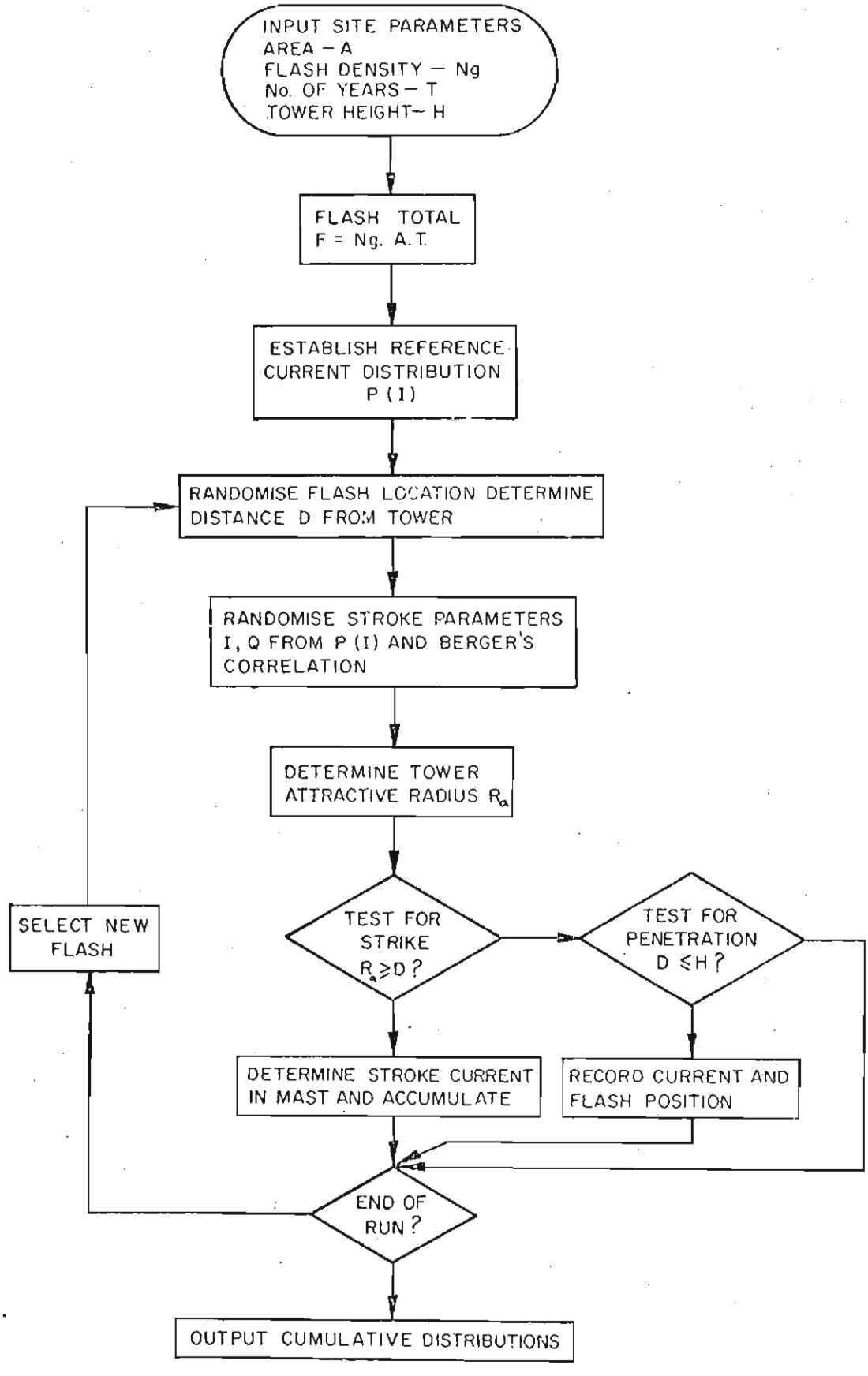

FIGURE 6A-3

MONTE-CARLO SIMULATION STUDY

Alternatively, in the event of a miss, the possibility that the stroke may have struck the ground within the 45° cone of protection, was also examined, by determining whether $D < H$. (The curves in Figure 6.2 clearly indicate that low current discharges could be associated with attractive radii less than the related structure heights.) Discharges meeting this criteria were termed "shielding failures" and their crest amplitudes and distances from the structure were also noted.

In this way, by examining a sufficiently large number of randomly selected flashes, a large number of strikes to a structure could be simulated - as well as a reasonable number of shielding failures. The reference criterion for the termination of a simulation run on a particular structure, was defined by the attainment of more than 200 strikes to that structure, although, in fact, runs involving up to 500 strikes to a particular structure were included in the study. Dependent upon the structure height (for the assumed ground flash density), this necessitated simulation runs extending up to equivalent periods of analyses between about 50 and 1 300 years (for structure heights decreasing from 500 to 20 m respectively).

The results for a typical analysis are shown in Figure 6A-4 - in this case, for a 200 m structure. (Although a rectangular co-ordinate system was used for convenience in graphical representation, the resultant strike incidence to the structure was per-unitised in terms of the ground flash incidence over an equivalent circular area having a radius of 1 250 m.)

The protective effect of the structure is clearly evident in this Figure, as seen by the reduced incidence of flashes to the ground in the structure vicinity. However, penetration of the 45° cone of protection by several flashes is also evident - as shown by the location of their termination points within the dotted locus given by $r = H$.

A summary of the results of this numerical study is given in Table 6A-1 for the range of structure heights examined.

FIGURE 6A-4 ..... /A-93

FIGURE 6A-4

SAMPLE PLOT FROM MONTE-CARLO SIMULATION STUDY (2000 FLASHES)

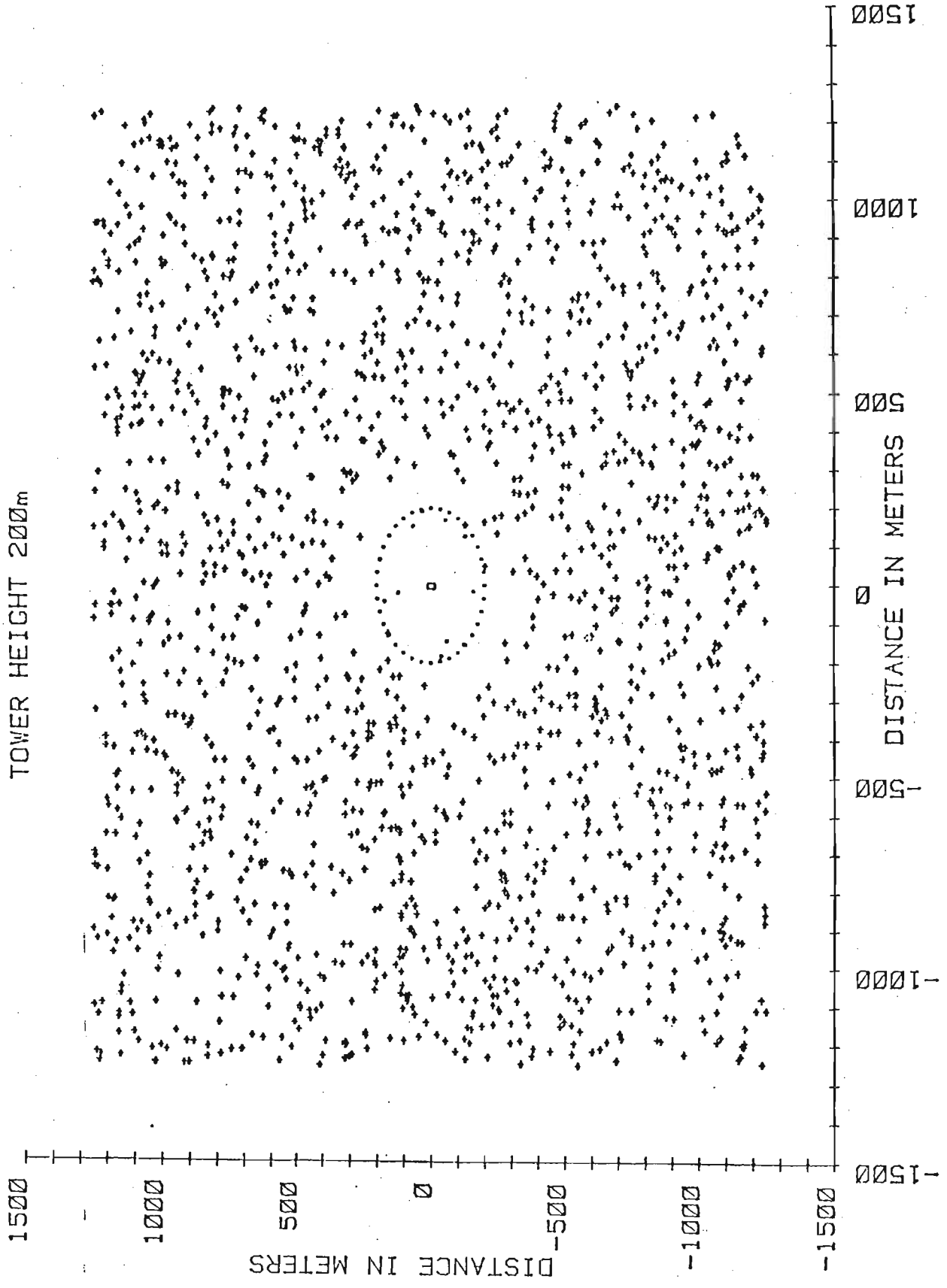

TABLE 6A-1: RESULTS OF MONTE CARLO STUDIES OF FLASHES TO TALL STRUCTURES

Tower height (m)	No. of flashes studied	No. of strikes to structure	SHIELDING FAILURES		
			Rate (per 10 000 flashes)	Maximum penetration I (kA)	Critical shielding angle (°)
20	82 118	213	-	-	-
50	20 422	211	-	-	-
100	11 520	311	1	7	35
200	5 498	382	20	15	31
300	2 394	301	29	16	30
400	3 014	501	96	21	27
500	2 112	501	180	22	21

(Note: The number of shielding failures have been normalised on the basis of 10 000 flashes within the area of interest. For an annual ground flash density of 1 $km^{-2}yr^{-1}$, the resultant base rate is equivalent to about one shielding failure per 2 000 years.)

In the cases of those structures that included shielding failures, the maximum currents I_M that penetrated the 45° cone of protection have been noted. In these instances also, the critical shielding angles θ_c have been determined from relating the closest distance of approach of these flashes to the tower d_c, to the corresponding tower height H (i.e. $\theta_c = \tan^{-1} d_c/H$).

The resultant variations in maximum penetration current I_M and critical shielding angle θ_c are shown graphically in Figure 6.3, together with a curve depicting a dramatic increase in the incidence of shielding failures as structure height increases.

In terms of the assumed ground flash density, the relative incidence of strikes to structures and the related dependency upon structure height - (as given in Table 6A-1) - leads to an estimation of the equivalent average attractive radius presented by the structure - in a manner similar to that applied elsewhere by the author in examining empirical data relating average flash incidence to structure height[16]. The resultant comparison between the empirically and numerically derived trends is given in Figure 6A-5, and a reasonable degree of agreement is apparent.

The ..... /A-95

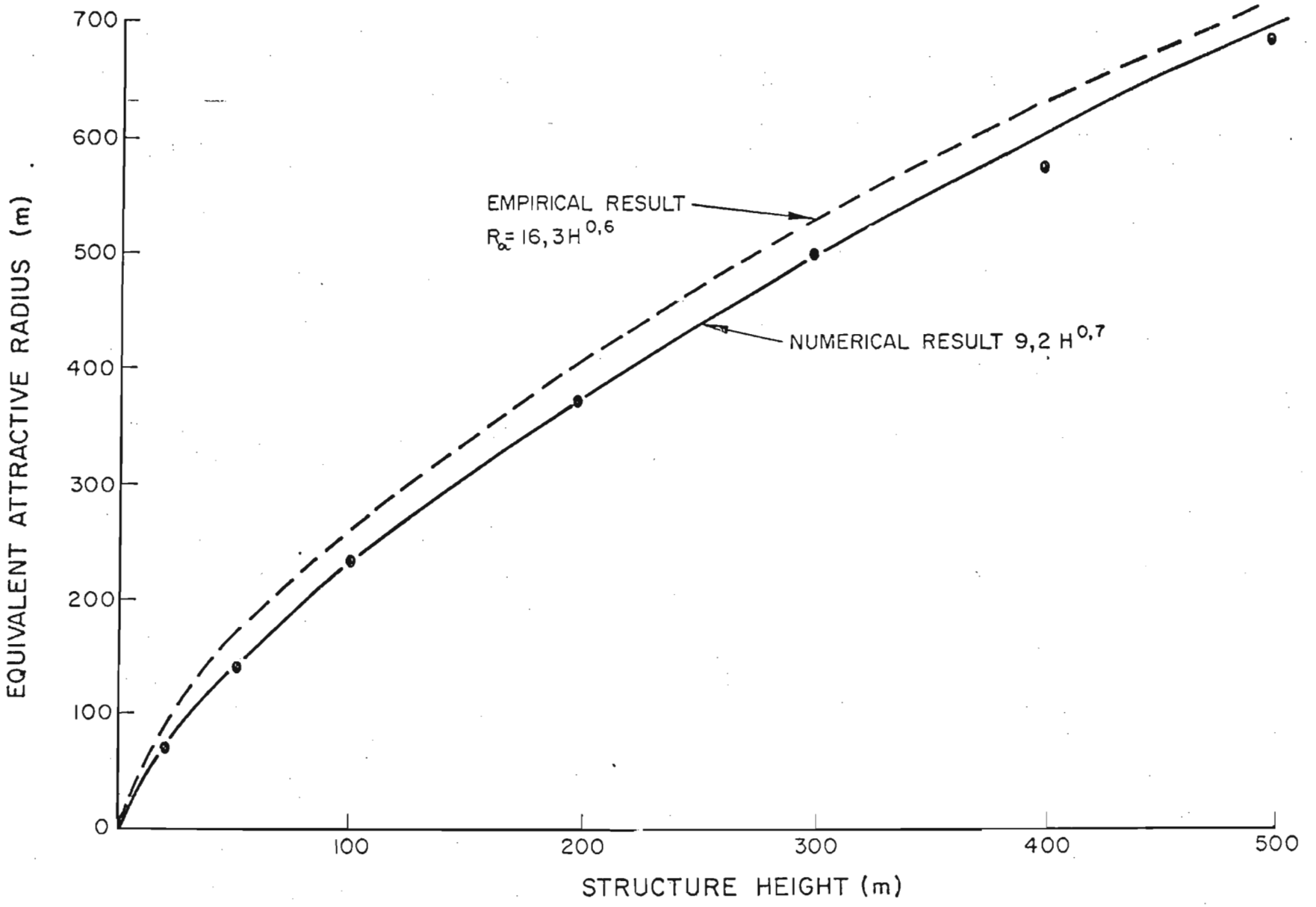

FIGURE 6A-5

COMPARISON BETWEEN EMPIRICAL AND NUMERICALLY DERIVED TRENDS IN STRUCTURE EQUIVALENT ATTRACTIVE RADIUS

The effect of structure height upon the distribution of peak current amplitudes

In the first section of this Appendix, attention was drawn to the considerable scatter evident in Berger's experimentally observed correlation between peak current amplitude I and impulse charge Q. Thus, although Berger's analysis indicates that this correlation may be expressed by the general relation;

$$I = kQ^{0,7}$$

where K has a mean value of about 10,6, the scatter in the data suggests that values for the factor K could lie in the range between about 1 and 20[14].

As a consequence, in examining the statistics of large samples (such as those of the Monte Carlo studies), while it is considered sufficiently accurate then to use the average correlation given by Berger's analysis, when studying individual flash by flash behaviour (such as the characteristics of individual strikes to structures) the author considers it necessary to take account of the wide scatter in this correlation.

Accordingly, in the course of the Monte Carlo simulations, a randomising routine was incorporated into that section of the program which analysed those flashes which were considered to strike the structure being studied. This routine randomly assigned values to the factor K in the correlation between charge and peak current. The source distribution from which these values were sampled was adjusted to cover the range of scatter present in Berger's data[14] and to yield average values of K in the range 10-11. This then provided the basis for the determination of the resultant peak currents discharged into a particular structure, on the occasion of each strike to that structure.

As previously noted, sufficient flashes were studied in the course of each simulation run to yield a meaningful sample of strikes to each structure - thereby allowing the evaluation of the associated cumulative frequency distributions of peak current amplitude. Having carried out these studies over a wide range of structure heights, it was thus possible to examine the effects of varying structure heights upon the resultant peak current amplitude distributions.

Examples of these distributions for three different structure heights are shown in Figure 6.4 - together with the CIGRE reference distribution. Approximating these numerically derived distributions by the log-normal form also allows an estimation of the relevant parameters of the distribution - as summarised in the table below:

TABLE 6A-2 ..... /A-97

TABLE 6A-2: EFFECTS OF STRUCTURE HEIGHT UPON THE DISTRIBUTION OF PEAK CURRENT AMPLITUDE

Structure height (m)	No. of flashes in sample	Log-normal approximation	
		Median (kA)	Standard deviation $\sigma_{\log I}$
20	213	30	0,83
50	211	34	0,62
100	311	33	0,68
200	382	33	0,64
300	301	33	0,73
400	501	34	0,69
500	501	34	0,68

For the sample sizes studied, the variations in these parameters are not statistically significant and these numerical analyses suggest therefore that structure height has no substantial effect upon the distribution of peak current amplitudes - subject to the assumptions of the original model.

APPENDIX 8A: LIGHTNING AND TALL STRUCTURES

As noted in the introductory review to this thesis (Chapter 1), the first results emerging from this research project were presented in a paper which was published by the author in June 1978. This paper also contained a general review of the incidence and characteristics of flashes to tall structures, and led to the expression of tentative conclusions regarding the influence of structure height upon the discharge process and upon certain flash parameters.

Much of the material contained in this paper is of direct relevance to the discussions of this thesis and in particular to the aspects examined in Chapters 4 and 6. This paper, and a further discussion thereof, were itemised as references (16) and (21) of the Bibliography. In view of their importance to the material of this thesis however, it was considered convenient to include these two references in this appendix - as set out below:

(a) "Lightning and tall structures"
Trans. SAIEE, Vol. 69, pp 238-252, 1978.

(b) Reply to discussion on "Lightning and tall structures"
Trans. SAIEE, Vol. 70, pp 121-125, 1979.

Research Paper No 4

Lightning and tall structures†

A J Eriksson* *Pr Eng, MSc (Eng) (Natal), MSAIEE*

SYNOPSIS

This paper reports upon a programme for the measurement of lightning currents and striking distances on a 60 m research mast. The programme has been in progress in South Africa for the past five years and the mast is situated in hilly terrain at an altitude of about 1 400 m.

Preliminary results suggest a median current amplitude of 41 kA for the first negative downward strokes. Measured striking distances have ranged from 50-250 m.

A review is made of data available from other regions of the world and it is concluded that the increasing incidence of upward flashes on tall structures with increasing structure height is largely responsible for the increased annual incidence of flashes to tall structures with increasing height. It is also concluded that the resultant current amplitude distributions for all flashes measured in tall structures should show a downward trend with increased structure height, due to the increasing contribution of upward flashes which statistically carry less current than downward flashes.

Contrary to present theories involving the use of electrogeometric modelling techniques, it is concluded that a tentative median value for the peak current amplitude of negative downward flashes to flat country is in the range of 40-50 kA and that this value shows little dependency with increasing structure height in the event of downward strikes to structures.

It is further suggested that present empirical relations between peak current amplitudes and striking distances may be erroneous and a new hypothesis involving a spatially diffuse leader in the striking mechanism is introduced.

SINOPSIS

Die referaat doen verslag oor 'n program vir die meet van weerligstrome en trefafstande op 'n 60 m-navorsingsmas, wat reeds die afgelope vyf jaar in Suid-Afrika plaasvind. Die mas is op 'n heuwelryke plek by 1 400 m bo seevlak opgerig. Voorlopige resultate dui op 'n gemiddelde stroomamplitude van 41 KA vir die eerste negatiewe afslae. Trefafstande het gewissel van 50 tot 250 m.

'n Oorsig word gegee oor gegewens wat uit ander wêreldstreke beskikbaar is en daaruit word afgelei dat die toenemende voorkoms van opwaartse blitse op hoë strukture met 'n toenemende strukturele hoogte grotendeels veroorsaak dat die voorkoms van blitse na strukture met 'n toenemende hoogte, jaarliks toeneem. Die gevolgtrekking word ook gemaak dat die gevolglike stroomamplitude verspreidings vir alle blitse wat in hoë strukture gemeet is, 'n afname behoort te toon namate die hoogte toeneem weens die toenemende aantal opwaartse blitse wat statisties minder stroom dra as afwaartse blitse.

In teenstelling met bestaande teorieë wat elektrogeometriesemodel-tegnieke benut, word daar tot die gevolgtrekking geraak dat 'n tentatiewe gemiddelde waarde vir die spitsstroomamplitude van negatiewe afblitse na plat plekke in die omgewing van 40-50 kA lê en dat dié waarde min beïnvloed word deur toenemende struktuurhoogte in die geval van afblitse na die strukture.

Daar word verder voorgestel dat bestaande empiriese verhoudings tussen spitsstroomamplitudes en trefafstande foutief mag wees en 'n hipotese wat 'n verspreide leier in die blitsmeganisme behels, word ingebring.

CONTENTS

†Paper first received December, 1977

†Presented at a meeting of the Institute in Johannesburg on 22nd June, 1978

*Power Electrical Engineering Division, National Electrical Engineering Research Institute, Council for Scientific and Industrial Research, Pretoria

1 Introduction

In many situations the most important question facing an electrical engineer concerned with lightning protection problems, whether these relate to power transmission and distribution systems, telecommunication installations or to buildings and structures, is an adequate knowledge of the engineering parameters of the lightning ground flash. The most important of these parameters (apart from the incidence of ground flashes in the area of concern), are the peak current amplitude (including its probability distribution) and the characteristics of the current waveshape, a knowledge of which is a fundamental requisite for the study of the electrical problems of lightning protection.

Over the past 80 years numerous workers have carried out measurements of lightning currents using a variety of techniques, some simple and others more sophisticated, and involving measurements on a variety of structures. Today, a considerable body of data has been accumulated, much of which has been obtained from magnetic links mounted on power transmission line towers or tall chimneys, and several cumulative frequency distributions of peak current amplitudes have been published (e.g., Lewis and Foust[1], Anderson and Jenner[2]).

The most comprehensive study of the current waveform characteristics of the lightning discharge is that carried out by Berger in Switzerland[3]. Over a 28-year period of measurement, he accumulated oscillographic recordings of current waveshapes during flashes to two towers (one 70 m and the other 80 m high), on top of Mount San Salvatore and situated some 650 m above Lake Lugano. The study embraced records of over 1 600 flashes, of which about 84 per cent were upward in

character, i.e., involved an upward leader breakdown process that progressed uninterruptedly from tower top towards the cloud.

In most electrical engineering situations, however, the ground flash of most practical concern is that involving a downward leader progression, as this type is most commonly encountered in comparatively flat terrain, or upon structures of moderate height, say less than 100 m. Berger's data have recently been subjected to detailed analysis[4] and the resultant cumulative frequency distribution curves for negative downward first and subsequent stroke peak current amplitudes are shown in Fig 1. The two distributions have median current amplitudes of 30 kA and 12 kA respectively.

Popolansky[5] has included 186 first stroke records (of both polarities) from Berger's data for downward first strokes, in a critical review of data available from measurements in some eight countries, (comprising a total of 618 current measurements), and has derived a resultant 'global' cumulative frequency distribution of current amplitudes. This distribution has a median amplitude of 28 kA, as shown in Fig 2, and is currently the most representative available for electrical engineering application.

In recent years several workers, including Ciano and Pierce[6], and Anderson[7], have indicated the possibility of regional variations in lightning parameters on a global scale, (apart from variations merely in lightning incidence), and attention has been drawn to differences between certain lightning parameters that have been measured in various parts of the world.

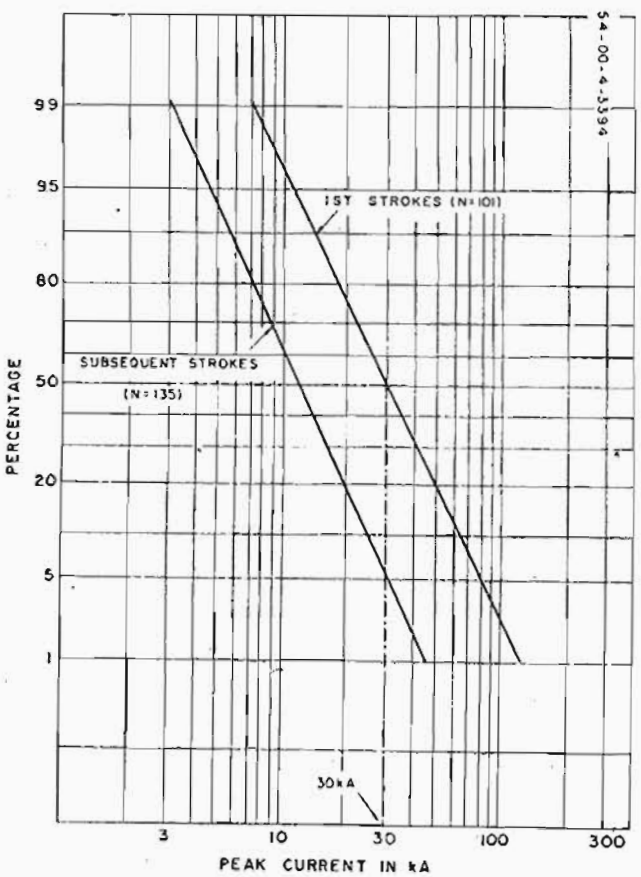

Fig 1 Cumulative frequency distribution of lightning current amplitudes for negative downward strokes — Berger.

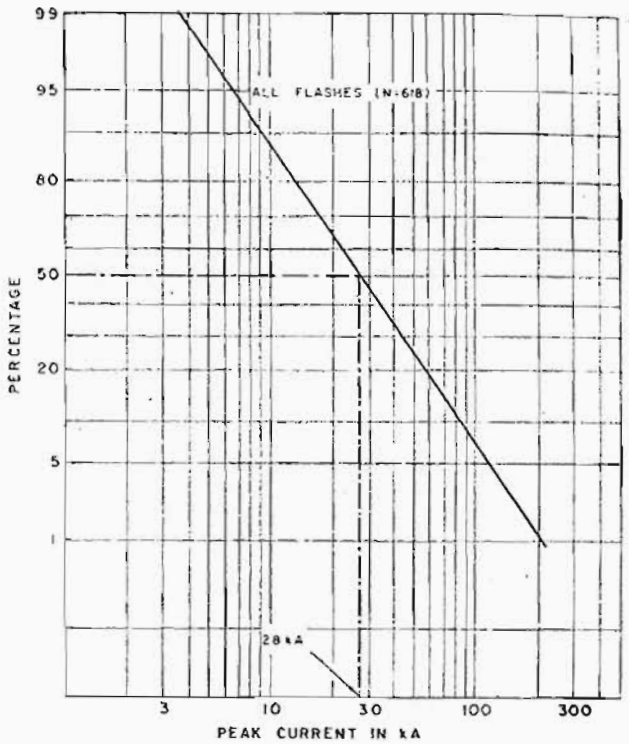

Fig 2 Combined cumulative frequency distribution of lightning current amplitudes — Popolansky.

At present, those aspects of South African electrical engineering practice which relate to lightning are based largely upon a knowledge of lightning parameters which has been accumulated from measurements in the more temperate northern regions of the world. In addition, the more densely industrialised and developed areas of South Africa tend to coincide with regions experiencing a high annual incidence of lightning.

Accordingly, in an attempt to characterise lightning parameters in these areas more rigorously, and also to determine to what extent lightning parameters locally differ from conditions measured elsewhere, the CSIR initiated a research programme in 1972 which is concerned primarily with the direct measurement of those parameters of the lightning discharge that are of prime importance to electrical engineers.

The purpose of this paper is to present the preliminary results emerging from this research programme and to examine these in relation to lightning observations in several other regions of the world.

2 The measurement of lightning parameters

At present the South African programme includes the following aspects:

(a) Direct measurement of the current waveform characteristics of strokes during flashes to structures — including current amplitudes, maximum rates of rise, polarity, charge transfer, etc.
This phase of the programme is also concerned with the development of indirect techniques for such measurements and includes a study of the features

of the high-speed electric field changes associated with ground flashes.

(b) A study of the striking process during discharges to structures and the influence of structures upon this process. An essential feature of this aspect is the study and measurement of lightning striking distances to structures and the relationship between striking distance and lightning peak current amplitude.

(c) A study of the incidence and characteristics of multiple-stroke ground flashes.

(d) A study of regional variations in thunderstorm electrical characteristics in various parts of South Africa.

The latter two sections of the programme are less directly related to lightning effects on tall structures, and as such will not be discussed further in this paper but have been reported on previously[8].

2.1 The research station

A central feature of the programme for recording lightning current waveforms is an automated station which, for logistic reasons, is situated on the CSIR campus, some 10 km east of Pretoria. This station comprises a 60 m tall mast and two adjacent huts that house the associated automatic power supply and instrumentation systems. The station is located upon a ridge about 80 m higher than the surrounding terrain, which is undulating in character and situated at an altitude of about 1 400 m above sea level.

The mast is built from triangular aluminium lattice section (having a side of 450 mm) and is comparatively unique in relation to lightning current measuring stations elsewhere in the world, in that the mast is raised upon insulators at the base and is supported by fully insulating stays (Fig 3). In the event of a lightning flash, this design has the double advantage that it confines the lightning current to the body of the mast itself and allows the current to be measured conveniently at the base of the mast during its passage across the insulated base section into the earth.

The situation of the mast and its height were chosen in an attempt to exert a moderate attractive influence upon nearby downward discharges, but it was hoped that this bias would not be so extreme that a high incidence of upward discharges would prevail — as has been the experience at similar stations such as those on Mount San Salvatore[3] or upon the Empire State Building[9], for example. The primary objective of the South African programme was that the data should be representative of, or applicable to practical electrical engineering situations — i.e. those involving the more common downward discharge, rather than the upward flash, the latter being a relatively 'unnatural' phenomenon principally encountered with very high structures such as television masts, or with structures situated upon mountain tops.

The Pretoria area experiences a mean annual keraunic level of about 70 thunderstorm days, and the average recorded annual ground flash density in this region is seven flashes per square kilometre. (The latter parameter has been determined over a nine-year period in the course

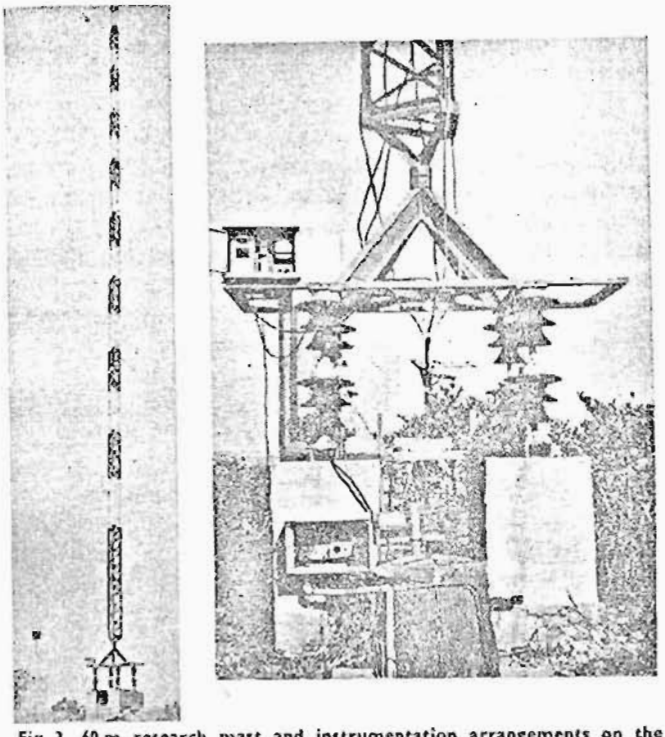

Fig 3 60 m research mast and instrumentation arrangements on the insulated base.

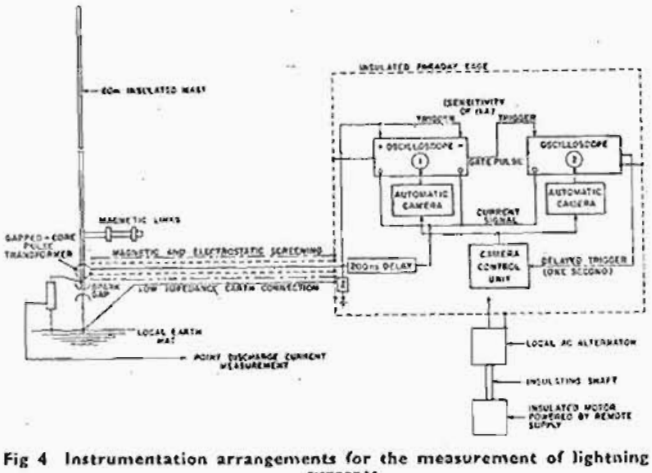

Fig 4 Instrumentation arrangements for the measurement of lightning currents.

of an associated CSIR project[10] which involves the development and use of lightning flash counters and lightning direction-finding techniques).

2.2 The measurement of lightning currents

All the instrumentation for this purpose is housed in one of the two huts at the automated station, and is interconnected in the manner shown schematically in Fig 4. The instrumentation hut is built as a fully insulated Faraday cage having only one connection to the site earth electrode via a low-impedance insulated copper strip.

The lightning currents entering the earth at the base of the mast are measured using a gapped core pulse transformer. This unit has a wide signal-frequency bandwidth extending from 1 Hz to 10 MHz (3 db points), and a sensitivity, when correctly terminated, of 1,25 V/kA. The output signals from this pulse transformer are routed

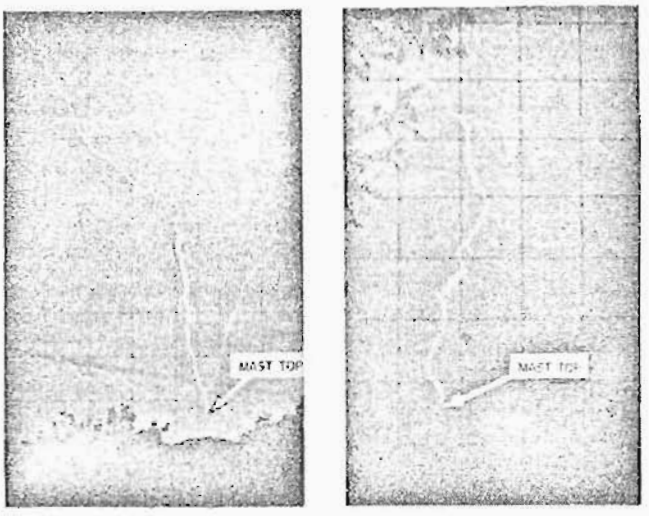

(a) Upward (Photographed from Camera 1) (b) Downward (Photographed from Camera 2)

Fig 5 Examples of upward and downward flashes recorded on the research mast.

through electrostatically and magnetically shielded cables to the recording instrumentation in the adjacent hut.

This instrumentation, which operates automatically, basically comprises a pair of high-speed oscilloscope and recording camera combinations, together with a controlling electronic trigger system. Magnetic links are mounted on the mast itself as a back-up measurement in the event of a complete instrumentation failure. In order to avoid power supply overvoltage surges, (which could arise due to transient differential potentials in the earth during the passage of lightning currents), the site power is supplied via an insulated motor-alternator set. In addition, the system includes a diesel generator set for standby power supply during outages. The station, with its associated instrumentation, is maintained in continuous automatic operation throughout the normal Transvaal summer thunderstorm season, which usually extends from September to April.

2.3 The measurement of lightning striking distances

This measurement is achieved photographically using two automatic framing cameras that are deployed approximately two and three kilometres respectively from the mast, and which view the mast from directions approximately at right angles to each other. These cameras, which incorporate graticules, or reference frames, in their fields of view, are run automatically during thunderstorms and record short-duration time exposures (typically of 15-60 s duration), of the terrain and general expanse of sky in the vicinity of the mast.

In the event of a flash to or from the mast, two-dimensional photographs of the discharge path are obtained simultaneously from the two cameras. These photographs are subsequently digitised and processed, using co-ordinate geometry and a specially developed computer program, to yield a set of three-dimensional co-ordinates defining the shape of the channel during the final stages of its progression in the vicinity of the mast. In the case of the more common downward flash, a study of this shape makes it possible to tentatively determine the striking distance. This has been defined[11] as that distance from the mast tip which has been reached by the downward progressing leader, at the instant when an upward interconnecting leader is initiated from the mast. It is assumed that at that instant the point of strike termination is determined. Implicit in this approach is the concept of an interconnection, or interception point between the upward and downward leaders, at a position remote from the mast tip. In analysing the geometries of those flashes photographed striking the mast, (although temporal resolution is absent), attempts are made to identify both the striking distance and this interconnection point from a study of the orientation of the discharge path.

An additional photographic system, which is also used for studying the striking process during flashes in the vicinity of the mast, employs a television camera, together with an automatic video tape recorder. The particular camera used incorporates a silicon-diode vidicon, which has the advantage that it is virtually burn-proof and allows an enhanced sensitivity. The video tape recorder may be played back frame by frame, which makes it possible to study in detail, for example, the temporal development of a multiple-stroke flash, subject to a frame resolution of 20 ms.

Both the framing cameras, as well as the closed-circuit television system, are controlled separately by an automatic radio switching unit, and are operated routinely during all thunderstorms in the vicinity of the mast.

3 Preliminary results

This research programme was initiated in 1972, the erection of the mast and research station being completed in September of that year. In November the top half of the mast collapsed during a severe storm owing to delamination of several of the original insulating supporting stays which were composed of an epoxy-bonded fibre-glass rod material. All stays were subsequently replaced by a nylon-based terylene fibre rope material (having an alkathene sheath for ultra-violet resistance), and the mast was recommissioned in May 1973. The recording station has been in continuous operation since that time, but owing to various operational problems, especially during the early development phase of the intrumentation techniques, several flashes have occurred during which no measurements were recorded.

A list of all the observed flashes is given in Table 1, while the salient features of these flashes are summarised in Table 2. A total of 25 flashes have occurred in the intervening five lightning seasons, giving a mean annual incidence of five flashes per year; (5,5 flashes per year, if expressed on a mast-month availability basis, to allow for the period of mast mechanical repair during the 1972/73 season).

Of these 25 flashes, 36 per cent occurred in the month of November, the monthly flash incidence for the remaining seven months of the season being about 9 per cent. Over the period of observation, station and instrumentation reliability has improved to the extent that the annual success rate in terms of measured flashes has increased from about 30 per cent in 1972/73 to over

Table 1
Summary of lightning flashes to the research mast

Date	Flash direction ↘	↘?	?	↗	↗?	Polarity	No. of strokes	Peak Current kA	Measurement (oscillographic and/or magnetic link)
1972-11-29	×					−	?	30	Mag
1972-11-29	×					−	?	?	—
1973-9-29			×			?	?	?	—
1973-9-29	×					?	?	?	—
1973-9-29			×			?	?	?	—
1973-10-15	×					?	?	?	—
1973-11-26				×		−	?	53	Mag
1973-11-26			×			−	?	?	—
1973-12-16	×					−	1	10	Mag + Osc
1974-1-4	×					−	3	36	Mag + Osc
1974-1-18		×				−	1	50	Osc
1974-1-18		×				−	3	58	Mag + Osc
1974-11-29			×			?	?	?	—
1974-11-29				×		?	?	?	—
1974-12-24	×					−	1	48	Mag + Osc
1974-12-25			×			?	?	?	—
1975-2-27	×					−	2	24	Mag
1975-11-2	×					−	1	20	Mag + Osc
1975-11-14				×		−	3	16	Mag + Osc
1976-2-7			×			−	1	>100	Mag + Osc
1976-9-28					×	?	1	<2	Mag
1977-2-22	×					−	3	87	Mag + Osc
1977-5-7					×	?	1	<1	Mag
1977-10-19	×					−	1	87	Mag + Osc
25 flashes	11	2	7	3	2				

Key
↘ — Downward-progressing leader
↘? — Suspected downward-progressing leader
? — Unknown direction of progression
↗ — Upward-progressing leader
↗? — Suspected upward-progressing leader

Table 2
Summarized features of the flashes recorded on the research mast

Total number of flashes recorded (1972-1977)	25
Mean number of flashes per year	5
Number of flashes on which current measurements were obtained	15
Total number of strokes recorded during the measured flashes	22
Incidence of observed downward flashes	52%
Incidence of observed upward flashes	20%
Observed ratio of downward/upward flashes	2,6:1
Observed incidence of negative flashes	60%
Observed incidence of positive flashes	0
Median current for first negative downward strokes	41 kA
Median current for all negative flashes	25 kA

95 per cent at the present.

From the available data, as indicated in Table 2, it would appear that the majority of flashes to the research mast have been of negative polarity and have progressed in the downward direction. This observation is encouraging since it suggests that one of the original objectives of the programme is being met — viz, that the influence of the mast as far as distortion, or intensification of the electrostatic field is concerned, is not so extreme as to result in a high incidence of the 'unnatural' upward flashes (as discussed in 2.1). The above results are, for example, in contrast to those obtained on Mount San Salvatore[3] where the incidence of upward flashes was about 84 per cent.

Figs 5(a) and (b) show examples of both downward and upward progressing flashes to the research mast, which were photographed with the framing camera system described in 2.3.

3.1 Results of lightning current measurements

As shown in Tables 1 and 2, current measurements to date have been made on a total of 15 flashes. An example of the resultant oscillograms is given in Fig 6 — in this case for a multiple-stroke flash.

Of the 15 measured flashes, 11 correspond to a downward direction of progression and the consequent cumulative frequency distribution of peak current amplitudes for negative first strokes is shown in Fig 7. Historically it has become common practice[4] to approximate such current amplitude distributions by the log-normal distribution. Consequently Fig 7 shows a regression line through the available data, the curve being based upon a log-normal fit together with 95 per cent confidence intervals. This distribution displays a median amplitude of 41 kA and a standard deviation $\sigma(\ell n\ I) = 0{,}71$ (where I = peak current amplitude). (For the available sample, the correlation coefficient for this regression is given by $r = 0{,}96$, which has significance at the 5 per cent level). These results suggest a 10 per cent probability of obtaining currents in excess of 123 kA.

By way of contrast reference may again be made to Figs 1 and 2 which show the cumulative distributions produced by Berger[4] for negative downward flashes, together with that obtained for all flashes by Popolansky[5]. These data indicate median and 10 per cent levels of incidence of 30 kA and 64 kA respectively in the case of Berger, and 28 kA and 82 kA respectively for Popolansky.

As illustrated by the confidence limits in Fig 7, however, the South African data at present comprise a small sample and thus may be considered as indicative of certain trends only.

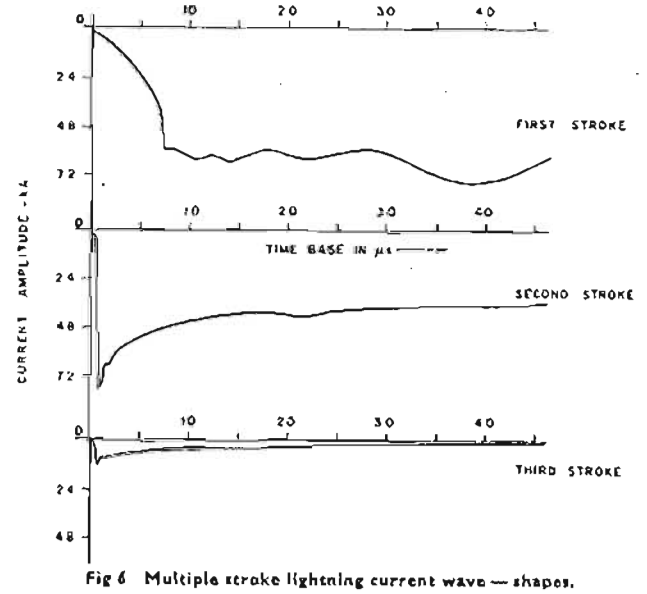

Fig 6 Multiple stroke lightning current wave — shapes.

For completeness it should also be noted that the median peak current amplitude for all negative flashes to the research mast (ie., including both upward and downward flashes) is 25 kA, (in contrast to the value of 41 kA obtained for downward flashes). At this stage it is considered that the samples of subsequent stroke and upward flash records are too small to permit separate analyses. Similar comments apply, at present, to the analysis of the waveform characteristics of the available records, i.e, in respect of such parameters as front duration, rate of rise, stroke charge, stroke duration, etc, although all such parameters are being determined from the data. It is interesting to note, however, that the oscillogram given in Fig 6 displays a maximum rate of rise of current on the wavefront of the second stroke, of about $1{,}8 \times 10^{11}$ A/s. As far as the writer is aware, this represents one of the severest records ever obtained. Berger's data[4], if extrapolated, suggests a probability of occurrence of about 1 per cent for such a rate of rise.

3.2 Results of measurements of striking distance

The dual camera system described in 2.3 was commissioned in October 1973 and operational problems were again experienced, especially in the early stages. Of the 20 flashes that have occurred since October 1973 13 have been successfully photographed from at least one direction, and four were photographed from both directions. Of the latter, three flashes were downward in character and were thus candidates for geometrical analysis of striking distance. (It may perhaps be noted that the main operational problems involve the loss of 220 V supply at one or the other, or occasionally both, of the two remote cameras during thunderstorms).

Figs 8(a) and (b) show an example of a recent flash which was photographed from both directions, together

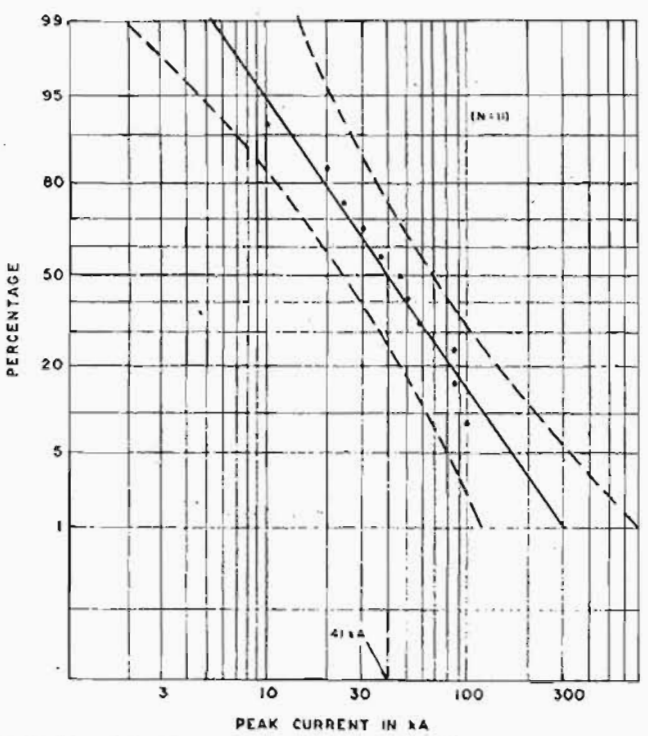

Fig 7 Cumulative frequency distribution of lightning current amplitudes for first negative downward strokes — research mast.

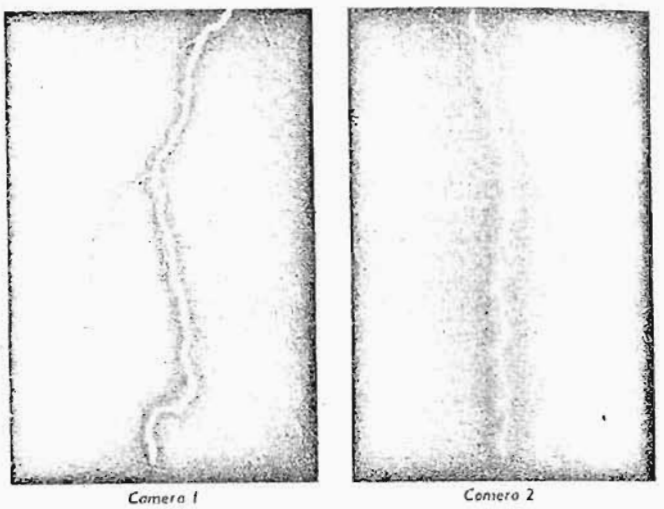

Fig 8(a) Downward flash to the research mast photographed from two directions.

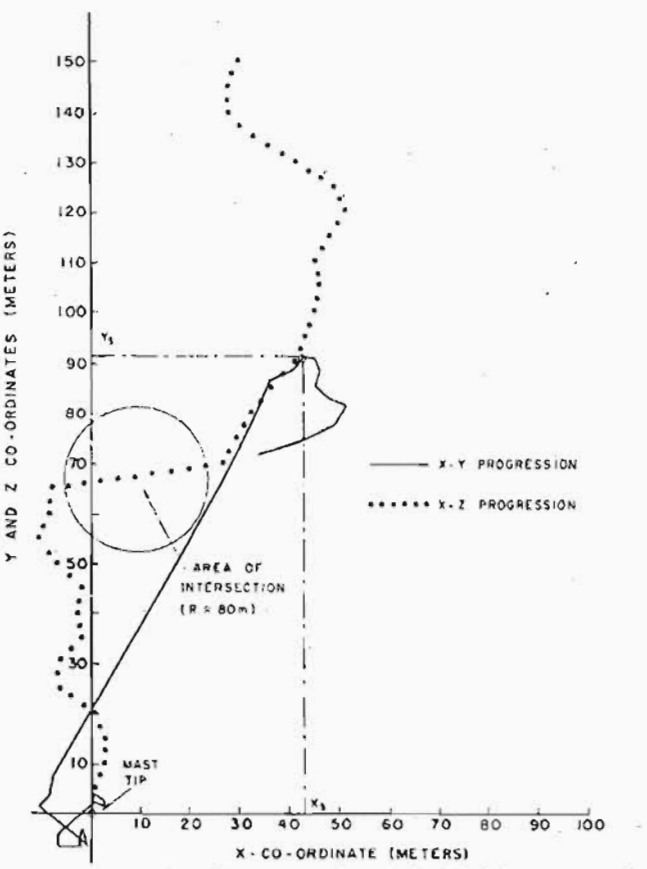

Fig 8(b) Reconstruction of flash progression (Flash-3) (Striking distance of 138 m).

with the resultant estimate of the striking distance as derived from the computerised analysis of flash geometry, while Fig 9 shows the relationship between the three available measurements of striking distance and the peak currents associated with the flashes involved. Following the experience gained in the three-dimensional studies, it was also possible to identify tentative interception points between the upward and downward leaders fairly readily, even in most of the two-dimensional photographs — in a manner similar to that adopted by Golde[12]. The resultant striking distance estimates must remain speculative, but are considered to be conservative.

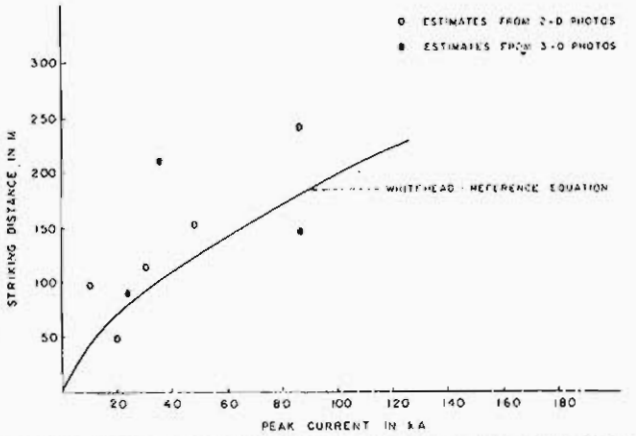

Fig 9 Relationship between striking distance and peak current amplitude as determined on the research mast.

Fig 9 therefore also includes five estimates which have been derived from geometrical study of unidirectional photographs.

4 Examination of data from other regions of the world

4.1 Introduction

In this section of the paper an attempt will be made to view the above preliminary South African data against a perspective of data available from various studies that have been carried out in other regions of the world. A further objective will be to consider general questions relating to lightning and tall structures — with particular regard to the possible influence of tall structures upon the amplitude distributions of lightning currents that may be observed in such structures.

As a general comment it may be noted in much of the discussion that follows that structure height has been adopted as a variable parameter for analysis. In fact the author considers this a gross (although largely unavoidable) simplification, since, as has been pointed out elsewhere[13], it is really the shape of the structure, or a dimensional relationship such as its 'slenderness ratio', that is the important consideration. In reality, the influence of a structure upon the lightning striking mechanism is determined by the degree to which the electrostatic field in the vicinity of a charged leader (or in extreme cases, the thundercloud field), is intensified by the presence of the structure. This in turn is a function of the shape of the structure rather than its height alone and, as has been shown in the case of tall masts or chimneys, the shape may be expressed in terms of the ratio between the height of the structure and its equivalent radius, H/R[13].

Previous measurement exercises elsewhere in the world have not taken the latter considerations into account and the writer has thus been forced to adopt height alone as a base parameter for comparative analysis. There may be some justification for this, since it is possible that most practical structures may have slenderness ratios (i.e., values for H/R), of somewhat similar orders of magnitude, simply for structural reasons.

In certain instances, however, such as structures situated on prominent mountains, the writer has found it necessary to introduce the concept of 'effective' height. For example, in the case of Berger's masts (70-80 m high) the resultant data in respect of flash incidence is totally inconsistent with that of structures of similar height. Clearly this is the consequence of the enhanced field intensification at the mast's top due to the shape and height of Mount San Salvatore. The latter, however, although 650 m above Lake Lugano, is electrically not equivalent to a tall 'thin' structure of similar height, and instead the adoption of an intermediate 'effective' height is considered reasonable. The data from this station suggest a height of about 300-400 m and accordingly, a value of 350 m has been assigned to this station. (A similar concept and magnitude has been used by Pierce[14].)

An additional problem encountered in attempting to draw comparisons amongst measurements made in various regions of the world lies in the fact that thunderstorm parameters and lightning incidence vary considerably throughout these regions. Accordingly, it is necessary to seek a common basis for comparison. Regional annual ground flash density would be the best parameter, but since this has not yet been accurately determined in many regions, a compromise is again inevitable. Not only because most of the available data are from the more temperate regions, but also in order to remain consistent with certain other studies[6], the writer has adopted a keraunic level of 30 thunderstorm days as the basis for linear normalisation of the relevant data.

It is recognised that the assumption of linearity between ground flash density and the annual keraunic level (although comparatively widely adopted[15]), may be erroneous.

In a preliminary survey of the results reported from 54 recording stations within the South African national lightning flash counter programme[10], the writer has obtained the tentative result:

$$N_g = 0{,}15(T_D)^{0{,}88} \text{ km}^{-2} \text{ yr}^{-1} \quad (1)$$

where N_g = annual ground flash density,
and T_D = annual number of thunderstorm days.

In the absence of further data therefore, the adoption of a linear basis for normalisation was considered a reasonable compromise.

4.2 The annual incidence of flashes to tall structures

The available data and source material are summarised in Table 3. These data correspond to a total of over 3 000 flashes in a sample of some 10 000 structure-years and include structures ranging in height from 22 m to over 540 m. The keraunic levels covered in the study range from 10 to almost 60 thunderstorm days.

In analysing these data structure heights have been grouped into intervals of 10 m increments and the mean flash incidence has been determined in each interval. The results are shown in Fig 10, together with a least-squares regression line which has been fitted to the data for structures more than 60 m tall. (The correlation coefficient for this regression, which is based upon 16 data pairs, is given as $r = 0{,}91$).

The equation of this line takes the form:

$$N_F = 1{,}48 \times 10^{-6} (H_s)^{2{,}8} \quad (2)$$

where N_F = annual number of flashes to a structure
H_s = height of structure in m.

4.3 The relative incidence of upward and downward flashes

The significance of the preceding observations becomes apparent when the relative incidence of upward flashes from tall structures is examined. In this regard, there are considerably less data published than those used in the analysis of flash incidence, but the available measured results are summarised in Table 4.

These data have been plotted in Fig 11, together with a least-squares regression line which takes the form:

$$P_u = 68{,}2\ \ell n\,(H_s) - 315{,}5 \quad (3)$$

Table 3
Incidence of flashes to tall structures

Source	Structure height in m	Regional keraunic level T_D (Note 1)	Annual frequency of recorded flashes, normalised to a T_D base of 30
Popolansky[17]	25	25	0,10
	35	,,	0,08
	45	,,	0,10
	55	,,	0,12
	65	,,	0,15
	75	,,	0,18
	85	,,	0,22
	95	,,	0,20
	115	,,	0,33
	540	,,	41,00
Müller Hillebrand[14]	28	10	0,16
	50	,,	0,18
	65	,,	0,35
	107	,,	0,38
	107	,,	2,24
	170	,,	2,24
	370	,,	25,6
Szpor et al[15]	24	22	0,02
	37	,,	0,04
	53	,,	0,03
	80	,,	0,18
	130	,,	0,40
	225	,,	2,13
Beck — as summarised in Clano and Pierce [4]	24	32	0,18
	31	,,	0,10
	31	,,	0,26
	60	,,	0,20
	60	,,	0,46
	70	,,	0,52
	90	,,	0,85
	105	,,	0,36
	110	,,	1,70
	170	,,	2,10
	340	,,	35,00
McCann[16]	400	31	23,00
Anderson and Jenner[3]	20	54	0,03
Berger[3] (negative flashes only)	350 (Note 2)	56	31,00

Note 1 In many instances, the values quoted for regional T_D are averages for many different structures distributed over one geographically similar area.
Note 2 A structure 'effective' height of 350 m has been assigned to this mountain-top station, as explained in 4.1.

where P_u is the relative percentage of upward flashes.

These data, and the associated analysis, suggest that structures having heights below 100 m will not normally experience upward flashes, while structures having heights greater than 450 m will virtually always display upward flashes. By way of comparison, a theoretical analysis by Horvath[16], is also included in Fig 11.

As noted earlier in 4.1 it is not strictly correct to generalise these observations in terms of structure height

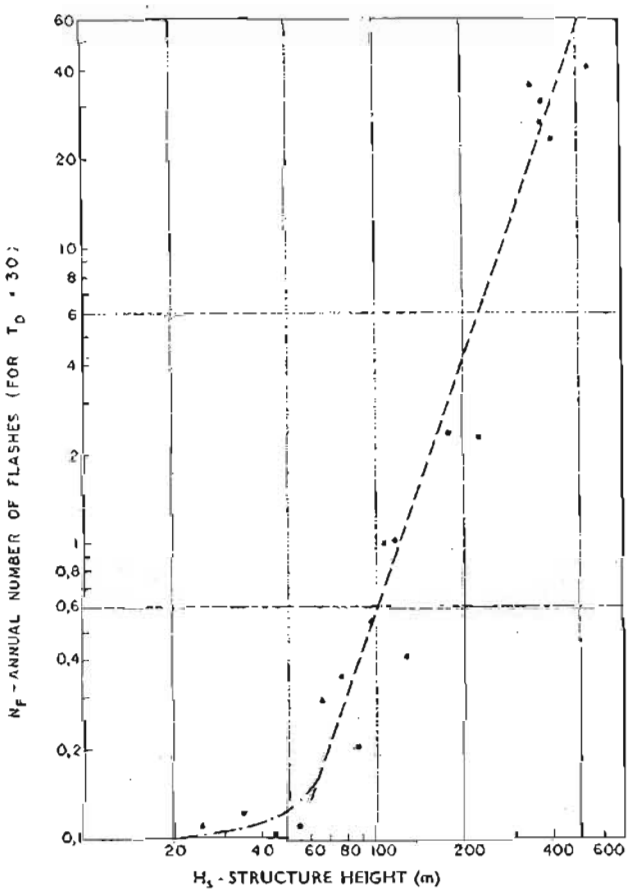

Fig 10 Relationship between structure height and the annual incidence of flashes.

Table 4
The relative incidence of upward flashes from tall structures

Source	Structure height in m	Relative frequency of occurrence of upward flashes
Pierce[14]	150	23%
	200	50%
	300	80%
	400	91%
McCann[16]	110	8%
	380	24%
	400	96%
Berger[3]	350 m*	84%
Gorin[21, 22]	540 m	92%**
Garbagnati[23]	500 m	98%

Notes *An effective height of 350 m has again been assigned to Berger's statistics. (See 4.1).
**50 per cent of the flashes recorded in this study were classified as 'unidentified'. The relative incidence of upward flashes is based upon analysis of only the identified data.

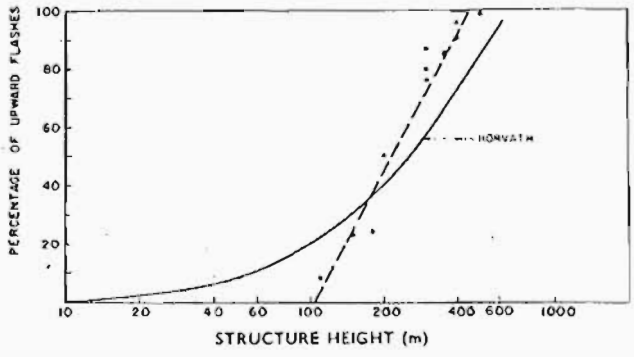

Fig 11 Relationship between structure height and the relative incidence of upward flashes.

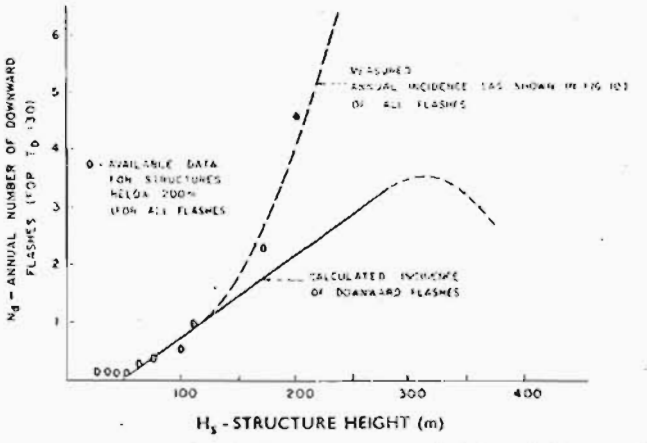

Fig 12 Derived relationship between structure height and the annual incidence of downward flashes.

alone, since it is the shape of the structure and the associated field intensification factor, which determine the relative probability that upward flashes will be initiated. This observation is borne out by the results from Berger's San Salvatore station, (84 per cent upward) which physically is situated some 650 m above the surrounding terrain (Lake Lugano). The data indicate, however, that electrically this mountain-top situation is equivalent to a tall 'thin' structure (such as those from which the remaining data are derived), having an effective height of about 350 m — thereby supporting the earlier adoption of this value.

The results presented in 4.2 may be used, together with the above analysis of the frequency of upward flashes, to estimate the relative contribution of downward flashes to the total annual incidence of flashes recorded in tal structures.

From equations (2) and (3), one may derive the expression:

$$N_D = aH_s^b \left\{1 - \left(\frac{a' + b' \ln H_s}{100}\right)\right\} \qquad (4)$$

where N_D = annual incidence of downward flashes to a tall structure in an area experiencing a keraunic level of 30 thunderstorm days, and a, b, a', b', are the corresponding constants from equations (2) and (3) respectively.

Substituting for structure heights in the range 50 to 400 m in equation (4), the resultant calculated curve relating structure height to the annual incidence of downward flashes is shown in Fig 12. This figure also includes the curve of equation (2), which shows the total incidence of all flashes to structures, as previously presented in 4.2.

Several points may be noted from the results of this analysis.

(a) The available data suggest that below about 50 m the annual flash incidence is comparatively insensitive to structure height. In general therefore, this would imply that the average attractive ranges of such structures do not vary significantly with structure heights below 50 m, but remain relatively constant.

The writer considers it probable, however, that this observation is merely an artefact of the data. The final stages of the discharge process in the vicinity of 'small' structures and the influence of the structures on the process, (i.e., the efficacy of shielding techniques), are complex, still requiring much clarification and additional data.

(b) In the range of structure heights between 50 m and about 300 m, the predicted annual incidence of downward flashes appears to be a linear function of structure height. In fact this function takes the form:

$$N_D = 1{,}42 \times 10^{-2} (H_s) - 0{,}68 \qquad (5)$$

over the range of heights concerned.

(c) This analysis also suggests that if the height of a structure is greater than about 350 m the number of downward flashes tends to decrease. Although this may be purely a fortuitous observation, reflecting the inadequacy of the data from which equations (2) and (3) were derived (as well as the use of height alone as a parameter), this could also imply that in such very tall structures the striking process is becoming modified (possibly as a consequence of space charge inhibition, for example), and the propensity of the structure towards intercepting downward leaders is subsequently reduced. One observation which may be in support of this hypothesis is the occasional termination of downward leaders on the flanks of very tall thin structures (such as the Ostankino[21] mast for example), which suggests some inhibitory mechanism at the tops of these structures.

Another factor, which may also contribute to the apparent decrease in downward flash incidence on very tall structures, is the possible depletion of charged areas of the cloud during upward flashes from these structures, thereby inhibiting the initiation of downward leaders. Even on those occasions when downward leaders have commenced within the cloud, it is possible that the additional field enhancement at a structure top may lead to the initiation of an upward leader from the structure, which in turn may subsequently intercept the downward leader, still within the cloud.

(d) There are insufficient data available to allow comparison of the predicted incidence of downward flashes with field data. As an example, however, equation (5) predicts an annual incidence of about 4,3 downward flashes on a 350 m tall structure. Over an

eighteen-year period of observation, the mean incidence of negative downward flashes observed by Berger (when normalised to a keraunic level of 30) is about 5,5 — which shows reasonable agreement.

4.4 Comparison with South African data

On the assumption that the majority of the unidentified flashes recorded at the South African lightning station were of the downward type, the data in Tables 1 and 2 indicate that the observed normalised annual flash incidence on the research mast is about 2,1 (normalised to a keraunic level of 30), and that the relative incidence of upward flashes is 20 per cent.

Substituting these values into the relations expressed by equations (2) and (3), leads to corresponding structure effective heights of 158 m and 138 m respectively, i.e., a mean height of 148 m.

It is considered not unreasonable to apply the concept of 'effective' height also in the case of the South African research mast, even though in this case this suggests a value in excess of the true structure height. This mast is unusually slender in relation to the majority of tall structures from which the available data are derived. The latter mostly involve tall chimneys or telecommunication masts, and for practical reasons their slenderness ratios (H/R) do not usually exceed 100, while the research mast has a slenderness ratio of 210. The work of Anderson et al[13] indicates that in a given uniform electrostatic field the intensification at a structure top will be enhanced by a factor 1,6, for an increase in slenderness ratio over the range 100 to 210. In addition, the research mast is situated upon a small hill some 80 m above the surrounding terrain, which would further enhance the field intensification at the structure top.

Accordingly, in the analysis below, a structure effective height of 148 m will be assigned to the South African research mast.

4.5 The effect of structure height upon current amplitude distributions

As in the preceding analysis, there appear to be scanty published data available relating the results of field measurements of lightning current peak amplitudes to structure height. In fact, many authors report current measurements in structures having a variety of heights, but combine these results in one general cumulative distribution (for example,[19]).

Popolansky[24], however, in an analysis of 209 current measurements in tall chimneys having various heights, has presented preliminary data, and his results, together with data from three other field measurement programmes, are summarised in Table 5. (These data include 14 measurements that have been recorded with magnetic links on 120 m tall radio masts in South Africa and which have been separately reported on by the author[8]).

These results, together with a least-squares regression line, are plotted on Fig 13 and suggest a decreasing trend with increasing height. For comparison, the South African research mast median of 25 kA for all negative flashes is also plotted — assuming an effective height of 148 m.

In the preceding sections, the relative incidence of

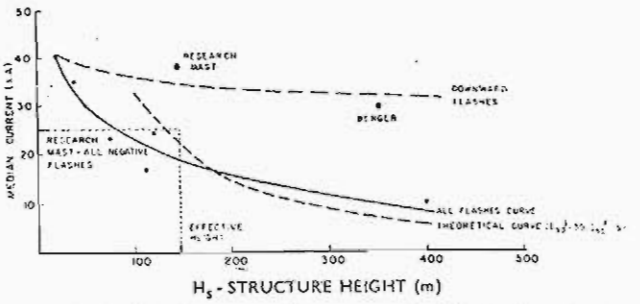

Fig 13 Relationships between median currents for all flashes, together with downward flashes only, as a function of structure height.

upward and downward flashes on tall structures has been discussed. It has been shown that the annual incidence of all flashes increases with increasing structure height and that this increase is largely the result of the increasing propensity toward upward flashes. Accordingly, in a set of current amplitude data, such as those presented in Table 5, which do not distinguish between upward and downward events, it would seem reasonable to assume that the resultant measured current amplitude distributions would include the contributions of both upward and downward flashes. On the basis of the previous analysis, it is suggested further that the relative 'mixing ratios' of downward and upward current amplitude distributions in turn would vary with increasing structure height, in accordance with the increasing incidence of upward flashes.

The theoretical curve shown in Fig 13 (which is included only as an example), illustrates this effect, being based upon the mixture of an upward flash distribution having an arbitrarily assigned median current of 5 kA, with a downward distribution having a median of 35 kA — the mixing ratio being determined by the data relating the incidence of upward flashes with increasing height — as previously presented in Fig 11 and equation (3). As might be expected from the respective median current amplitudes, this mixture leads to a downward trend in the resultant combined median current amplitude, with increasing structure height.

Unfortunately, published data regarding the peak current amplitude distributions of downward and upward flashes separately are very sparse, since the majority of field measurements have involved the use of magnetic links. The available data for downward negative flashes, which comprise only Berger's measurements and the preliminary results from the South African research mast, are also plotted in Fig 13, together with a line indicating a suggested trend. (The latter is, of course, only speculative.)

The only comprehensive analysis of the parameters of upward flashes is that recently prepared by Berger[25]. In the case of first upward strokes for negative flashes, he obtained a median current of only 250 A. Of prime importance here, however, is the threshold level of measurement, which in Berger's field stations was less than 40 A. Golde[26] has pointed out that over 50 per cent of negative flashes initiated by upward leaders involve only continuous-current discharges, which are not followed by high-current impulses, and the peak current amplitudes of which do not usually exceed several hundred amperes. (By way of contrast, Garbagnati's

Table 5
Current amplitude distribution as a function of structure height

Source	Structure height in m	Median current amplitude in kA, for all negative flashes
Popolansky[24]	22-55	34,6
	55-65	29,7
	65-85	22,9
	85-140	16,3
Anderson[1]	20	40,0
Hagenguth et al[7]	400	10,0
Eriksson[8]	120	24,3

data[23] from mountain-top measurements in Italy indicate that for first strokes of negative upward flashes the median current amplitude is 25 kA. However, the threshold level for measurement was 3 kA and Berger's data suggest that 96 per cent of all upward flashes would in fact be excluded from the Italian sample.)

In similar vein, the majority of magnetic link field measurements of lightning current amplitudes involve threshold levels in the range of 1 to 2 kA and as a consequence, the resultant combined distributions of upward and downward flashes would include drastically truncated distributions as far as the upward current contributions are concerned. It is expected, however, that owing to the increasing contribution of upward flashes in the total sample, the resultant trend would remain the same: i.e., a decrease in median current (for all flashes) with increasing structure height.

Several concluding points arising out of the preceding analysis may be noted, (which will be further discussed in section 5):

(a) The data sample presented in Table 5 is small and, as Golde has pointed out[26], may not be considered adequate. However, the resultant trend toward a decrease in median current for all flashes with increasing height, (as shown in Fig 13), is at least consistent with the concept of a mixture of downward and upward flashes having individually high and low median-current amplitudes respectively, and involving a mixing ratio which is determined by the relative incidence of upward flashes.

(The previous remarks notwithstanding, it is recognised that the trend in Popolansky's data in particular[23] (as presented in Table 5), is not fully consistent with the observation expressed in Section 4.3, that structures having heights below about 100 m will not normally experience upward flashes. This conclusion may be a reflection upon the data, but could equally reflect the inadequacy of adopting structure height alone as a parameter for comparative analysis.)

(b) The available data with regard to downward negative flashes alone, indicate median-current amplitudes of the order of 30 to 40 kA for structure heights in the range 150 to 350 m. This result may be compared with a median value of 40 kA for all flashes measured in a structure height of 20 m[7] (for which it may be assumed that the contribution of upward flashes was negligible). This suggests little height dependency as far as negative downward flashes are concerned. (It should perhaps again be emphasised that the preceding analyses of Sections 4.2 and 4.3 preclude the assignment of a structure height of only 70 m to Berger's San Salvatore field station).

(c) The data and the trends depicted are wholly inconsistent with predictions of current amplitude distributions based upon the application of electrogeometric modelling techniques of analysis — such as those of Sargent[27], which suggest an increase in median-current amplitudes with increasing structure height and a median-current amplitude to flat ground of about 15 kA.

5 Discussion

5.1 Regional variations in lightning parameters

As mentioned in the Introduction, one of the principal objectives of the South African research programme is to determine to what extent the engineering parameters of the lightning discharge, as measured locally, differ from those measured in the more temperate regions of the world, the most important parameter for consideration being that of current amplitude. However, as the preceding analysis in Section 4 has shown, the incidence and character of lightning flashes is influenced to a considerable degree by the dimensions of the structure upon which lightning measurements are recorded. Therefore these influences must be clarified and fully accounted for before any regional comparisons may be attempted; alternatively, the results of measurements from structures displaying comparable geometries only, may be compared.

At this stage, on the above basis, it is considered that there are insufficient adequately resolved data available from other regions of the world to permit effective regional comparisons with the South African measurements. For example, the fact that the local median current of 41 kA for first negative downward strokes is higher than Popolansky's global median of 28 kA, may be interpreted as a tendency toward more intense discharges locally. This conclusion is considered unjustified, however, since Popolansky's data, being based upon a large variety of structures displaying a wide range of heights (and gathered using several different measurement techniques and various threshold levels) will inevitably include both upward and downward flashes, (as well as measured currents of both polarities), and their relative contribution to these data is unknown.

Somewhat more significance may possibly be ascribed to the observed differences between the South African and Swiss field stations in respect of median currents for first negative downward strokes (41 kA and 30 kA respectively). Again, however, due to the differences in the effective heights of the structures and in the absence of any further understanding of the influence of structure height (or preferably dimensions) upon these current distributions, it is felt that no significant interpretations may be attributed to these differences. In addition, although the South African preliminary median of 41 kA for first negative downward strokes shows good agree-

ment with the Rhodesian median of 40 kA[7] (all flash data, of which 94 per cent were negative), the South African sample of data is still too small, as evidenced by the 95 per cent confidence limits shown in Fig 7, to allow meaningful comparisons to be made.

It must be concluded therefore that considerably more data of an adequately resolved character must be obtained, both locally and in other regions of the world, before any significant conclusions may be drawn as to regional variations in lightning peak current amplitudes.

5.2 The distribution of peak current amplitudes during strokes to the ground

Several authors have derived predicted reference peak current amplitude distributions of lightning strokes to flat ground from an analysis of measured distributions in structures of specific height. These reference distributions then form the basis for design and performance studies (usually involving Monte Carlo techniques of analysis) upon various transmission line geometries. Contemporary values for the median amplitudes of these reference current distributions lie in the range 13 to 18 kA[27], [28], [29].

However, as already noted in 4.5, the available data in respect of measured peak current amplitude distributions totally contradict these predictions, and if extrapolated from structures having heights of only 20 m to level ground, suggest a median value in the range 40 to 45 kA for first downward strokes.

The only data available regarding values of lightning current during strikes to flat country are those presented by Uman[30], which are derived from measurements of electric field waveforms and the subsequent interpretation of these in terms of a transmission line return stroke model. Two sets of data are reported: the first set is based upon an analysis of 98 strokes in 21 flashes within a distance of 10 km, and a median current of 37 kA is obtained. (The reported limits to this value, in terms of the ranges of return stroke velocities, are 30 to 50 kA). The second set of data is derived from an analysis of 63 strokes in 18 more distant flashes, and a median current of 12 kA is obtained. (The latter determination involves an assumed value of return stroke velocity which, as Uman points out, could be subject to considerable error). It should be noted also that this analysis covers all strokes within a flash and consequently it may be expected that the resultant distributions will display lower currents than would be obtained if first strokes only were considered.

Accordingly, it would appear that these data are also not in support of a low median current for strikes to flat country and it must be concluded therefore, in the absence of further data, that there is little justification for the use of reference current amplitude distributions having median values as low as those currently being adopted. In fact, a value of the order of 40 kA for first downward strokes would appear to be indicated.

5.3 Implications in relation to electrogeometric models and to striking distance considerations

Geometrical studies of the problems of lightning protection have dated from Franklin's original work — as reviewed recently by Golde[31]. The electrogeometric technique of analysis[32] has developed into a powerful medium for theoretical study of the performance of transmission line designs, and is now widely adopted.

As pointed out in 4.5, however, predictions of current amplitude distributions based upon the application of electrogeometrical modelling techniques are not supported by the available data relating structure height and peak current amplitudes.

An assumption which is fundamental to the electrogeometric technique of analysis is that of a functional relationship between the prospective stroke peak current amplitude and the associated striking distance, during a flash to a particular structure. Such relationships normally take the form[31]:

$$R_s = \mathrm{k}(I)^{\mathrm{b}} \tag{6}$$

where R_s = striking distance
I = peak current amplitude
k, b are empirical constants, usually derived from a study of the performance of existing transmission line designs.

A basic weakness in the application of this form of relationship in many engineering studies is the absence of any allowance for the influence of the structure itself upon the striking process and upon the consequent striking distances. Anderson et al[13] have pointed out that the striking process is dependent upon the structure-dimensional relationships.

More recently, Whitehead[33] has recognised this and has introduced a modified form of functional relationship:

$$R_s^* = R_s\{1 + E_i I_F^2 \exp(-R_s/\mathrm{H})\} \tag{7}$$

where R_s^* = modified striking distance to a structure of height H;
E_i = field intensification factor which takes into account the structure slenderness ratio;
I_F = factor which relates the prospective stroke current to the median of a reference current amplitude distribution.

R_s in this case is a reference striking distance to the ground and is given by $R_s = 10.\mathrm{I}^{0,65}$ (8)

It is considered that the above expression is a considerable improvement upon equation (6). However, in contradiction of the data in 4.5, an inescapable consequence of the application of this concept in an electrogeometrical modelling approach is that there still should be a tendency toward recording higher peak current amplitudes in structures of increasing height.

In physical terms, a relationship between striking distance and leader charge would be preferred, since, as has been shown elsewhere[13], it is the magnitude of the charge on the leader (and the distribution of this charge), together with the field intensification in the vicinity of a structure, which determines the distance over which the final stages of the lightning breakdown process take place. The adoption of a relation between striking distance and

peak current is more convenient for engineering purposes and relies upon the observation from Berger's data[4] that there is a good correlation between peak current and impulse charge.

At this stage, reference should again be made to the tentative results of the measurement of striking distance to the research mast — as presented in Section 3.2 and Fig 9. If all the data points are considered, a trend of increasing striking distance with increasing current is suggested. However, if only those three points which were obtained from full three-dimensional analyses are examined, considerable scatter is evident.

By way of comparison, the curve for Whitehead's reference striking distance to ground[33] is also included in Fig 9 (equation (8)) and, if the data measured on the research mast may be considered to be meaningful, this comparison would suggest that the influence of the mast upon the striking distance is less pronounced than consideration of the mast electrostatic field intensification factor would have indicated.

It is recognised that the measurement technique adopted for the photographic estimation of striking distances is subject to several possible major errors. For example, as Golde has recently pointed out[31], the influence of downwind plumes of space charge (not in the sense of downward leader diversion, but purely as a fortuitous interceptor providing a high conductivity return path to the mast) is impossible to take into account. In most instances, however, when examining the geometry of flashes to the mast it has been possible to distinguish the path of the upward leader (usually vertically oriented initially), an interconnecting element, and a point of leader interception, or persistent progression toward an interception point. (It is considered that the geometry displayed in Figs 8(a) and (b) is a good example of this process).

In considering these tentative results, as well as the previous data relating structure height and the median values of the peak current amplitude distributions, the postulate may be introduced that the assumption of a strong functional relationship between striking distance and peak current (or more accurately, impulse charge), may in fact be erroneous. (Such a conclusion would be necessary to account for the absence of a trend toward increasing current amplitudes in structures of increasing height).

In fact, the writer considers it possible that the present common practice of simulating the leader as a single geometrical element bearing all the prospective impulse charge (distributed according to some functional relationship with leader length), may be an oversimplification of the physical situation. (Such a representation will always lead logically to a functional relationship between striking distance and peak current).

In practice, as shown in time-resolved photography and as frequently observed in the writer's video recordings, the downward leader comprises both a macro- and micro-structure of fine branches — usually all of comparatively similar luminosity. On the macro-scale, these are distributed spatially over quite large volumes of the space between cloud and ground (dimensions being in the range 100 m to 5 km). A similar spatial distribution

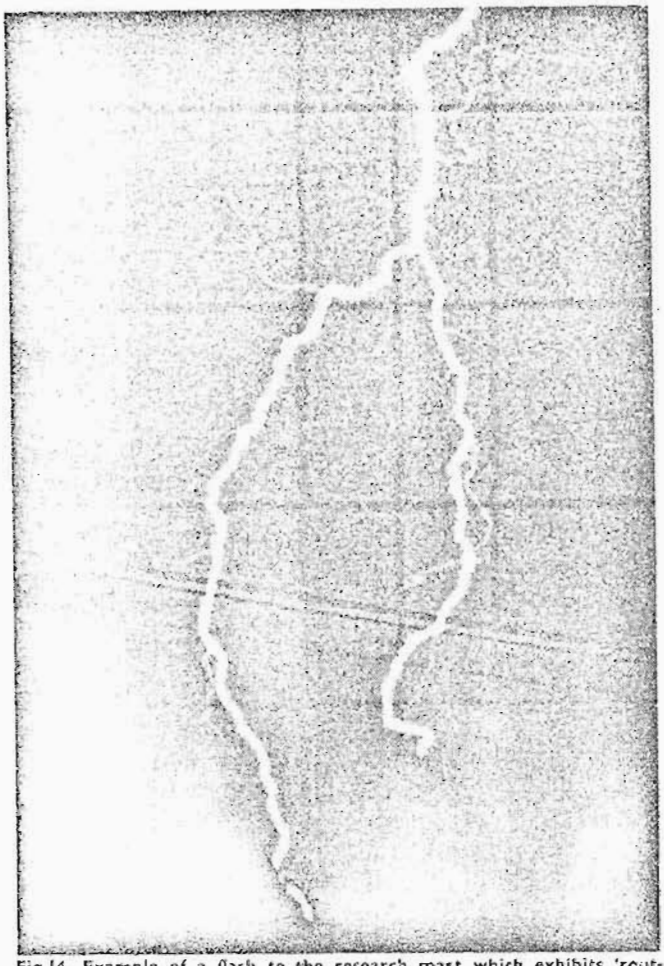

Fig 14 Example of a flash to the research mast which exhibits 'root-branching'.

has been reported by Proctor from VHF spherics recordings[34]. It is considered possible therefore that the total leader charge is spatially distributed in a rather diffuse fashion and that the final point of strike termination is more dependent upon the approach of one leader branch (or group of branches) to a structure. It is therefore suggested that on the micro-scale, in the vicinity of a structure, the striking process still involves the interception of downward and upward leaders, but that the local electrostatic fields in the immediate vicinity are dominated by the magnitude and distribution of charges in these nearby elements of the leader, rather than by the total charges being lowered. The hypothesis of such a mechanism is supported by the occurrence of simultaneous root-branched flashes, which have been observed by several authors, and an example of which is shown in Fig 14[35].

On the above basis therefore, it is suggested that there may well still be a functional relationship between striking distance and the integral effect of those elements of leader charge which enter the immediate proximity of a structure. There should thus also be an influence of the structure upon this striking process, owing to the enhancement of the local field caused by the structure. However, it may well be incorrect to assume a similar functional relationship in terms of the peak current, since this is more dependent upon the total macro-charge lowered by the complete leader structure, than upon

those micro-charges whose local spatial distribution determines the point of strike.

In consequence therefore, such a hypothesis precludes the assumption of a functional relationship between striking distance and prospective peak current. In turn, application of the concept in an electrogeometric modelling approach would lead to a lack of dependency of any predicted current amplitude distributions upon structure height. This tentative conclusion is thus in support of the observations expressed in 4.5.

5.4 Aspects related to lightning protection

In Section 4.3, an expression was derived which related the anticipated annual incidence of downward strikes to the height of the structure concerned (over a height range 50 to 300 m), viz: (equation (5));

$$N_D = 1{,}42 \times 10^{-2} (H_s) - 0{,}68.$$

In many engineering applications and lightning-protective installations it is common practice to assume a mean annual equivalent 'collection area' A, for the structure involved. This implies that the annual incidence of downward flashes intercepted by the structure may be given by:

$$N_D = A\, N_g \tag{9}$$

where N_g = annual ground flash density in the region of interest.

The data presented in 4.3 were based upon a mean annual keraunic level of 30 thunderstorm days and it is necessary therefore to relate this level to an equivalent ground flash density.

This question was previously examined in 4.1, where a linear relationship was assumed and the writer reported a tentative result for South African data: (Equation (1)).

$$N_g = 0{,}15\,(T_D)^{0{,}88} \text{km}^{-2}\ \text{yr}^{-1}$$

where T_D = annual number of thunderstorm days.

This indicates a value for $N_g = 3{,}0\ \text{km}^{-2}\ \text{yr}^{-1}$ for a keraunic level of 30.

Applying this value to equations (5) and (9), the structure equivalent collective area A may be expressed as:

$$A = 4{,}73 \times 10^{-3} (H_s) - 2{,}3 \times 10^{-5}\ \text{m}^2 \tag{10}$$

In this regard, the concept of an equivalent mean protective radius R may also be introduced, ie.

$$A = \pi R^2 \tag{11}$$

after substitution into equation (10); R may be expressed as:

$$R = 39\,(H_s - 48)^{\frac{1}{2}} \tag{12}$$

(for $50 < H_s < 300$)

For $20 < H_s < 50$, it was found in 4.3 that the annual incidence of downward flashes was virtually independent of structure height and was approximately 0,1 flashes per year. Thus, from equation (11), for an annual ground flash density of $3{,}0\ \text{km}^{-2}\ \text{yr}^{-1}$, this implies a minimum equivalent protective radius for structures having heights in this range:

$$R_{min} = 103\ \text{m} \tag{13}$$

Expressions (12) and (13) for mean protective radius may be combined and the results are shown in Fig 15 as a function of structure height.

For comparison, this figure also shows the equivalent protection afforded by the commonly adopted concept of a 45° cone of shielding, as well as Golde's proposal that $R \simeq 2H$[36]. The latter in particular shows reasonable agreement with the empirical results up to structure heights of about 300 m.

It should be emphasised that the above empirical approach is based upon data describing the mean annual incidence of flashes to tall structures. As such, any dependency of striking distance upon leader charge variations is not taken into account. As an example, Fig 15 also depicts the range of striking distances estimated from the research mast records, for a structure effective height of 148 m.

It should also be noted that the data in Fig 12 (upon which this analysis is based) indicate a decreasing trend in flash incidence above structure heights of about 300 m. This would imply a similar decrease in protective radius, as has been depicted in Fig 15.

As a general comment, although the adoption of height as a parameter for analysis is considered inadequate, the above discussion and empirical results do suggest that the concept of a 45° cone of protection is acceptable as far as the shielding afforded by isolated tall structures is concerned — subject only to the possible short range effects of weakly charged leaders.

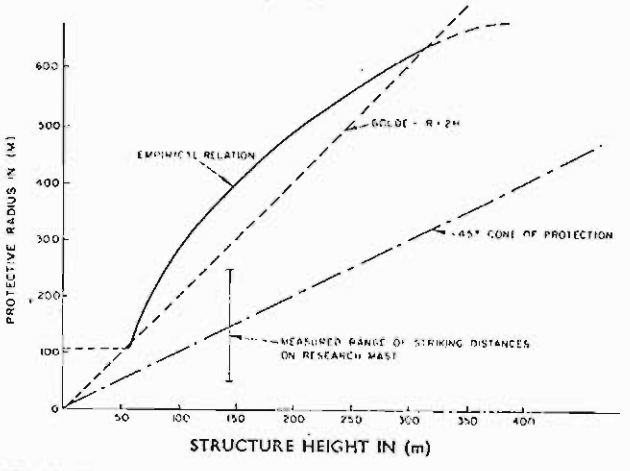

Fig 15 Relationship between protective radius and structure height.

6 Summarising remarks and conclusion

This paper has reported briefly upon the central features of a South African lightning parameter research programme and, following five years of observation, preliminary data have been presented in respect of peak

current amplitudes and striking distances. (Figs 7 and 9 respectively).

The South African data have been examined in relation to results available from similar measurement programmes elsewhere in the world and several important observations may be noted.

In particular, attention has been drawn to the influence of structure dimensions upon the striking process and the consequent relationship between the incidence of lightning flashes and height of structure. The importance of upward-progressing flashes has also been emphasised and it is noted that these contribute largely to the increasing incidence of flashes as structure height is increased (Fig 12).

Although data are very sparse, it would appear that the distribution of the current amplitudes of the first strokes of negative downward-progressing flashes is largely independent of the height of the structure, and, contrary to present theoretical approaches, that the adoption of a median value of the order of 40 to 45 kA for flashes to flat country is indicated.

It is pointed out that the increasing contribution of upward flashes to the total incidence of flashes in tall structures should lead to a decrease in measured current amplitudes (for all flashes), with increasing structure height, and it is observed that preliminary data are in support of this trend (Fig 13).

It is also suggested that the available data, although very limited, are not at all in support of several fundamental aspects of the electrogeometric concept, including in particular, the common assumption of a relationship between striking distance and prospective peak current, and a tentative physical mechanism involving a spatially diffuse leader is postulated in explanation of this observation.

Clearly, however, it is recognised that much of the preceding discussion is based upon an inadequate sample of data and that in terms of the observed trends, the resultant conclusions must needs be only speculative.

It is apparent that there is an unfortunate dearth of adequately resolved lightning current data, both in respect of flash direction and polarity, as well as in terms of structure dimensions, and in view of the important questions that have been raised in this preliminary analysis it is essential that further data should be gathered both locally and globally.

Acknowledgements

The author wishes to record his appreciation to the Council for Scientific and Industrial Research and to the Director of the National Electrical Engineering Research Institute for the opportunity and permission to publish this paper. He also wishes to express his gratitude to the reviewers for helpful comments and constructive criticism.

7 References

1 LEWIS, M V, and FOUST, C M: 'Lightning investigations on transmission lines, VII'. *AIEE Trans Vol 59, No 4*, p 227, April 1940.
2 ANDERSON, R B, and JENNER, R D: 'A summary of eight years of lightning investigation in Southern Rhodesia'. *Trans SAIEE*, p 215-294, July-September 1954.
3 BERGER, K: 'Messungen und Resultate der Blitzforschung auf dem Monte San Salvatore bei Lugano, der Jahre 1963-1971.' *Bull SEV, Vol 63, No 24*, p 1403-1422, November 1972.
4 BERGER, K, ANDERSON, R B, and KRÖNINGER, H: 'Parameters of lightning flashes'. *Electra No 41*, p 23-27, July 1975.
5 POPOLANSKY, F: 'Frequency distribution of amplitudes of lightning currents', *Electra No 22*, p 139-147, May 1972.
6 CIANO, N, and PIERCE, E T: 'A ground-lightning environment for engineering usage', *Stanford Research Institute Tech Report 1*, August 1972.
7 ANDERSON, R B: 'A comparison between some lightning parameters measured in Switzerland with those in Southern Africa', *CSIR Special Report ELEK 6*, May 1971.
8 ERIKSSON, A J: 'The measurement of lightning and thunderstorm parameters — results for the 1976/77 season'. *CSIR Special Report ELEK 124*, June 1977.
9 HAGENGUTH, J H, and ANDERSON, J G: 'Lightning to the Empire State Building Part 3'. *AIEE Trans Vol 71*, pp 641-649, 1952.
10 ANDERSON, R B, VAN NIEKERK, H R, and MEAL D V: Ninth progress report on the development and testing of lightning flash counters in the Republic of South Africa during 1977. *CSIR Special Report ELEK 122*, May 1977.
11 ERIKSSON, A J: 'The striking distance of a lightning flash'. *CSIR Special Report ELEK 46*, June 1974.
12 GOLDE, R H: 'Lightning protection' (Edward Arnold, London 1973), p 33.
13 ANDERSON, R B, ERIKSSON, A J, and KRÖNINGER, H: 'Lightning and tall structures — some preliminary observations'. *4th Int Conf on Gas Discharges. IEE Conf Publication No 143*, Sept, 1976.
14 PIERCE, E T: 'Triggered lightning and some unsuspected lightning hazards'. *Stanford Research Institute Scientific Note 15*, Jan, 1972.
15 PRENTICE, S: 'Frequency of lightning discharges'. *Lightning Vol 1, chapter 14*, (Academic Press, London, 1977). Edited by R H Golde, p 481.
16 HORVATH, T: 'Gleichwertige fläche und relativ einshlagsgefahr als charakteristiche ausdrücke des schutzeffektes von blitzableitern'. *Int Blitzshutzkonf*, Munich, 1971.
17 POPOLANSKY, F: 'Preliminary report on lightning observations on high objects in CSSR'. *Private Communication*, August 1976.
18 MÜLLER-HILLEBRAND, D: 'On the frequency of lightning flashes to high objects — a study on the Gulf of Bothnia'. *Tell Vol 12, No 4*, pp 444-449, November 1960.
19 SZPOR, S, MILADOWSKA, K, and WIECKNOWSKI, J: 'Lightning current records on industrial chimneys in Poland'. *Pro, 1974 Session of CIGRÉ, Paris, Paper No 33-10*, August 1974.
20 MCCANN, E D: 'The measurement of lightning currents in direct strokes'. *AIEE Trans Vol 63*, pp 1 157-1 164, 1944.
21 GORIN, B N: 'Lightning discharges to the Ostankino television tower'. *Electrichestvo, No 2*, pp 24-29, Feb 1972 (CE Trans 6038).
22 GORIN, B N, LEVITOV, V I, and SHKILEV, A V: 'Distinguishing features of lightning strokes to high construction'. *4th Int Conf on Gas Discharges. IEE Conf Publication No 143*, Sept 1976.
23 GARBAGNATI, E, GUIDICE, E, LO PITARO, G B, and MAGAGNOLI, U: 'Survey of the characteristics of lightning stroke currents in Italy — results obtained in the years from 1970 to 1973'. *ENEL Report R5/63-27*, September 1974.
24 POPOLANSKY, F: 'The dependence of polarity of lightning current on the frequency distribution measured on objects with various heights in CSSR'. *Private Communication*, 1974.
25 BERGER, K: 'Parameters of upward lightning flashes'. *Private Communication*, June 1977.
26 GOLDE, R H: 'Lightning currents and Related Parameters'. *Lightning Vol 1, chapter 9*, (Academic Press, London 1977). Edited by Golde, p 335.
27 SARGENT, M A: 'The frequency distribution of current magnitudes of lightning strokes to tall structures'. *IEEE Trans PAS-91, No 5*, Sept/Oct 1972.
28 BROWN, G N, and THUNANDER, S: 'Frequency of distribution arrester discharge currents due to direct strokes'. *IEEE Trans PAS-95, No 5*, Sept/Oct 1976.
29 LINCK, H: 'The lightning exposure of tall structures'. *Private Communication*, June 1977.
30 UMAN, M A, MCLAIN, D K, FISCHER, R J, and KRIDER, E P: 'Currents in Florida lightning return strokes'. *J Geophys Res, Vol 78, No 18*, pp 3 530-3 537, June 1973.
31 GOLDE, R H: 'The Lightning Conductor'. *Lightning Vol 2, Chapter 17*, (Academic Press, London 1977). Edited by R. H. Golde, p 545-576.
32 ARMSTRONG, H R, and WHITEHEAD, E R: 'Field and analytical studies of transmission line shielding'. *IEEE Trans PAS, 87*, p 270-281, 1968.
33 WHITEHEAD, E R: 'Analytical speculation on improved geometric models of the lightning flash and transmission line environment and discussion'. *Private Communications*, August 1976 and June 1977.
34 PROCTOR, D: 'VHF radio pictures of lightning'. *PhD Thesis, University of Witwatersrand*, 1977.
35 ERIKSSON, A J: 'An unusual lightning flash?' *Weather, Vol 35, No 3*, p 102, March 1977.

Author's Replies

It is indeed gratifying to receive, as well as a challenging task to respond to, the thoughtful and comprehensive comments that have been presented by the contributors to the discussion on this paper, and I am highly appreciative of their kind remarks and the extent and scope of their contributions.

The first contribution, presented by **Dr C F Boyce**, is indeed most welcome, since he has re-emphasised the very real engineering motivations for active lightning research in South Africa and has highlighted the unique 'victim laboratory' nature of the Witwatersrand industrial complex. Subject to the availability of resources, I heartily endorse his comments on the possibility of extending the research work of this paper to additional structures. The role of corona discharge and the influence of local space charge (as discussed by Malan[1] and subsequently examined by Golde[2]) is certainly an important and relatively unexplored area of research as far as tall structures are concerned, and the prospects of studying the behaviour of one or two local structures are currently being investigated.

Several common areas of discussion present themselves in the contributions prepared by **Dr Anderson** and **Dr Stringfellow** and I propose therefore to respond to the relevant aspects of both of these two discussions in the following section.

First, both Dr Anderson and Dr Stringfellow have rightly criticised my initial procedure of normalising the global data on the assumption of a linear relationship between ground flash density (N_g) and regional keraunic level (T_D).

In the examination of this data, I recognised that this assumption was a poor compromise, but considered it unavoidable in the absence of reliable global data on either regional ground flash densities or the dependency of ground flash density upon keraunic level. The adoption of linear normalisation was based upon well-established precedents in many regions of the world, as shown in Prentice's analysis of the problem[3]; it is still, in fact, employed in modern engineering practice by Darveniza[4], amongst others. However, I concur completely with both Dr Anderson and Dr Stringfellow that the correct basis of normalisation should be in terms of ground flash density, and Dr Stringfellow is to be commended for his elegant derivation of equivalent ground flash densities and subsequent normalisation of my global data.

In this context, subsequent to the preparation of the original paper, an analysis has been carried out of the first three years of data available from the national survey of ground flash density[5]. This programme involves the deployment of some 300 RSA 10 ground flash counters around the country. In examining the data, it was possible to correlate the local keraunic levels as recorded by the various counter observers, with the corresponding ground flash densities determined from the counters' registrations, over a three-year period of analysis. The results are shown in Fig 1, together with a power-curve fit through the data. A total of 120 observations was available and the sample ranged from keraunic levels of 3 to 110 thunderstorm days. The power curve fit takes the form (correlation coefficient $r = 0{,}82$):

$$N_g = 0{,}023 T_D^{1{,}3} \qquad (1)$$

and it is interesting to observe that the exponent is less than the value of 1,67 obtained by Popolansky — as anticipated by Dr Anderson in his comments on Popolansky's analysis of the relationship between CIGRÉ counter registrations and keraunic level. Thus, although the continued usage of keraunic levels in engineering studies is generally to be discouraged in favour of the direct measurement of ground flash density, it is suggested that the above relationship (being derived from direct measurement) may offer a more realistic basis for normalisation — in contrast to the many empirical assumptions currently adopted. It is possible that the range in storm incidence and intensity encountered across South Africa may not correspond to that observed elsewhere in the world, but it is encouraging to note that the power curve in equation (1) corresponds well also with the trend indicated by the available global data — as shown in Fig 2, which depicts the data collated by Prentice[3] from many regions of the world.

For the sake of comparison, Fig 2 also shows the commonly assumed linear relationship:

$$N_g = 0{,}1\, T_D$$

which was the basis for normalisation of the data in the paper; it is clear, when compared with the new relationship as expressed in equation (1), that errors of the order of 50 per cent may well be possible at the lower end of the scale.

Accordingly, in response to Dr Anderson and Dr Stringfellow's comments, I have reprocessed the global data in Table 3 of the paper using the new relationship:

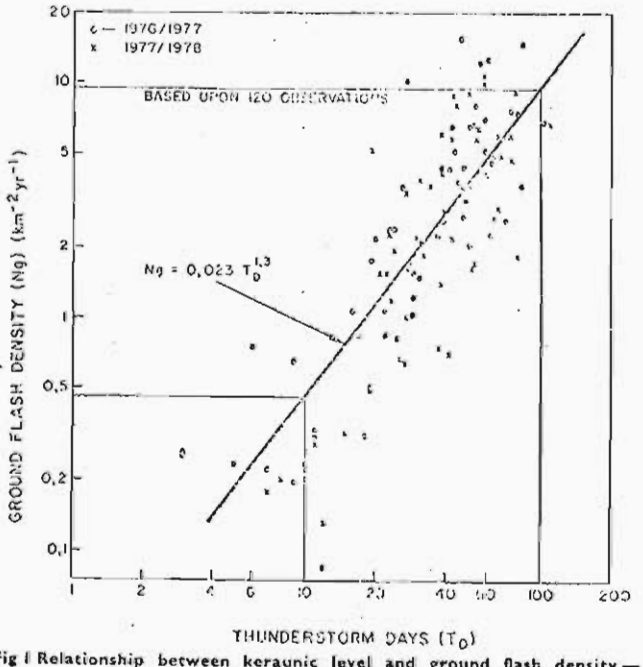

Fig 1 Relationship between keraunic level and ground flash density — South African flash counter data.

$$N_g = 0{,}023\ T_D^{1,3}$$

The resultant normalised data, showing annual flash incidence as a function of structure height, is shown in Fig 3, together with an exponential curve fitted through the data using a least squares technique. This relationship takes the form (for $N_g = 1\ \text{km}^{-2}\text{yr}^{-1}$):

$$N_F = 0{,}041 \exp(0{,}015\ H_s) \qquad (2)$$

It may be noted that this reprocessing has removed the discontinuity evident in the original Fig 10 of the paper — as remarked upon by Dr Stringfellow. For further comparison, the polynomial relationship derived by Dr Stringfellow has also been drawn through the reprocessed data shown in Fig 3 of this discussion, and there is a general similarity between the trend of the exponential relationship in equation (2) and that of this polynomial.

Having arrived at this modified relationship, I have repeated the approach originally adopted in the paper and followed by Dr Stringfellow in his discussion, and have re-derived relationships for the incidence of downward flashes as a function of structure height and for the resultant equivalent attractive radius, namely:

$$N_D = 8{,}33 \times 10^{-4}\ H_s^{1,22}\ (\text{for } N_g = 1\ \text{km}^{-2}\text{yr}^{-1}) \qquad (3)$$

and thus,

$$R = 16{,}3\ H_s^{0,61} \qquad (4)$$

The resultant modified dependency of attractive radius on increasing structure height is shown in Fig 4, together with the curve estimated by Dr Stringfellow.

It is interesting to observe that the modified curves both still approach the general trend of the $R = 2H$ relationship as noted in the paper, being therefore in general agreement with the points made by Dr Anderson in his discussion of this aspect.

I agree with Dr Anderson that the apparent downturn in the incidence of downward flashes, and thus in attractive radius as structure height is increased, may be an artefact of the data (or of some of the relationships fitted to the data) and it is clear that more accurate data will be required before this aspect can be clarified.

As a general comment on the above remarks, it should however be noted that, although the relationships expressed in equations (1) to (4) are considered to be more meaningful, being based upon an analysis of ground flash density rather than the compromise approach originally adopted in the paper, no attempts have been made to determine the best-fit functions through the modified data, since I still consider that the quality of the original data does not justify this level of treatment.

Dr Anderson also emphasised the probablistic nature of flash incidence and, in response to his examples, I have applied the Poisson equation to an estimation of the incidence of downward flashes to the research mast over a 5-year period of analysis, assuming a regional ground flash density of $7\ \text{km}^{-2}\text{yr}^{-1}$. The resulting predicted incidence is shown in Fig 5 as a function of structure

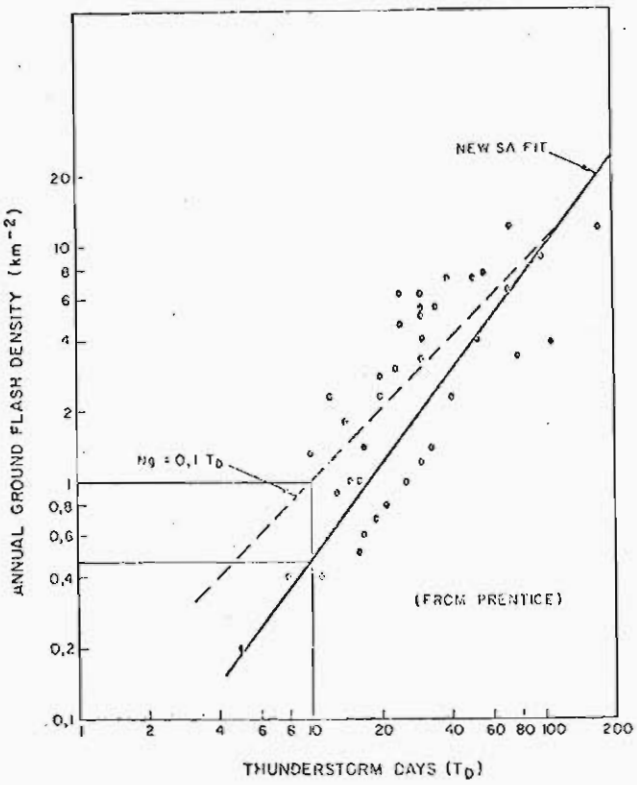

Fig 2 Relationship between keraunic level and ground flash density — global data.

attractive radius. It is seen that the observed 5-year incidence of downward flashes to the research mast is best accounted for by a structure with an attractive radius of about 320 m. Assuming that $R \approx 2H$, as indicated by the results shown in Fig 4, the above observation accords reasonably well with the estimate of an effective height of 148 m which was assigned to the research mast in section 4.4 of the paper. (In fact, by a happy coincidence, applying the modified relationships of this discussion, the mean effective height of the research mast increases to about 160 m.)

Two important points may therefore be noted:

(1) There is an overall consistency amongst these observations, whatever approach is adopted, and the general qualitative trends of the paper remain unaltered. These indicate essentially that tall isolated structures appear to display approximate average attractive radii, $R \approx 2H$, as far as downward flashes are concerned.

(2) The above remarks have no influence on the tentative conclusions in the paper concerning the dependencies of median current amplitudes upon structure height or upon the proposed adoption of a median amplitude of about 40 kA for negative downward flashes to flat country. (It should also be noted that the research mast current amplitude data, although consistent with the latter observations, comprise too small a sample to be statistically significant and are not essential for the substantiation of these observations, which arise consistently out of the limited data available from structures elsewhere in the world.)

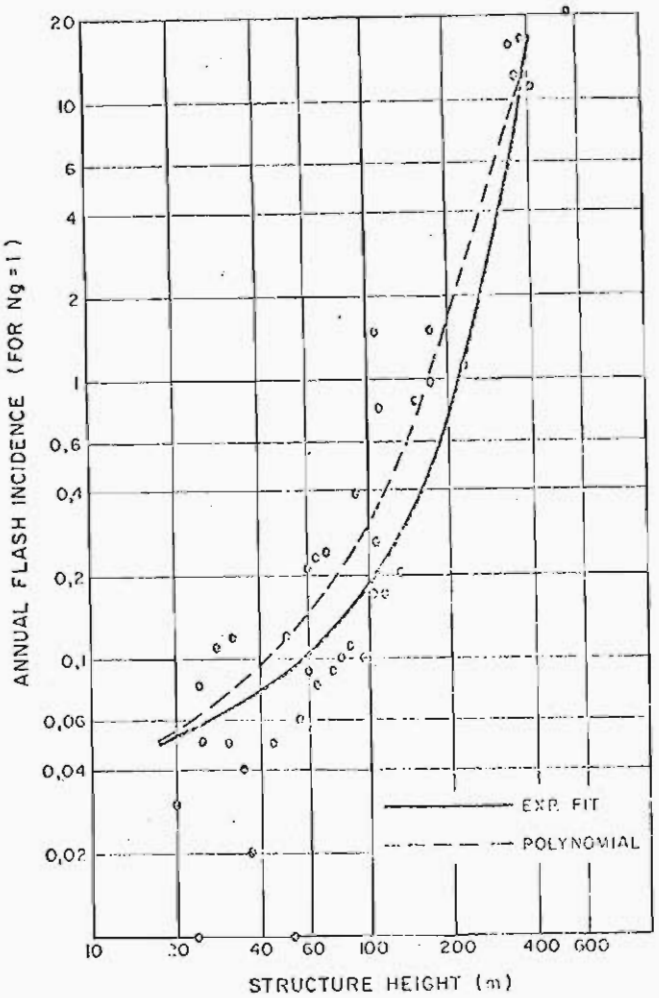

Fig 3 Relationship between structure height and annual flash incidence — on the basis of ground flash density.

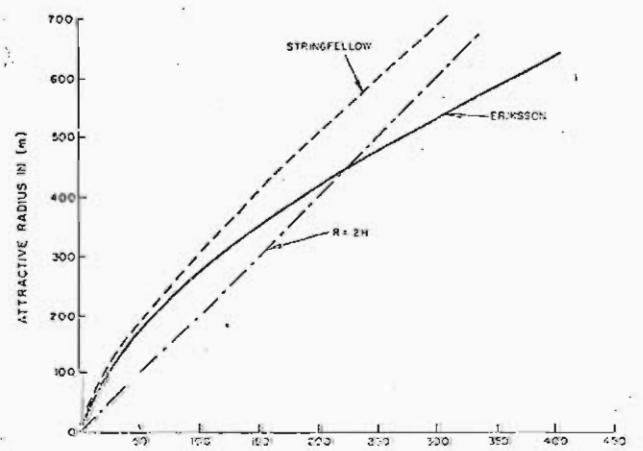

Fig 4 Relationship between attractive radius and structure height.

In the remainder of his discussion Dr Anderson has drawn attention to the lack of understanding of the final stages of a flash to a structure and has itemised several of the important factors which have to be taken into account — with particular emphasis on the role of the relative velocities of the downward and upward connecting leaders. I agree completely with his remarks in this regard and believe that this is an important aspect

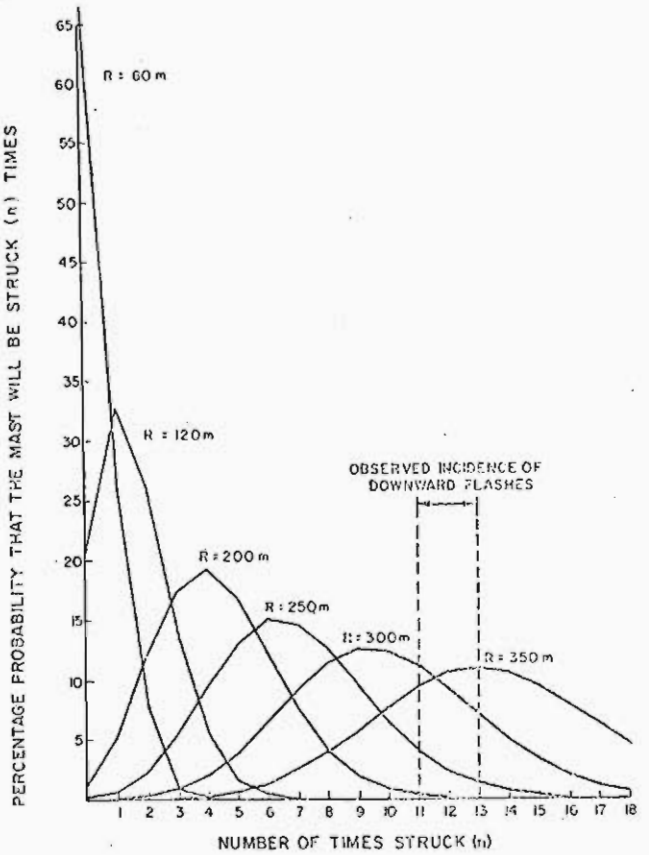

Fig 5 Predicted incidence of strikes to the research mast as a function of attractive radius (for a five-year period and a ground flash density of 7 km^{-2} yr^{-1})

of the problem — as emphasised recently also in the work of Allibone and Dring[6].

While it is generally agreed that the final stages of a downward flash involve the interception of the downward leader by a short upward rising connecting leader — in the event of flashes both to the ground and to tall structures (and involving upward leader lengths varying over a range of 5-300 m) a comprehensive understanding of this process must be capable of accounting for several relatively paradoxical observations:

(a) On the one hand, the electrogeometric concept (which essentially relates the downward leader striking distance to the leader charge) is apparently successful in predicting shielding failures, or penetrations, within transmission line geometries with dimensions in the range of about 5-20 m;

(b) On the other hand, evidence is available of the initiation of upward leaders from structures, during the approach of downward leaders, but which fail to intercept these leaders, the ground flash ultimately terminating elsewhere. An example recently recorded on the research mast, using the CCTV system, is shown in Fig 6. Although of poor quality due to the limited line resolution, this depicts the approach of a downward leader to within about 300 m of the mast, together with the initiation of an upward leader at least 60 m in extent, but the associated still photographs from the remote cameras indicate the final termination of this ground flash

at a point some 3 km away from the mast.

Apart from the influence of relative leader velocities, I therefore consider that the branched nature of the downward leader is an important feature of the process. Attention should also be drawn to Proctor's work[7] which suggests that the downward leaders that emerge from the clouds and ultimately lead to ground flashes may merely be branches of an extensive and complex process of inter-cloud breakdown.

As far as the engineering problems of lightning protection are concerned, I suspect that it may well become necessary to represent the complexity of the final stages of the process with a two-element concept of 'striking distance'. The first would relate to the macro-scale or 'blundering' approach of the branched downward leader and to the general intensification of the electrostatic fields in the vicinity of structures while the second would involve the probability of approach and the relative velocity of a branched element which may or may not penetrate a particular shielding geometry.

For the interim, and in response to Mr Rapley's questions, in the absence of a better understanding of the process, I suggest that there are several important aspects which are not necessarily fully taken into account in conventional protection practices.

(1) The role of the upward connecting leader should not be neglected, and I consider that advantage can accrue from the provision of preferential points of leader initiation on protection schemes in the form of short vertical finials at strategic positions on the air terminal system.

(2) In complex geometries, such as those discussed by Mr Rapley, the probabilistic nature of the process should also be taken into account. An engineering approach which has been found useful employs the Poisson equation; together with a striking distance relationship such as that expressed by equation (8) of the paper, and a known distribution of peak current amplitudes to arrive at an estimate of the probability of failure of a particular protection arrangement. The final decision on that arrangement should be based upon a study of the risk of failure and the consequences of the penetration of a given magnitude of current, and should also take cognisance of the economies of the situation.

I hope that in this discussion I have taken note of most of the points raised by the contributors and I should like once more to express my appreciation of their very pertinent and constructive contributions.

I record also my gratitude to the Council for Scientific and Industrial Research, and to the Director of the National Electrical Engineering Research Institute in particular, for the opportunity and permission to publish these remarks.

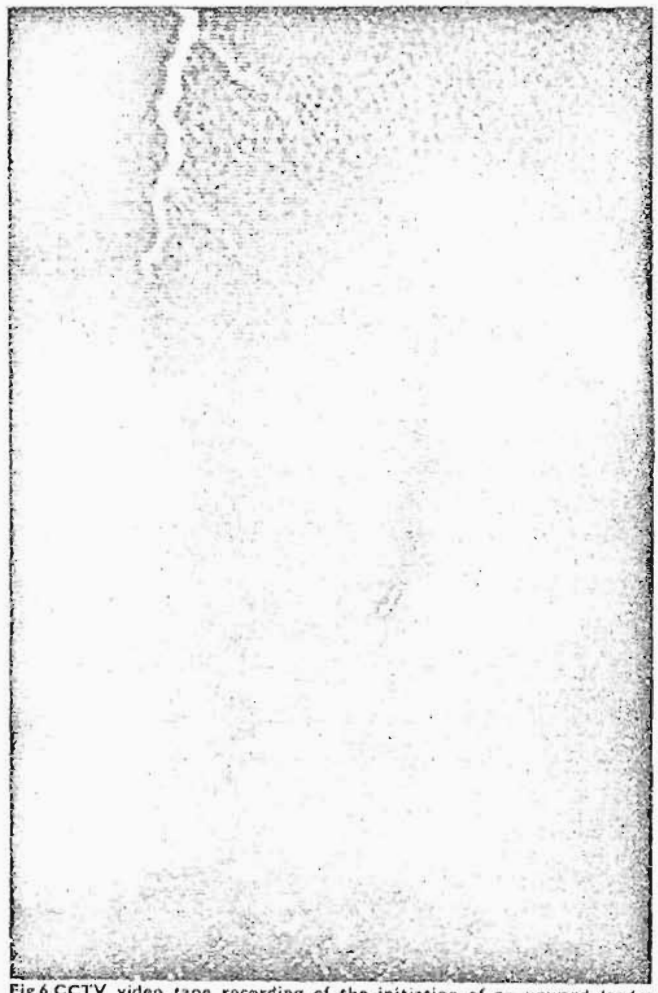

Fig 6 CCTV video tape recording of the initiation of an upward leader during the approach of a downward leader near the research mast.

References

1 MALAN, D J: 'Lightning and its effect on high structures', *Trans SAIEE*, Vol 60, Pt 2, November 1969, pp 241-242.
2 GOLDE, R H: 'Lightning and tall structures', *Proc IEE*, Vol 125, No 4, April 1978, pp 347-351.
3 PRENTICE, S A: 'Frequency of lightning discharge', *Lightning*, Vol 1, Chapter 14, (Academic Press, London, 1977) edited by Golde, pp 472-474.
4 DARVENIZA, M: 'Modelling for lightning performance calculations', *Private communication, 1978.*
5 ANDERSON, R B, VAN NIEKERK, H R, MEAL, D V and SMITH, M A: 'Tenth progress report on the development and testing of lightning flash counters in the Republic of South Africa during 1977/78'. *CSIR Special Report Elek 148, July 1978.*
6 ALLIBONE, T E and DRING, D: 'Lightning and the long spark; the significance of leader-stroke velocity', *Proc R Soc Lond A* 357, pp 15-35, 1977.
7 PROCTOR, D: 'VHF radio pictures of lightning', *PhD Thesis*, University of the Witwatersrand, 1977.